UNIVERSITAT DE BARCELONA

Structural Genomic Alterations in Hepatocellular Carcinoma and Novel Combination Therapies

Roger Esteban Fabró

Structural Genomic Alterations in Hepatocellular Carcinoma and Novel Combination Therapies

Doctoral thesis submitted by:

Roger Esteban Fabró

To obtain the degree of Doctor by the University of Barcelona.

Tutored by:

Prof. Josep Maria Llovet i Bayer

Full Professor of Medicine – University of Barcelona

Professor of Research – Institut d'Investigacions Biomèdiques August Pi I Sunyer (IDIBAPS), Hospital Clínic de Barcelona

PhD Program in Medicine and Translational Research

Faculty of Medicine and Health Sciences. University of Barcelona.

December 2022

Josep M Llovet, MD, PhD
Professor of Medicine-Hepatic Oncology
Professor of Research-ICREA
Director, Master in Translational Medicine
University of Barcelona
Head, Translational Research in Liver Cancer Lab
Liver Unit, IDIBAPS
Rosselló 149-153
08036 Barcelona
Catalonia, Spain
Office: +34-932279155
E-mail: jmllovet@clinic.cat
Assistant: Ariadna Farré (afarrec@clinic.cat)

Barcelona, 12 de desembre de 2022

Jo, Dr. Josep M. Llovet i Bayer, Catedràtic de Medicina a la Universitat de Barcelona, cap del Laboratori de Recerca Translacional en Oncologia Hepàtica de l'Institut d'Investigacions Biomèdiques August Pi i Sunyer (IDIBAPS) – Universitat de Barcelona – Hospital Clínic, Professor ICREA i director del Màster Oficial de Medicina Translacional de la Universitat de Barcelona,

CERTIFICO:

Que la tesi doctoral titulada "Structural Genomic Alterations in Hepatocellular Carcinoma and Novel Combination Therapies" presentada per Roger Esteban Fabró per optar al títol de Doctor en Medicina i Recerca Translacional per la Universitat de Barcelona s'ha realitzat sota la meva direcció i compleix tots els requisits necessaris per ser defensada davant el Tribunal d'Avaluació corresponent.

Dr. Josep M. Llovet i Bayer

Conformitat de l'estudiant de doctorat:

Roger Esteban Fabró

Al Dr. Josep Maria Llovet,

per confiar en mi i brindar-me les oportunitats i experiències que m'han permès arribar fins aquí.

A tots els membres del Laboratori Translacional en Oncologia Hepàtica de l'IDIBAPS,

per haver-me guiat, ensenyat, ajudat, suportat, acompanyat i motivat a seguir endavant, fent possible aquesta etapa de creixement professional i personal.

To all members of the Liver Cancer Program at Mount Sinai and friends in NYC,

for being the best colleagues and friends and making the city shine in a period of pandemic and uncertainty.

Als meus pares i família,

per ser la base més sòlida sobre què recolzar-me i créixer.

The present thesis has been supported by a doctoral training grant (BES-2017-081286) from MCIN/AEI/10.13039/501100011033 and the European Social Fund (ESF), and a mobility grant from Fundació Universitària Agustí Pedro i Pons.

List of content

Abbreviations

AFP	Alpha fetoprotein
ALIOS	American lifestyle-induced obesity syndrome
APC	Antigen-presenting cell
BCLC	Barcelona Clinic Liver Cancer
BS	Broad CNA score
cDC	Conventional dendritic cell
CIN	Chromosomal instability
CNA	Copy-number alteration
CR	Complete response
CTL	Cytotoxic lymphocyte
CXCR2	C-X-C Motif Chemokine Receptor 2
DC	Dendritic cell
DEN	Diethylnitrosamine
DNA	Deoxyribonucleic Acid
FC	Fold-change
FDA	Food and Drug Administration
FDR	False discovery rate
FS	Focal CNA score
GZMB	Granzyme B
HBV	Hepatitis B virus
HCC	Hepatocellular carcinoma
HCV	Hepatitis C virus
HGDN	High-grade dysplastic nodule
HLA	Human leukocyte antigen
ICI	Immune checkpoint inhibitor
IFN-γ	Interferon gamma
IHC	Immunohistochemistry
LGDN	Low-grade dysplastic nodule
LOH	Loss of heterozygosity
MDSC	Myeloid-derived suppressive cell

MHC	Major histocompatibility complex
MPO	Myeloperoxidase
MSI-H	Microsatellite instability-high
NAFLD	Non-alcoholic fatty liver disease
NASH	Non-alcoholic steatohepatitis
NE	Neutrophil elastase
NET	Neutrophil extracellular trap
NGS	Next-generation sequencing
NK	Natural killer (cell)
NLR	Neutrophil-to-lymphocyte ratio
NTP	Nearest template prediction
OR	Objective response
ORR	Objective response rate
OS	Overall survival
PD	Progressive disease
PFS	Progression-free survival
PMN-MDSC	Polymorphonuclear myeloid-derived suppressor cell
PR	Partial response
RCT	Randomized controlled trial
RNA	Ribonucleic acid
RNA-seq	RNA sequencing
ROS	Reactive oxygen species
SD	Stable disease
SNP	Single-nucleotide polymorphism
SNV	Single-nucleotide variant
ssGSEA	Single-sample gene set enrichment analysis
TAM	Tumor-associated macrophage
TAN	Tumor-associated neutrophil
TCGA	The Cancer Genome Atlas
TCR	T cell receptor

TGF-β	Transforming growth factor β
TKI	Tyrosine kinase inhibitor
TME	Tumor microenvironment
TLS	Tertiary lymphoid structures
TMB	Tumor mutational burden
Treg	T regulatory cell
VEGF	Vascular endothelial growth factor
VEGFR	Vascular endothelial growth factor receptor
WES	Whole-exome sequencing
WGS	Whole-genome sequencing

List of articles composing the thesis

The present thesis has the form of a compendium of three published articles.

<u>Study 1</u>: **Copy number alteration burden differentially impacts immune profiles and molecular features of hepatocellular carcinoma.**

Laia Bassaganyas*, Roser Pinyol*, **Roger Esteban-Fabró***, Laura Torrens, Sara Torrecilla, Catherine E. Willoughby, Sebastià Franch-Expósito, Maria Vila-Casadesús, Itziar Salaverria, Robert Montal, Vincenzo Mazzaferro, Jordi Camps, Daniela Sia, and Josep M Llovet. Copy number alteration burden differentially impacts immune profiles and molecular features of hepatocellular carcinoma. Clinical Cancer Research 2020; 26: 6350-6361.

**Shared first authorship.*

Impact factor: 13.801, 1st quartile. Subject Areas: Cancer Research. (Source: JCR).

Aim:

1. To determine the biological and clinical impact of chromosomal instability in hepatocellular carcinoma and to reveal its association with antitumor immunity.

<u>Study 2</u>: Cabozantinib Enhances Anti-PD1 Activity and Elicits a Neutrophil-Based Immune Response in Hepatocellular Carcinoma.

Roger Esteban-Fabró*, Catherine E. Willoughby*, Marta Piqué-Gili, Carla Montironi, Jordi Abril-Fornaguera, Judit Peix, Laura Torrens, Agavni Mesropian, Ugne Balaseviciute, Francesc Miró-Mur, Vincenzo Mazzaferro, Roser Pinyol, Josep M. Llovet. Cabozantinib Enhances Anti-PD1 Activity and Elicits a Neutrophil-Based Immune Response in Hepatocellular Carcinoma. Clinical Cancer Research 2022; 28:2449-2460.

**Shared first authorship.*

Impact factor: 13.801, 1st quartile. Subject Areas: Cancer Research. (Source: JCR).

Aim:

2.1. To explore the antitumoral and immunomodulatory effects of cabozantinib alone and in combination with anti-PD1.

Study 3: CXCR2 inhibition limits NASH-HCC immunotherapy

Jack Leslie, John B G Mackey, Thomas Jamieson, Erik Ramon-Gil, Thomas M Drake, Frédéric Fercoq, William Clark, Kathryn Gilroy, Ann Hedley, Colin Nixon, Saimir Luli, Maja Laszczewska, Roser Pinyol, **Roger Esteban-Fabró**, Catherine E Willoughby, Philipp K Haber, Carmen Andreu-Oller, Mohammad Rahbari, Chaofan Fan, Dominik Pfister, Shreya Raman, Niall Wilson, Miryam Müller, Amy Collins, Daniel Geh, Andrew Fuller, David McDonald, Gillian Hulme, Andrew Filby, Xabier Cortes-Lavaud, Noha-Ehssan Mohamed, Catriona A Ford, Ximena L Raffo Iraolagoitia, Amanda J McFarlane, Misti V McCain, Rachel A Ridgway, Edward W Roberts, Simon T Barry, Gerard J Graham, Mathias Heikenwälder, Helen L Reeves, Josep M Llovet, Leo M Carlin, Thomas G Bird, Owen J Sansom, Derek A Mann. CXCR2 inhibition limits NASH-HCC immunotherapy. **Gut** 2022;71(10):2093-2106.

Impact factor: 31.84, 1st quartile. Subject Areas: Gastroenterology and Hepatology. (Source: JCR).

Aim:

2.2. To evaluate the capacity of a CXCR2 inhibitor to re-sensitize NASH-HCC to anti-PD1 therapy.

Thesis summary (Catalan)

Títol

Caracterització de les alteracions estructurals genòmiques en carcinoma hepatocel·lular i estudi de noves teràpies.

Introducció

El càncer de fetge és el sisè tipus de càncer més diagnosticat al món i la tercera causa de mortalitat associada a càncer [1]. Un 90% dels casos corresponen al carcinoma hepatocel·lular, (CHC), que normalment es desenvolupa en el context d'una cirrosi hepàtica[2]. De tots els pacients de CHC, un 50-60% estan exposats a teràpies sistèmiques al llarg de la seva vida; recentment, la combinació de la immunoteràpia atezolizumab (anticòs monoclonal contra PD-L1, que permet desencadenar una resposta immunitària antitumoral) amb bevacizumab (anticòs monoclonal contra VEGFA, un factor de creixement responsable de l'angiogènesi o formació de nous vasos sanguinis) s'ha convertit en el tractament estàndard en primera línia en CHC avançat. Tot i així, només un 30% dels pacients responen a aquest tractament, essent la mitjana de supervivència dels pacients inferior als dos anys[3]. Per tant, és necessari descobrir biomarcadors de resposta o resistència per identificar els pacients que es beneficiaran de les teràpies disponibles i aprofundir en el coneixement sobre els mecanismes de la immunitat antitumoral per millorar les alternatives terapèutiques. De fet, els tumors desenvolupen mecanismes per evadir la resposta immunitària, entre d'altres acumulen alteracions genòmiques que els emmascaren i eviten la resposta immunitària. L'aneuploïdia és una alteració genòmica derivada de la inestabilitat dels cromosomes que suposa l'acumulació d'alteracions en el nombre de còpies (CNAs), i aquestes poden ser àmplies o focals. En certs tipus de càncer l'acumulació de CNAs àmplies s'associa a resistència a immunoteràpia, però el seu impacte biològic en CHC no s'ha descrit detalladament[4,5].

Per altra banda, l'elevada taxa de resistència primària a atezolizumab-bevacizumab (70%) emfatitza la necessitat de desenvolupar noves estratègies terapèutiques[2]. Atès que les immunoteràpies mostren millors resultats en tumors amb un context pro-inflamatori[6] i que les molècules pro-angiogèniques són immunosupressores, l'activitat antitumoral de la immunoteràpia podria ser estimulada promovent la infiltració o reactivació de les cèl·lules del

sistema immunitari usant teràpies de combinació amb agents antiangiogènics[7]. En aquest context, l'inhibidor de receptors tirosina quinases cabozantinib és un candidat prometedor.

A occident, els increments en la incidència d'obesitat i síndrome metabòlica s'associen a un augment dels casos de CHC atribuïbles a la esteatohepatitis no alcohòlica (EHNA), una malaltia hepàtica crònica deguda a la inflamació secundària al dipòsit de lípids al fetge[2,8]. Recentment, els tumors de EHNA-CHC s'han descrit com a menys sensibles a la immunoteràpia a causa de l'expansió d'un subgrup de limfòcits infiltrants en el microambient amb un perfil disfuncional[9]. D'altra banda, els neutròfils són un altre tipus de cèl·lula immunitària que presenta un comportament plàstic i pot ésser pro- o anti-tumorigènic[10]. Per tant, la modulació del seu funcionament podria ser un mecanisme per rescatar la resistència a la immunoteràpia associada a EHNA-CHC.

Hipòtesi

La hipòtesi d'aquesta tesi és que la identificació de trets moleculars/alteracions estructurals associats a la immunitat antitumoral en el carcinoma hepatocel·lular i l'avaluació de noves teràpies de combinació amb immunoteràpies permetran identificar biomarcadors candidats de resposta o resistència a la immunoteràpia i opcions terapèutiques més efectives per estimular la resposta immunitària antitumoral.

Objectius

Els objectius específics d'aquesta tesi doctoral són:

1. Determinar l'impacte biològic i clínic de la inestabilitat cromosòmica en carcinoma hepatocel·lular i identificar la seva associació amb la immunitat antitumoral.

2. Avaluar l'impacte de teràpies moleculars combinades amb immunoteràpia en models preclínics de carcinoma hepatocel·lular. Específicament:
   2.1. Explorar els efectes anti-tumorals i immunomoduladors de cabozantinib en monoteràpia i en combinació amb anti-PD1.
   2.2. Avaluar la capacitat d'un inhibidor de CXCR2 per re-sensibilitzar el CHC associat a esteatohepatitis no alcohòlica (EHNA) a la teràpia amb anti-PD1.

Mètodes

Estudi #1 (Bassaganyas *et al.*, Clin Cancer Res 2020): Es van analitzar les dades de *SNParray* de 452 parelles de mostres de teixit tumoral i adjacent de CHC i 25 nòduls displàstics. Per quantificar les càrregues genòmiques en alteracions en el nombre de còpies (CNAs) àmplies i focals es va fer servir l'eina web CNApp[11], que permet extreure *broad* i *focal scores* (BS i FS), respectivament. A continuació, aquestes dades es van integrar amb els perfils transcriptòmics, mutacionals i de metilació de les mostres, amb la seva composició immune i amb dades clinicopatològiques.

Estudi #2 (Esteban-Fabró *et al.*, Clin Cancer Res 2022): Es van utilitzar dos models murins singènics de CHC basats en la injecció subcutània de les línies cel·lulars Hepa1-6 i Hep53.4 (n=80 i 40, respectivament). Els animals es van aleatoritzar als 4 grups experimentals cabozantinib, anti-PD1, la combinació o placeb. Es van avaluar els trets moleculars i la composició immunològica de les mostres tumorals dels models amb citometria de flux, immunohistoquímica i anàlisi transcriptòmic. Alhora, s'extragué sang que s'avaluà mitjançant citometria de flux i un panell de citoquines. Els efectes observats amb cabozantinib es validaren amb dades transcriptòmiques d'un model de xenograft derivat de tumors colorectals. Finalment, les dades transcriptòmiques de tres cohorts de pacients de CHC (cohort 1: n=167, cohort 2: n=57, *The Cancer Genome Atlas*: n=319) permeteren agrupar els pacients segons perfils d'expressió similars als dels animals tractats amb la combinació anti-PD1 i cabozantinib, i se n'avaluà el valor predictiu.

Estudi #3 (Leslie *et al.*, Gut 2022): Es va caracteritzar la infiltració de neutròfils en CHC humà i en tres models de EHNA-CHC: model ortotòpic sobre fetge EHNA, model DEN-ALIOS i model deficient en colina i amb dieta rica en greixos. En els dos primers models es va administrar anti-PD1, un inhibidor de CXCR2 (AZD5069), la combinació o vehicle. Els efectes moleculars de les teràpies sobre el microambient tumoral van ser avaluats amb citometria de masses associada a imatge, seqüenciació d'ARN i citometria de flux. A més, aprofundint en el mecanisme d'acció de les teràpies, es va avaluar el següent *in vivo*: (1) administració d'anti-CD8a per reduir les cèl·lules T $CD8^+$, (2) ús de ratolins iCCR (*knockout* de CCR1, 2, 3 i 5) per impedir el reclutament de cèl·lules dendrítiques (CDs), (3) tractament amb anti-XCL1 per bloquejar la interacció entre CDs i cèl·lules T $CD8^+$, i (4) transfusió de neutròfils immadurs per avaluar la seva capacitat antitumoral.

Resultats

Estudi #1 (Bassaganyas *et al.*, Clin Cancer Res 2020):

1. Explorant les dades de 26 tipus de càncers diferents disponibles públicament (*The Cancer Genome Atlas*), les distribucions d'alteracions genòmiques estructurals (BS i FS) en CHC presentaren valors intermedis. El CHC és un dels 14 tipus tumorals de la cohort de TCGA on el *Broad Score* (BS) correlacionà negativament amb la quantitat d'infiltrat immunitari.
2. Els CHCs amb baixa càrrega de CNAs àmplies (baix BS) eren més diploides i enriquits en la classe immune del CHC, específicament la subclasse immune activa, caracteritzada per una major activació de la resposta immunitària adaptativa contra el tumor. Per tant, presentaren més senyalització antitumoral, infiltrat immune i activitat citolítica, i eren transcriptòmicament similars a mostres d'altres tipus tumorals que responen a anti-PD1.
3. Els CHCs amb alta càrrega de CNAs àmplies (alt BS) eren més poliploides i estaven enriquits en processos de proliferació i de reparació de l'ADN, mentre que presentaren una baixa infiltració immunitària.
4. Alts nivells de CNAs focals (alt FS) s'associaren a trets clàssics de proliferació, mutacions en *TP53*, signatures moleculars de mal pronòstic i trets histopatològics de tumors agressius com una pobra diferenciació i invasió vascular. Els valors de FS no s'associaren a cap tret immunitari.
5. Els nòduls displàstics i CHCs molt inicials que presentaven alguna CNA àmplia també s'associaren a una manca de perfils d'activitat immune antitumoral.
6. S'observaren diversos mecanismes que podrien justificar l'associació entre l'acumulació de CNAs àmplies i una falta d'enriquiment en trets moleculars d'immunitat antitumoral:
    a. Els tumors amb BS baixos presentaren una major proporció de neoantígens observats respecte els estimats segons la seva càrrega mutacional.
    b. Els CHCs amb BS alts presentaren delecions que afecten gens de la maquinària de presentació antigènica (com *HLA-DQB1*).
    c. Els valors alts de BS s'associaren amb una hipometilació general, fet que podria indicar una influència epigenètica en els perfils immunitaris del CHC.
    d. L'acumulació de delecions àmplies s'associà amb un menor infiltrat immunitari en major mesura que els guanys.

Estudi #2 (Esteban-Fabró *et al.*, Clin Cancer Res 2022):

1. La combinació de cabozantinib i anti-PD1 resultà en una reducció significativa del temps fins a resposta objectiva *versus* la resta de tractaments, induint alhora una major inhibició del creixement tumoral i una major taxa de resposta. Tant cabozantinib com la combinació causaren una reducció significativa en el volum de tumor viable i un augment en la taxa de necrosi tumoral.
2. Els efectes antiangiogènics de cabozantinib i de la combinació es confirmaren amb una reducció observada en la tinció de CD31, amb l'absència de vasos encapsulant clústers tumorals, amb una reducció en signatures transcriptòmiques d'angiogènesi i amb un enriquiment en firmes d'hipòxia. La combinació també s'associà amb la major reducció en signatures de proliferació i reparació de l'ADN.
3. L'avaluació de les poblacions infiltrants al tumor (citometria de flux, immunohistoquímica i anàlisi transcriptòmica) revelà que cabozantinib i la combinació induïren un reclutament significatiu de neutròfils. L'activitat dels neutròfils va ser el procés més significativament associat amb els 100 gens sobre-expressats únicament per la combinació.
4. Addicionalment, la totalitat dels tumors tractats amb anti-PD1 i la combinació recapitularen la classe immune del CHC. La combinació s'associà significativament amb l'enriquiment en signatures d'expressió d'inflamació, immunitat innata i adaptativa i la reducció de vies de senyalització de TGF-β i β-catenina. Tant cabozantinib com la combinació causaren una reducció en la infiltració de limfòcits T $CD8^+$ $PD1^+$ i de cèl·lules T reguladores.
5. A nivell sistèmic, cabozantinib i la combinació augmentaren les proporcions de cèl·lules T i T $CD8^+$ circulants, i reduïren el rati de neutròfils/limfòcits a la sang. La combinació causà un augment específic de les proporcions de cèl·lules T i T $CD8^+$ memòria/efectores, i dels nivells de les quimiocines CCL27 i IL-16.
6. Analitzant les dades transcriptòmiques de mostres de CHC humà, es definiren tres grups (*Neutrophil Enriched*, *Neutrophil Depleted* i *Tumor-only Neutrophil Depleted*) en funció de l'enriquiment en una signatura de neutròfils actius que s'associà al tractament amb la combinació en els models murins. En destacà el grup enriquit en neutròfils (*Neutrophil Enriched,* 25% de CHCs), amb alts nivells de la signatura en teixit adjacent i tumoral, que

presentà una manca d'exclusió immune, una manca de trets proliferatius i de cèl·lules desdiferenciades, i s'associà amb una millor prognosi.

Estudi #3 (Leslie *et al.*, Gut 2022):

1. Es va detectar l'expressió de CXCR2 entre neutròfils infiltrats en fetge EHNA humà i en tumors de pacients i de models murins d'EHNA-CHC. En models murins, els neutròfils associats a tumor presentaren enriquiment en gens inflamatoris i pro-tumorals.
2. Utilitzant models murins de NASH-CHC resistents a la immunoteràpia amb anti-PD1, aquesta resistència es va superar mitjançant el co-tractament amb l'inhibidor de CXCR2 AZD5069, que va ser capaç de perllongar significativament la supervivència, reduir la càrrega tumoral i impedir la proliferació cel·lular dels tumors.
3. L'avaluació de l'infiltrat immunitari revelà que la combinació de l'inhibidor de CXCR2 amb anti-PD1 augmentà la infiltració de cèl·lules T $CD8^+$ i la quantitat de clústers de cèl·lules T granzim B-positives. Aquestes agrupacions també es trobaven enriquides en cèl·lules dendrítiques convencionals (CDc) $XCR1^+$ i neutròfils immadurs proliferatius.
4. La combinació, que augmentà el nombre de neutròfils infiltrants, induí alhora una re-programació dels neutròfils cap a un perfil anti-tumoral: els neutròfils infiltrants en tumors de ratolins tractats amb la combinació es trobaren enriquits en processos de cicle cel·lular, fagocitosi, presentació d'antígens i desgranulació.
5. El tractament basat en la transfusió de neutròfils inflamatoris immadurs en combinació amb anti-PD1 va tenir un efecte anti-tumoral similar a la combinació amb l'inhibidor de CXCR2, i alhora augmentà les cèl·lules T $CD8^+$ i les cèl·lules dendrítiques convencionals infiltrants. En paral·lel, la reducció de les cèl·lules T CD8+, CDc i el bloqueig de les interaccions entre CDc i cèl·lules T $CD8^+$ causà una reducció de l'activitat anti-tumoral de la combinació. Per tant, els resultats indicaren que aquestes cèl·lules són necessàries per al benefici terapèutic de la combinació.

Conclusions

- Existeix una associació significativa entre les càrregues genòmiques de CNAs amplis o focals i diversos trets moleculars del CHC. Els CHCs amb altes càrregues de CNAs amplis exhibeixen trets d'exclusió immune, mentre que baixes càrregues de CNAs amplis s'associen a perfils d'activació de la immunitat antitumoral. Aquestes dades suggereixen que la inestabilitat cromosòmica és un tret diferencial del càncer que impacta sobre la immunogenicitat dels tumors, fet que podria influenciar la capacitat de resposta dels pacients a la immunoteràpia.

- La combinació de cabozantinib amb anti-PD1 presenta una major eficàcia que les monoteràpies i promou la immunitat anti-tumoral a través de l'estimulació d'una resposta innata guiada per la infiltració de neutròfils en combinació amb una resposta immune adaptativa. Els CHCs humans que presenten trets moleculars semblants als observats en models experimentals que responen a la combinació cabozantinib + anti-PD1, com ara l'activació de neutròfils, podrien presentar una resposta favorable a aquesta estratègia terapèutica.

- Els neutròfils associats a tumor es poden manipular selectivament a través de la inhibició de CXCR2 per tal d'adoptar un perfil anti-tumoral. La combinació d'un inhibidor de CXCR2 amb la immunoteràpia anti-PD1 augmenta l'eficàcia d'anti-PD1 en models preclínics de NASH-CHC i és un candidat prometedor per ser avaluat en assaigs clínics.

Thesis summary

Title

Structural Genomic Alterations in Hepatocellular Carcinoma and Novel Combination Therapies

Introduction

Primary liver cancer is the sixth most diagnosed cancer and the second leading cause of cancer-related death worldwide[1]. Around 90% of cases correspond to hepatocellular carcinoma (HCC), which normally arises in the setting of a chronic liver disease[2]. Of all HCC patients, 50-60% will be ultimately exposed to systemic therapies, where the combination of atezolizumab and bevacizumab has become the standard of care in first line. However, only around 30% of patients respond to this therapy[3]. Therefore, there is a need for biomarkers of response/resistance and more knowledge on the mechanisms behind antitumor immunity. In line with this, aneuploidy – the presence of copy-number alterations (CNAs) in chromosome segments due to chromosomal instability- has been linked to immune evasion in some cancer types. In HCC, the biological implications of aneuploidy profiles have not been thoroughly described [4,5].

The elevated rates of primary resistance to atezolizumab-bevacizumab (70%) highlight the need to develop novel therapeutic strategies[2]. Given that immunotherapeutic agents show better results among tumors with an inflammatory microenvironment[6] and that proangiogenic molecules are immunosuppressive, the antitumor activity of immunotherapy could be enhanced by promoting the infiltration or reactivation of immune cells in combinatorial strategies with antiangiogenic agents[7]. In this context, the tyrosine kinase inhibitor (TKI) cabozantinib is a promising candidate for combination with ICIs.

In Western countries, an increasing prevalence of obesity and metabolic syndrome is leading to a higher fraction of HCCs attributed to non-alcoholic steatohepatitis (NASH)[2,8]. Recently, NASH-HCC has been reported as less responsive to immunotherapy due to an expansion of a subset of exhausted infiltrating $CD8^+$ T cells[9]. Considering the growing evidence for pro- and anti-tumor functions of neutrophils in cancer and HCC[10], neutrophil phenotype modulation could be a mechanism to overcome NASH-HCC immunotherapy resistance.

Hypothesis

The identification of molecular features/structural genomic alterations linked to antitumor immunity in HCC and the assessment of novel combinatorial strategies with immunotherapies will reveal candidate biomarkers of response or resistance to immunotherapeutic agents and more effective therapeutic options to enhance the antitumor immune response.

Aims

The specific objectives of the doctoral thesis are:

1. To determine the biological and clinical impact of chromosomal instability in hepatocellular carcinoma and to reveal its association with antitumor immunity.
2. To evaluate the impact of molecular therapies combined with ICIs in preclinical models of HCC. Specifically:
    2.1. To explore the antitumoral and immunomodulatory effects of cabozantinib alone and in combination with anti-PD1.
    2.2. To evaluate the capacity of a CXCR2 inhibitor to re-sensitize NASH-HCC to anti-PD1 therapy.

Methods

Study #1 (Bassaganyas *et al.*, Clin Cancer Res 2020): We analyzed SNP array data from 452 paired tumor/adjacent resected HCCs and 25 dysplastic nodules. We used the CNApp web tool[11] to quantify the CNA burdens of each sample and generate broad and focal scores (BS and FS), which were then correlated with transcriptomic, mutational and methylation profiles, tumor immune composition, and clinicopathologic data.

Study #2 (Esteban-Fabró *et al.*, Clin Cancer Res 2020): This study was performed using two syngeneic murine HCC models based on C57BL/6J mice bearing subcutaneous Hepa1-6 or Hep53.4 tumors (n=80 and 40, respectively). Animals were randomized to receive cabozantinib, anti-PD1, their combination or placebo. Molecular and immune effects on tumor samples were assessed with flow cytometry, IHC and transcriptome analysis, while blood samples were evaluated with flow cytometry and cytokine profiling. Cabozantinib-

related effects were validated in transcriptomic data from a colorectal cancer patient-derived xenograft model. Finally, transcriptomic data from three human HCC cohorts (cohort1: n=167, cohort 2: n=57, The Cancer Genome Atlas: n=319) were used to cluster patients according to combination-like expression features and to assess their impact on overall survival.

Study #3 (Leslie *et al.*, Gut 2022): neutrophil infiltration was characterized in human HCC and in three mouse models of NASH-HCC: an orthotopic on Western diet model, a DEN/ALIOS model and a choline-deficient high-fat diet model. Animals from the first two models were administered anti-PD1, AZD5069, the combination or vehicle, and the molecular effects of the therapies on the tumor immune microenvironment were evaluated by imaging mass cytometry, RNA-seq and flow cytometry. Anti-CD8a was administered for $CD8^+$ T cell depletion, iCCR mice (CCR1, 2, 3 and 5 knockout) with DEN/ALIOS treatment was used to impair dendritic cell (DC) recruitment, anti-XCL1 was used to block cDC-$CD8^+$ T cell interactions and neutrophil transfusions were performed in the orthotopic NASH-HCC model.

Results

Study #1 (Bassaganyas *et al.*, Clin Cancer Res 2020):

1. We used the TCGA pan-cancer data (10,635 patients) to rank HCC based on CNApp-derived BS and FS, quantifying genomic burdens of broad and focal CNAs, respectively. We observed that BS and FS distributions in HCC were intermediate among all cancer types. In addition, HCC was one of the 14 tumor types where BS negatively correlated with transcriptomic estimates of immune infiltration, while FS did not.
2. HCCs with a low burden of broad CNAs (low BS) were more diploid and were enriched in the HCC immune class, specifically the active subclass, which is characterized by the activation of an adaptive immune response. Low BS samples displayed high inflammatory and antitumor immunity signaling, higher immune infiltrate and cytolytic activity estimates, and were transcriptionally similar to tumors responding to anti-PD1.
3. HCCs with high burden of broad CNAs (high BS) were more polyploid, had an enrichment in transcriptomic features of DNA repair and proliferation and low immune infiltration.

4. High levels of focal CNAs (high FS) were linked to classical proliferative features, TP53 mutation, poor survival signatures and features of aggressive tumors like poor cell differentiation and vascular invasion. FS did not correlate with immune features.
5. Dysplastic nodules and very early HCCs with broad CNAs were also linked to reduced features of active antitumor immunity, suggesting that the impact of broad CNAs on immunity may be seen even at early stages of hepatocarcinogenesis.
6. We observed several potential mechanisms that could explain the differential immune profiles based on broad CNA levels:
    a. Low BS HCCs had a significantly higher ratio of observed/expected neoantigens, rendering more neoantigens than expected by their lower mutation burdens.
    b. Specific losses of antigen presentation machinery genes (such as *HLA-DQB1*) were enriched in high BS tumors.
    c. High BS HCCs have a widespread hypomethylation, which may indicate an epigenetic influence on HCC immune profiles[12].
    d. The accumulation of broad CNA losses had a stronger association with reduced immune infiltration estimates as compared to broad CNA gains, like previous observations in melanoma[13].

Study #2 (Esteban-Fabró *et al.*, Clin Cancer Res 2020):

1. Combination treatment induced a significantly shorter time to objective response versus the rest of treatment arms. It also induced the greatest anti-tumor growth effect and the greatest objective response rate (ORR). In addition, both cabozantinib and combination treatments induced a significant reduction in viable tumor volume and increased tumor necrosis.
2. The antiangiogenic effects in cabozantinib and combination arms were confirmed by reduced CD31 staining, absence of vessels encapsulating tumor clusters, reduced enrichment in transcriptomic signatures of angiogenesis and more enrichment in hypoxia-related signatures. Combination was also associated with the greatest reduction in gene expression signatures of proliferation and DNA repair.
3. Immune population assessment of infiltrating immune cells (with flow cytometry, immunohistochemistry and transcriptomic analysis) revealed that cabozantinib and

combination induced a significant recruitment of intratumor neutrophils. In addition, neutrophil antitumor activity was the biological process most significantly associated with the 100 genes uniquely upregulated by the combination.

4. Further immune characterization revealed that all anti-PD1 and combination-treated samples recapitulated the immune class of HCC. Combination was significantly associated with upregulation of transcriptomic pathways of inflammation, innate and adaptive immunity and with downregulation of TGFβ and β-catenin pathways. Cabozantinib and combination induced a reduction in $CD8^+$ $PD1^+$ lymphocytes and intratumoral T regulatory cells.
5. At the systemic level, cabozantinib and combination increased the proportions of circulating T and $CD8^+$ T cells and reduced the neutrophil-to-lymphocyte ratio in blood. Combination specifically increased the proportions of circulating memory/effector T and $CD8^+$ T cells, and the levels of the chemoattractants CCL27 and IL-16.
6. We defined three human HCC clusters (*Neutrophil Enriched*, *Neutrophil Depleted* and *Tumor-only Neutrophil Depleted*) based on enrichment in a signature reflecting the neutrophil activation in combination-treated mice. The Neutrophil Enriched cluster (25% of patients), with high active neutrophil enrichment in tumor and adjacent tissue, presented a lack of immune exclusion, reduced stem cell and proliferation features, and was linked to longer survival.

Study #3 (Leslie *et al.*, Gut 2022):

1. $CXCR2^+$ expression was detected specifically among infiltrating neutrophils in human NASH and within the tumor of both human and mouse models of NASH-HCC. In mouse models, tumor-associated neutrophils (TANs) express inflammatory and pro-tumor neutrophil genes.
2. Using preclinical models of NASH-HCC that are resistant to anti-PD1 therapy, we observed that such resistance is overcome by co-treatment with the CXCR2 small molecule inhibitor AZD5069, which can extend survival, reduce tumor burden and impair tumor cell proliferation.

3. The combination of anti-PD1 and CXCR2 inhibitor increased $CD8^+$ T cell infiltration and induced a higher number of Granzyme B^+ T cell clusters. These clusters were also enriched in conventional $XCR1^+$ dendritic cells and immature proliferating neutrophils.
4. The combination, which increased the number of TANs, also induced a TAN re-programming from a pro- to an anti-tumor phenotype: combination-treated TANs were enriched in cell cycle, phagocytosis, antigen presentation and degranulation processes.
5. The treatment based on the transfusion of immature inflammatory neutrophils in combination with anti-PD1 had a similar anti-tumor effect than the combination with the CXCR2 inhibitor. It also increased intratumor $CD8^+$ T cells and conventional dendritic cells. In parallel, depletion of $CD8^+$ T cells, of cDC1s and blockade of cDC-$CD8^+$ T cell interactions impaired the anti-tumor activity of the combination. Therefore, our results suggest that these cells are required for the therapeutic benefit of the combination.

Conclusions

- There are differential associations between broad and focal genomic CNA burdens and several HCC molecular features. HCCs with high burdens of broad CNAs exhibit immune exclusion features, while low broad CNA burdens are linked to immune active profiles. These data constitute evidence in favor of chromosomal instability as a cancer hallmark impacting tumor immunogenicity, which may influence patient response to immunotherapies.
- The combination of cabozantinib with anti-PD1 enhances anti-tumor immunity by bringing together innate neutrophil-driven and adaptive immune responses, a mechanism of action which could broaden the spectrum of responders in HCC. Human HCC tumors enriched in combination-like neutrophil features display a favorable molecular and clinical profile, suggesting the benefit of this combination for HCC treatment.
- TANs can be selectively manipulated through CXCR2 inhibition to adopt an anti-tumor phenotype. The combination of CXCR2 antagonism with anti-PD1 therapy enhances the efficacy of anti-PD1 in preclinical models of NASH-HCC and is a promising candidate for clinical testing.

Introduction

1. Cancer: impact and biology

1.1. The global burden of cancer

Cancer is defined as the group of diseases in which abnormal cells divide without control and have the potential to invade other parts of the body[14]. It is a remarkable health problem globally which caused an estimated 19.3 million new cases and 10 million deaths worldwide in 2020[1]. Of these, the most diagnosed cancers were female breast (11.7% of the total new cases), lung (11.4%), colorectal (10%), prostate (7.3%), stomach (5.6%) and liver (4.7%); and the most common causes of death by cancer were lung (18%), colorectal (9.4%), liver (8.3%), stomach (7.7%) breast (6.9%) and esophagus (5.5%)[1]. Of note, incidence and mortality of cancer types differ significantly across geographic regions and between genders; this reflects societal, economic and lifestyle disparities. However, based on growth and ageing of the world population, the incidence of cancer is expected to rise across all regions and up to 28.4 million new cases globally in 2040. This could be further exacerbated particularly in developing countries where an epidemiologic transition is likely to increase the prevalence of known cancer risk factors such as smoking, excessive body weight or sedentarism[1]. Such data reinforce the need to escalate efforts to control the disease through prevention measures and efficacious cancer care to achieve a global cancer control. In this context, translational research is crucial to convert the increasing knowledge on the biological principles of cancer into successful clinical implementations[15].

1.2. Cancer Biology

Tumorigenesis is a multistep process based on the acquisition of a set of fundamental traits (**hallmarks of cancer**) by cancer cells[16]. In 2000, Hanahan and Weinberg published 'The Hallmarks of Cancer', a review of cancer research literature that was essential for conceptualizing the pathogenic route that a normal tissue undergoes to become a malignant tumor[17]. These hallmarks are acquired thanks to **enabling characteristics**, which act as facilitators of cell transformation. In a recent revision of this model, the following framework of hallmarks and enabling characteristics were proposed[18] (**Figure 1**).

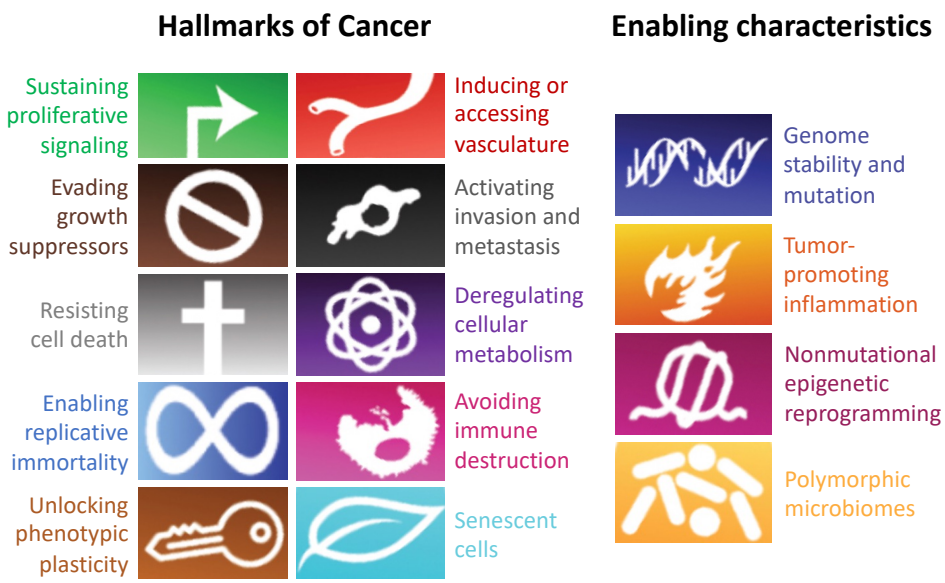

Figure 1 | Hallmarks of Cancer and enabling characteristics. Adapted from Hanahan Cancer Discovery 2022[18].

1.2.1. Hallmarks of Cancer

- *Sustaining proliferative signaling:* cancer cells can increase the production and release of growth factors or present structural changes inducing ligand-independent activation of receptors to continuously promote their progression through the cell cycle.

- *Evading growth suppressors*: capacity to bypass proliferation inhibition signals, which mostly depend on the activity of tumor suppressor genes.

- *Resisting cell death*: tumor cells present alterations in the sensor systems that trigger apoptosis, the mechanism of programmed death for old or damaged cells in order to avoid the propagation of DNA errors and promote cell homeostasis in the tissues.

- *Enabling replicative immortality*: in cancer cells, the enzyme complex telomerase is reactivated and allows the maintenance of telomeres (the ends of chromosomes) in the successive cell divisions. Without telomere shortening, cancer cells can undergo an unlimited number of growth-and-division cycles.

- *Inducing angiogenesis*: cancer cells can release angiogenic factors to trigger the formation of tumor-associated vasculature, which provides nutrients and oxygen and evacuates waste products from the tumor tissue, enabling cell proliferation and metastasis.

- *Activating invasion and metastasis*: The invasion capability -linked to the loss of adherent junctions, expression of matrix-degrading enzymes and increased motility- allows cancer cells to escape the primary tumor mass, occupy adjacent tissues and travel to distant sites where they may form new colonies -metastases-, which are the cause of 90% of human cancer deaths.

- *Deregulation of cellular energetics*: cancer cells can reprogram their glucose metabolism limiting it largely to glycolysis, adjusting to the energy requirements to sustain uncontrolled cell proliferation.

- *Avoiding immune destruction*: to escape detection by the immune system, which is constantly monitoring tissues and eliminating arising malignant cells, tumors develop mechanisms such as avoiding immune recognition, suppressing immune reactivity or preventing T-cell infiltration.

- *Unlocking phenotypic plasticity*: to avoid proliferation arrest, malignant cells can exit the state of terminal differentiation reached by normal cells. This can be reached by de-differentiation back to progenitor-like states, undifferentiated progenitor cells halting their differentiation process, or by a switch in the differentiation program (transdifferentiation) towards a more favorable cell phenotype.

- *Senescent cells*: in certain contexts, senescent (non-dividing and metabolically active) cells in the tumor microenvironment are capable of stimulating tumor development and malignant progression.

1.2.2. Enabling characteristics

- *Genome instability and mutation*: a succession of alterations in the genomes of cancer cells (mutations) allows the acquisition of oncogenic traits. Specific mutant genotypes in subsets of cancer cells are linked to a selective advantage and enable their outgrowth and dominance in the local tissue environment.

- *Tumor-promoting inflammation*: tumor-infiltrating immune cells can promote several hallmark capabilities by supplying molecules to the microenvironment such as growth factors, survival factors limiting cell death, proangiogenic factors, enzymes modifying the extracellular matrix and promoting invasion, etc.

- *Non-mutational epigenetic reprogramming*: many cancers harness global changes in their epigenetic landscapes, reprogramming gene-regulation networks to alter gene expression and favor the acquisition of hallmark capabilities.

- *Polymorphic microbiomes*: the human body is colonized by a large variety of microorganisms –approximately 40 trillion cells-, which may contribute to human health and disease. For instance, some have promoting or protective effects on cancer development, progression, and response to therapies.

Of note, genomic instability in cancer cells and the inflammatory state of premalignant and malignant lesions are relevant determinants of the tumor phenotypes and may inform on their capacity to respond to therapies. These characteristics are further discussed below.

1.3. Genomic instability and mutation in cancer

The acquisition of many of the hallmarks presented above rely upon the accumulation of alterations in the genomes of cancer cells. Such accumulation allows the generation of altered genotypes in subclones of cells that have a selective advantage, allowing them to outgrow the rest of cells and dominate in a local tissue environment, promoting cancer progression[16]. The increased tendency to accumulate DNA alterations during cell division is known as **genomic instability**. It can be caused by multiple elements: an increased sensitivity to

mutagenic agents, a breakdown in one or more components of the genomic maintenance machinery and/or a dysfunction in the surveillance system that monitors the genomic integrity and induces senescence or apoptosis of damaged cells[19].

The acquired DNA alterations in somatic cells, known as **somatic mutations**, are the result of cell-intrinsic processes (e.g., DNA damage or decay of nucleotides over time) or exposures to external agents (e.g., cigarette smoke or ultraviolet light). **Germline mutations**, which are inherited from parents, are less frequent and are linked to hereditary cancer predisposition and normally affect DNA repair genes[20].

All molecular aberrations that involve the modification of the underlying DNA sequence are called **structural mutations**, which can be further subdivided into single-base substitutions, insertions and deletions (indels), copy-number alterations (CNAs) and chromosomal rearrangements. Further details on these types of structural mutations are given in the sections below.

In addition to the previous, cancer cells can also present **insertional mutagenesis** or the integration of exogenous DNA sequences within the genome, resulting in the deregulation of genes that lead to oncogenic development. These sequences are generally from viruses like Epstein Barr virus, Hepatitis B virus, human papilloma virus, human T lymphotropic virus 1 and human herpes virus 8[21].

The study of somatic mutations has advanced dramatically with the advent of genome-wide sequencing, which has shown that every tumor harbors thousands of somatic mutations (and epigenetic alterations). However, only a small fraction of them (around 3-8) are **drivers** – located in genes that provide a growth advantage over surrounding cells when mutated-. The remaining mutations are **passengers**. These occur coincidentally during the tumorigenic process[21,22] and do not confer a selective growth advantage to the tumor cell. Currently, only ~570 cancer driver genes have been described of the >20,000 genes in the human genome[23].

1.3.1. Single-base substitutions and indels

Single-base substitutions or single nucleotide variants (SNVs) involve replacements of one base for another and can be divided into **transitions** (exchanges between bases of the same class, purine or pyrimidine) and **transversions** (a purine being replaced by a pyrimidine or vice

versa). When a SNV affects an exon, it can induce a change in the codified amino acid. Depending on the type of codon change, SNVs can be classified as **synonymous or silent mutations** (the new codon encodes the same amino acid than in the wild-type gene), **non-synonymous or missense mutations** (the new codon encodes a different amino acid) and **nonsense mutations** (the new codon is a stop codon causing a truncated protein)[24] (**Figure 2**).

Insertions and deletions (indels) comprise insertions and deletions of one or a few bases in the DNA sequence. **Frameshift indels** are those that cause a shift in the reading frame of the protein, altering all the codons that are read after the mutation. Sometimes, **inframe indels** occur if 3 (or a multiple of 3) bases are inserted or deleted, since the reading frame is not modified (**Figure 2**).

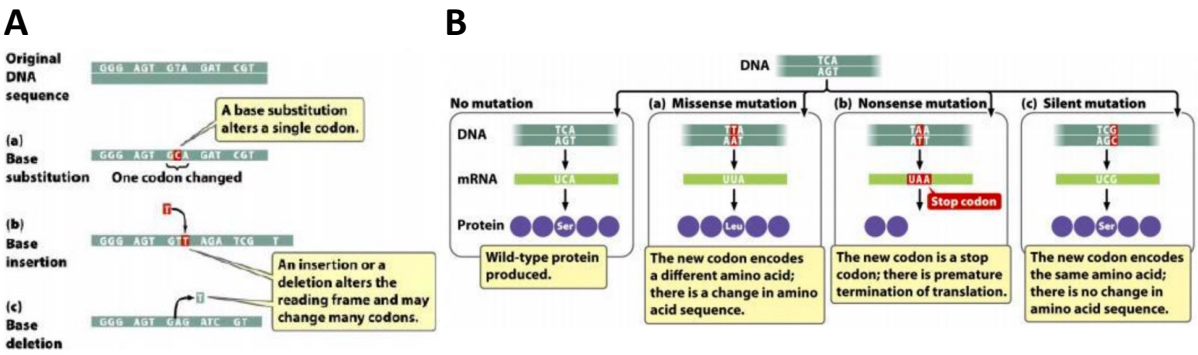

Figure 2 | Single-base substitutions and indels. (A) Representation of SNVs and indels. (B) Types of SNVs based on how they alter the codon sequence. Obtained from Krebs *et al.* Genes are DNA. Lewin's Genes XI 2013[24].

Of note, in common solid tumors like breast, colon, pancreas or brain, an average of 33 to 66 genes displays mutations that alter their protein sequence (40 for HCC, **Figure 3**). About 95% of these mutations are SNVs, of which 90.7% are missense mutations, 7.6% are nonsense mutations, and 1.7% result in alterations of splice sites or untranslated regions adjacent to start and stop codons. The remaining 5% of alterations are indels of one or a few bases[25].

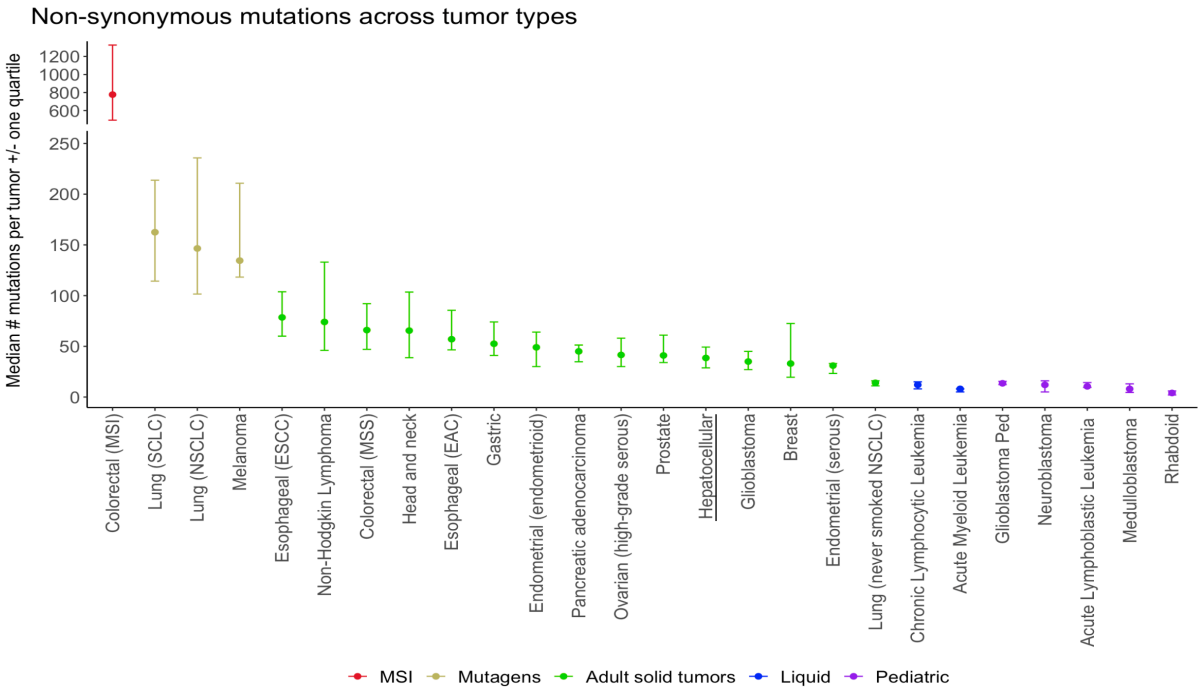

Figure 3 | Number of non-synonymous somatic mutations in multiple human cancer types. Horizontal bars represent the 1st and 3rd quartiles. MSI, microsatellite instability; SCLC, small cell lung cancers; NSCLC, non–small cell lung cancers; ESCC, esophageal squamous cell carcinomas; MSS, microsatellite stable; EAC, esophageal adenocarcinomas. Data from Vogelstein *et al.* Science 2013[25].

1.3.2. Copy-Number alterations (CNAs) and aneuploidy

Aneuploidy is a common feature of human cancer, present in ~90% of solid tumors[26]. It is defined as a state in which a cell does not contain the exact multiple of the haploid chromosomal complement, therefore having an unbalanced genomic status (**Figure 4A**)[27]. Aneuploidy encompasses numerical aberrations (whole chromosome gains and/or losses) and structural or segmental aberrations (gains and/or losses of sub-chromosomal regions)[27–30]. Regarding its origin, a major source of aneuploidy is believed to be **chromosomal instability** (**CIN**), defined as an ongoing elevated frequency of mitotic errors that leads to gains and losses of whole chromosomes or parts thereof[31–33]. These aberrant mitoses are mainly due to chromosome mis-segregations, lagging chromosomes during anaphase, pre-mitotic structural defects due to replication stress and even cancer-cell extrinsic events like glucose deprivation, hypoxia, or extracellular medium acidification[33–35]. Therefore, CIN causes a rapid acquisition of aneuploidy in cancer cells.

Generally, tumor aneuploidy is assessed through somatic copy-number alterations (CNAs). These can either be **broad CNAs**, which span most of a chromosome or the majority (≥50%)

of its arm, and mainly occur through mitotic chromosome missegregations[26]; or **focal CNAs**, typically defined as deletions or amplifications affecting a limited region in a chromosome arm and which tend to occur due to inappropriate repair of DNA double strand breaks[26]. Focal CNAs have been analyzed differently over the years, varying from restrictive definitions limiting their lengths to less than 3 Mb[36,37], to recent genomic studies defining those somatic CNAs spanning less than 50% of a chromosome arm as focal events[5,38,39]. Pan-cancer studies have revealed that there is a median of 11 focal amplifications, 12 focal deletions, 3 broad amplifications and 5 broad deletions per cancer sample, as well as 1 **copy-neutral loss-of-heterozygosity** (**LOH**), which is a genomic event where one allele is deleted and the other is duplicated[39]. In HCC, an average burden of 8.7 CNAs per patient has been reported[40]. Of note, although broad CNAs tend to be less frequent and do not involve multi-copy gains or homozygous deletions, they may cause large gene dosage imbalances in the expression of hundreds to thousands of genes.

In terms of the consequences of aneuploidy, it promotes a dual cellular state: generally, adverse effects of aneuploidy (i.e., defects in cell proliferation, proteotoxic stress and p53 activation) impair tumorigenesis, but these negative cellular outcomes are attenuated in the presence of aneuploidy-tolerating mutations (e.g., TP53 inactivation), increased ploidy or balancing aneuploidies (occurrence of alterations that counteract the protein imbalances resulting from the accumulation of CNAs)[27] (**Figure 4B**). In this scenario, aneuploidy leads to intratumor genetic diversity and the ability to undergo selective evolution, which is required for processes like metastasis and resistance to anticancer therapies[33,34]. For this reason, the genomic imbalances caused by aneuploidy may be relevant for tumor progression and may enhance even further the generation of more DNA structural alterations, causing a negative effect on patients' survival[5,41].

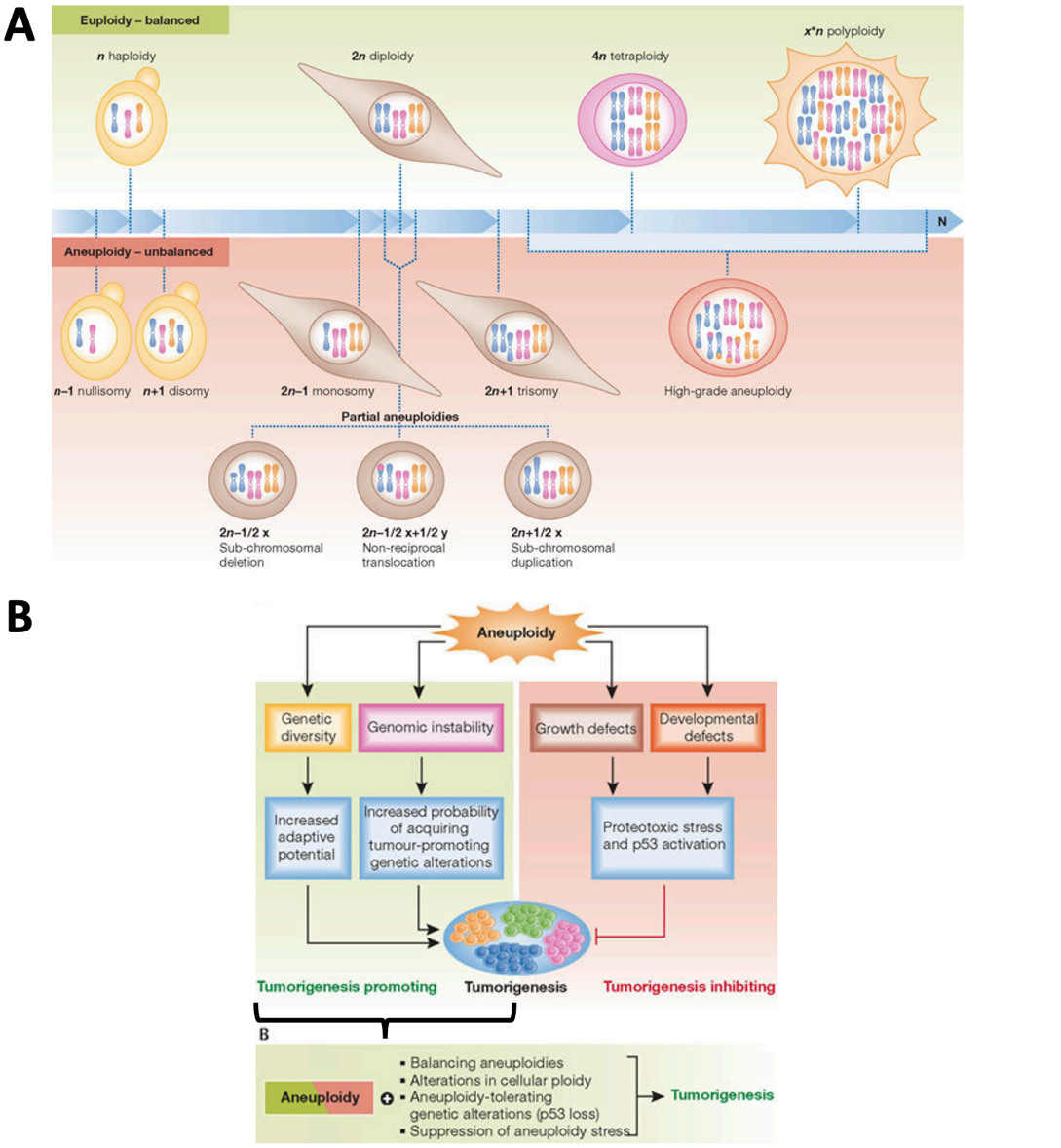

Figure 4 | Aneuploidy and its impact on tumorigenesis. (A) Aneuploidy is defined as a deviation from an euploid genomic state with a range of possible aberrant karyotypes. (B) Although aneuploidy is mostly associated with cellular stress and inhibition of tumorigenesis, specific conditions give aneuploid cells enhanced tumorigenic potential. Adapted from Pfau *et al.* EMBO Rep 2012[27].

1.3.3. Chromosomal rearrangements

Chromosomal rearrangements originate from a DNA break that is rejoined to another DNA segment that was not originally contiguous to the breakpoint. This results in the formation of **gene fusions**, which can be tumorigenic due to the overexpression of one of the genes involved or the generation of a fusion protein with oncogenic potential; for example, the rearrangement between *BCR* (in chromosome 22) and *ABL* (in chromosome 9) generates a fusion protein with constitutively activated *ABL* and a deregulated cell cycle[21].

1.4. The immune system in cancer

1.4.1. Infiltrating immune cells and the cancer-immunity cycle

A tumor can be defined as a heterogeneous mixture of resident host cells, infiltrating cells, secreted factors and extracellular matrix. Of those, the tumor microenvironment (TME) includes the immune cells, stromal cells, blood vessels and extracellular matrix surrounding tumor cells[42]. During tumor growth, a dynamic interaction between tumor cells and the TME is established to support the survival of cancer cells, local invasion and metastatic dissemination[43].

The function of the immune system in the context of cancer is to detect and eliminate tumor cells as non-self-entities[42]. Depending on the specificity of the response, anti-tumor immunity can be classified into innate and adaptive. **Innate immune cells**, composed of natural killer (NK) cells, eosinophils, basophils, and phagocytic cells, including macrophages, monocytes, mast cells, neutrophils and dendritic cells (DCs), participate in tumor suppression either by directly killing tumor cells or by triggering adaptive immune responses[43–45]. Conversely, the **adaptive immune cells** are lymphocytes, which can orchestrate a response against tumor cells based on the identification of tumor-specific antigens (or neoantigens), which are novel peptide sequences induced by the accumulation of somatic mutations[44]. Lymphocytes can be split into B cells, which play a role in humoral immune responses (the generation of antibodies against tumor neoantigens), and T cells, involved in cell-mediated immune responses[46–48].

To escape immune surveillance, tumors modify the composition and phenotype of infiltrating immune populations to diminish the effects of tumor-antagonizing cells and favor the activity of tumor-promoting cells. **Table 1** summarizes the functions of the main pro- and anti-tumor immune cells.

Table 1 | Main protumor and antitumor immune cell types. [42–49]

Effect	Cell types	Roles in cancer
Tumor-antagonizing	**CD8+ Cytotoxic T lymphocytes (CTLs)**	Identification and killing of tumor cells presenting target neoantigens through FasL-mediated apoptosis. Secretion of IFN-γ and TNFα to induce cytotoxicity in cancer cells.
	CD4+ T helper lymphocytes	Secretion of IL-2 to promote CTL proliferation, cross-presentation of tumor antigens to CTLs and secretion of costimulatory molecules to shape CTL phenotypes.
	B cells	Formation of tertiary lymphoid structures (TLS), antibody production, antigen presentation to T cells, production of IFN-γ.
	NK cells	Tumor cell killing inducing apoptosis via perforin and granzyme production. Secretion of proinflammatory chemokines (e.g. IFN-γ, TNF, IL-6).
	Dendritic cells (DC)	Antigen presentation to T cells and generation of costimulatory signals for T cell activation. Initiators of adaptive immune responses.
	M1-polarized tumor-associated macrophages (TAMs)	Production of pro-inflammatory cytokines and reactive oxygen species (ROS) for tumor cell killing.
	N1-polarized tumor-associated neutrophils (TANs)	Release of granules with cytotoxic compounds. Secretion of pro-inflammatory cytokines and chemokies.
Tumor-promoting	**CD4+ Regulatory T cells (Tregs)**	Prevention of an effective antitumor immune response through multiple mechanisms, including suppression of CD8+ T cells via TGF-β and IL-10 signaling.
	Myeloid-derived suppressor cells (MDSCs)	Enhancing angiogenesis through the production of MMP9, prokineticin 2 and VEGF. Induction of cancer cell migration towards endothelia (metastasis promotion). Inhibition of T cell function through the production of arginase, iNOS, TGF-β and IL-10.
	M2-polarized tumor-associated macrophages (TAMs)	Production of anti-inflammatory cytokines (e.g IL-4, IL-10, IL-13). Induction of angiogenesis (VEGF production) and extracellular matrix (ECM) remodeling to promote tumor progression and metastasis. Morphologically similar to monocytic MDSCs (M-MDSCs).
	N2-polarized tumor-associated neutrophils (TANs)	Promotion of tumor growth and invasion through ECM modification via matrix metalloprotease-9 (MMP-9) and angiogenesis via VEGF. Morphologically similar to polymorphonuclear MDSCs (PMN-MDSCs).
	B cells	Production of cytokines to recruit MDSCs and inhibit CTL function (e.g. IL-10 and TGF-β).

Considering the immune actors above, effective killing of cancer cells by the adaptive immune system is dependent on the completion of a multi-step process called the **cancer-immunity cycle**, encompassing the following (**Figure 5**): (1) tumor-specific neoantigens are captured by antigen-presenting cells (APCs, mostly DCs) for processing if they receive positive proinflammatory signals (chemokines and other factors from dying tumor cells); (2) APCs present the antigens to T cells (via major histocompatibility complex molecules, MHCs, binding T-cell receptors, TCRs); (3) effector T cells are primed and activated against the cancer-specific antigens in lymph nodes; (4) effector T cells traffic into the tumor; (5) infiltrate into the tumor; (6) specifically recognize tumor cells expressing their cognate antigen through the interaction between TCR and MHC-I expressed by cancer cells; and (7) kill the target tumor cell, releasing more tumor antigens to be recognized by APCs and continuing the cycle[50]. Of note, the innate immune system is crucial for the maintenance of this cycle and can amplify

the immune response: innate immune cells participate in the T cell priming, expansion and infiltration at the tumor site, in addition to having a direct tumoricidal effect (phagocytosis and cytotoxicity)[45].

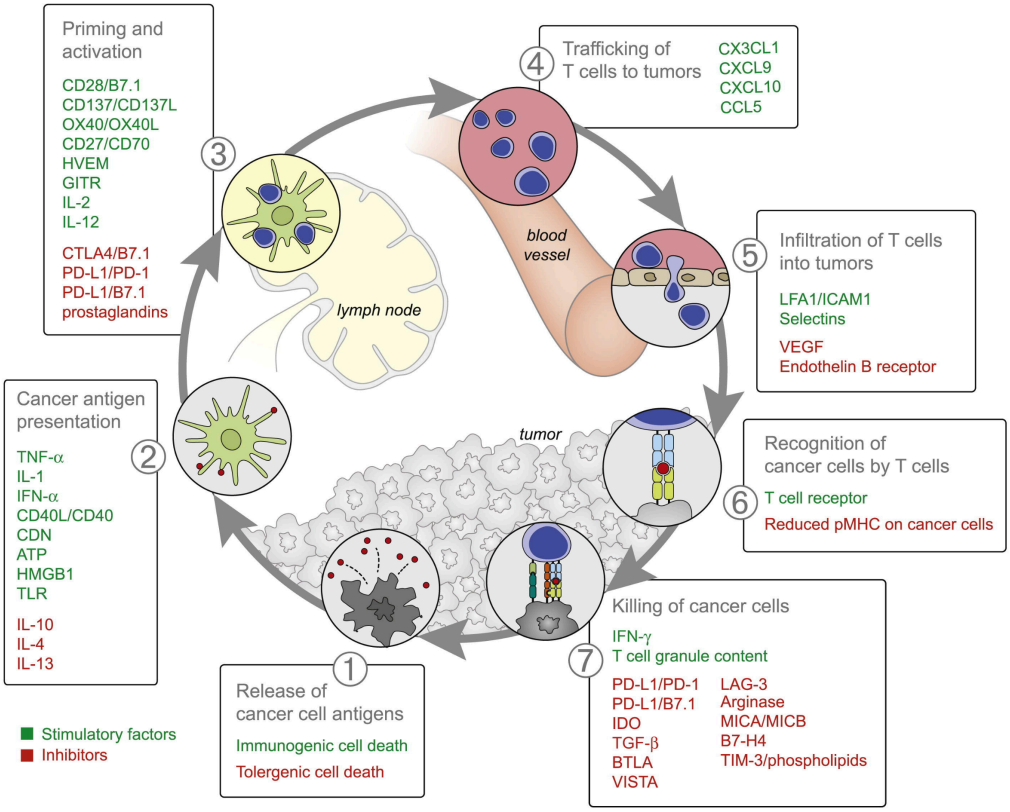

Figure 5 | The cancer-immunity cycle, with associated stimulatory and inhibitory factors. Obtained from Chen *et al.* Immunity 2013[50].

1.4.2. Mechanisms of immune evasion in cancer

In optimal conditions, innate and adaptive immunity cooperate to detect the presence of a developing tumor and destroy it before it is clinically apparent. However, rare tumor cell variants may have acquired the ability to overcome immune recognition and/or destruction and survive the anti-cancer immunity processes to ultimately become a progressively growing tumor[51]. The **cancer immunoediting** is a conceptual framework that integrates the mechanisms by which the immune system affects cancer development and progression. It includes the processes of **elimination** of new tumor cells, **equilibrium** involving the survival of rare tumor cell variants, and **escape** of immunosurveillance to generate a full-blown tumor[51].

In cancer patients, the cancer-immunity cycle does not function optimally. The mechanisms that tumors utilize to evade immunosurveillance are multiple and can be linked to every step of the cycle (**Figure 5**)[50]. Regarding cancer antigen presentation (steps 1-2 in **Figure 5**), tumors can **modulate the phenotype of DCs to interfere with their function and maturation**, and therefore with an effective presentation of antigens to T cells. They can do so by releasing soluble factors like VEGF, IL-10, TGF-β, M-CSF and IL-6, and through physiological stimuli like hypoxia and lactic acid in the TME[50,52]. **Impeding the trafficking of cytotoxic T cells (CTLs) to tumors** (step 4) can be achieved by the disruption of T cell-attracting chemokines produced in the TME, such as CCL2, CCL3, CCL4, CCL5, CXCL9, CXCL10 and CXCL11[53]. Tumors can also **block CTL extravasation and infiltration into tumors** (step 5), which requires their adhesion to the vascular endothelium, through the release of angiogenic molecules (e.g. VEGF, basic fibroblast growth factor -bFGF-, endothelins) that downregulate adhesion molecule expression on endothelial cells (e.g. intercellular adhesion molecule-1, ICAM-1, and vascular cell adhesion molecule, VCAM-1)[54,55]. Once CTLs reach the tumor bed, they encounter multiple obstacles before reaching the target tumor cell. Tumors can **recruit and induce local expansion of immune suppressive cells**, like $CD4^+$ Treg cells and MDSCs. Tregs suppress CTL expansion and cytokine secretion (IFNγ, TNFα) nonspecifically through the secretion of soluble mediators (TGFβ, IL-10, and IL-35), the generation of adenosine and cytolysis via TRAL and granzyme B, while also inducing DC immunotolerant phenotypes[56]. MDSCs, in turn, contribute to CTL suppression by arginase I, reactive oxygen species (ROS), IL-10, and TGFβ production[57]. CTLs also face the **expression of surface molecules by tumor cells inducing cell death** (FasL, TRAIL)[58] and attenuation of their function due to **deprivation of metabolic substrates** via competitive consumption by the tumor and hypoxic and acidic conditions of the extracellular medium[52,59,60]. After overcoming the barriers of the tumor vasculature and stroma, T cells need to recognize cancer cells presenting antigens via major histocompatibility complex (MHC) molecules (step 6). Many tumors **eliminate the presentation of neoantigens through MHC molecules** through loss of expression or downregulation of such molecules, which can be achieved by selective pressure from mutation, genetic loss, or epigenetic silencing of expression[52,61].

Finally, a common mechanism of many tumors to **avoid T cell priming and activation** (step 3) **and killing of cancer cells** (step 7) is to **induce the expression of immune suppressive**

checkpoint molecules in tumor cells and leukocytes (**Figure 6**)[52], with the goal to overcome the co-stimulatory signals that are needed on top of the MHC-TCR interaction to induce effector T cell activity. Among other immune checkpoints, cytotoxic T lymphocyte associated antigen 4 (CTLA4) predominantly acts as a regulator of $CD4^+$ T cell priming in the lymph nodes (step 3 of the cancer immune cycle) and enhances the Treg cell ability to suppress effector $CD8^+$ T cell function[62]. In parallel, given that activated T cells express the co-inhibitory receptor programmed cell death protein 1 (PD1), tumors promote the expression of its ligand PD-L1 by tumor and stromal cells; this promotes an exhausted state of T cells, becoming functionally disabled (Steps 6-7). The identification of these molecules has led to the development of immune checkpoint inhibitors (ICIs), cancer immunotherapies interrupting these immunosuppressive interactions and restoring the ability of T cells to eliminate antigen-expressing cancer cells[52,62].

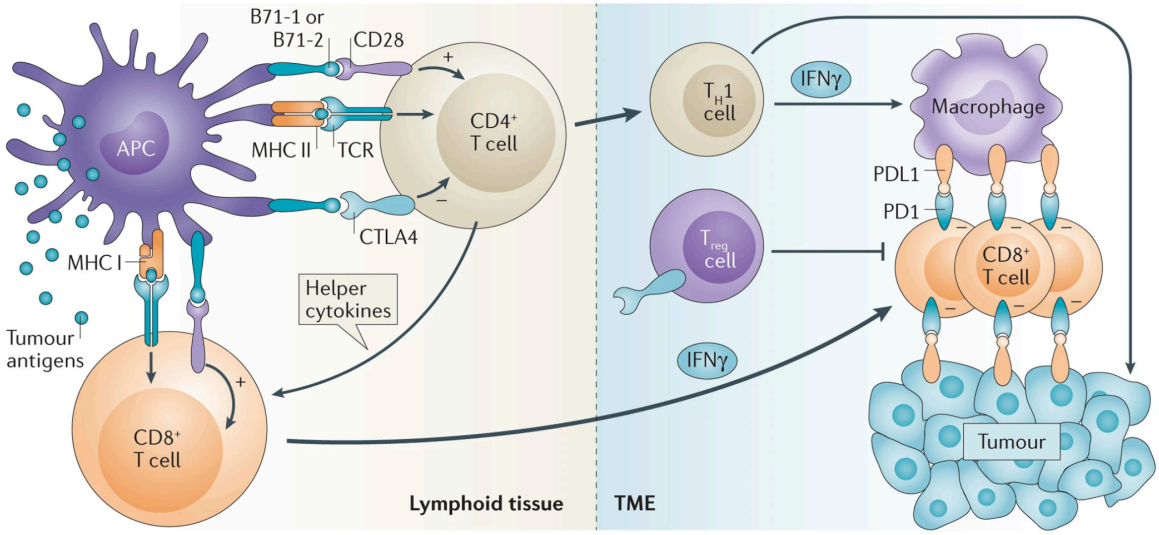

Figure 6 | The role of the immune checkpoints PD1 and CTLA4. $CD8^+$ T effector (Teff) cells are thought to be the major type of immune cell affected by the programmed cell death protein 1 (PD1) immunosuppressive checkpoint pathway. In contrast, cytotoxic T lymphocyte associated antigen 4 (CTLA4) predominantly regulates the activity of both effector and regulatory (Treg) $CD4^+$ T cell subtypes. Obtained from Topalian *et al.* Nature Reviews Cancer 2016[62].

1.4.3. Evidence of correlation between CNAs and immune evasion

Chromosomal instability (CIN) is the source of a variety of copy-number alteration (CNA) profiles among tumor cells inside a tumor. In turn, these CNAs can have large phenotypic impacts through the alteration of the expression of many genes[63]. Such intratumor heterogeneity, in face of the selective pressure exerted by the immune system, could allow

the selection of subclones with specific alterations in immune-related genes or with deletions in immunogenic neoantigens[64,65]. Pan-cancer evaluations of the impact of CNAs on the hallmarks of cancer revealed that distinct types of aneuploidy impact differently the cancer transcriptomic profiles: while -in general- the genomic loads of focal CNAs are linked to proliferation markers and affect strongly patient survival, broad CNAs are associated with a reduced cytotoxic immune infiltrate[4,5,63]. Moreover, in highly aneuploid melanomas, broad CNAs are associated with poor responses to immunotherapy[5,66,67]. The mechanistic rationale behind the association of broad CNAs with immune escape remains unresolved, although multiple candidate mechanisms have been proposed, including aneuploidy causing specific losses in immune-related genes[13], aneuploidy-derived proteotoxic stress weakening tumor antigen presentation on MHC molecules[5,68] or global demethylation helping to reduce aneuploidy-induced immunogenicity[12]. Although the association of CNAs with immune evasion has been described in multiple cancer types, the present thesis aimed to thoroughly define the impact of CNA burdens on HCC molecular and immune features given the limited evidence available for this cancer type.

1.4.4. Neutrophils and cancer

Neutrophils are key mediators of the innate inflammatory response as the first effector cell to reach an inflammation site, exerting antimicrobial and inflammatory functions through phagocytosis, degranulation, release of neutrophil extracellular traps (NETs) and antigen presentation[69]. Until recently, they were overlooked in cancer pathogenesis as their lifespan was believed to be too short (7-10h in blood) to have an important effect[10]. However, they accumulate in the peripheral blood of advanced-stage cancer patients and a high circulating neutrophil-to-lymphocyte ratio (NLR>5) is a robust biomarker of poor outcome in many cancers[70–72].

To date, only limited evidence is available on the phenotype and function of intratumor neutrophils (or tumor-associated neutrophils, TANs) in patients with cancer, and data is mostly restricted to early stages of the diseae[10,71]. Although TANs have been associated with poorer outcomes in a pan-cancer basis[73], this seems to vary across cancer types and to depend on neutrophil location (intratumoral or peritumoral)[74–76] and tumor stage[77,78]. The

hypothesis that local molecular cues from different tumor regions or disease stages may modulate neutrophil phenotypes could explain this observation[71]; for example, it has been proposed that the invasive tumor front dominated by TGF-β signaling and peritumoral GM-CSF and TNF signaling can induce neutrophil pro-tumor phenotypes in colorectal and hepatocellular carcinomas[79,80].

Initial evidence of TAN functions in mouse models of cancer revealed that neutrophils have a phenotypic plasticity that depends on specific features of the TME: in a TGF-β-rich environment, neutrophils acquire a pro-tumor "N2" phenotype[81], while interferon signaling and TGF-β depletion polarize them towards an anti-tumor "N1" phenotype[81–83] (**Table 1**). In mouse and in human, these phenotypic changes are based on shifts in the expression patterns of multiple cytokines, chemokines, adhesion molecules and granule-associated proteins; since N1-N2 are extremes of a wide spectrum of intermediate phenotypes[71,78], the identification of robust markers is difficult. Nevertheless, upregulation of CCL17 (Treg chemoattractant), arginase (promoting T cell inhibition) and matrix metalloproteinase 9 (MMP9, promoting angiogenesis) are linked to N2 neutrophil functions[84–86]. In contrast, the N1 phenotype correlates with an enhanced capacity to degranulate, to produce pro-inflammatory cytokines and chemokines, to activate adaptive immunity acting like an APC (expressing MHC-I and MHC-II molecules), and to induce direct cell killing through increased oxidative burst and phagocytosis[71,78].

Given their plasticity and capacity to interact with other innate and adaptive immune cell populations, clinically targeting TANs to suppress them or modulate their phenotype may shed light on their role in cancer and reveal novel immunotherapeutic approaches[10,71].

2. Hepatocellular carcinoma

2.1. Epidemiology and risk factors of HCC

Primary liver cancer is the sixth most diagnosed cancer and the third leading cause of cancer-related death worldwide, with approximately 906,000 new cases and 830,000 deaths reported in 2020[1] (**Figure 7A**). Moreover, by 2025 its incidence is expected to raise to >1 million individuals[2]. **Hepatocellular carcinoma (HCC)** is the most common form of primary liver cancer accounting for around 90% of cases[2]. Incidence and mortality rates are the highest

in East Asia and Africa, although they are increasing in different parts of Europe and the USA[2]; in fact, HCC has been reported as the fastest increasing cause of cancer-related death in the USA since the early 2000s[87].

Around 90% of HCC cases arise in the setting of an underlying chronic liver disease, and cirrhosis from any etiology is the strongest risk factor for HCC. The major risk factors generating chronic liver damage are chronic alcohol consumption, diabetes or obesity-related NASH and viral infection by HBV or HCV; other less-prevalent risk factors are cirrhosis induced by primary biliary cholangitis, haemochromatosis and α1-antitrypsin deficiency[2]. As depicted in **Figure 7B**, the global distribution of the major risk factors is heterogeneous and explains the regional differences in the burden of HCC:

- **Hepatitis B virus (HBV)** infection accounts for ~60% of cases in Asia and Africa, is the leading etiology in South America and is less prevalent (~20% of cases) in Western countries. As a DNA virus, HBV can induce insertional mutagenesis, integrating into the host genome and activating oncogenes; this can lead to the onset of HCC in the absence of cirrhosis in a subset of cases[2,88].

- **Hepatitis C virus (HCV)** infection is the most common etiology in North Africa, Western Europe, North America and Japan. HCV is an RNA virus which does not integrate into the host genome; thus, the risk of HCC is derived from the induction of chronic inflammation leading to cirrhosis or chronic liver damage. Although there have been dramatic improvements in HCV treatment during the last 5 years with the new direct-acting antiviral agents, causing >90% of sustained virologic responses (SVR), there is over 2% of patients with HCV-induced cirrhosis that continue to have a persistent risk of HCC even after SVR[2].

- **Non-alcoholic steatohepatitis (NASH)** is a rapidly increasing risk factor predicted to become predominant in high income regions in the near future. Currently, it represents ~15-20% of cases in the West. It is a form of **non-alcoholic fatty liver disease (NAFLD)**, a term that encompasses a range of chronic liver disease forms that mostly occur in people with diabetes mellitus and obesity. NAFLD ranges from only excessive hepatocyte triglyceride accumulation (non-alcoholic fatty liver) to **NASH**, defined as a

non-alcoholic fatty liver plus inflammation and hepatocyte injury. Of note, 25-30% of NASH-HCCs occur in the absence of cirrhosis[2].

- **Alcohol abuse** is the leading etiology in Central and Eastern Europe. Excessive alcohol intake leads to alcoholic liver disease, cirrhosis and HCC. Alcohol can also interact with other HCC risk factors like viral hepatitis or diabetes. The potential pro-carcinogenic mechanisms of alcohol include the mutagenic effects of acetaldehyde and the production of ROS due to excessive hepatic iron deposition[2,89].

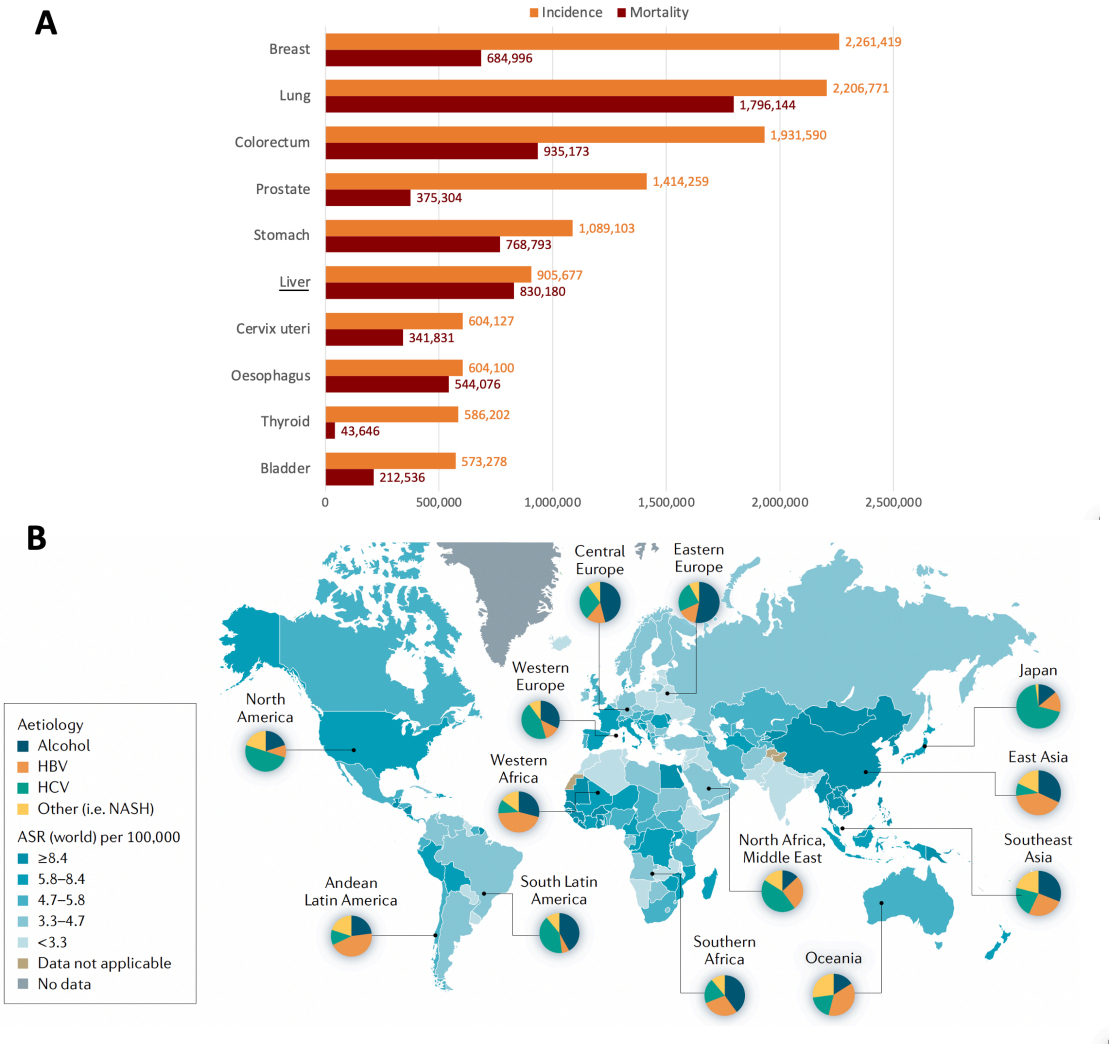

Figure 7 | Epidemiology and risk factors of liver cancer and HCC. (A) Estimated number of liver cancer incident cases and deaths worldwide, in both sexes and all ages (top-10 most incident cancers in 2020). **(B)** Incidence of HCC according to geographical area and etiology. Modified from Sung H *et al.*, Cancer J Clin 2021[1] and Llovet JM *et al.*, Nat Rev Dis Prim 2021[2].

Moreover, especially in cirrhotic patients, **age** and **gender** are sociodemographic factors which have also been linked to the risk of HCC: individuals over 70 years old have the highest HCC incidences, and the **male predominance** of HCC is evident with a male-to-female ratio of 3:1[2].

Finally, some carcinogenic **cofactors** can increase the risk of HCC in the presence of other risk factors: **tobacco smoke; aflatoxin B1**, which synergizes with HBV to induce HCC and is a common food contaminant in Southeast Asia and Sub-Saharan Africa; and **aristolochic acid**, frequently used in Asian traditional medicine[90,91].

2.2. Molecular pathogenesis of HCC

HCC development is a multistep process where **genetic** factors interact with **environmental** exposures. The early steps of hepatocyte malignant transformation rely upon the co-ocurrence of multiple elements, including a genetic predisposition, reciprocal interactions between viral and non-viral risk factors, the cellular microenvironment and the severity of the underlying chronic liver disease[2]. In fact, ~80% of HCCs develop in a cirrhotic background following a sequence of histopathological phases from the emergence of pre-cancerous dysplastic nodules (low-grade dysplastic nodules, LGDNs, and high-grade dysplastic nodules, HGDNs) which can turn into early-stage HCC and continue developing into more advanced stages, accumulating genetic and microenvironment alterations[91]. On the other hand, ~20% of HCCs develop in the context of a chronic liver disease without cirrhosis; this can be caused, for example, by insertional mutagenesis of the HBV genome or by malignant transformation of hepatocellular adenoma[92,93]. Of note, the cell of origin of HCC is debated between transformed mature hepatocytes, liver stem cells and transit-amplifying cell populations[2,91,94].

2.2.1. Molecular landscape of HCC

Evidence from recent translational genomic studies enabled the description of the molecular landscape of HCC. On average, HCC tumors present 40-60 somatic point mutations, most of which are *passengers*; however, some of them are *drivers* and occur in genes that play a role in tumor progression[95] (**Table 2**). The most mutated driver gene in HCC is ***TERT*** (~60%), followed by ***CTNNB1*** and ***TP53*** (~29% and ~27%, respectively). These three alterations

constitute the most frequent trunk events in HCC, mutations arising at early stages of carcinogenesis and being ubiquitous across all tumor regions[96,97]. In addition to these, focal copy-number alterations are also recurrent in HCC, mostly gains in 8q24.21 affecting *MYC* (12%) and 11q13.3 involving -among others- *CCND1* and *FGF19* (6-7%), as well as losses in 9p21.3 involving *CDKN2A* (2%)[95] (**Table 2**).

Table 2 | Key oncogenic drivers and pathways de-regulated in HCC

Altered pathway	Altered gene	Type of alteration	% prevalence in HCC (range)
Telomere maintenance	*TERT*[a]	Promoter-activating mutation	55 (44–59)
		High-level focal amplification	6 (1–9)
		Viral insertion	3 (1–5)
Cell cycle regulation	*TP53*[a]	Loss-of-function mutation	27 (18–31)
		Homozygous deletion	2 (0–2)
	ATM	Loss-of-function mutation	4 (2–5)
	RB1	Loss-of-function mutation	4 (3–5)
		Homozygous deletion	5 (4–6)
	CDKN2A	Loss-of-function mutation	2 (1–3)
		Homozygous deletion	5 (4–6)
	MYC	High-level focal amplification	12 (4–18)
	CCND1[a]	High-level focal amplification	7 (5–7)
WNT–β-catenin signaling	*CTNNB1*[a]	Activating mutation	29 (23–36)
	AXIN1	Loss-of-function mutation	7 (4–10)
	APC	Loss-of-function mutation	2 (0–3)
Chromatin remodeling	*ARID1A*	Loss-of-function mutation	8 (4–12)
	ARID2	Loss-of-function mutation	7 (3–10)
	KMT2A	Loss-of-function mutation	3 (0–4)
	KMT2C	Loss-of-function mutation	3 (2–5)
	KMT2B	Loss-of-function mutation	2 (0–4)
	BAP1	Loss-of-function mutation	2 (0–5)
	ARID1B	Loss-of-function mutation	1 (0–3)
Ras–PI3K–mTOR	*RPS6KA3*	Unclassified	4 (3–6)
	PIK3CA[b]	Activating mutation	2 (1–4)
	KRAS[b]	Activating mutation	1 (0–1)
	NRAS	Activating mutation	0 (0–1)
	PDGFRA[b]	Mutation	1 (0–4)
	EGFR[b]	Activating mutation	1 (0–2)
	PTEN	Loss-of-function mutation	1 (0–2)
FGF signaling	*FGF19*[b]	High-level focal amplification	6 (5–6)
VEGF pathway	*VEGFA*[b]	High-level focal amplification	5 (1–8)
Oxidative stress	*NFE2L2*[c]	Activating mutation	4 (2–6)
	KEAP1[c]	Activating mutation	3 (2–5)
Hepatocyte differentiation	*ALB*	Mutation	9 (5–13)
	APOB	Mutation	8 (1–10)
JAK–STAT	*IL6ST*	Mutation	2 (0–3)
	JAK1[a]	Mutation	1 (0–3)
TGF-β signaling[a]	*ACVR2A*	Loss-of-function mutation	4 (1–10)
IGF signaling[a]	*IGF2R*	Mutation	1 (0–2)

IGF, Insulin Growth Factor; mTOR, mammalian Target of Rapamycin; STAT, Signal Transducer and Activator of Transcription; TGFβ, Transforming Growth Factor β. [a]Targetable by a drug in testing phases. [b]Targetable by an FDA-approved drug. [c]Targetable by mTOR inhibitors in testing phases. Adapted from Llovet JM *et al*., Nature Cancer Reviews 2022.

As a result of the recurrent alterations in the TERT promoter, ~80% of HCCs display overexpression of telomerase and therefore enhanced **telomere maintenance**, avoiding senescence and cell death due to telomere shortening[40,95,97]. Around 30-50% of cases display an oncogenic **activation of the Wnt-β-catenin pathway**, caused by activating mutations in *CTNNB1* or inactivating mutations/deletions in *AXIN1* or *APC*[40,95,98,99]. Other frequent alterations are responsible for **altering cell cycle control** (such as those in *TP53*, *RB1*, *CCND1*, *CDKN2A*, *MYC* or *ATM*), cause **epigenetic modifications** (loss-of-function alterations in *ARID1A*, *ARID2*, *KMT2A* and *KMT2C*), induce a **deregulation of the oxidative stress pathway** (activating *NFE2L2*, *KEAP1*) and **activate the oncogenic tyrosine kinase receptor-RAS-PI3K signaling**, either directly (e.g. loss-of-function mutations in *RPS6KA3* and *PTEN*, activating *PIIK3CA*, *FGF19* amplification and scarce RAS family gene alterations) [40,95,98,99] or indirectly through upstream signaling from the insulin growth factor (IGF) pathway (*IGF2R*)[100]. Of note, additional mutated genes in HCC are involved in the **JAK/STAT signaling** (*IL6ST*, *JAK*), **TGF-β signaling** (*ACVR2A*) and **hepatocyte differentiation** (*ALB*, *APOB*).

Surprisingly, of the 34 most mutated genes in HCC (**Table 2**), only 6 are targetable by an FDA-approved drug and another 8 are being assessed in early phase trials[91]. Two clear examples of targetable mutations are the high-level focal amplifications in 11q13 (6%) and 6p21 (5%), leading to FGF19 and VEGFA overexpression, respectively. In the first case, the anti-tumoral benefit of a fibroblast growth factor receptor 4 (FGFR4) inhibitor was demonstrated at the clinical level in HCCs with FGF19 overexpression[101,102]. In the second case, although drugs targeting VEGFA (bevacizumab) or VEGFRs (regorafenib, cabozantinib, lenvatinib) are available, there is no specific information on specific clinical benefits for patients with VEGFA amplification[91]. This highlights the unmet need for effective treatment for HCC and/or biomarker definition to identify patients responding to available therapies.

2.2.2. Mutational signatures in HCC

During chronic liver damage, cirrhosis and hepatocarcinogenesis, hepatocytes accumulate genetic mutations which follow distinct patterns that are dependent on the driving mutational mechanism of each tumor. Such patterns can be represented through the **mutational signatures** and in certain cases they have been linked to exposures to particular

environmental risk factors or endogenous cellular processes[103]. In HCC, DNA sequencing analyses have revealed enrichments in specific mutational signatures from the catalog of somatic mutations in cancer (COSMIC): signatures SBS1 and SBS5 are common and reflect clock-like mutations accumulating over successive cell divisions with age; SBS16 has been linked to alcohol intake; SBS4 and SBS29, to tobacco smoking; and SBS22 and SBS24 are linked to aristolochic acid and aflatoxin B1 exposures and are found mostly in Asian and African patients, respectively[95,103,104]. These observations reflect the role of the liver in detoxifying multiple metabolites, which can damage the genome of hepatocytes[2].

2.2.3. Molecular classification of HCC

The integration of genomic, transcriptomic, epigenomic, histopathological and clinical data on HCC tumors has allowed the identification of different HCC molecular classes[98,105–110]. The most extended HCC molecular classification is based on the proliferation and the non-proliferation classes (~50% of cases each, **Figure 8**)[105].

- The **HCC proliferation class** includes tumors with mutations in TP53 and focal amplifications in the 11q13 locus (*FGF19* or *CCND1*), is more frequently found in HBV-associated HCC and has the worst prognosis. Chromosomal instability and global DNA hypomethylation represent additional hallmarks of this class. In its turn, it is subdivided into two subclasses[105,106]: the **Proliferation-progenitor cell subclass** or S2 (~25-30% of HCCs), including tumors with activated classic cell proliferation pathways (e.g. RAS-MAPK, PI3K-AKT-mTOR, MET and IGF signaling) together with progenitor cell markers (e.g. *EPCAM* and AFP); and the **Proliferation-Wnt-TGFβ subclass** or S1 (~20% of HCCs), which displays a non-canonical activation of the Wnt pathway.

- The **HCC non-proliferation class** or S3 accounts for 50% of patients and is more prevalent in alcohol and HCV-associated HCCs. It is characterized by less aggressive tumors, reduced vascular invasion, well-to-moderate histological differentiation and low AFP levels[111], as well as chromosomal stability and frequent *TERT* promoter mutations. At least two subgroups have been found within this class: the **Wnt-β-catenin *CTNNB1* subclass**, which presents frequent *CTNNB1* mutations and activation of the Wnt-β-

catenin pathway driving an immune excluded phenotype with low immune infiltration[112]; and the **Interferon subclass**, with a highly activated IL6-JAK-STAT signaling pathway, with a more inflamed tumor microenvironment[106].

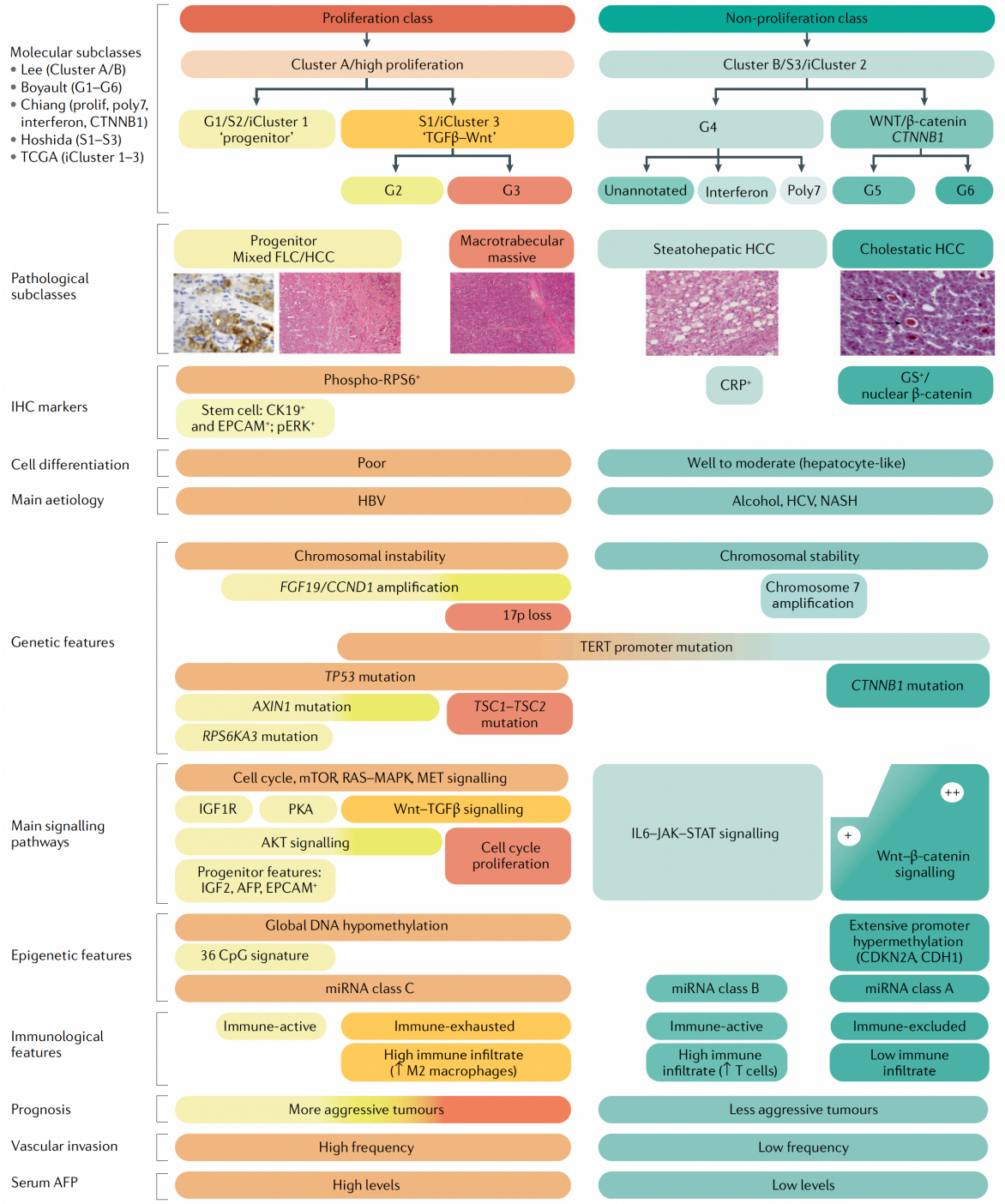

Figure 8 | HCC Molecular classification. Hepatocellular carcinoma can be subdivided into two major molecular classes based on their transcriptome, which are also associated with genomic, histopathological and clinical characteristics. FLC, fibrolamellar carcinoma; IHC, immunohistochemistry; FLC, TCGA, The Cancer Genome Atlas; AFP, α-fetoprotein; HBV, hepatitis B virus; HCV, hepatitis C virus; NASH, non-alcoholic steatohepatitis; miRNA, microRNA. Obtained from Llovet *et al.*, Nat Rev Dis Prim 2021[2].

2.3. Tumor microenvironment in HCC

2.3.1. Overview of immune cell infiltrate types

An altered microenvironment is a key enabling characteristic of cancer and is known to participate in all stages of malignant progression[2]. In HCC, the main cell types in the tumor immune infiltrate found to impact patient outcomes include:

- **$CD8^+$ cytotoxic T cells (CTLs)**: their association with better overall survival has been widely demonstrated in several cancer types, including HCC[113]. However, the search for additional markers to distinguish between CTL functional states has revealed some associations with treatment resistance. In human NASH, a subset of auto aggressive $CD8^+PD1^+$ T cells induce hepatocyte cell death, promote NASH pathogenesis and impair immune surveillance, thereby favoring HCC occurrence and progression[114]. In addition, the presence of terminally exhausted $CD39^{hi}$ TOX^{hi} $PD\text{-}1^{hi}$ CD8 T cells is linked to resistance to neoadjuvant PD1 blockade[115].
- **$CD4^+$ helper T cells**: the T_{H1} subtype and its related cytokines (e.g., IFN-γ) are linked to good clinical outcomes in HCC, while HCCs with aggressive features (vascular invasion and metastasis) upregulate T_{H2}-related cytokines (e.g., IL-4 and IL-10) [113,116].
- **Regulatory T cells (Treg)**: high tumor Treg infiltrate has been proposed as an independent prognostic factor for poor overall survival in HCC[116], and a high Treg to effector T cell ratio is associated with reduced clinical benefit of atezolizumab plus bevacizumab[117].
- **B cells**: despite being abundant in the TME and key players in the humoral adaptive immunity, there is no clear prognostic value for B cells.
- **Tumor-associated macrophages (TAMs)**: In HCC, TAMs arise from tissue-resident macrophages (Kupffer cells) or monocyte-derived macrophages that infiltrate the tumor[118]. TAM abundance has been linked to poor prognosis in HCC[119]; particularly, greater proportions of pro-tumor M2 macrophages (**Table 1**) have been linked to worse clinical outcomes in HCC[113,116,119].
- **Dendritic cells (DCs)**: subsets of DCs with distinct functions and morphology have been identified, including anti-tumoral type 1 DCs, and regulatory type 2 DCs.

- **Myeloid-derived suppressor cells (MDSCs)**: this heterogeneous population of immature and immunosuppressive myeloid cells has been found in increased numbers in tumor tissue and peripheral blood from patients with HCC, and elevated counts correlate with tumor progression[120,121].
- **Tumor-associated neutrophils (TANs)**: in HCC, multiple studies indicate that neutrophils, if present, are predominantly located in the peritumoral stroma rather than being intratumoral, although both intra- and peritumor TANs have been associated with poorer overall survival (OS)[71,76,80,86,122]. Single-cell RNA-seq characterization of TANs showed that $CCL4^+$ TANs can recruit TAMs and $PD\text{-}L1^+$ TANs can suppress T cell cytotoxicity.

2.3.2. Known mechanisms of immune evasion in HCC

Aside from the recruitment of suppressive immune populations and the known mechanisms of evasion in cancer seen above, specific signaling pathways linked to immune evasion are especially relevant in HCC. First, approximately 29% of HCCs display an activating mutation in the *CTNNB1* gene (**Table 2**), and the activation of the **Wnt/β-catenin** signaling pathway is a feature associated with the lack of immune infiltration[107,109]. Of note, in HCC the activation of β-catenin signaling downregulates the chemokines CCL4 and CCL5, which induce the infiltration of dendritic cells and T cells[112].

In parallel**, Wnt/TGF-β** signaling in HCC is linked to activation of the stroma and stromal deposition through fibroblast activity, T cell exhaustion with impaired cytotoxic activity and immunosuppressive components like M2 macrophages, upregulation of myeloid chemoattractants and downregulation of NK cell activators[108,109].

Furthermore, **VEGF** expression from HCC tumor cells has a pro-angiogenic effect and generates a pro-tumorigenic microenvironment favoring the recruitment of Tregs, MDSCs and TAMs and reducing the infiltration of CTLs and the function of DCs[123,124] (**Figure 9**). Therefore, inhibiting the VEGF/VEGFR pathway could help to enhance anti-tumor immunity in HCC[2,106,123].

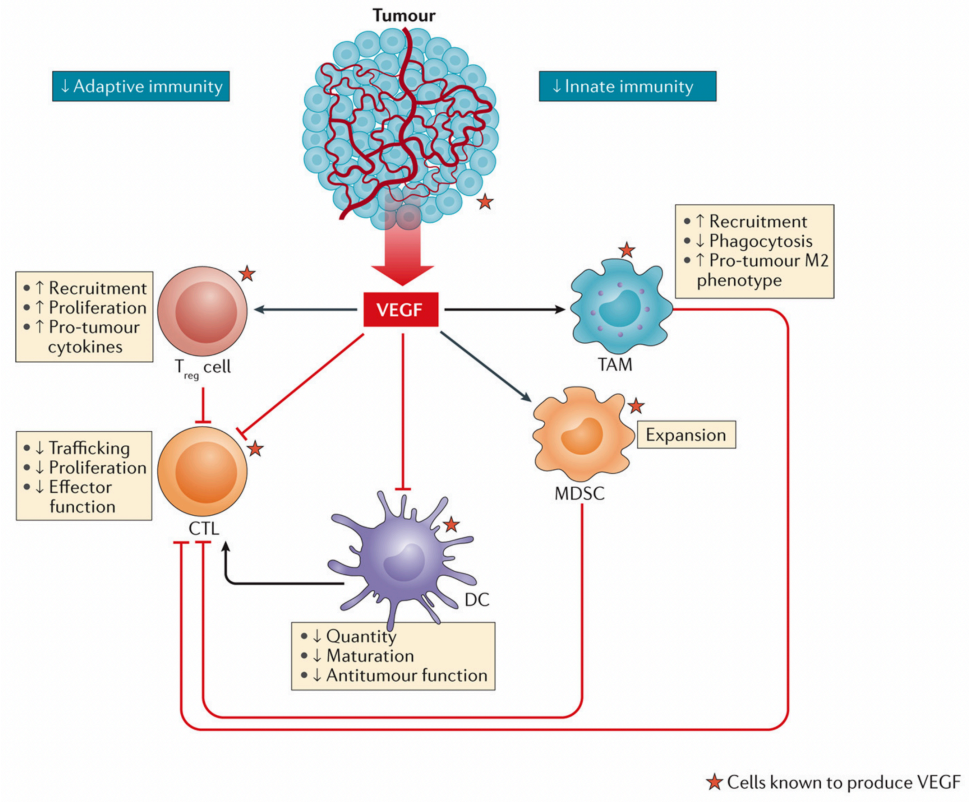

Figure 9 | VEGF pathway activation has direct effects on tumor-infiltrating immune cells. VEGF from tumor and immune cells promotes immunosuppressive functions of innate and adaptive immune cells. Modified from Fukumura *et al.* Nat Rev Clin Oncol 2018[123].

2.3.3. Immune classification and role of NASH etiology in HCC immune profiles

From the immunological standpoint, HCC can be classified into the **Inflamed class** and the **non-Inflamed class** [109]. The **Inflamed class** (~30-35% of HCCs, **Figure 10**) includes the **Immune class** (~25% of HCCs), which displays a high level of immune infiltration, PD1-PD-L1 signaling and enrichment in signatures of response to ICIs in other tumor types[108] (**Figure 10**). In turn, the Immune class can be subdivided into the **Immune Active** subclass, with elevated interferon signaling, expression of adaptive immune response genes and a favorable prognosis, and the **Immune Exhausted** subclass, with an activated stroma and high TGF-β signaling[108]. In addition, the Inflamed class also includes the **Immune-like** subclass, a subset of HCCs with unique features of strong interferon signaling and immune activation along with *CTNNB1* mutations[109]. Notably, Inflamed tumors were described to be enriched in HCC patients responding to anti-PD1/PD-L1 therapies[125] (**Figure 10**).

Regarding the ~65% of HCCs comprising the **Non-inflamed** class, two subclasses have been identified depending on the immune escape mechanism: an **Intermediate** class with *TP53* mutations, high chromosomal instability and deletions in interferon and antigen presentation machinery genes; and an **Excluded** class with *CTNNB1* mutations and immune desertification[109].

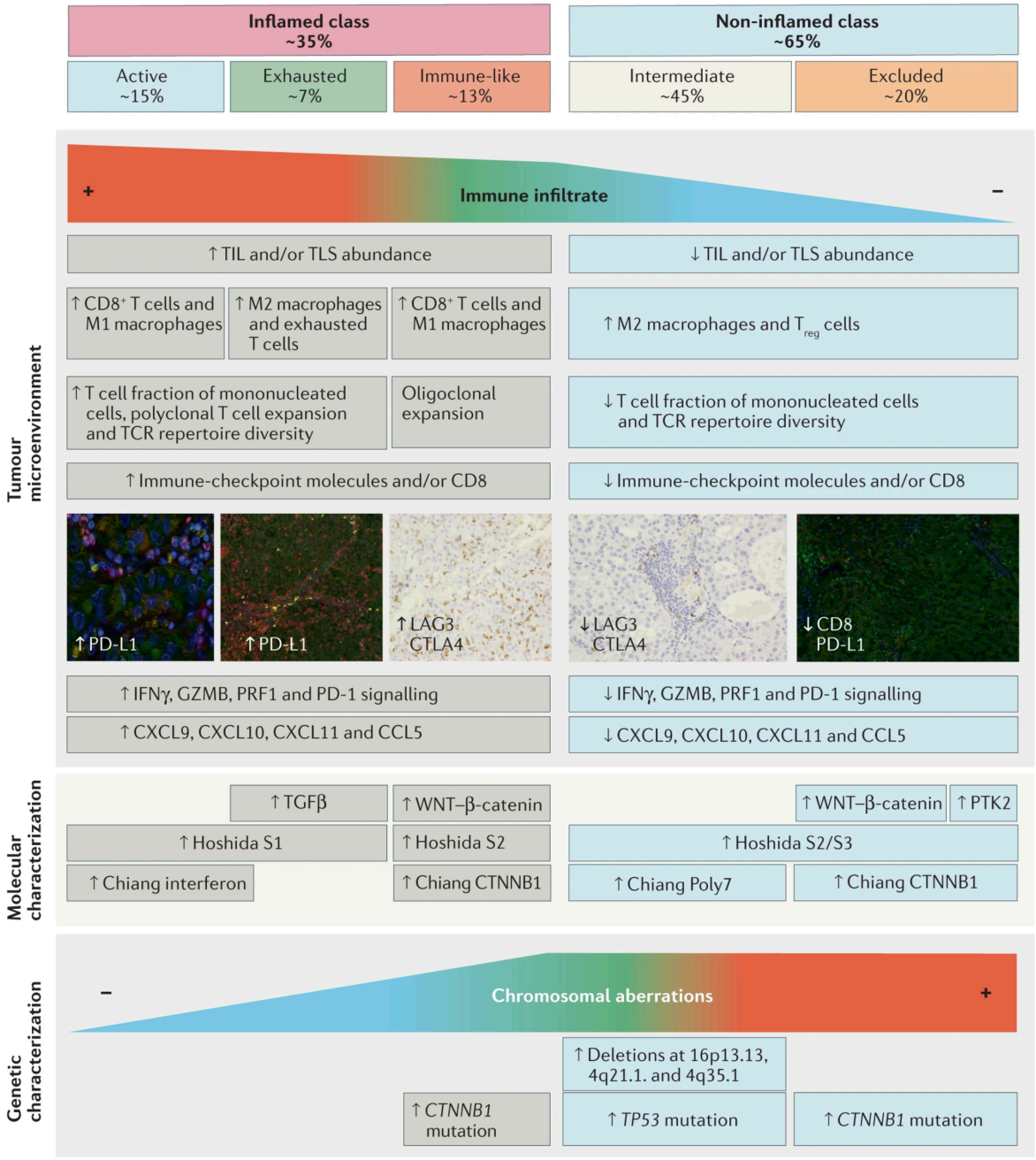

Figure 10 | HCC immune classification. Hepatocellular carcinoma can be classified based on immune-related features in the Inflamed class and the Non-inflamed class, with several subclasses based on specific immune activation or evasion mechanisms. TCR, T-cell receptor; TIL, tumor-infiltrating lymphocyte; TLS, tertiary lymphoid structure; Treg, regulatory T cell. Adapted from Llovet *et al.* Nat Rev Clin Oncol 2021[2].

Recent evidence from NASH-HCC studies revealed several particularities in the molecular and immune profiles of tumors from this etiology. NASH-related HCCs are enriched in inflammation-related signatures, Wnt-TGFβ signaling and immunosuppression features[126]. In fact, in the setting of human NASH, auto-aggressive $CD8^+PD1^+CXCR6^+$ T cells present in the liver induce hepatocyte cell death, enhance NASH pathogenesis and impair immune surveillance favoring HCC occurrence and progression with an immunotherapy-resistant tumor profile[9]. In fact, a meta-analysis with >1600 advanced HCC patients revealed that immunotherapy did not improve survival in patients with non-viral HCC [9].

2.4. Clinical management of HCC

2.4.1. Diagnosis, staging and management

Given that the subclinical course of HCC is prolonged, several surveillance protocols have been developed for early diagnosis among high-risk patients; these are based on liver nodule detection through abdominal ultrasound and its confirmation with non-invasive radiological approaches or liver biopsy[2]. Despite surveillance efforts, ~50% of cases globally are diagnosed at advanced stages, especially in developing countries. Since HCC develops in most cases (~80-90%) among cirrhotic patients, their overall health status is often limiting the therapeutic options. Currently, the most widely recognized clinical algorithm for the management of HCC is the Barcelona Clinic Liver Cancer (BCLC) staging system, which classifies patients into 5 stages based on disease extension, liver function and performance status, and links them to specific treatment recommendations (**Figure 11**)[2,90]. In summary, patients with a **very early HCC** (**BCLC 0**) are candidates for local curative treatments, including resection and ablation, and have low recurrence rates; those with **early HCC** (**BCLC A**) are candidates for the curative approaches of resection, ablation and transplantation, depending on liver-related variables, have high recurrence rates (~70% at 5 years) and a median survival beyond 60 months; **Intermediate HCC** cases (**BCLC B**) are amenable to transarterial chemoembolization, achieving survival rates of 26-30months; **advanced HCC** patients (**BCLC C**) are eligible for systemic therapies, including tyrosine kinase inhibitors (TKIs) and immune checkpoint inhibitors (ICIs), achieving survival rates of ~19 months; finally, **terminal HCC** patients (**BCLC D**) are given best supportive care.

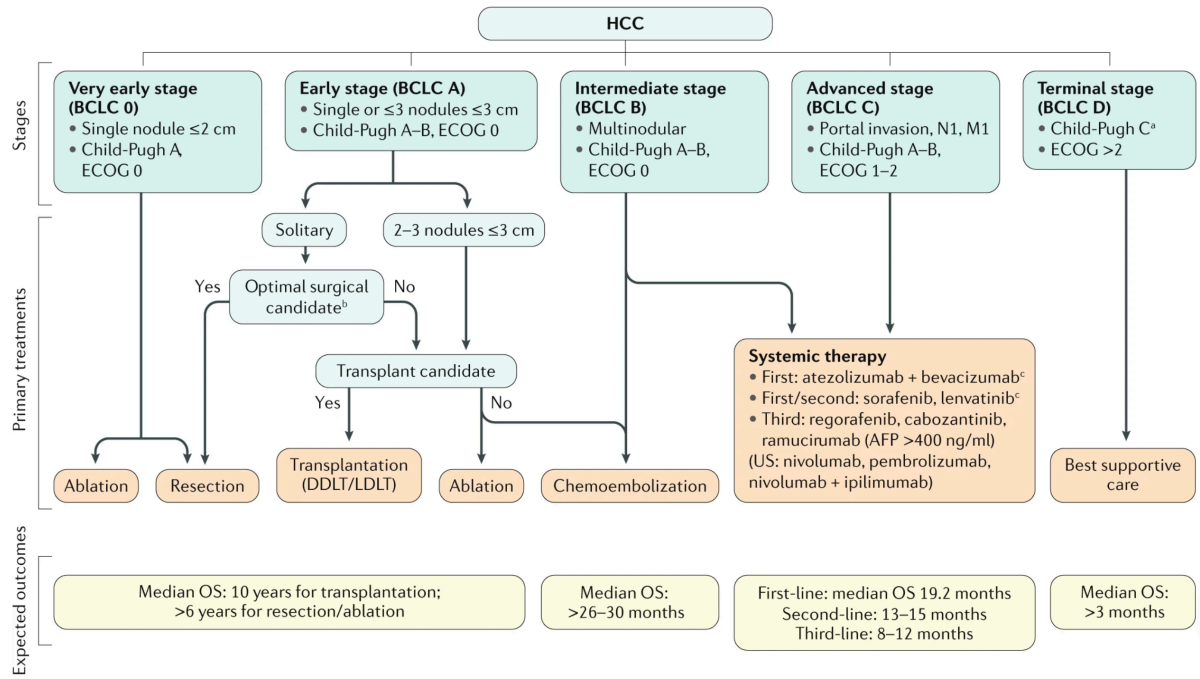

Figure 11 | The Barcelona Clinic Liver Cancer (BCLC) staging system. Clinical management algorithm using the BCLC classification, which is based on disease extension, liver function and performance status. AFP, α-fetoprotein; DDLT, deceased-donor liver transplantation; ECOG, Eastern Cooperative Oncology Group; HCC, hepatocellular carcinoma; LDLT, living-donor liver transplantation; M1, distant metastasis; N1, lymph node metastasis; OS, overall survival; RCT, randomized controlled trial; TACE, transarterial chemoembolization. [a]Patients with end-stage liver disease Child-Pugh class C should first be considered for liver transplantation. [b]Patients with preserved hepatic function Child-Pugh class A with normal bilirubin and no portal hypertension are optimal candidates for hepatic resection. [c]Sorafenib and lenvatinib are also considered first-line treatment in case of contraindication for atezolizumab + bevacizumab. Obtained from Llovet *et al.* Nat Rev Clin Oncol 2021[2].

2.4.2. Systemic therapies and biomarkers of response in HCC

It is estimated that ~50-60% of HCC patients will ultimately be exposed to systemic therapies during their lifespan[127]. Of the patients receiving systemic therapies, ~50-70% are progressing from surgery or locoregional therapies, while ~30-50% are treatment naïve[128].

The landscape of systemic therapies in HCC is based on two kinds of agents: receptor tyrosine kinase inhibitors (TKIs) and immune-checkpoint inhibitors (ICIs)(**Figure 12**). The first systemic therapy to be approved in HCC as a first-line drug for advanced cases was the TKI **sorafenib** in 2008, after the breakthrough SHARP trial demonstrating an overall survival (OS) benefit compared to placebo (median of 10.7 versus 7.9 months) [129]. Ten years later, the TKI **lenvatinib**, with a higher potency blocking VEGF receptors and the FGFR family, demonstrated non-inferiority compared to sorafenib (median OS of 13.6 versus 12.3 months)[130].

In the second line setting, the TKIs **regorafenib**, **cabozantinib** and **ramucirumab** have been approved for the treatment of HCC patients progressing to sorafenib[131–133]: regorafenib, a TKI targeting VEGFR1-3, was the first agent approved for patients progressing on sorafenib [131]; cabozantinib, a TKI that targets VEGFR2, MET and AXL, demonstrated improvements in median OS and progression-free survival [131–133]; in turn, ramucirumab, an anti-VEGF monoclonal antibody, is the only biomarker-guided therapy for HCC, which is indicated for patients with baseline alpha-fetoprotein levels above 400 ng/dl[133].

In the recent years, immunotherapies with ICIs have emerged as promising treatment options for multiple solid tumors like HCC. ICIs are monoclonal antibodies directed against negative regulators of the T cell immune function (e.g. PD1, PDL1, CTLA4), expressed by tumor or immune cells, aiming to stimulate an adaptive antitumor immune response. In HCC, the combination of the ICI **atezolizumab** (anti-PDL1) **plus bevacizumab** (anti-VEGF) has become the **standard of care in first line** after demonstrating superiority versus sorafenib (median OS 19.2 vs. 13.4 months with a 30% ORR)[3]. However, its primary resistance rate of ~70% and <2-year progression-free survival[3] leave room for improvement with new strategies. Recently, the combination of **tremelimumab** (anti-CTLA-4) **plus durvalumab** (anti-PD-L1) has demonstrated superiority over sorafenib for OS (median OS 16.4 vs. 13.8 months with a 20% ORR) [134], but it is not yet approved. In addition, promising phase Ib/II studies, the ICI **pembrolizumab** (anti-PD1) and the combination of **nivolumab** (anti-PD1) **plus ipilimumab** (anti-CTLA4) led to FDA accelerated approval in the second line setting (the latter extending median duration of response to 21.7 months)[135,136]. Finally, **cabozantinib plus atezolizumab** has shown superiority over sorafenib in terms of PFS[137].

Except elevated serum AFP levels predicting response to ramucirumab, approved systemic agents in HCC are missing associated predictive biomarkers[2,91]. The reasons behind this are multiple. Firstly, it is estimated that ~25% of HCC tumors present actionable mutations, but their low prevalence (<10% in most cases) is a major drawback in the design of proof-of-concept studies[95,127]. In addition, the most common mutations in HCC are not targetable with existing drugs (TERT, TP53, CTNNB1). Secondly, HCC is clinically diagnosed with non-invasive imaging according to the guidelines[2,90,91], limiting access to tissue specimens for biomarker discovery in randomized controlled trials (RCTs). Thirdly, an elevated intratumor heterogeneity in up to 25% of patients is also an obstacle to find robust biomarkers[138,139].

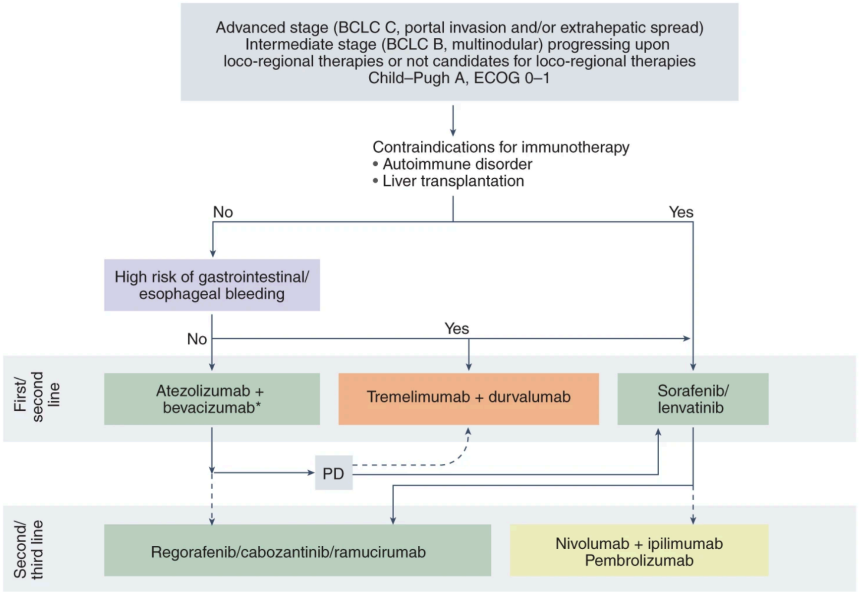

Figure 12 | Treatment strategy for HCC with systemic therapies. Green, regulatory-body-approved regimes based on phase III studies. Orange, positive combinations versus sorafenib, but drugs are not yet approved. Yellow, treatments that received FDA accelerated approval based on phase II studies. *Around 70–80% of patients are expected to receive this regime. PD, progressive disease. Obtained from Llovet *et al*. Nature Cancer 2022[91].

A limited number of RCTs have been designed to enrich for biomarker-based populations, and none has been based on molecular or immune HCC classes[91]. Currently, like in many other solid tumor types, multiple candidate biomarkers of response to immunotherapeutic agents and combinations are under investigation in HCC. Data from non-randomized studies of nivolumab and pembrolizumab monotherapies suggested that protein PD-L1 expression could be associated with response, although methodological heterogeneity and small sample sizes limit interpretation[2,136,140]. Additional candidates are tumor lymphocytic infiltration[141], gene expression signatures reflecting inflamed phenotypes[109], signatures capturing anti-tumor immunity pathways enriched in responders (e.g. interferon and antigen presentation for ICI monotherapy[125,142] or T effector cells in atezolizumab plus bevacizumab[117]) and *CTNNB1* mutational status[107,112]. In addition, recent data have revealed that non-viral HCCs, including nonalcoholic steatohepatitis (NASH)-related HCCs, are less responsive to immunotherapy due to the intratumor accumulation of a population of dysfunctional activated $CD8^{+}PD1^{+}$T cells[114].

2.4.3. Overview of drug immunomodulation in HCC

Immunotherapeutic strategies have an improved efficacy among tumors with an inflammatory microenvironment –the so-called *hot tumors*– and efficacy is reduced in tumors with decreased immune infiltration –*cold* tumors–[6]. In HCC, pembrolizumab and nivolumab monotherapies show long-lasting responses (beyond 16 months) but only in a subset of 15%-20% of patients and this failed to significantly extend overall survival (OS) in phase III trials[136,140,143,144]. Efforts are being made to broaden the spectrum of responders to ICIs by promoting vascular normalization and the infiltration or re-activation of specific immune cell types through combination strategies with anti-angiogenic agents, given that pro-angiogenic molecules such as VEGF, angiopoietins or PDGF have immunosuppressive roles that undermine the anti-tumor immunity elicited by ICIs[7,123,145] (**Figure 13**). The immunomodulation induced by combinations relies upon enhancing both dendritic cell (DCs) and cytotoxic T lymphocyte activity and inhibiting tumor-associated macrophages (TAMs), regulatory T (Treg) cells and myeloid-derived suppressor cells (MDSCs)[2]. Clear evidence of the success of this therapeutic strategy in HCC is the breakthrough IMbrave150 trial positioning atezolizumab (anti-PD-L1) plus bevacizumab (anti-VEGF) as standard of care in frontline[2,3].

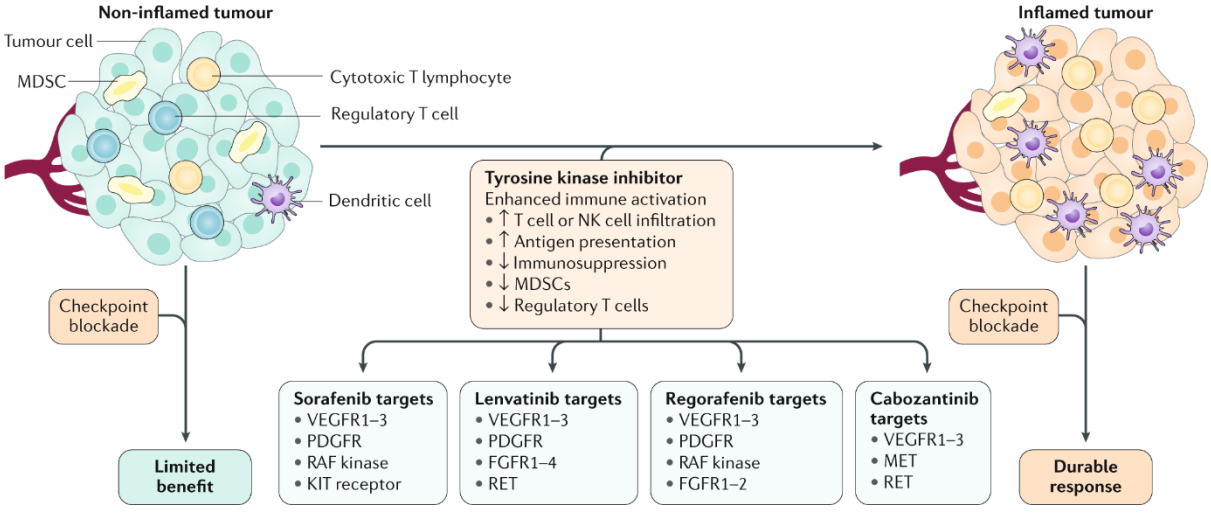

Figure 13 | Potential effects of the combinations of ICIs and TKIs. Role of TKIs in the switch from a non-inflamed tumor (*cold tumor*) towards an inflamed tumor (*hot tumor*). Adapted from Llovet *et al.* Nat Rev Clin Oncol 2021[2].

Although the candidate anti-angiogenic combinatorial agents are expected to expand antitumor effects and reactivate an inflammatory response, molecular evidence from preclinical studies suggest that they may have specific immunomodulatory mechanisms, most

likely due to differences in target molecules and/or affinities[117,146,147]. On one hand, atezolizumab-bevacizumab causes an increase in total intratumor $CD8^+$ T cells and in their proliferating and GZMB-expressing antigen-specific subpopulations, as well as in conventional dendritic cells, while also reducing T regulatory cell proliferation (a feature that was also found in post-treatment human biopsies)[117]. On the other hand, regorafenib-anti-PD1 combination enhances cytotoxic lymphocyte recruitment and activation due to vessel normalization causing a better regorafenib delivery, which in turn promotes Stat1 signaling and tumor CXCL10 production, that further recruits more cytotoxic T cells into the tumor[146]. Conversely, lenvatinib-anti-PD1 combination increases T cells and dendritic cells in the tumor coupled with a lenvatinib-induced reduction of T regulatory cell infiltration and TGFβ immunosuppressive signaling[147].

Considering the above, the potential of the TKI cabozantinib as a combinatorial agent with anti-PD1 was not thoroughly explored in HCC. Cabozantinib targets VEGFRs, MET, AXL, RET, KIT, TIE2 and FLT3, relevant players in angiogenesis, proliferation and epidermal-to-mesenchymal transition[148,149]. Also, in addition to its anti-angiogenic and anti-proliferative activity[149], immune-modulatory effects have been reported in experimental prostate cancer models[150]. The immunomodulatory role of cabozantinib in HCC has been addressed in this thesis.

Aside from targeting pro-angiogenic pathways, immune modulation can also be achieved by immune-oncology combinations where complementary checkpoint molecules or immune-related pathways are targeted simultaneously. For example, co-targeting CTLA4 synergizes with anti-PD1/anti-PD-L1 activity through regulation of T-cell activation in lymph nodes and tissues: CTLA4 inhibition results in expansion of a population of $ICOS^+$ effector helper T-cells while engaging subsets of exhausted-like $CD8^+$ T cells[151].

Finally, exploring the modulation of additional immune cell populations could also be of interest in a combination setting. Considering the growing evidence for both pro- and anti-tumor neutrophil functions in multiple cancer types[10], the present thesis also discusses modulation of neutrophil biology with a CXCR2 small molecule inhibitor to enhance anti-PD1 efficacy, particularly in the setting of anti-PD1-resistant NASH-HCC.

Hypothesis and aims

Rationale

Primary liver cancer is the sixth most diagnosed cancer and the second leading cause of cancer-related death worldwide[1]. Around 90% of cases correspond to hepatocellular carcinoma (HCC), which normally arises in the setting of a chronic liver disease[2]. Of all HCC patients, 50-60% will be ultimately exposed to systemic therapies, where the combination of atezolizumab and bevacizumab has become the standard of care in first line. However, only around 30% of patients respond to this therapy[3]. Therefore, there is a **need for biomarkers of response/resistance and more knowledge on the mechanisms behind antitumor immunity**. In line with this, aneuploidy – the presence of copy-number alterations (CNAs) in chromosome segments due to chromosomal instability- has been linked to immune evasion in some cancer types[4,5]. **In HCC, the biological implications of aneuploidy profiles have not been thoroughly described** (Study 1).

The elevated rates of primary resistance to atezolizumab-bevacizumab (70%) highlight the **need to develop novel therapeutic strategies**[2]. Given that immunotherapeutic agents show better results among tumors with an inflammatory microenvironment[6] and that proangiogenic molecules are immunosuppressive, the antitumor activity of immunotherapy could be enhanced by promoting the infiltration or reactivation of immune cells in combinatorial strategies with antiangiogenic agents[7]. In this context, the **tyrosine kinase inhibitor (TKI) cabozantinib is a promising candidate for combination with ICIs** (Study 2).

In Western countries, an increasing prevalence of obesity and metabolic syndrome is leading to a higher fraction of HCCs attributed to non-alcoholic steatohepatitis (NASH)[2,8]. Recently, NASH-HCC has been reported as less responsive to immunotherapy due to an expansion of a subset of exhausted infiltrating $CD8^+$ T cells[9]. Considering the growing evidence for pro- and anti-tumor functions of neutrophils in cancer and HCC[10], **neutrophil phenotype modulation could be a mechanism to overcome NASH-HCC immunotherapy resistance** (Study 3).

Hypothesis

The identification of molecular features/structural genomic alterations linked to antitumor immunity in HCC and the assessment of novel combinatorial strategies with immunotherapies will reveal candidate biomarkers of response or resistance to immunotherapeutic agents and more effective therapeutic options to enhance the antitumor immune response.

Aims

The specific objectives of the doctoral thesis are:

1. To determine the biological and clinical impact of chromosomal instability in hepatocellular carcinoma and to reveal its association with antitumor immunity.

2. To evaluate the impact of molecular therapies combined with ICIs in preclinical models of HCC. Specifically:

    2.1. To explore the antitumoral and immunomodulatory effects of cabozantinib alone and in combination with anti-PD1.

    2.2. To evaluate the capacity of a CXCR2 inhibitor to re-sensitize NASH-HCC to anti-PD1 therapy.

Results

Study 1: Copy number alteration burden differentially impacts immune profiles and molecular features of hepatocellular carcinoma

Laia Bassaganyas*, Roser Pinyol*, **Roger Esteban-Fabró***, Laura Torrens, Sara Torrecilla, Catherine E Willoughby, Sebastià Franch-Expósito, Maria Vila-Casadesús, Itziar Salaverria, Robert Montal, Vincenzo Mazzaferro, Jordi Camps, Daniela Sia, Josep M Llovet.

**Shared first authorship.*

Clinical Cancer Research. 2020 Sep; 26(23): 6350-6361. (IF: 13.801, Q1)

Summary

It is estimated that 50-60% of HCC patients undergo systemic therapies in their lifespan, most of which are in advanced disease stages (40% of the diagnosed cases)[2,127]. In advanced HCC, only around 30% of patients respond to the current standard of care, atezolizumab (anti-PDL1 antibody) plus bevacizumab (anti-VEGF antibody)[3]; therefore, there is a **need for biomarkers of response/resistance and more knowledge on the mechanisms behind antitumor immunity**. In line with this, aneuploidy – the presence of copy-number alterations (CNAs) in chromosome segments due to chromosomal instability- has been linked to immune evasion in some cancer types [4,5]. Specifically, the accumulation of broad CNAs (spanning ≥50% of a chromosome arm) has been correlated with decreased leukocyte infiltration and response to immunotherapy in non-small cell lung cancer and melanoma [4,5]. Conversely, focal CNAs (<50% of a chromosome arm) have been more strongly associated with proliferation and worse prognosis [4,5]. However, the direction and intensity of these associations may not be common in all cancer types[152–154]. **In HCC, the biological implications of aneuploidy profiles based on broad and focal CNA landscapes have not been thoroughly described**.

Given the above, we aimed at **determining the biological and clinical impact of aneuploidy assessed through the burdens of broad and focal CNAs to reveal its association with antitumor immunity in HCC**. Namely, we aimed (1) to define and characterize aneuploidy profiles in HCC through scores capturing broad and focal CNA landscapes; (2) to evaluate the association of aneuploidy profiles with molecular and clinical characteristics; and (3) to characterize immune profiles linked to broad or focal CNA loads.

For this study we analyzed SNP array data from 452 paired tumor/adjacent resected HCCs and 25 dysplastic nodules. We used the CNApp web tool[11] to quantify the CNA burdens of each sample and generate broad and focal scores (BS and FS), which were then correlated with transcriptomic, mutational and methylation profiles, tumor immune composition, and clinicopathologic data.

Our findings were the following:

1. We used the **TCGA pan-cancer** data (10,635 patients) to rank HCC based on CNApp-derived BS and FS, which quantify genomic burdens of broad and focal CNAs, respectively. We observed that **BS and FS distributions in HCC were intermediate** among all cancer types. In addition, **HCC was one of the 14 tumor types** where **BS negatively correlated** with transcriptomic estimates of **immune infiltration**, while FS did not.

2. HCCs with a **low burden of broad CNAs** (low BS) were more **diploid** and were enriched in the **HCC immune class**, specifically the **active subclass**. Low BS samples displayed high inflammatory and antitumor immunity signaling, higher immune infiltrate and cytolytic activity estimates, and were transcriptionally similar to tumors responding to anti-PD1.

3. HCCs with **high burden of broad CNAs** (high BS) were more **polyploid**, had an enrichment in transcriptomic features of **DNA repair and proliferation** and **low immune infiltration**.

4. **High levels of focal CNAs** (high FS) were linked to classical **proliferative features**, **TP53 mutation**, **poor survival** signatures and features of **aggressive tumors** like poor cell differentiation and vascular invasion. FS did not correlate with immune features.

5. **Dysplastic nodules and very early HCCs with broad CNAs** were also linked to **reduced features of active antitumor immunity**, suggesting that the impact of broad CNAs on immunity may be seen even at early stages of hepatocarcinogenesis.

6. We observed several **potential mechanisms** that could explain the differential immune profiles based on broad CNA levels:
    a. **Low BS** HCCs had a significantly **higher ratio of observed/expected neoantigens**, rendering more neoantigens than expected by their lower mutation burdens. TP53 mutation was linked to higher mutations and neoantigen burdens in those samples.
    b. **Specific losses of antigen presentation machinery genes** (such as *HLA-DQB1*) were enriched in **high BS** tumors.
    c. **High BS** HCCs have a **widespread hypomethylation**, which may indicate an epigenetic influence on HCC immune profiles[12].
    d. The accumulation of **broad CNA losses** had a **stronger association with reduced immune infiltration** estimates as compared to broad CNA gains, like previous observations in melanoma[13].

In conclusion, our study revealed differential associations between broad and focal genomic CNA burdens and several HCC molecular features. HCCs with high burdens of broad CNAs exhibit immune exclusion features, while low broad CNA burdens are linked to immune active profiles. These data constitute evidence in favor of chromosomal instability as a cancer hallmark impacting tumor immunogenicity, which may influence patient response to immunotherapies.

CLINICAL CANCER RESEARCH | TRANSLATIONAL CANCER MECHANISMS AND THERAPY

Copy-Number Alteration Burden Differentially Impacts Immune Profiles and Molecular Features of Hepatocellular Carcinoma

Laia Bassaganyas[1], Roser Pinyol[1], Roger Esteban-Fabró[1], Laura Torrens[1], Sara Torrecilla[1], Catherine E. Willoughby[1], Sebastià Franch-Expósito[2], Maria Vila-Casadesús[3], Itziar Salaverria[4,5], Robert Montal[1], Vincenzo Mazzaferro[6], Jordi Camps[2], Daniela Sia[7], and Josep M. Llovet[1,7,8]

ABSTRACT

Purpose: Chromosomal instability is a hallmark of cancer that results in broad and focal copy-number alterations (CNAs), two events associated with distinct molecular, immunologic, and clinical features. In hepatocellular carcinoma (HCC), the role of CNAs has not been thoroughly assessed. Thus, we dissected the impact of CNA burdens on HCC molecular and immune features.

Experimental Design: We analyzed SNP array data from 452 paired tumor/adjacent resected HCCs and 25 dysplastic nodules. For each sample, broad and focal CNA burdens were quantified using CNApp, and the resulting broad scores (BS) and focal scores (FS) were correlated with transcriptomic, mutational, and methylation profiles, tumor immune composition, and clinicopathologic data.

Results: HCCs with low broad CNA burdens (defined as BS ≤ 4; 17%) presented high inflammation, active infiltrate signaling, high cytolytic activity, and enrichment of the "HCC immune class" and gene signatures related to antigen presentation. Conversely, tumors with chromosomal instability (high broad CNA loads, BS ≥ 11; 40%), displayed immune-excluded traits and were linked to proliferation, *TP53* dysfunction, and DNA repair. Candidate determinants of the low cytotoxicity and immune exclusion features of high-BS tumors included alterations in antigen-presenting machinery (i.e., HLA), widespread hypomethylation, and decreased rates of observed/expected neoantigenic mutations. High FSs were independent of tumor immune features, but were related to proliferation, *TP53* dysfunction, and progenitor cell traits.

Conclusions: HCCs with high chromosomal instability exhibit features of immune exclusion, whereas tumors displaying low burdens of broad CNAs present an immune active profile. These CNA scores can be tested to predict response to immunotherapies.

Introduction

Liver cancer is the fourth leading cause of cancer-related death and a major health problem globally (1). Among liver cancers, hepatocellular carcinoma (HCC) is the most common form (∼90% of primary liver cancers), with more than 850,000 new cases per year worldwide, and is a type of tumor that occurs more commonly among men (1). Despite recent major advances in the understanding of the molecular pathogenesis of HCC, current therapeutic options remain limited, with curative approaches only available for a minority of patients diagnosed at early stages (2, 3). Of note, around 40% of patients with HCC are diagnosed at advanced stages, where the kinase inhibitors sorafenib and lenvatinib are first-line standard systemic therapies, while regorafenib, cabozantinib, and ramucirumab are administered in second line (2). Only recently, the first-line combination therapy with the immune checkpoint inhibitor (ICI) atezolizumab and the VEGF inhibitor bevacizumab [mAbs against programmed cell death 1 ligand 1 (PD-L1) and VEGF-A, respectively], showed significantly improved survival rates in patients with unresectable HCC compared with the standard-of-care sorafenib in the IMbrave 150 phase III clinical trial (4). Response rates in this trial and in phase I/II trials testing nivolumab and pembrolizumab (anti–PD-1) or combinations of nivolumab and ipilimumab (anti–CTLA-4; refs. 5–7) ranged between 15% and 30% of patients, highlighting the need for biomarkers of response/resistance in HCC and an overall better comprehension of the tumor immune responses (8).

In this regard, we have recently characterized the immune landscape of HCC tumors and identified the HCC immune class, a subgroup of approximately one-third of HCCs whose immune profile is characterized by high tumor-infiltrating lymphocytes (TIL), high expression levels of PD-L1 and PD1, and markers of cytolytic activity (9). In addition, we have described the HCC exclusion class, with exclusion of TILs and other "cold" tumors traits, which is prevalent in approximately 30% of HCCs (10).

Copy-number changes of chromosomal segments, also known as aneuploidy, are a common feature of human cancers and have been proposed as a driving force of tumorigenesis (11). Aneuploidy encompasses broad somatic copy-number alterations (CNAs), involving

[1]Liver Cancer Translational Research Group, Liver Unit, Institut d'Investigacions Biomèdiques August Pi i Sunyer (IDIBAPS), Hospital Clínic, Universitat de Barcelona, Barcelona, Catalonia, Spain. [2]Gastrointestinal and Pancreatic Oncology Group, Institut d'Investigacions Biomèdiques August Pi i Sunyer (IDIBAPS), Barcelona, Catalonia, Spain. [3]Bioinformatics Unit, CIBERehd, Barcelona, Catalonia, Spain. [4]Lymphoid Neoplasms Program, Institut d'Investigacions Biomèdiques August Pi i Sunyer (IDIBAPS), Barcelona, Catalonia, Spain. [5]Tumores Hematológicos, Centro de Investigación Biomédica en Red de Cáncer (CIBERonc), Madrid, Spain. [6]Gastrointestinal Surgery and Liver Transplantation Unit, National Cancer Institute, Milan, Italy. [7]Mount Sinai Liver Cancer Program, Division of Liver Diseases, Tisch Cancer Institute, Icahn School of Medicine at Mount Sinai, New York, New York. [8]Institució Catalana de Recerca i Estudis Avançats (ICREA), Barcelona, Catalonia, Spain.

Note: Supplementary data for this article are available at Clinical Cancer Research Online (http://clincancerres.aacrjournals.org/).

L. Bassaganyas, R. Pinyol, and R. Esteban-Fabró contributed equally as co-first authors of this article.

Corresponding Author: Josep M. Llovet, Institut d'Investigacions Biomediques August Pi i Sunyer (IDIBAPS), C/Rosselló 153, Barcelona, Catalonia, 08036, Spain. Phone: 349-3227-9155; E-mail: jmllovet@clinic.cat

Clin Cancer Res 2020;26:6350–61

doi: 10.1158/1078-0432.CCR-20-1497

Translational Relevance

In hepatocellular carcinoma (HCC), immune checkpoint inhibitors achieve responses in 15%–20% of patients, however, there is no established biomarker predictive of response. Recently, several pan-cancer studies have uncovered that chromosomal alterations strongly associated with specific immune traits recapitulating known "immune/inflamed" and "excluded/noninflamed" tumor subtypes. These subtypes have been linked to potential response or primary resistance to checkpoint inhibitors, respectively. Because the intensity and direction of the interaction between copy-number alterations (CNAs) and tumor immunity are not uniform in all cancer types, and different tissue-specific features may affect the immune response of tumors, we analyzed the particularities of HCC. Here, we propose a strategy based on the CNA profile of each tumor that allows its classification into active/excluded immune profiles. Our study revealed that while HCCs with high loads of broad CNAs [high broad score (BS)] present immune-excluded features and proliferation signatures, tumors with low levels of broad CNAs (low BS) displayed immune active hot features. We hypothesize that the immune profile of low-BS HCCs may indicate a favorable response to immunotherapies.

large portions of chromosomes, and smaller focal CNAs. Recently, it has been uncovered that the loads of broad and focal CNAs differentially correlate with gene expression markers related to hallmarks of cancer, cell proliferation, and immune evasion (12, 13), suggesting that they are involved in the carcinogenic process through distinct mechanisms. While high levels of focal events correlate with proliferation markers (12) and can have increased prognostic value compared with broad CNAs (14), high levels of broad events are strongly associated with markers of immune evasion (in several tumor types) and with a reduced response to immunotherapy [e.g., in non–small cell lung cancer (NSCLC) and melanoma; refs. 12, 13, 15]. Thus, the interaction between the cancer genome and the immune system might be regulated through a general gene dosage imbalance governing over specific gene alterations. Nevertheless, none of the above-mentioned studies, or any other published, have specifically deepened on such analysis in HCC. In addition, recent reports have shown that the intensity and direction of the association between CNAs and tumor immunity may not be universal in all cancer types (15–18), underlining the need to investigate the impact of aneuploidy considering the tumor tissue–specific context.

In a previous work, we assessed whether the number of statistically significant recurrent amplifications or deletions in HCC correlated with the immune classes (9), but a thorough characterization of the CNA burden was unaddressed. Thus, we analyzed the effect of focal and broad CNA loads using a newly described scoring strategy (19) and correlated the scores with molecular and immune features. Our findings suggest that HCCs with high burden of broad CNAs correlated with immune exclusion profiles and proliferation signatures; on the other hand, tumors with lower burdens of broad CNAs were enriched in the HCC immune class (9) and proinflammatory pathways, presented higher cytolytic activity, and exhibited absence of *CTNNB1* mutations. Consequently, we propose that the "hot" tumor traits of HCCs with low CNA burdens may make them potential candidates to a sustained favorable response to ICIs. In contrast, the "noninflamed" traits and reduced cytotoxic immunophenotype of HCCs with higher levels of broad CNAs are consistent with the notion that broad events may be implicated in immune escape mechanisms and could be indicators of resistance to immunotherapies, as observed in other cancer types (12).

Materials and Methods

Study cohorts

A total of 452 samples were analyzed (Supplementary Fig. S1A), including a discovery cohort ($n = 107$; ref. 20) and a validation cohort [$n = 345$; The Cancer Genome Atlas (TCGA); ref. 21]. The main clinicopathologic features of these two cohorts are summarized in Supplementary Table S1. The HEPTROMIC cohort is characterized by mostly Caucasian patients, median age 66 years, males (78%), with Hepatitis C virus (HCV)-related HCC (46%), at early stages of the disease (86% BCLC 0–A), undergoing resection for single tumors (77%), and with α-fetoprotein < 400ng/mL (85%) in patients with well-preserved liver function (Child-Pugh A, 98% and platelet count > 100,000, 82%). At pathologic examination, 36% of tumors presented microvascular invasion and 24% satellites. Patients from TCGA cohort were characterized by a median age of 61 years, 68% males, with 12% of cases related to HCV infection, at early stages of the disease (75% AJCC-T1 and AJCC-T2), and the majority of them presented a well-preserved liver function (Child-Pugh A, 91% and platelet count >100,000, 94%). At pathologic examination, 35% of tumors presented microvascular invasion. In addition to these two cohorts, previously published premalignant samples ($n = 25$) and very early HCCs (veHCC, $n = 18$) were also included in the study (20, 22). Finally, a publicly available transcriptome dataset corresponding to 65 pretreatment samples of patients with cancer treated with anti–PD-1 (23) was used to run the subclass mapping. More details on the cohorts have been included in Supplementary Data.

CNA data processing and determination of the CNA level

The HEPTROMIC and TCGA-Liver HCC (LIHC) SNP array data, and the CNApp web tool (19), were used to quantify the individual CNA burdens of each sample, and to generate the broad and focal CNA scores (BS and FS, respectively). Details are provided in the Supplementary Data.

Additional information related to Material and Methods is provided in the Supplementary Data.

Results

Profiling broad and focal CNAs in human HCC

To determine the impact of the genomic imbalances in the molecular and immune features of HCC, we analyzed 452 samples profiled by SNP array: 107 HCC samples (HEPTROMIC, discovery cohort) and 345 HCC samples (TCGA-LIHC, validation cohort; Supplementary Fig. S1). Using the validated CNApp resegmentation approach (see Materials and Methods), we first generated each sample's genome-wide CNA landscape, and then categorized the detected chromosomal amplifications and deletions into broad and focal events (12). HCC tumors displayed a median of 6.8 and 8.3 broad CNAs per sample in the HEPTROMIC and TCGA-LIHC cohorts, respectively; and a median of 21.0 and 30.3 focal CNAs per sample. In terms of lengths, broad chromosomal fragments had, respectively, a median size of 69.7 and 62.4 Mb (HEPTROMIC, range of 9.5–243 Mb and LIHC-TCGA, range of 8.8–245 Mb). Focal CNAs had a median length of 1.7 Mb in HEPTROMIC and 0.6 Mb in LIHC-TCGA, and 84% of all focal CNAs were below 12 Mb [ref. 24; 81% in HEPTROMIC ($n = 107$) and 85% in LIHC-TCGA ($n = 345$); Supplementary Fig. S1]. Overall, no major

differences were identified between the CNA landscapes of the two cohorts (Supplementary Fig. S1), and the profiled landscapes of the most frequent events were consistent with previously published analysis applying the GISTIC algorithm on other HCC cohorts (24–26). Briefly, the most recurrent broad gains in the two cohorts ($n = 452$) were in 1q (52%) and 8q (47%), and the most frequent broad losses were in 8p (52%) and 17p (45%). We also detected slightly less prevalent broad losses in 4q (30%), 6q (24%), and 16q (28%). CNApp also identified frequent high focal gains, characteristic of HCC, such as the ones located in 5p15.33 [in 63/452 HCCs (14%); involving *TERT*], in 11q13.3 (>6%; affecting *CCND1* and *FGF19*), or in 6p21.1 (10%; including *VEGFA*), among others. Despite the similar genomic landscapes, the two analyzed cohorts presented some differences at the clinicopathologic level (Supplementary Table S1). TCGA-LIHC patients were at more advanced stage and presented poorer liver function. Median age was also slightly different [66 in HEPTROMIC vs. 61 in TCGA ($P < 2.6E-5$)] and etiology distribution differed in the two cohorts, HCV-related HCC in HEPTROMIC accounted for 45% of cases and alcohol-related HCC in TCGA-LIHC accounted for 32% of cases. These differences, however, did not impact the CNA profiles as no significant associations were found between CNAs and the analyzed clinicopathologic variables. Next, we quantified the load of broad and focal CNAs in each sample using CNApp. The power of CNApp at capturing the actual fraction of altered genome through scores has been previously demonstrated using TCGA pan-cancer dataset of more than 10,000 samples (19). To summarize, for each tumor, CNApp provided a BS and a FS accounting for the number, amplitude, and length of broad and focal segments.

To rank the aneuploidy levels of HCC among the cancer spectrum, we conducted a pan-cancer analysis using the CNApp-derived BSs and FSs of 10,635 TCGA samples representing 33 tumor types (ref. 19; Supplementary Table S2). This analysis revealed that in HCC, the BS and FS distributions were intermediate when compared with the other 32 tumor types (**Fig. 1A** and **C**).

To explore the impact of the CNA profiles on the molecular and immune characteristics of the tumors, we categorized each sample into high/low-BS and high/low-FS according to the BS and FS quartiles. The threshold for high-BS tumors was set at ≥11 (the top quartile of both TCGA pan-cancer cohort and the discovery cohort) and for low-BS tumors at ≤4 (coinciding with the bottom quartile in the discovery cohort). In terms of FS, low-FS samples were defined as those with FS ≤ 13.5, while high FS was defined as those with FS ≥ 47, considering the quartile values in the discovery cohort. Overall, 17% of the analyzed tumors presented low broad CNA burdens (75/452) and 40% of the tumors presented high loads of broad CNAs (183/452). In terms of focal events, 20% of cases were low-FS (92/452) and 43% were high FS (196/452).

Burdens of broad and focal CNAs are associated with distinct molecular features

Stratifying HCC tumors according to their BS and assessing the correlation with molecular and immune features revealed that HCCs with fewer broad genomic imbalances (i.e., those with low BS) were characterized by high inflammation (increase of hallmarks of inflammatory response, TNFα, and IL2-JAK-STAT signaling) and IFN signaling (**Fig. 2A**). Interestingly, these tumors presented enrichment of the HCC immune class and active immune subclass (9) when compared with tumors with higher BS ($P = 0.02$ and $P = 0.04$, respectively; **Fig. 2A**). In addition, low-BS tumors were deficient in S2 (27) proliferative traits ($P = 0.006$), presented significant activation of different immune-related pathways, and had LXR/FXR/RXR signaling as one of the top canonical pathways ($P < 0.001$; Supplementary Table S3).

In terms of ploidy, we found 40% of HCCs being polyploid (3.9 ± 0.7 sets of chromosomes on average), and the remaining 60% being diploid (2 ± 0.2 sets of chromosomes). Of note, polyploid tumors were significantly enriched in high-BS HCCs [17/25 (68%) in the discovery cohort, $P < 0.001$ and 69/158 (44%) in the validation cohort; $P < 0.0001$; Supplementary Tables S5 and S6]. Low-BS HCCs were mainly diploids ($P = 0.002$; Supplementary Tables S5 and S6). At the clinicopathologic level, none of the variables assessed (including etiology and tumor stage) were linked to low BS (Supplementary Table S4).

On the other hand, HCC tumors with high burden of broad CNAs presented a completely different molecular profile. High-BS tumors were characterized by hallmarks of mismatch repair and proliferation and presented low immune infiltration, inferred from the tumor transcriptomic profile (**Fig. 2A**; Supplementary Table S5; ref. 28). Consistently, they were significantly excluded from the HCC immune class ($P = 0.02$). Pathway analysis further supported these findings, providing cell-cycle control of chromosomal replication and DNA damage as top canonical pathways (Supplementary Table S3). In addition, integrative pathway analysis (IPA) revealed a role for the arginase pathway in these tumors. The parallel evaluation of TCGA cohort confirmed these observations (Supplementary Fig. S2; Supplementary Table S6).

When classifying the tumors according to their FS, we observed that those with high levels of focal events were characterized by classical proliferative features and were associated with poor survival signatures both in the discovery and in the validation cohorts (**Fig. 3A**; Supplementary Fig. S3A; Supplementary Tables S7 and S8). Consistently, transcriptome-based pathway analysis revealed cell-cycle–related pathways as the top canonical pathways for high-FS tumors. In addition, these tumors were enriched in the HCC proliferation subclass (ref. 24; $P < 0.004$) and were excluded from the CTNNB1 subclass (ref. 24; $P = 0.032$). This molecular profile was aligned with *CTNNB1* mutations being significantly excluded from high-FS tumors ($P < 0.001$), while *TP53* mutations were enriched among them ($P < 0.001$; Supplementary Fig. S3A; Supplementary Table S8). In addition, high-FS tumors were positive for the signatures of hepatic progenitors (ref. 29; $P = 0.004$), CK19 (refs. 30, 31; $P = 0.01$), vascular invasion (ref. 32; $P = 0.02$), MET (ref. 33; $P = 0.029$), and late TGFβ signaling (ref. 34; $P = 0.005$). At the clinicopathologic level, these tumors were associated with poor cell differentiation ($P < 0.001$; Supplementary Tables S7 and S8). Interestingly, we did not find a significant association between FS and tumor immune profiles (**Fig. 3A**; Supplementary Fig. S3; Supplementary Tables S7 and S8). Despite displaying traits of poor prognosis, FS status did not correlate with patient's overall survival. Levels of broad CNAs were also not associated with patient's outcome.

Overall, and as in other cancer types, burdens of broad CNAs, but not focal, have an impact on the HCC immune profile, and this also supports a differential role for focal and broad events as determinants of HCC antitumor immunity.

Low broad CNAs loads correlate with the HCC immune class, and high burdens of broad CNAs correlate with immune exclusion

As mentioned above, low-BS tumors presented hallmarks of inflammatory and IFN signaling and were characterized by immune traits as seen by an enrichment of the HCC immune class (9). Chemokine and cytokine signaling as well as signatures of innate (cytotoxicity mediated by natural killer cells, monocytes, and dendritic cells) and adaptive

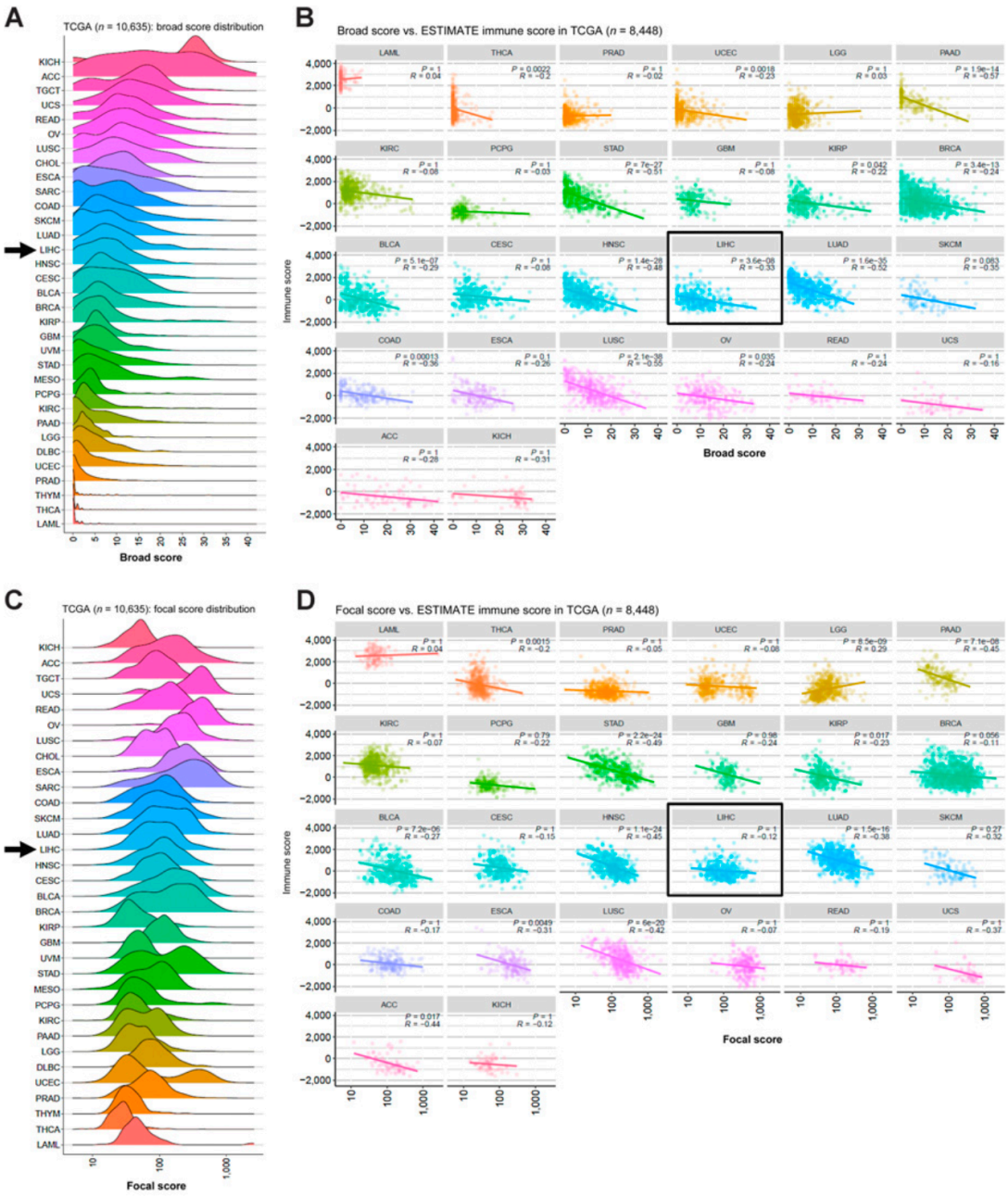

Figure 1.

Diagrams representing CNApp BS and FS distributions and their correlation with the ESTIMATE immunity score in a pan-cancer cohort. **A,** BS distribution across 33 cancer types from TCGA. **B,** Dot plots displaying the correlation between BS and ESTIMATE-derived immune score per cancer type. **C,** FS distribution across 33 cancer types from TCGA. **D,** Dot plot with FS and immune score correlations per cancer type. P, Spearman correlation *P* value; R, Spearman regression coefficient. Arrow in **A** and **C** and box in **B** and **D** indicate HCC. TCGA cancer project abbreviations: ACC, adrenocortical carcinoma; BLCA, bladder urothelial carcinoma; BRCA, breast invasive carcinoma; CESC, cervical squamous cell carcinoma and endocervical adenocarcinoma; COAD, colon adenocarcinoma; ESCA, esophageal carcinoma; GBM, glioblastoma multiforme; HNSC, head and neck squamous cell carcinoma; KICH, kidney chromophobe cell carcinoma; KIRC, kidney renal clear cell carcinoma; KIRP, kidney penal papillary cell carcinoma; LAML, acute myeloid leukemia; LGG, brain lower grade glioma; LUAD, lung adenocarcinoma; LUSC, lung squamous cell carcinoma; OV, ovarian serous cystadenocarcinoma; PAAD, pancreatic adenocarcinoma; PCPG, pheochromocytoma and paraganglioma; PRAD, prostate adenocarcinoma; READ, rectum adenocarcinoma; SKCM, skin cutaneous melanoma; STAD, stomach adenocarcinoma; THCA, thyroid carcinoma; UCEC, uterine corpus endometrial carcinoma; UCS, uterine carcinosarcoma.

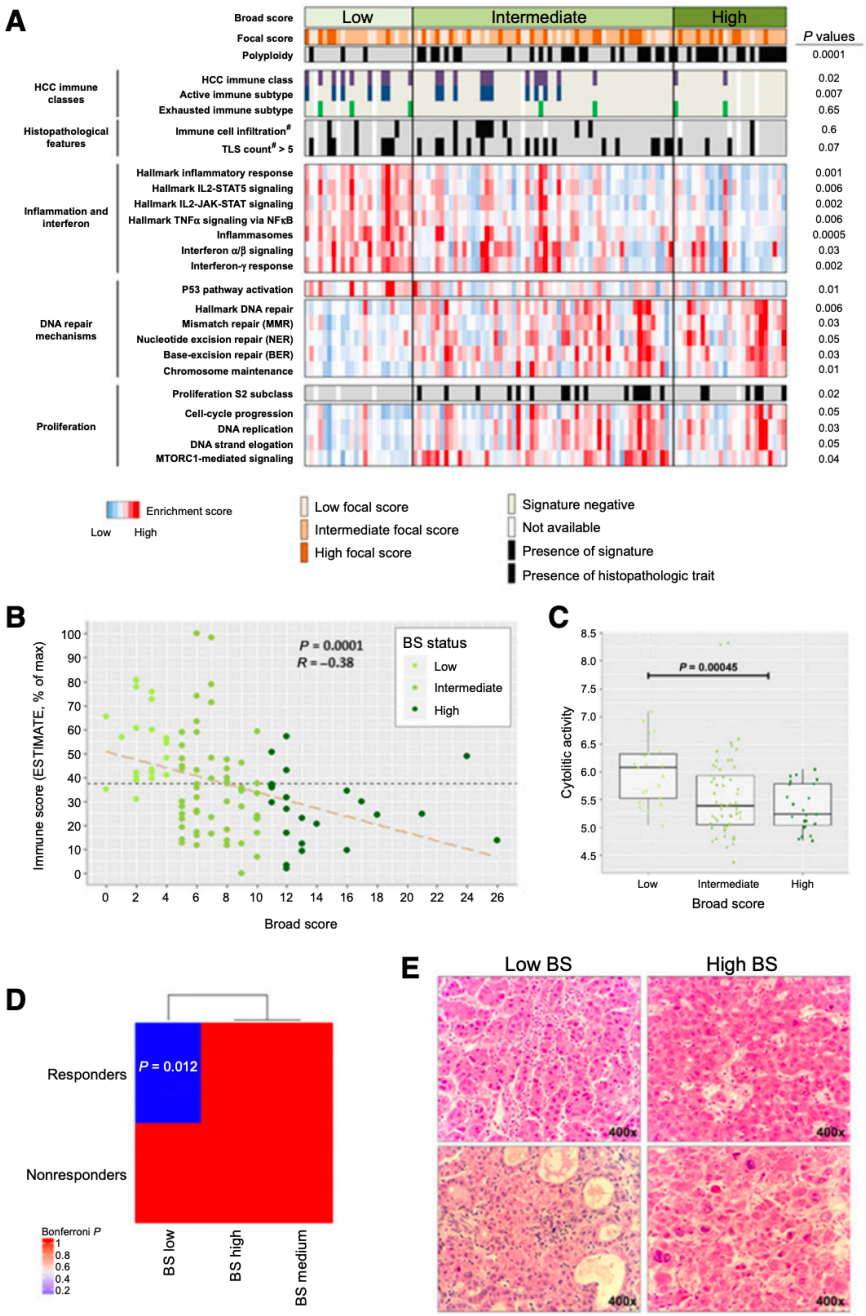

Figure 2.

HCC tumors with a low burden of broad copy-number chromosomal alterations display higher immune infiltration when compared with HCCs with higher loads of broad events. **A,** Scores to quantify the burden of broad and focal chromosomal alterations (BS and FS) were computed using CNApp. Tumors with low burdens of broad chromosomal alterations (low BS) were significantly associated with the HCC immune class, and were mainly diploid and had functional p53. In contrast, tumors with high BS were markedly polyploid, and were enriched in cell proliferation features and DNA repair hallmarks including *TP53* mutations/losses. #, pathologically assessed. Displayed *P* values were calculated comparing low-BS tumors with high-BS tumors. **B,** Transcriptome-based estimation of immune cell infiltration in HCC negatively correlates with broad CNA burdens ($n = 102$, discovery cohort). Data are presented normalized to the maximum immune score. r, Spearman rank correlation coefficient. **C,** BS-low HCC tumors exhibited significantly higher cytolytic activity compared with the rest ($n = 102$, discovery cohort). **D,** Molecular similarity between low-BS HCC patients and tumors responsive to PD-1 therapy. Submap analysis was applied considering two groups in the HCC cohort (low BS vs. rest) and two groups (anti–PD-1 responders and nonresponders) in the anti–PD-1–treated dataset. Low-BS HCC tumors were significantly similar to tumors responding to anti–PD-1 ($P = 0.01$). **E,** Representative images of immune cell infiltration in low-BS and high-BS HCC tumors from the HEPTROMIC cohort.

immunity (cytotoxic T cells, Th lymphocytes, and B- and T-cell receptor signaling) were also enriched in low-BS tumors (Supplementary Fig. S4A). Interestingly, expression levels of immune checkpoints such as programmed cell death 1 (PD-1) and CTLA-4 were higher in these tumors compared with HCCs with intermediate or high BS (Supplementary Fig. S4A). The presence of higher immune infiltrate in low-BS HCCs was confirmed at the pathologic level and by using transcriptome-based independent algorithms (**Fig. 2**; refs. 28, 35, 36). First, pathologic assessment of tumor immune infiltrates in our cohort revealed a trend toward higher immune cell infiltration ($P = 0.054$) and higher count of tertiary lymphoid structures (TLS; $P = 0.06$; **Fig. 2A** and **E**; Supplementary Table S5) in low-BS tumors. TLS density has been reported to correlate with $CD8^+$ and $CD4^+$ T-cell density in tumors and its presence is associated with favorable prognosis (37, 38). Second, levels of immune cell infiltrate were inferred from the tumor whole-genome expression profiles (28), and

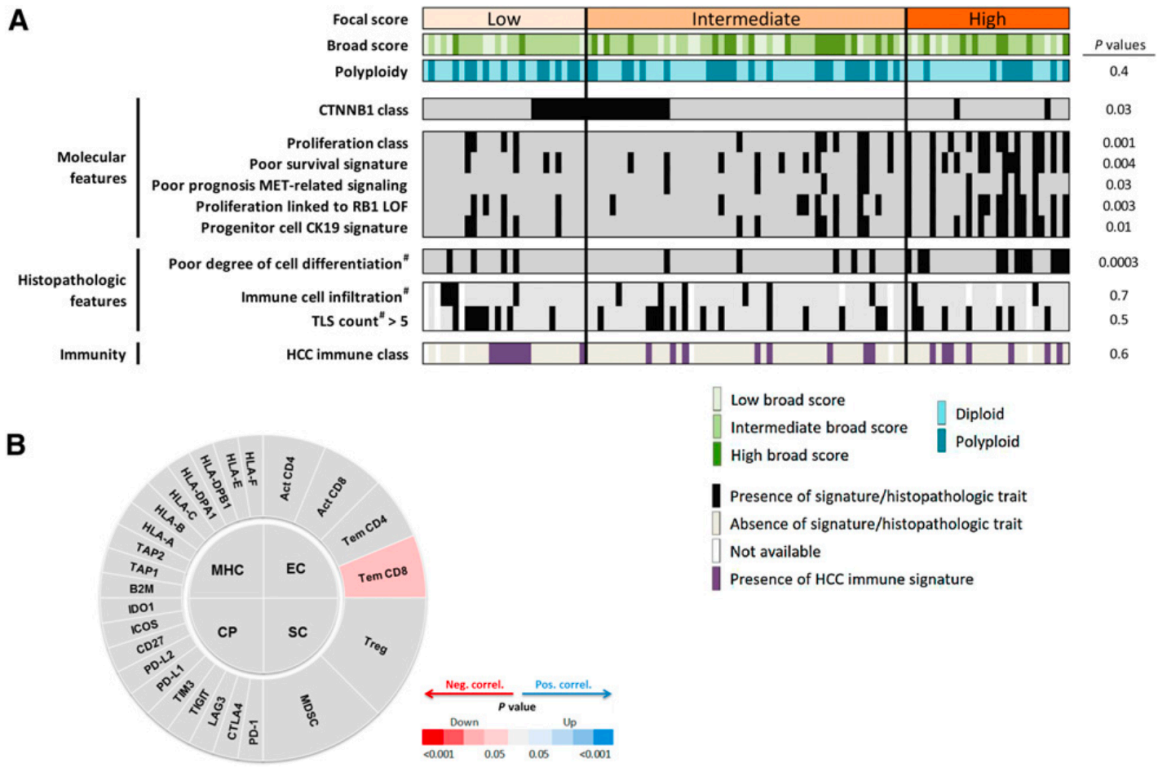

Figure 3.

HCC tumors with a high burden of focal copy-number chromosomal alterations exhibit proliferation and poor prognosis traits, but no association with tumor immunity. **A,** Tumors with a high level of focal events (high FS) were enriched in poor prognosis and proliferation signatures, and presented a higher degree of cell differentiation. HCCs with low or intermediate levels of focal CNAs (low FS and intermediate FS) were enriched in WNT-CTNNB1 signaling. FSs were not associated with immune signaling. #, pathologically assessed. **B,** Immunophenoscore diagram correlating FS with expression features from effector cells (ECs), immune checkpoints (CP), MHC-related components (MHC), and suppressor cells (SP). FSs did not correlate with any of the immunophenoscore groups of genes.

were found significantly increased among HCCs with low CNA burden (low BS; $P = 0.0001$; **Fig. 2B**). Third, we adapted the immunophenoscore (ref. 35; Supplementary Table S9) to further dissect the transcriptome of our discovery and validation cohorts and confirmed the above-mentioned immune traits of low-BS HCCs (Supplementary Figs. S2C and S4B). We also inferred the cytolytic activity of each tumor (36) and observed that it was higher in tumors with reduced broad CNA burdens ($P < 0.001$; **Fig. 2C**). In addition, we performed a submap analysis comparing the molecular profile of our HCC tumors grouped according to BS with a publicly available molecular print of treated tumors (23), classified according to their response to anti–PD-1 treatment. Remarkably, we only observed a significant association between low-BS tumors and tumors responding to anti–PD-1 therapy ($P = 0.01$; **Fig. 2D**). Furthermore, we identified significantly elevated expression of HLA-A molecules in BS-low tumors when compared with the rest ($P < 0.001$; Supplementary Fig. S4). Finally, pathway analysis revealed several ILs and IFNγ among the top upstream regulators in low-BS HCC tumors (Supplementary Table S3), as well as a consistent association with different immune-related pathways [antigen presentation ($P < 0.001$); communication between innate and adaptive immune cells ($P < 0.001$); differential regulation of cytokines ($P < 0.001$); IL17-mediated production of immune cells ($P < 0.001$); and B-cell development ($P < 0.001$)].

Regarding HCC tumors with a high burden of broad CNAs (high BS), in addition to low immune infiltration, they were significantly excluded from the HCC immune class ($n = 2/25$; $P = 0.02$) and the HCC active immune subclass ($n = 0/25$; $P = 0.01$; Supplementary Table S5). This was mirrored in TCGA cohort, where high-BS tumors had significantly less HCC immune class patients compared with low-BS tumors (17% vs. 37%; $P = 0.006$). In addition, in both cohorts, high-BS HCCs were not related to immunosuppressive features (Supplementary Figs. S2C and S4B). This is consistent with the notion that aneuploidy may play a role as a mechanism of tumor immune evasion (12).

In this regard, a previous study analyzing the aneuploidy profile of 12 cancer types (not including HCC) proposed that high levels of CNAs were drivers of immune exclusion (12). Thus, we assessed whether our scores were associated with immunity in a large spectrum of cancer types. To this end, we correlated the BSs and FSs from 10,635 TCGA samples representing 27 tumor types with a transcriptomic surrogate of the immune infiltrate level: the immune score from the ESTIMATE tool (28). Strikingly, in terms of broad alterations, we observed a significant negative correlation between immune score and BS in 14 of the 27 tumor types analyzed, including HCC (**Fig. 1B** and **D**). In terms of focal events, our FS correlated significantly with the immune score in 12 of 27 tumor types, but HCC was not among them (**Fig. 1B** and **D**). This places HCC in the subset of tumors were broad

aneuploidy events adversely affect immune cell action against tumors (12), but also corroborates that the relation between immunity and CNAs is not universal across cancer types, highlighting the importance of considering the tumor-specific context (15–18).

Preneoplastic lesions and very early HCC tumors with high loads of broad CNAs also present reduced immune features

Following the identification of immune features associated to low-BS HCCs, we sought to explore whether the burden of broad copy-number changes (BS) could also influence the modulation of the immune system at the early stages of hepatocarcinogenesis. To this end, we analyzed 25 premalignant dysplastic nodules and 18 veHCCs (20, 22). Because the preneoplastic lesions presented very few broad chromosomal rearrangements, we categorized them according to the presence or absence of broad CNAs, rather than computing their BSs. Overall, we found the presence of broad alterations in four of the 25 (16%) analyzed dysplastic nodules ("presence" being equivalent to "BS-high") and it was linked to reduced molecular features of active antitumor immunity (Supplementary Fig. S5). More precisely, BS-high dysplastic nodules displayed trends toward reduced cytolytic activity values (Supplementary Fig. S5A) and toward reduced immune cell infiltration (Supplementary Fig. S5B). On the other hand, lesions without broad CNAs presented enrichment of effector cell features, immune checkpoints, MHC-related components, and suppressor cells (Supplementary Fig. S5C and S5D). Similarly, analysis of veHCCs also revealed a significant negative correlation between BS and cytolytic activity, as well as the expression-derived immune score reflecting immune infiltration (Supplementary Fig. S6).

Overall, our results suggest that there is a continued association between BS and immunity throughout the hepatocarcinogenic process, from dysplastic nodules to veHCCS to more advanced tumors.

Potential mechanisms determining the distinct molecular and immune landscapes of tumors with different types of copy-number profiles

Tumor mutational burden, neoantigens, and *TP53* status

The fact that differences in broad CNA burdens were associated with distinct immune profiles suggests that mechanisms related to overall gene imbalance may contribute to determining the activation of molecular and immune pathways in HCC. Here, we assessed the potential contribution of the mutational load (both silent and non-silent mutations), the *TP53* status, the total predicted neoantigens, and the ratio of observed/expected neoantigens in determining the different HCC immune characteristics of specific CNA profiles. For this purpose, we used the genomic profiles of 179 patients available from TCGA HCC cohort (36), that presented an average of reported nonsilent mutations per megabase of 2.5 (tumor mutational burden, TMB), with only 2% of the samples (n = 6/302) with TMB > 10 mutations/Mb (39). Our analysis on the total number of mutations per sample revealed that this was significantly lower among low-BS tumors as compared with the rest (P = 0.023; **Fig. 4A**). Consistently, pan-cancer studies have described increased mutational burdens among tumors with increased aneuploidy (15). Because the ability to trigger a tumor immune response does not only depend on the number of mutations, but also on their antigenicity, we also calculated the ratio of observed/expected neoantigens. This ratio measures how much the number of observed neoepitopes (defined on the basis of the mutation's potential to bind HLA with high affinity, and taking into account the gene expression) deviates from the number of expected neoantigens (inferred using a pan-cancer empirical model) in each sample (36). Interestingly, we observed that low-BS tumors displayed higher ratios of observed/expected neoantigens when compared with high-BS tumors (P = 0.015) and that BS negatively correlated with this ratio (P = 0.028; **Fig. 4B**). In terms of mutations, low-BS tumors presented a positive correlation between total number of mutations and ratio of observed/expected neoantigens (P = 0.028), whereas such correlation was not observed in the rest of the cohort (**Fig. 4C**). Overall, this suggests that, despite presenting lower loads of mutations, low-BS tumors rendered more neoantigens than expected. In contrast, the higher mutational burdens together with the lower ratios of observed/expected neoantigens among high-BS tumors point toward a negative selection of neoantigens that could be rendering higher rates of less immunogenic mutations among tumors accumulating broad CNAs (**Fig. 4A–D**).

We next assessed whether our observed association between CNA burden and immune infiltration further depended on the mutational status of *TP53*, given its role in preventing genome mutations. We observed that the total number of mutations (silent and nonsilent) was independent from the *TP53* mutational status among high-BS tumors, whereas for the rest of tumors, the number of mutations was higher when *TP53* was nonfunctional (P = 0.018; **Fig. 4E**). A similar observation was made regarding neoantigen burdens, predicted neoantigens were independent from the *TP53* status only in high-BS tumors. In the rest of tumors, those with mutated *TP53* displayed significantly higher numbers of predicted neoantigens as compared with those with wild-type *TP53* (P = 0.0082; Supplementary Fig. S7A). Thus, our analysis suggests that *TP53* could have a role in shaping the immunogenicity of tumors that do not accumulate high loads of broad genomic imbalances.

T-cell–related and antigen-presenting machinery–related mechanisms

In addition, we assessed whether amplification or deletion of specific immune-related genes could contribute to explain the link between immunity and BS levels in HCC. Screening the CNApp segmentation output, we identified copy-number losses significantly enriched in high-BS tumors from the discovery and validation cohorts, potentially contributing to the observed immune phenotype. These included losses in genes from the antigen presentation machinery, T-cell receptor components, and immune checkpoints (Supplementary Fig. S7). Remarkably, few of these alterations were detected in low-BS tumors. Among others, we found significant losses of *HLA-DQB1*, coding for the type MHC class II heterodimer, in high-BS tumors [65/158 high-BS HCCs (35%) vs. 6/51 low BS (12%); P < 0.0001]. This was accompanied by a significant reduction of HLA-DQB1 expression in high-BS tumors compared with low-BS tumors in the discovery cohort (P = 0.002) and a trend in the validation cohort. Of note, the loss of HLA-DQB1 could mediate a deficit in cytotoxic cell responses in high-BS HCCs. In this regard, in lung cancer, HLA-DQB1 expression on tumor cells has been positively correlated with CD4- and CD8-positive lymphocyte infiltration (40).

Epigenetic features

In addition, considering recent evidence revealing the correlation between global demethylation and CNAs across different tumor types (41), and given that this may promote immune evasion in tumors with high copy-number load, we analyzed the methylation data available for our cohorts. In the discovery cohort, we observed that among the 17,090 probes differentially methylated between low-BS tumors and the rest, 13,252 (77%) presented higher methylation levels (Supplementary Fig. S8). Similarly, in the validation cohort, 65,361

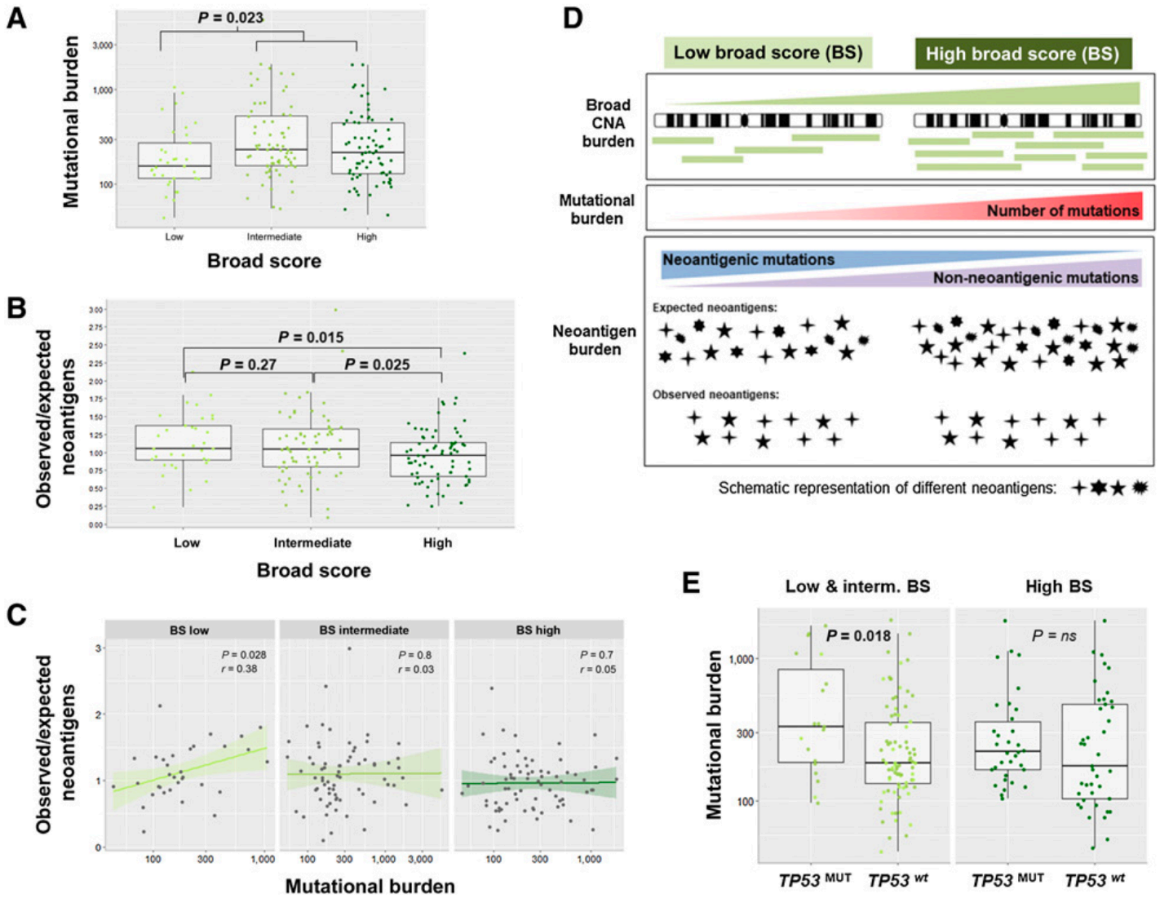

Figure 4.

Impact of the mutational landscape in HCC CNA profiles. **A,** HCC tumors with a low burden of broad CNAs (low BS) exhibited a significantly lower mutational load (silent + nonsilent mutations) when compared with the rest ($n = 179$, LIHC-TCGA; $P = 0.023$). **B,** BS-high tumors were associated with lower ratios of observed/expected neoantigens, suggesting a negative selection of low immunogenic mutations in these tumors ($n = 179$). **C,** Mutational burden in HCC significantly correlated with the ratio of observed/expected neoantigens only in BS-low tumors. **D,** Diagram summarizing the relationship between broad CNA loads, mutational burden, and observed/expected neoantigens in HCC. **E,** Total number of mutations in HCC tumors characterized by high burdens of broad CNAs (high BS) was not related to *TP53* mutational status. In contrast, low-BS HCCs (and intermediate) tumors with nonfunctional *TP53* (*TP53*^{MUT}) displayed a significantly higher number of mutations compared with those with wild-type *TP53* (*TP53*^{wt}). r, Spearman rank correlation coefficient.

(88%) of 74,195 differentially methylated probes displayed higher methylation levels among low-BS samples as compared with the rest (Supplementary Fig. S8). Therefore, our data align with the fact that the accumulation of broad CNAs leads to a widespread hypomethylation (41), and suggest an impact of epigenetic regulation in HCC immune profiles. The fact that low-BS tumors are characterized by high immune infiltration and higher methylation levels aligns with our previous observation that tumors within the HCC immune class present higher overall levels of methylation (9).

Specific contribution of CNA gains and losses

Here, we questioned whether CNA gains and losses contributed equally in determining the tumor immune profile. This was motivated by a report in melanoma suggesting that the total number of genes with copy-number losses was a marker of resistance to immune checkpoint–related treatments (42). Similar to melanoma, we observed a significant negative correlation between broad losses and cytolytic activity in HCC, both in the discovery and validation cohorts ($P = 0.0004$ in HEPTROMIC and $P = 0.01$ in LICH-TCGA; Supplementary Fig. S9). Thus, the more broad losses the tumors have, the less cytolytic activity they present; and therefore, less chances to respond to ICIs. This was also consistent with our finding that high-BS HCCs are depleted from tumor immune features and suggest that CNA losses may contribute more to this phenotype. No consistent correlations were found in terms of gains (neither broad nor focal) and in terms of focal losses.

Discussion

CNAs are considered a hallmark of cancer. Recently, pan-cancer studies have described broad and focal CNA burdens as genomic features able to determine tumor immune infiltration and immune exclusion in several cancer types (12, 15). Notably, the strength and direction of this immunogenomic correlations may not be common in

all cancer types (16–18), mainly due to the different context of each tumor (43, 44). The impact of CNAs in the setting of HCC has not been comprehensively addressed. Here, we used data from a high-resolution whole-genome SNP array to understand the immune and molecular impact of genomic CNA burdens in HCC, taking into account each tumor's landscape determined using CNApp (19). Similar to other tumor types, in HCC we observed that different broad copy-number landscapes presented distinct immune profiles, while focal CNAs did not impact tumor immunity. Specifically, we observed that HCC tumors with a high burden of broad chromosomal alterations were linked to DNA repair and proliferation signatures and presented immune exclusion. On the other hand, tumors with low levels of broad CNAs displayed features of immunologically "hot" HCCs, higher immune infiltration and cytolytic activity, as well as upregulation of proinflammatory cues. Thus, like it has been described in melanoma (12), we hypothesized that HCCs with low BS might represent potential responders to immunotherapies, whereas high-BS HCCs, potential nonresponders. Our hypothesis is sustained by the fact that (i) tumors responding to anti–PD-1 treatment have a molecular profile similar to low-BS HCCs and (ii) patients with tumors responding to anti–CTLA-4 or anti–PD-L1 correlate with the expression of IFNγ and GZMB, both overexpressed among low-BS tumors (45–47). With regard to focal events, HCCs with a high burden of focal CNAs were characterized by pro-proliferative and more aggressive features, and exhibited no *CTNNB1* mutations. Overall, in our study we propose a strategy to classify HCCs (which usually do not present high TMB) into immune/inflamed and excluded/noninflamed tumors based on CNAs, regardless of the mutational load. This classification expands on our proposed HCC immune classification (9, 10). In particular, we propose a BS ≤ 4 (low BS) as a putative marker to identify patients with HCC with inflamed tumors, and BSs ≥ 11 (high BS) for HCCs lacking immune-related features (**Fig. 5**). The fact that immune traits may be predicted by broad, but not focal CNA loads, is consistent with the above-mentioned pan-cancer study (12). According to this study, tumors with fewer broad copy-number events may sustain higher infiltration of cytotoxic immune cells, and the genetic variability induced in high-BS tumors may provide tumor cells with an advantage to avoid immunologic recognition. However, because no molecular data of patients with HCC treated with immunotherapies are publicly available to date, the predictive value of the scores warrants validation.

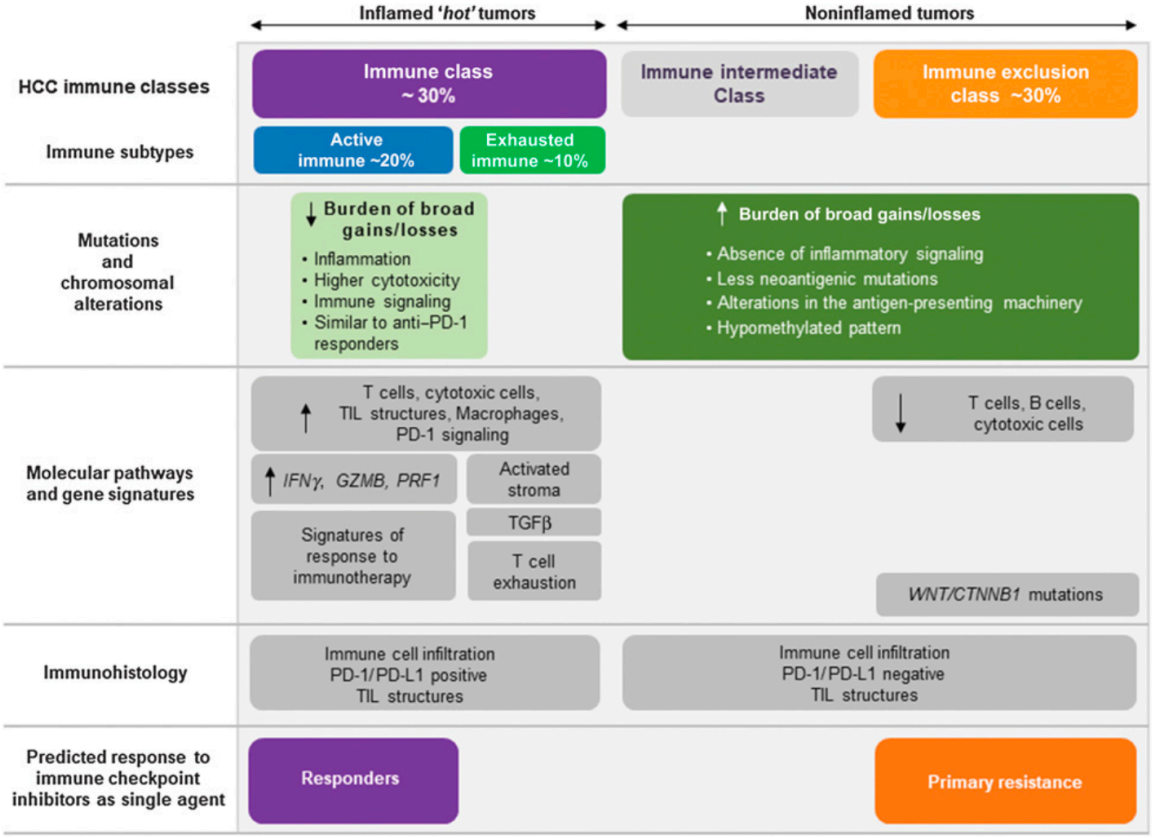

Figure 5.
Immune classification of HCC. Our results complement the previously proposed immune classification of HCC (9, 10). Tumors with low burden of broad CNAs (i.e., those with low BS) presented inflammatory features and were enriched in the HCC immune class. The HCC immune class has been previously reported to display high levels of immune cell infiltration, expression of PD-1 and/or PD-L1, activation of IFNγ signaling, and markers of cytolytic activity (such as granzyme B and perforin 1). On the other hand, HCCs with high loads of broad CNAs lacked immune features, paralleling the HCC exclusion class, were enriched in *CTNNB1* mutations, and are proposed to represent those tumors with innate resistance to anti–PD-1/PD-L1 inhibitors.

We also analyzed the potential mechanisms by which an increase in broad CNA burdens might be associated with exclusion of immune infiltration. It has been described that neoepitopes drive cytolytic activity in tumors (36), and therefore, high mutational loads could render higher neoantigen burdens and greater immune infiltration. In this study, we observed that low-BS HCCs displayed lower burdens of mutations in comparison with high-BS tumors. However, the ratio of observed/expected neoepitopes was lower among high-BS tumors, suggesting that the accumulation of broad CNAs would be linked to an enhanced pruning of neoantigenic mutations, regardless of overall mutation burden. Because the antitumor immune responses are conditioned by the functional presentation of tumor antigens (48), such pruning could contribute to the decreased antitumor immunity features of high-BS HCCs. Of note, an additional reason could be the reduced antigenicity of neoantigenic mutations among high-BS tumors. In other cancer types, it has been reported that not only the number of neoantigens was a determinant of the tumor immune status, but also the ability of neoantigens to induce an immune response (49, 50).

In addition, specific CNAs involving immune-related genes could impact the tumor immune features. In particular, gene losses involved in antigen presentation, found enriched among high-BS HCCs (i.e., HLA-DQB1), could drive the failure to attract effector T cells in these tumors. This, and the fact that high-BS HCCs were enriched in arginine degradation pathways, suggests that these tumors may evade immune destruction by impairing the MHC-mediated antigen presentation, as in lung cancer (48), rather than developing an immunosuppressive microenvironment. Overall, our findings are in concordance with recent studies on NSCLC (TRACERx; ref. 51). Tumors sparsely infiltrated exhibited decreased neoantigen editing indicative of copy-number losses of clonal neoantigens, and dysfunction in the neoantigen-presenting machinery, among the mechanisms of immune evasion (48, 51).

In parallel, the demethylation observed in high-BS tumors could also promote lack of immune infiltration (41). Even though our data suggest potential explanations, further mechanistic studies will be required to determine the causality between tumor CNA burden and antitumor immunity.

On the other hand, the observation that HCCs with high levels of broad CNAs were markedly polyploid, with proliferative features, and associated with poor prognosis signatures, is consistent with a recent publication (52) that proposes ploidy as a prognosis marker.

With regard to focal copy-number events, the fact that high-FS HCCs were more proliferative is consistent with data from other tumor types (12), and has even been demonstrated experimentally through the depletion of *CDKN2A* in human cell lines (53).

Finally, we observed that our findings in HCC were extensible to preneoplastic lesions and very early HCCs. Although further confirmatory studies using larger cohorts would be required, these data align with the idea that CNAs may contribute to the escape from antitumor immune pressure (12, 54).

Overall, our study revealed differential associations between broad and focal genomic CNA burdens and several molecular features of HCC. Most importantly, our data reinforce the evidence supporting a differential role for broad CNAs in determining antitumor immune profiles in HCC and provide evidence in favor of chromosomal stability as a hallmark of tumor immunogenicity, and consequently, patient response to immunotherapies.

Disclosure of Potential Conflicts of Interest

C.E. Willoughby reports grants from Instituto de Salud Carlos III (ISCIII) and the European Social Fund [Sara Borrell Fellowship (CD19/00109)] during the conduct of the study. R. Montal reports personal fees from Servier and Roche outside the submitted work. J.M. Llovet reports grants and personal fees from Bayer HealthCare Pharmaceuticals, Eisai Inc, and Bristol Myers-Squibb, grants from Boehringer-Ingelheim and Ipsen, and personal fees from Celsion Corporation, Exelixis, Eli Lilly, Roche, Genentech, Glycotest, Nucleix, Can-Fite Biopharma, and AstraZeneca outside the submitted work. No potential conflicts of interest were disclosed by the other authors.

Authors' Contributions

L. Bassaganyas: Conceptualization, resources, data curation, formal analysis, supervision, validation, methodology, writing-review and editing. **R. Pinyol:** Conceptualization, data curation, formal analysis, validation, investigation, writing-original draft, writing-review and editing. **R. Esteban-Fabró:** Conceptualization, resources, data curation, formal analysis, validation, investigation, writing-original draft, writing-review and editing. **L. Torrens:** Formal analysis, writing-review and editing. **S. Torrecilla:** Formal analysis, writing-review and editing. **C.E. Willoughby:** Writing-review and editing. **S. Franch-Expósito:** Conceptualization, resources, software, writing-review and editing. **M. Vila-Casadesús:** Data curation, software. **I. Salaverria:** Conceptualization, formal analysis, writing-review and editing. **R. Montal:** Investigation, writing-review and editing. **V. Mazzaferro:** Resources, writing-review and editing. **J. Camps:** Conceptualization, investigation, writing-review and editing. **D. Sia:** Writing-review and editing. **J.M. Llovet:** Conceptualization, resources, supervision, funding acquisition, investigation, writing-review and editing.

Acknowledgments

We would like to thank Dr. Carla Montironi for her contribution in the article. This study has been developed, in part, in the Centre Esther Koplowitz from IDIBAPS/CERCA Programme/Generalitat de Catalunya. The results shown here are, in part, based on data generated by TCGA Research Network: http://cancergenome.nih.gov/. J.M. Llovet was supported by grants from the European Commission Horizon 2020 Program (HEPCAR, proposal number 667273-2), the U.S. Department of Defense (CA150272P3), the NCI (P30 CA196521), the Samuel Waxman Cancer Research Foundation, the Spanish National Health Institute (MICINN, SAF-2016-76390 and PID2019-105378RB-I00), through a partnership between Cancer Research UK, Fondazione AIRC, and Fundación Científica de la Asociacion Española Contra el Cáncer (HUNTER, ref. C9380/A26813), and by the Generalitat de Catalunya (AGAUR, SGR-1358). L. Bassaganyas, R. Esteban-Fabró, and R. Montal were supported by a Beatriu de Pinos grant (AGAUR, 2016BP00161), a MICINN fellowship (BES-2017-081286), and a FSEOM-Boehringer Ingelheim grant, respectively. D. Sia was supported by the Klion Young Scientist award and the PhD Scientist Innovative Research award. C.E. Willoughby was supported by a Sara Borrell fellowship (CD19/00109) from the ISCIII and the European Social Fund. J. Camps was supported by grants from the Instituto de Salud Carlos III and cofunded by the European Regional Development Fund (CPII18/00026 and PI17/01304), the CIBEREHD program, and the Agència de Gestió d'Ajuts Universitaris i de Recerca, Generalitat de Catalunya (2017 SGR 1035). S. Franch-Expósito was supported by a CIBEREHD contract.

The costs of publication of this article were defrayed in part by the payment of page charges. This article must therefore be hereby marked *advertisement* in accordance with 18 U.S.C. Section 1734 solely to indicate this fact.

Received April 20, 2020; revised July 8, 2020; accepted August 28, 2020; published first September 1, 2020.

References

1. Ferlay J, Colombet M, Soerjomataram I, Mathers C, Parkin DM, Piñeros M, et al. Estimating the global cancer incidence and mortality in 2018: GLOBOCAN sources and methods. Int J cancer 2019;144:1941–53.

2. Llovet JM, Montal R, Sia D, Finn RS. Molecular therapies and precision medicine for hepatocellular carcinoma. Nat Rev Clin Oncol 2018;15:599–616.
3. Llovet JM, Zucman-Rossi J, Pikarsky E, Sangro B, Schwartz M, Sherman M, et al. Hepatocellular carcinoma. Nat Rev Dis Prim 2016;2:16018.
4. Galle PR, Finn RS, Qin S, Ikeda M, Zhu AX, Kim T-Y, et al. Patient-reported outcomes (PROs) from the phase III IMbrave150 trial of atezolizumab (atezo) + bevacizumab (bev) vs sorafenib (sor) as first-line treatment (tx) for patients (pts) with unresectable hepatocellular carcinoma (HCC). J Clin Oncol 2020;38:476.
5. El-Khoueiry AB, Sangro B, Yau T, Crocenzi TS, Kudo M, Hsu C, et al. Nivolumab in patients with advanced hepatocellular carcinoma (CheckMate 040): an open-label, non-comparative, phase 1/2 dose escalation and expansion trial. Lancet 2017;389:p2492–502.
6. Zhu AX, Finn RS, Edeline J, Cattan S, Ogasawara S, Palmer D, et al. Pembrolizumab in patients with advanced hepatocellular carcinoma previously treated with sorafenib (KEYNOTE-224): a non-randomised, open-label phase 2 trial. Lancet Oncol 2018;19:940–52.
7. Yau T, Kang Y-K, Kim T-Y, El-Khoueiry AB, Santoro A, Sangro B, et al. Nivolumab (NIVO) + ipilimumab (IPI) combination therapy in patients (pts) with advanced hepatocellular carcinoma (aHCC): results from CheckMate 040. J Clin Oncol 2019;37:4012.
8. Sharma P, Hu-Lieskovan S, Wargo JA, Ribas A. Primary, adaptive, and acquired resistance to cancer immunotherapy. Cell 2017;168:707–23.
9. Sia D, Jiao Y, Martinez-Quetglas I, Kuchuk O, Villacorta-Martin C, Castro de Moura M, et al. Identification of an immune-specific class of hepatocellular carcinoma, based on molecular features. Gastroenterology 2017;153:812–26.
10. Pinyol R, Sia D, Llovet JM. Immune exclusion-Wnt/CTNNB1 class predicts resistance to immunotherapies in HCC. Clin Cancer Res 2019;25:2021–3.
11. Sansregret L, Vanhaesebroeck B, Swanton C. Determinants and clinical implications of chromosomal instability in cancer. Nat Rev Clin Oncol 2018;15:139–50.
12. Davoli T, Uno H, Wooten EC, Elledge SJ. Tumor aneuploidy correlates with markers of immune evasion and with reduced response to immunotherapy. Science 2017;355:eaaf8399.
13. Thorsson VV, Gibbs DL, Brown SD, Wolf D, Bortone DS, Ou Yang TH, et al. The immune landscape of cancer. Immunity 2018;48:812–30.
14. Smith JC, Sheltzer JM. Systematic identification of mutations and copy number alterations associated with cancer patient prognosis. Elife 2018;7:e39217.
15. Taylor AM, Shih J, Ha G, Gao GF, Zhang X, Berger AC, et al. Genomic and functional approaches to understanding cancer aneuploidy. Cancer Cell 2018;33:676–89.
16. Budczies J, Seidel A, Christopoulos P, Endris V, Kloor M, Győrffy B, et al. Integrated analysis of the immunological and genetic status in and across cancer types: impact of mutational signatures beyond tumor mutational burden. Oncoimmunology 2018;7:e1526613.
17. Jiménez-Sánchez A, Cybulska P, Mager KLV, Koplev S, Cast O, Couturier DL, et al. Unraveling tumor–immune heterogeneity in advanced ovarian cancer uncovers immunogenic effect of chemotherapy. Nat Genet 2020;52:582–93.
18. Braun DA, Hou Y, Bakouny Z, Ficial M, Sant' Angelo M, Forman J, et al. Interplay of somatic alterations and immune infiltration modulates response to PD-1 blockade in advanced clear cell renal cell carcinoma. Nat Med 2020;26:909–18.
19. Franch-Expósito S, Bassaganyas L, Vila-Casadesús M, Hernández-Illán E, Esteban-Fabró R, Díaz-Gay M, et al. CNApp, a tool for the quantification of copy number alterations and integrative analysis revealing clinical implications. Elife 2020;9:50267.
20. Villanueva A, Portela A, Sayols S, Battiston C, Hoshida Y, Méndez-González J, et al. DNA methylation-based prognosis and epidrivers in hepatocellular carcinoma. Hepatology 2015;61:1945–56.
21. Ally A, Balasundaram M, Carlsen R, Chuah E, Clarke A, Dhalla N, et al. Comprehensive and integrative genomic characterization of hepatocellular carcinoma. Cell 2017;169:1327–41.
22. Torrecilla S, Sia D, Harrington AN, Zhang Z, Cabellos L, Cornella H, et al. Trunk mutational events present minimal intra- and inter-tumoral heterogeneity in hepatocellular carcinoma. J Hepatol 2017;67:1222–31.
23. Prat A, Navarro A, Paré L, Reguart N, Galván P, Pascual T, et al. Immune-related gene expression profiling after PD-1 blockade in non–small cell lung carcinoma, head and neck squamous cell carcinoma, and melanoma. Cancer Res 2017;77:3540–50.
24. Chiang DY, Villanueva A, Hoshida Y, Peix J, Newell P, Minguez B, et al. Focal gains of VEGFA and molecular classification of hepatocellular carcinoma. Cancer Res 2008;68:6779–88.
25. Guichard C, Amaddeo G, Imbeaud S, Ladeiro Y, Pelletier L, Maad IB, et al. Integrated analysis of somatic mutations and focal copy-number changes identifies key genes and pathways in hepatocellular carcinoma. Nat Genet 2012;44:694–8.
26. Schulze K, Imbeaud S, Letouzé E, Alexandrov LB, Shinde J, Soysouvanh F, et al. Exome sequencing of hepatocellular carcinomas identifies new mutational signatures and potential therapeutic targets. Nat Genet 2015;47:505–11.
27. Hoshida Y, Nijman SMBS, Kobayashi M, Chan Ja, Brunet J-P, Chiang DY, et al. Integrative transcriptome analysis reveals common molecular subclasses of human hepatocellular carcinoma. Cancer Res 2009;69:7385–92.
28. Yoshihara K, Shahmoradgoli M, Martínez E, Vegesna R, Kim H, Torres-Garcia W, et al. Inferring tumour purity and stromal and immune cell admixture from expression data. Nat Commun 2013;4:2612.
29. Lee J, Heo J, Libbrecht L, Chu I, Kaposi-Novak P, Calvisi DF, et al. A novel prognostic subtype of human hepatocellular carcinoma derived from hepatic progenitor cells. Nat Med 2006;12:410–6.
30. Andersen JB, Loi R, Perra A, Factor VM, Ledda-Columbano GM, Columbano A, et al. Progenitor-derived hepatocellular carcinoma model in the rat. Hepatology 2010;51:1401–9.
31. Villanueva A, Hoshida Y, Battiston C, Tovar V, Sia D, Mazzaferro V, et al. Combining clinical, pathology, and gene expression data to predict recurrence of hepatocellular carcinoma. Gastroenterology 2011;140:1501–12.
32. Mínguez B, Hoshida Y, Villanueva A, Toffanin S, Cabellos L, Thung S, et al. Gene-expression signature of vascular invasion in hepatocellular carcinoma. J Hepatol 2011;55:1325–31.
33. Kaposi-Novak P, Lee J-S, Gòmez-Quiroz L, Coulouarn C, Factor VM, Thorgeirsson SS. Met-regulated expression signature defines a subset of human hepatocellular carcinomas with poor prognosis and aggressive phenotype. J Clin Invest 2006;116:1582–95.
34. Coulouarn C, Factor VM, Thorgeirsson SS. Transforming growth factor-beta gene expression signature in mouse hepatocytes predicts clinical outcome in human cancer. Hepatology 2008;47:2059–67.
35. Charoentong P, Finotello F, Angelova M, Mayer C, Efremova M, Rieder D, et al. Pan-cancer immunogenomic analyses reveal genotype-immunophenotype relationships and predictors of response to checkpoint blockade. Cell Rep 2017;18:248–62.
36. Rooney MSS, Shukla SAA, Wu CJJ, Getz G, Hacohen N. Molecular and genetic properties of tumors associated with local immune cytolytic activity. Cell 2015;160:48–61.
37. Sautès-Fridman C, Petitprez F, Calderaro J, Fridman WH. Tertiary lymphoid structures in the era of cancer immunotherapy. Nat Rev Cancer 2019;19:307–25.
38. Calderaro J, Petitprez F, Becht E, Laurent A, Hirsch TZ, Rousseau B, et al. Intratumoral tertiary lymphoid structures are associated with a low risk of early recurrence of hepatocellular carcinoma. J Hepatol 2019;70:58–65.
39. Hoadley KA, Yau C, Hinoue T, Wolf DM, Lazar AJ, Drill E, et al. Cell-of-origin patterns dominate the molecular classification of 10,000 tumors from 33 types of cancer. Cell 2018;173:291–304.
40. Zhang L, Li M, Deng B, Dai N, Feng Y, Shan J, et al. HLA-DQB1 expression on tumor cells is a novel favorable prognostic factor for relapse in early-stage lung adenocarcinoma. Cancer Manag Res 2019;11:2605–16.
41. Jung H, Kim HS, Kim JY, Sun JM, Ahn JS, Ahn MJ, et al. DNA methylation loss promotes immune evasion of tumours with high mutation and copy number load. Nat Commun 2019;10:4278.
42. Roh W, Chen PL, Reuben A, Spencer CN, Prieto PA, Miller JP, et al. Integrated molecular analysis of tumor biopsies on sequential CTLA-4 and PD-1 blockade reveals markers of response and resistance. Sci Transl Med 2017;9:eaah3560.
43. Bianchi JJ, Zhao X, Mays JC, Davoli T. Not all cancers are created equal: Tissue specificity in cancer genes and pathways. Curr Opin Cell Biol 2020;63:135–43.
44. Ben-David U, Amon A.Context is everything: aneuploidy in cancer. Nat Rev Genet 2020;21:44–62.
45. Tumeh PC, Harview CL, Yearley JH, Shintaku IP, Taylor EJM, Robert L, et al. PD-1 blockade induces responses by inhibiting adaptive immune resistance. Nature 2014;515:568–71.
46. Rizvi NA, Hellmann MD, Snyder A, Kvistborg P, Makarov V, Havel JJ, et al. Mutational landscape determines sensitivity to PD-1 blockade in non-small cell lung cancer. Science 2015;348:124–8.
47. Chan TA, Wolchok JD, Snyder A. Genetic basis for clinical response to CTLA-4 blockade in melanoma. N Engl J Med 2015;373:1984.

48. Rosenthal R, Cadieux EL, Salgado R, Bakir MA, Moore DA, Hiley CT, et al. Neoantigen-directed immune escape in lung cancer evolution. Nature 2019;567:479–85.
49. McGranahan N, Furness AJSS, Rosenthal R, Ramskov S, Lyngaa R, Saini SK, et al. Clonal neoantigens elicit T cell immunoreactivity and sensitivity to immune checkpoint blockade. Science, 2016;351:1463–9.
50. Turajlic S, Litchfield K, Xu H, Rosenthal R, McGranahan N, Reading JL, et al. Insertion-and-deletion-derived tumour-specific neoantigens and the immunogenic phenotype: a pan-cancer analysis. Lancet Oncol 2017;18:1009–21.
51. Jamal-Hanjani M, Wilson GA, McGranahan N, Birkbak NJ, Watkins TBK, Veeriah S, et al. Tracking the evolution of non–small-cell lung cancer. N Engl J Med 2017;376:2109–21.
52. Hélias-Rodzewicz Z, Lourenco N, Bakari M, Capron C, Emile J-FF. CDKN2A depletion causes aneuploidy and enhances cell proliferation in non-immortalized normal human cells. Cancer Invest 2018;36:338–48.
53. Bou-nader M, Caruso S, Donne R, Celton-Morizur S, Calderaro J, Gentric G, et al. Polyploidy spectrum: a new marker in HCC classification. Gut 2020;69:355–64.
54. Meylan M, Petitprez F, Lacroix L, Di Tommaso L, Roncalli M, Bougoüin A, et al. Early hepatic lesions display immature tertiary lymphoid structures and show elevated expression of immune inhibitory and immunosuppressive molecules. Clin Cancer Res 2020;26:4381–9.

Study 2: Cabozantinib enhances anti-PD1 activity and elicits a neutrophil-based immune response in hepatocellular carcinoma

Roger Esteban-Fabró*, Catherine E Willoughby*, Marta Piqué-Gili, Carla Montironi, Jordi Abril-Fornaguera, Judit Peix, Laura Torrens, Agavni Mesropian, Ugne Balaseviciute, Francesc Miró-Mur, Vincenzo Mazzaferro, Roser Pinyol, Josep M Llovet.

**Shared first authorship.*

Clinical Cancer Research, 2022 Jun;28(11):2449-2460. (IF: 13.801, Q1)

Summary

The treatment landscape for advanced HCC has changed dramatically after the positive results of the phase III IMbrave150 trial, which positioned atezolizumab plus bevacizumab, the first combination therapy and first treatment regimen involving an immunotherapy, as the standard of care in first line[3]. Despite extending median overall survival to 19.2 months, primary resistance rates are high at around 70%; this highlights the need to develop more efficacious therapeutic strategies and predictive biomarkers[2]. Given that immunotherapeutic agents show better results among tumors with an inflammatory microenvironment[6] and that proangiogenic molecules are immunosuppressive, the antitumor activity of immunotherapy could be enhanced by promoting the infiltration or reactivation of immune cells in combinatorial strategies with antiangiogenic agents[7]. In this context, the **tyrosine kinase inhibitor (TKI) cabozantinib is a promising candidate for combinatory strategies**: in addition to its anti-angiogenic and anti-proliferative activity[149], immune-modulatory effects have been reported in experimental prostate cancer models[150].

In light of the above, we aimed **to explore the antitumoral and immunomodulatory effects of cabozantinib alone and in combination with anti-PD1**. Specifically, we aimed (1) to evaluate the efficacy of cabozantinib alone and combined with anti-PD1 in a syngeneic murine HCC model; (2) to investigate the mechanism of action and immunomodulatory effects of cabozantinib and the combination; and (3) to identify combination-like molecular profiles in human HCC.

This study was performed using two syngeneic murine HCC models based on C57BL/6J mice bearing subcutaneous Hepa1-6 or Hep53.4 tumors (n=80 and 40, respectively). Animals were randomized to receive cabozantinib, anti-PD1, their combination or placebo. Tumor samples were used for flow cytometry, IHC and transcriptome analysis, while blood samples were used for flow cytometry and cytokine profiling. Cabozantinib-related effects were validated in transcriptomic data from a colorectal cancer patient-derived xenograft model. Finally, transcriptomic data from three human HCC cohorts (cohort1: n=167, cohort 2: n=57, The Cancer Genome Atlas: n=319) were used to cluster patients according to combination-like expression features and to assess their impact on overall survival.

Our findings were the following:

1. **Combination** treatment induced a **significantly shorter time to objective response** versus the rest of treatment arms. It also induced the **greatest anti-tumor growth effect** and the **greatest objective response rate** (ORR). In addition, **both cabozantinib and combination** treatments induced a significant **reduction in viable tumor volume** and **increased tumor necrosis**.

2. The **antiangiogenic effects** in **cabozantinib and combination** arms were confirmed by reduced **CD31 staining**, absence of **vessels encapsulating tumor clusters**, reduced enrichment in transcriptomic **signatures of angiogenesis** and more enrichment in **hypoxia-related signatures**. Combination was also associated with the greatest reduction in gene expression signatures of proliferation and DNA repair.

3. Immune population assessment of infiltrating immune cells (with flow cytometry, immunohistochemistry and transcriptomic analysis) revealed that **cabozantinib** and **combination** induced a significant **recruitment of intratumor neutrophils**. In addition, **neutrophil antitumor activity** was the biological process most significantly associated with the 100 genes uniquely upregulated by the **combination**.

4. Further immune characterization revealed that all **anti-PD1 and combination**-treated samples recapitulated the **immune class of HCC**. **Combination** was significantly associated with **upregulation** of transcriptomic pathways of **inflammation, innate and adaptive immunity** and with **downregulation** of **TGFβ** and **β-catenin** pathways.

Cabozantinib and **combination** induced a **reduction in CD8+ PD1+ lymphocytes** and **intratumoral T regulatory cells**.

5. At the systemic level, **cabozantinib** and **combination increased** the proportions of **circulating T and CD8$^+$ T cells** and **reduced** the **neutrophil-to-lymphocyte ratio** in blood. **Combination** specifically increased the proportions of **circulating memory/effector T and CD8$^+$ T cells**, and the levels of the chemoattractants **CCL27** and **IL-16**.

6. We defined three **human HCC clusters** (*Neutrophil Enriched*, *Neutrophil Depleted* and *Tumor-only Neutrophil Depleted*) based on enrichment in a signature reflecting the neutrophil activation in combination-treated mice. The **Neutrophil Enriched cluster** (25% of patients), with high active neutrophil enrichment in tumor and adjacent tissue, presented a **lack of immune exclusion**, **reduced stem cell and proliferation** features, and was linked to **longer survival**.

Overall, our data suggests that the combination of cabozantinib with anti-PD1 enhances anti-tumor immunity by bringing together innate neutrophil-driven and adaptive immune responses, a mechanism of action which could broaden the spectrum of responders in HCC. Human HCC tumors enriched in combination-like neutrophil features display a favorable molecular and clinical profile, suggesting the benefit of this combination for HCC treatment.

CLINICAL CANCER RESEARCH | TRANSLATIONAL CANCER MECHANISMS AND THERAPY

Cabozantinib Enhances Anti-PD1 Activity and Elicits a Neutrophil-Based Immune Response in Hepatocellular Carcinoma

Roger Esteban-Fabró[1,2], Catherine E. Willoughby[1], Marta Piqué-Gili[1], Carla Montironi[1], Jordi Abril-Fornaguera[1], Judit Peix[1], Laura Torrens[1,2], Agavni Mesropian[1], Ugne Balaseviciute[1], Francesc Miró-Mur[3], Vincenzo Mazzaferro[4,5], Roser Pinyol[1], and Josep M. Llovet[1,2,6]

ABSTRACT

Purpose: Immune checkpoint inhibitors combined with antiangiogenic agents produce benefits in the treatment of advanced hepatocellular carcinoma (HCC). We investigated the efficacy and immunomodulatory activity of cabozantinib alone and combined with anti-PD1 in experimental models of HCC, and explored the potential target population that might benefit from this combination.

Experimental Design: C57BL/6J mice bearing subcutaneous Hepa1-6 or Hep53.4 tumors received cabozantinib, anti-PD1, their combination, or placebo. Tumor and blood samples were analyzed by flow cytometry, IHC, transcriptome, and cytokine profiling. Cabozantinib-related effects were validated in a colorectal cancer patient-derived xenograft model. Transcriptomic data from three human HCC cohorts (cohort 1: $n = 167$, cohort 2: $n = 57$, The Cancer Genome Atlas: $n = 319$) were used to cluster patients according to neutrophil features, and assess their impact on survival.

Results: The combination of cabozantinib and anti-PD1 showed increased antitumor efficacy compared with monotherapy and placebo ($P < 0.05$). Cabozantinib alone significantly increased neutrophil infiltration and reduced intratumor $CD8^+PD1^+$ T-cell proportions, while the combination with anti-PD1 further stimulated both effects and significantly decreased regulatory T cell (Treg) infiltration (all $P < 0.05$). In blood, cabozantinib and especially combination increased the proportions of overall T cells ($P < 0.01$) and memory/effector T cells ($P < 0.05$), while lowering the neutrophil-to-lymphocyte ratio ($P < 0.001$ for combination). Unsupervised clustering of human HCCs revealed that high tumor enrichment in neutrophil features observed with the treatment combination was linked to less aggressive tumors with more differentiated and less proliferative phenotypes.

Conclusions: Cabozantinib in combination with anti-PD1 enhanced antitumor immunity by bringing together innate neutrophil-driven and adaptive immune responses, a mechanism of action which favors this approach for HCC treatment.

Introduction

Hepatocellular carcinoma (HCC) is the most common form of primary liver cancer, which is the third leading cause of cancer-related death and a major health problem globally (1, 2). Around 50%–60% of patients will be ultimately exposed to systemic therapies, where the combination of atezolizumab and bevacizumab has become the standard of care in first line. In the phase III IMbrave150 trial, this combination demonstrated significantly better overall survival (OS) and progression-free survival (PFS) versus sorafenib (median OS 19.2 vs. 13.4 months; refs. 3, 4), the multikinase inhibitor which had been the previous standard of care for advanced HCC for the past 12 years (5). This marks the first combination therapy and first treatment regimen involving an immunotherapy to induce a greater survival benefit for patients with HCC compared with existing therapies, although objective responses (OR) were restricted to 30% of patients (3). Single-agent immune checkpoint inhibitors (ICI)—that is, nivolumab and pembrolizumab—had also shown promising results over the past decade, with median OS of 13–16 months reported in patients with advanced HCC (6, 7). However, no ICI monotherapy significantly extended OS in phase III trials. In addition, recent data have revealed that nonviral HCC, particularly nonalcoholic steatohepatitis (NASH)-related HCC, might be less responsive to immunotherapy due to the intratumor accumulation of a population of dysfunctional activated $CD8^+PD1^+$ T cells (8). Thus, there is an unmet need to better understand the complex mechanisms underlying antitumor immunity and explaining response and resistance to immunotherapies, to favor the development of more efficacious therapeutic strategies with immunotherapies (9), including combination therapies.

Given that immunotherapeutic strategies show better results among tumors with an inflammatory microenvironment (10), efforts are being made to enhance the antitumor activity of ICIs by promoting the infiltration or reactivation of immune cells in tumors which lack an inflamed profile. One approach to this is via the

[1]Translational Research in Hepatic Oncology Laboratory, Liver Unit, Institut d'Investigacions Biomèdiques August Pi i Sunyer (IDIBAPS), Hospital Clínic, University of Barcelona, Barcelona, Catalonia, Spain. [2]Mount Sinai Liver Cancer Program, Division of Liver Diseases, Tisch Cancer Institute, Icahn School of Medicine at Mount Sinai, New York, New York. [3]Systemic Autoimmune Diseases, Vall d'Hebron Institut de Recerca (VHIR), Barcelona, Catalonia, Spain. [4]Department of Surgery, Fondazione IRCCS Istituto Nazionale dei Tumori, Milan, Italy. [5]Department of Oncology, University of Milan, Milan, Italy. [6]Institució Catalana de Recerca i Estudis Avançats (ICREA), Barcelona, Catalonia, Spain.

Note: Supplementary data for this article are available at Clinical Cancer Research Online (http://clincancerres.aacrjournals.org/).

R. Esteban-Fabró and C.E. Willoughby contributed equally to this article.

Corresponding Author: Josep M. Llovet, Translational Research in Hepatic Oncology Laboratory, Liver Unit, IDIBAPS-Hospital Clinic, University of Barcelona, C/Rosselló 153, 08036, Barcelona, Catalonia, Spain. Phone: 34-93-227-9155; E-mail: jmllovet@clinic.cat

Clin Cancer Res 2022;28:2449–60

doi: 10.1158/1078-0432.CCR-21-2517

Translational Relevance

Hepatocellular carcinoma (HCC) is the most common type of liver cancer, which is the third leading cause of cancer-related death worldwide. The combination of immune checkpoint inhibitors with antiangiogenic agents produces survival benefits in advanced HCC, but only for around 30% of patients, so new strategies to overcome tumor-intrinsic resistance are urgently needed. Here we used preclinical models to explore the efficacy and immunologic impact behind combining cabozantinib and anti-PD1 therapy for the treatment of HCC. We provide evidence that cabozantinib in combination with anti-PD1 enhances antitumor immunity by bringing together innate neutrophil-driven and adaptive immune responses, which is associated with greater antitumor responses than either monotherapy, thus providing a mechanistic rationale supporting this combination as a new treatment strategy for HCC. We also identify a subgroup of human HCC with reduced enrichment of active neutrophil phenotypes which displays significantly worse outcomes, and may therefore benefit the most from this combination.

combination of ICIs with antiangiogenic agents, in light of the reported immunosuppressive role of proangiogenic molecules (mainly VEGF, angiopoietins, hepatocyte growth factor and the platelet-derived growth factor family; refs. 11, 12). Encouraging results have been obtained for combinations of ICIs plus antiangiogenic therapies in preclinical studies (13, 14), as well as in clinical trials across different cancer types including HCC (3, 15, 16).

Cabozantinib, a tyrosine kinase inhibitor (TKI), proved its efficacy in a phase III trial with patients with advanced HCC who had progressed on sorafenib, and extended median OS to 10.2 months from 8.0 months with placebo (17). Among other kinases, cabozantinib targets VEGFR, AXL, and MET, key factors in pathways promoting angiogenesis, proliferation, and epithelial-to-mesenchymal transition (18, 19). Therefore, the combination of cabozantinib and ICIs may lead to enhanced clinical benefits over monotherapies in HCC, and in fact, the combination of nivolumab + cabozantinib conveyed a median PFS of 5.5 months in patients with advanced HCC, with median OS not reached (20). The phase III study assessing the combination of atezolizumab + cabozantinib (COSMIC-312; ref. 21) reported in the first interim analysis a significant improvement in PFS versus sorafenib (HR: 0.63; 99% CI, 0.44–0.91; $P = 0.0012$), and a nonsignificant trend in terms of OS impact (22). Studies in experimental models of prostate cancer have also suggested that cabozantinib may have immunomodulatory activity (23); however, this has not yet been explored in HCC.

Our study explored the antitumoral, mechanistic, and immunomodulatory effects of cabozantinib alone and in combination with anti-PD1 in two preclinical HCC mouse models. The combination of cabozantinib with anti-PD1 (i) was associated with greater efficacy than any single treatment alone, (ii) enhanced neutrophil recruitment and neutrophil activation profiles, and (iii) decreased $CD8^+PD1^+$ T and regulatory T cell (Treg) infiltration in the tumor. Finally, human HCC data revealed that tumors with neutrophil-based enrichment are linked with better molecular and clinical features. Therefore, the combination of cabozantinib and anti-PD1 has the potential to bring together the activation of adaptive and innate immune responses against the tumor in patients with HCC.

Materials and Methods

Experimental mouse models

Immunocompetent murine models of HCC were generated by subcutaneously implanting 5×10^6 Hepa1-6 cells (model 1) or 5×10^6 Hep 53.4 cells (model 2) suspended in Matrigel (50% volume for volume) into the right flank of male 5-week-old C57BL/6 mice (model 1: $n = 80$, model 2: $n = 40$). When tumors reached a volume of 200–300 mm^3, animals were randomly assigned to receive: (i) placebo: Hamster IgG 10 mg/kg i.p. every 3 days for a total of five doses; (ii) cabozantinib: 30 mg/kg orally daily until the end of the study; (iii) anti-PD1: Hamster anti-murine PD1 mAb J43 (BioXCell) intraperitoneal at 10 mg/kg every 3 days for a total of five doses; or (iv) combination of cabozantinib with anti-PD1. Tumor volume measurements were taken every 2–3 days using bilateral callipers, and tumor response rates were calculated as described in the Supplementary Materials and Methods. In model 1, 6 mice per group were randomly selected and culled on day 14 of treatment for pharmacodynamic analyses. The remaining 14 mice per group were monitored until their tumor volume surpassed 1,500 mm^3 or reached day 32 of treatment (Supplementary Fig. S1). Model 2 was used as validation and all animals were culled at day 14. Animal experiments were approved by the corresponding review board. As a further independent model, we also analyzed the RNA sequencing (RNA-seq) data from paired human colorectal cancer patient-derived xenograft (PDX) models treated with cabozantinib (30 mg/kg daily orally) or vehicle (24).

Flow cytometry

Peripheral blood samples were collected by cardiac puncture under deep terminal anesthesia and subjected to red blood cell lysis. Tumor tissues were minced with forceps and scissors, followed by chemical and mechanical disaggregation. The resulting single-cell suspensions were incubated with antibody conjugates to identify specific populations of myeloid (dendritic cells, macrophages, and neutrophils) and lymphoid (leukocytes, $CD4^+$ T cells, $CD8^+$ T cells, Tregs, PD1-expressing $CD8^+$ T cells, memory T cells, and B cells) immune cells, and stained with a viability dye (Supplementary Tables S1–S3) and in the presence of a Fc receptor blocking reagent. Samples were analyzed on a 5-laser Fortessa flow cytometer (BD Biosciences) using BD FACSDiva software v8.0.

Gene expression profiling of mouse tumors

Gene expression profiling of mouse tumor samples was performed using a whole-genome microarray platform (GeneChip Mouse Genome 430 2.0 Array, Affymetrix; GSE174770). Mouse expression data were retrieved, quality checked, and processed through RMA using the R package *affy* (v.1.62.0). After quality filtering, probe-gene correlates were identified with the R package *htmg430pmprobe* (v.2.18.0). Subsequently, the mouse gene expression matrix was humanized using the mouse-human orthologs data available in ENSEMBL (retrieved using BioMart) and Mouse Genome Informatics (MGI, informatics.jax.org). Molecular Signature Database gene sets (MSigDB, broadinstitute.org/msigdb) and previously reported gene signatures representing different states of inflammation, HCC subclasses, or distinct immune cell populations (25–28) were tested using enrichment tools implemented in GenePattern [ref. 29; gene set enrichment analysis (GSEA) and single-sample GSEA (ssGSEA)]. In addition, the GenePattern module Comparative Marker Selection (CMS) was used to identify differential gene expression between treated and untreated tumors (FDR < 0.05, FC ≥ 1.5), and the Enrichr tool (30) was used to evaluate enrichment in specific pathways and

biological functions among the differentially expressed genes (DEG; Supplementary Tables S5 and S6). We considered as neutrophil-related genes those DEGs classified within biological functions linked to neutrophil activity. A signature reflecting the specific molecular effect of combination therapy (CAP-100) was retrieved by selecting the upregulated genes in the combination arm versus placebo and deducting those genes commonly upregulated between the combination and the monotherapies.

Human samples and molecular profiling

We analyzed the gene expression data of 167 paired HCC tumor and tumor-adjacent liver obtained by our group (25, 31) from untreated, surgically resected fresh-frozen samples (cohort 1: Heptromic, GSE63898). Supplementary Table S7 depicts the clinical features of the subset of 167 patients, and a complete description of the full cohort can be found elsewhere (25, 31). In addition, we used a second cohort of 57 untreated patients with HCC with paired expression data from the tumor and tumor-adjacent liver (cohort 2: Supplementary Table S7, GSE174570). Samples from both cohorts were collected through the International HCC Genomic Consortium under the corresponding Institutional Review Board approval for each center. We also used the survival and expression data of 319 patients with HCC publicly available from The Cancer Genome Atlas (TCGA; ref. 32).

RNA extractions from fresh-frozen samples were performed as reported previously (31), and RNA profiling was conducted using the Human Genome U219 Array Plate (Affymetrix). The processing of transcriptome data (normalization, background correction, and filtering) was carried out as described previously (31). Prediction of mRNA-based signature positivity was performed with GenePattern's nearest template prediction (NTP) module, and gene expression signature enrichment as well as differential gene expression analysis were carried out as with the mouse tumor expression data. K-medoids clustering was used for the unsupervised classification of samples according to the enrichment in gene expression signatures (Supplementary Fig. S9). The optimal number of clusters was determined as the k with the maximum silhouette width.

Statistical analysis

Statistical analyses were performed using R (version 3.6.1). Specifically, nonparametric tests were used for the comparison of distribution of continuous variables (Wilcoxon or Kruskal–Wallis tests). For the assessment of correlations between two continuous variables, we used Spearman rank correlation coefficient test. Univariate analysis of survival was conducted using the log-rank test, while a multivariate Cox proportional hazards model was conducted to identify independent predictors of survival. In the event of a multiple comparison testing, Benjamini–Hochberg correction was applied unless specified otherwise. In general, adjusted P values <0.05 (two-sided) were considered to be statistically significant and are denoted as follows (unless stated otherwise in specific analyses): *, $P < 0.05$; **, $P < 0.01$; ***, $P < 0.001$. NS indicates not significant, $P > 0.05$.

Data availability

Data generated or analyzed by the authors is available in Gene Expression Omnibus at GSE174770, GSE60939, GSE63898, and GSE174570.

Full details of the Materials and Methods are given in the Supplementary Data.

Results

Cabozantinib plus anti-PD1 treatment displayed higher antitumor efficacy as compared with the monotherapies

We used subcutaneous murine models of HCC to assess the antitumor efficacy of cabozantinib, anti-PD1, and combination (Supplementary Fig. S1), and evaluated tumor response rate according to RECIST adapted for murine models. In the Hepa1-6 model, the combination of cabozantinib and anti-PD1 most rapidly induced an OR out of all treatment arms, with statistically significant improvements versus cabozantinib alone or anti-PD1 monotherapy, as well as placebo (median time to OR: 12.6 days for combination vs. 20.1 days for cabozantinib monotherapy, with time to OR not reached in the anti-PD1 and placebo arms; $P < 0.05$; **Fig. 1A**; Supplementary Fig. S2A). Of note, cabozantinib and anti-PD1 monotherapies also significantly accelerated time to achieve an OR compared with placebo ($P < 0.05$). In addition, the combination treatment induced the highest OR and complete response rates (CRR; 70% ORR and 15% CRR), followed by cabozantinib (35% ORR and 5% CRR) and anti-PD1 (25% ORR and 15% CRR), and all treatment-induced ORRs were significantly higher as compared with placebo (0% ORR, $P < 0.05$; **Fig. 1B**). All treatments also delayed tumor growth versus placebo ($P < 0.05$), and no adverse clinical signs or loss in starting body weight were detected throughout the study (Supplementary Fig. S2B and S2C). These findings were also recapitulated in the Hep53.4 model (Supplementary Fig. S2D–S2F).

Excised HCC tumors were then evaluated at the molecular and histopathologic level. First, examination of the tumor sections revealed that cabozantinib and combination treatments were associated with significant reductions in viable tumor volume and increases in the percentage of tumor necrosis (**Fig. 1C**). On the other hand, and confirming the antiangiogenic activity of cabozantinib (18, 19, 24), IHC detection of endothelial cells by CD31 staining revealed that only placebo and anti-PD1 tumors contained marked or moderate levels of vascular endothelial cells, and cabozantinib-treated tumors (monotherapy and combination) were associated with significantly reduced areas of $CD31^{+}$ staining compared with placebo ($P < 0.05$; **Fig. 1D**). In addition, only cabozantinib and combination-treated tumors displayed an absence of vessels encapsulating tumor clusters (VETC; **Fig. 1D**).

Analysis of the tumor whole-genome expression profile revealed the impact of therapies in reducing proliferation and angiogenesis. Regarding proliferation, using the NTP and ssGSEA modules of GenePattern, we observed that placebo-treated tumors were associated with the Chiang proliferation (26) and the Boyault G3 (28) subclasses of HCC, and also displayed increased expression of a wide array of proliferation and DNA repair signatures (**Fig. 1E**). Furthermore, administration of cabozantinib (monotherapy or combination) significantly impacted angiogenesis by reducing VEGF and endothelial cell signaling and promoting enrichment in molecular signatures of hypoxia (**Fig. 1E**). Combination was the only treatment associated with a significant reduction in proliferation and DNA repair signatures as compared with placebo, with a similar but nonsignificant trend also observed in cabozantinib monotherapy–treated tumors. Taken together, these data demonstrate that cabozantinib treatment induced antiproliferative effects in the tumors and these were more marked when administered in combination with anti-PD1.

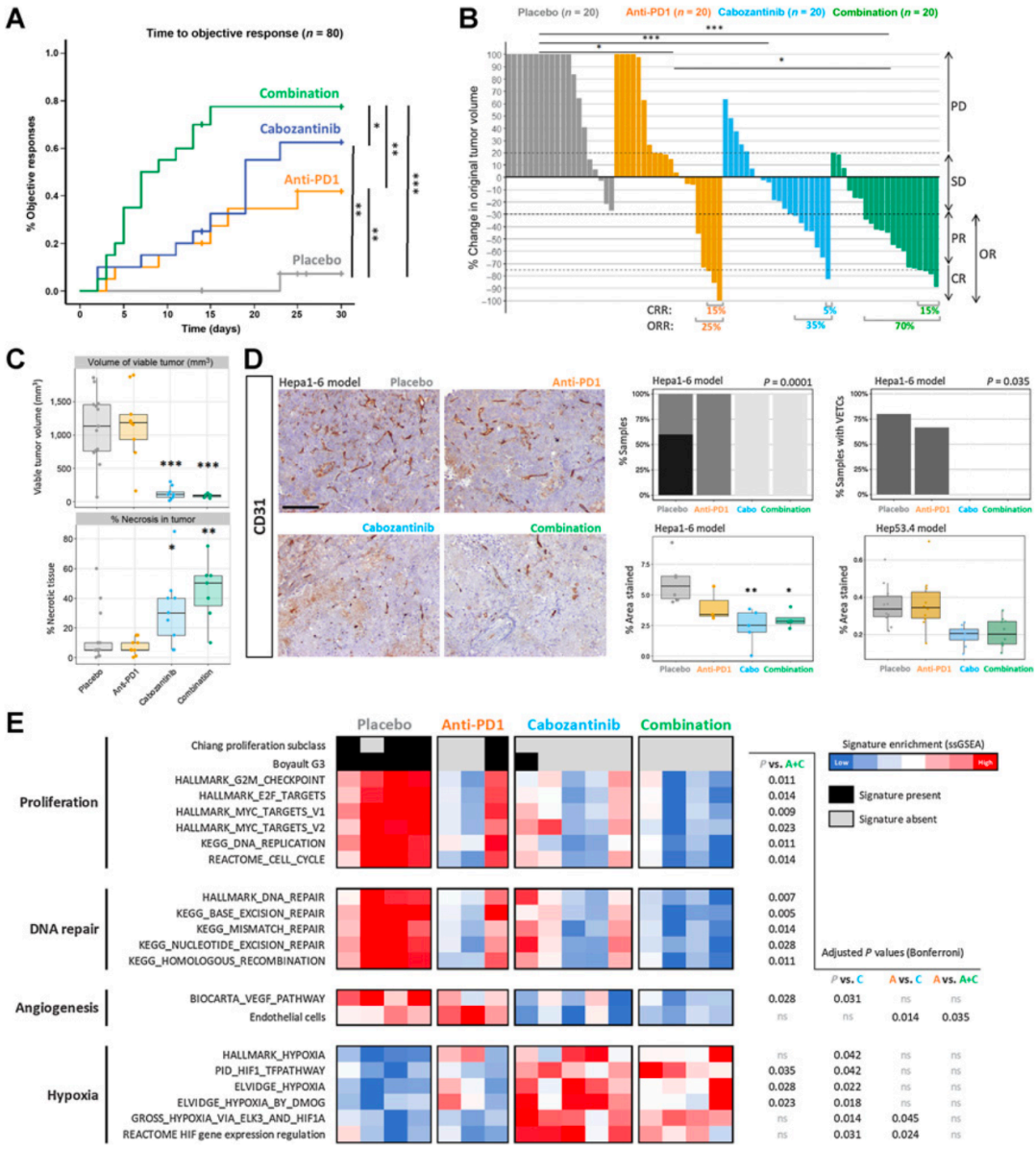

Figure 1.

Cabozantinib + anti-PD1 has a strong antitumor activity and promotes vascular normalization in a murine HCC model. C57BL/6J mice bearing Hepa1–6 tumors were treated with anti-PD1 or placebo IgG ± oral cabozantinib ($n = 20$ mice/arm). **A,** Time taken to achieve an OR (log-rank test P values depicted). **B,** Waterfall plot of tumor response at day 14 according to RECIST (Fisher exact test P values depicted). The Y-axis is capped at +100% and therefore only the first doubling in tumor volume is accurately depicted. CR, complete response; OR, objective response; PD, progressive disease; PR, partial response; SD, stable disease. **C,** Volume of viable tumor (mm^3) and % of tumor necrosis from tumors at day 32 (compared vs. placebo). **D,** Representative images of CD31 staining across the four treatment groups, 100× magnification (left, scale bar = 200 μm). Plots on the right depict the proportion of samples with mild, moderate, or marked CD31 staining; the quantification of tumor vascular endothelial cells stained with CD31 (compared vs. placebo, and validation in the Hep53.4 model); and the percentage of samples with VETCs. Images taken at 100× magnification. Scale bar = 200 μm. **E,** Heatmap reflecting enrichment in signatures of proliferation, DNA repair, angiogenesis, and hypoxia obtained through NTP and ssGSEA. *, $P < 0.05$; **, $P < 0.01$; ***, $P < 0.001$; ns, $P > 0.05$.

Combination treatment induced intratumoral neutrophil infiltration

Immune population analysis using flow cytometry, IHC, and transcriptomic data revealed that cabozantinib administration promoted the recruitment of neutrophils in the tumor tissue. Specifically, through flow cytometry, we observed median 2.5- and 1.8-fold increases in the prevalence of tumor-infiltrating neutrophils in cabozantinib and combination treatment arms versus placebo ($P < 0.05$ vs.

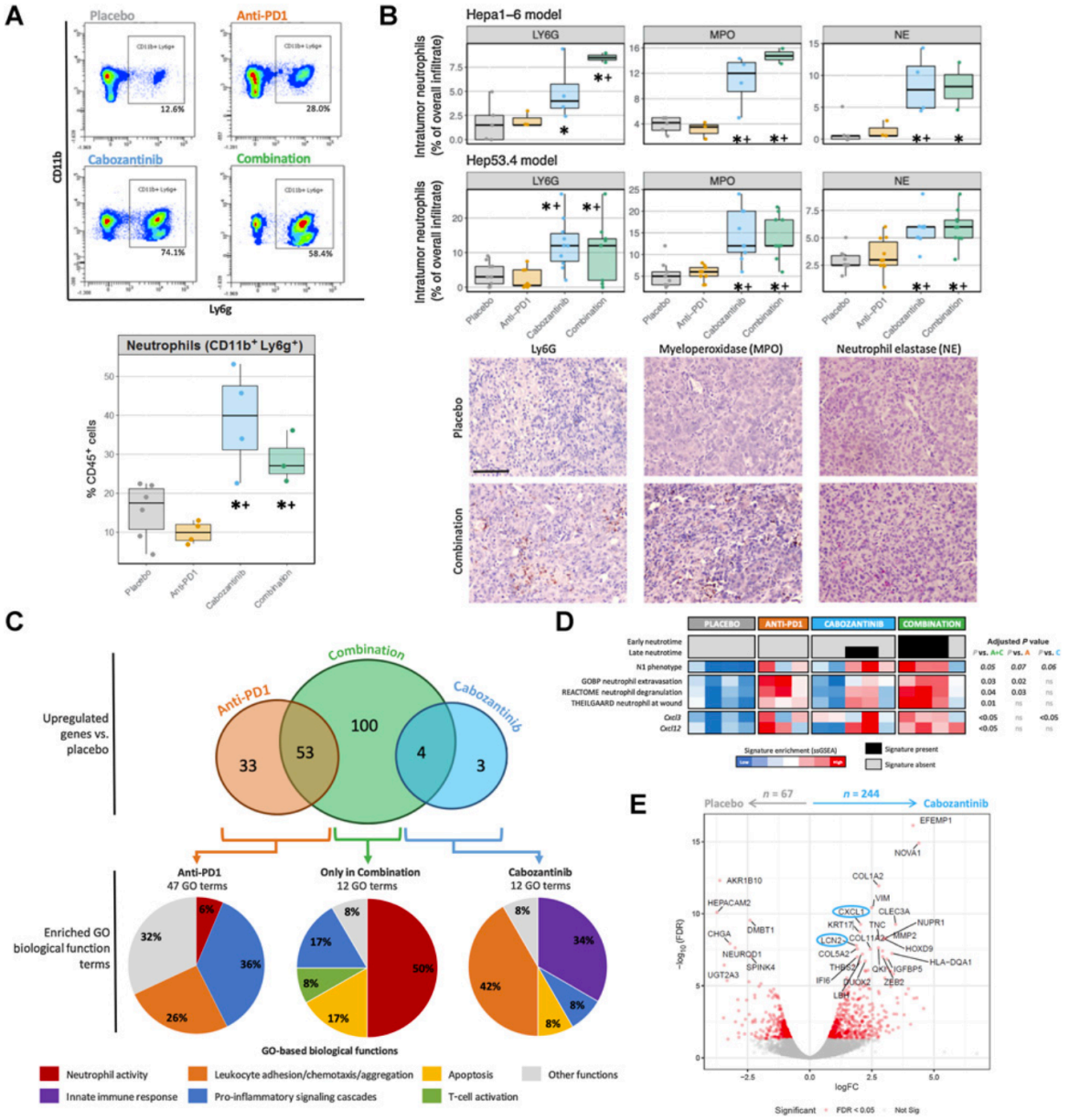

Figure 2.

Cabozantinib treatment induces intra-tumoural neutrophil infiltration and activation in preclinical models. **A,** Representative flow cytometry results for the Ly6G gating among $CD45^+CD11b^+$ cells (top), and resulting proportions of intratumoral neutrophils ($CD11b^+Ly6G^+$) across treatment arms (bottom). Data are depicted as the median percentage ± interquartile range of $CD45^+$ cells. **B,** The mean percentage of the overall tumor immune infiltrate corresponding to intratumoral immune cells positive for the neutrophil markers Ly6G, MPO and NE, as determined by IHC across treatment arms in Hepa1-6 and Hep53.4 tumors (top). Representative images from Hepa1-6 tumors taken at 200× (bottom, scale bar = 100 μm). **C,** Venn diagram for the number of overexpressed genes among treatment groups as compared with placebo, FDR <0.05, fold change (FC) ≥ 1.5. Bottom pie charts depict the distribution of the Gene Ontology (GO)-based biological function terms found to be significantly enriched (FDR < 0.05) in each group of genes using Enrichr analysis. **D,** Heatmap representing sample enrichment in neutrophil-related signatures and expression of differentially-expressed chemokines. **A**, **C**, and **D** data obtained from the Hepa1-6 model. **E,** Volcano plot of DEGs from the colorectal cancer PDX model by Song and colleagues (24), as determined by RNA-seq in paired tumors after 3 days of treatment, with significant DEGs in red and top neutrophil-related genes circled in blue. *, $P < 0.05$ and FDR < 0.1 compared with placebo; $^+$, $P < 0.05$ and FDR < 0.1 compared with anti-PD1.

placebo and anti-PD1; **Fig. 2A**). Furthermore, in combination-treated animals, the increased proportion of neutrophils coincided with high ESTIMATE immune cell infiltrate scores (33), suggesting that neutrophils were a prevalent immune subtype in these higher infiltrated tumors (Supplementary Fig. S2G). We further assessed neutrophil intratumor infiltration and activation by IHC using a panel of three markers: Ly6G, which is expressed by neutrophils and granulocytes; myeloperoxidase (MPO), which is expressed by active polymorphonuclear cells including neutrophils; and neutrophil elastase (NE), which is expressed in the lysosomal granules of active neutrophils. Overall, we observed a significantly elevated percentage of stained cells in tumors from the cabozantinib (median 4% for Ly6G, 12% for MPO, 8% for NE) and combination (8.5% for Ly6G, 15% for MPO, 4% for NE) arms versus placebo (1.5% for Ly6G, 4.2% for MPO, 0.5% for NE; $P < 0.05$; **Fig. 2B**). These data suggest that active neutrophils are significantly increased in the intratumoral regions of mice treated with combination and cabozantinib, whereas no changes in peritumor neutrophil infiltration were observed across treatment groups (Supplementary Fig. S4A and S4B). These findings were also recapitulated in the Hep53.4 model (**Fig. 2B**), and when compared with Hep53.4 tumor samples treated with the antiangiogenic lenvatinib ± anti-PD1 also generated by our lab (34), this effect was revealed to be cabozantinib specific (Supplementary Fig. S2H).

To further investigate this observation, we extracted DEGs (FDR < 0.05, fold change > 1.5) among the treatment groups through CMS analysis of tumor transcriptomic data. Combination treatment had the greatest impact reshaping the molecular profile of the tumor, because it was associated with the greatest number of DEGs compared with placebo at 157 genes, followed by anti-PD1 with 86 DEGs, while only seven genes were significantly upregulated by cabozantinib. The 100 genes exclusively upregulated in the combination arm were used to generate the cabozantinib plus anti-PD1 100-gene signature (CAP-100), capturing the specific molecular effect of the combination (Supplementary Table S5). Gene Ontology (GO) enrichment analysis revealed that CAP-100 was significantly associated with 12 biological function GO terms, of which six (50%) were linked to neutrophil activity ($P < 0.05$; **Fig. 2C**; Supplementary Table S6). The antitumor neutrophil phenotype in the combination arm was further supported by higher enrichments in gene expression signatures of the N1 neutrophil profile (35), neutrophil activity, and maturation (late neutrotime; ref. 36; **Fig. 2D**). In parallel, the seven genes upregulated by cabozantinib monotherapy were associated with the chemotaxis and migration of leukocytes, fundamentally neutrophils (5/12 GO terms; 42%), and with innate immunity responses (4/12 GO terms, 34%; **Fig. 2C**; Supplementary Table S6). On the other hand, the 86 genes upregulated by anti-PD1 monotherapy were linked to broader proinflammatory signaling cascades (17/47 GO terms; 36%) and chemotaxis of a wide variety of leukocyte subpopulations (12/27 GO terms, 26%).

We then validated the molecular effect of cabozantinib using RNA-seq data from colorectal cancer tumors in a PDX model (ref. 24; Supplementary Fig. S3A). GO enrichment analysis of the 244 genes upregulated by cabozantinib versus placebo revealed a positive regulation of neutrophil chemotaxis (Supplementary Fig. S3B; **Fig. 2E**), and GSEA identified an enrichment in neutrophil-, inflammation-, hypoxia-, and apoptosis-related pathways (Supplementary Fig. S3C).

Combination of cabozantinib and anti-PD1 induces a strong inflammatory phenotype

To further investigate the immunomodulatory roles of cabozantinib and its combination with anti-PD1, we assessed several infiltrating lymphoid and myeloid immune populations along with the tumor transcriptomic profiles. Regarding antitumor immunity features, anti-PD1 and combination induced a higher enrichment in stromal and immune microenvironment components based on expression data (Supplementary Fig. S4D). Flow cytometry analysis revealed a specific reduction in the proportions of the exhausted $CD8^+PD1^+$ T-cell subpopulation induced by cabozantinib and combination (mean 7% and 6% of $CD45^+$ cells; $P < 0.05$ vs. 25% in placebo and 35% in anti-PD1; **Fig. 3A**), even though no significant differences in the IHC counts of infiltrating $CD8^+$ and $CD4^+$ T cells were observed (Supplementary Fig. S4E and S4F). In addition, the location of CD8 positivity was mostly intratumoral in combination and anti-PD1 tumors (means of 73% and 60%, respectively; $P < 0.05$ vs. 26% in placebo; **Fig. 3C**), suggesting a higher capacity to infiltrate the tumor parenchyma to exert their effector function.

Aligning with these results, transcriptomic analysis revealed that all anti-PD1 and combination-treated tumors recapitulated the HCC Immune Class (25), compared with none in the placebo arm (**Fig. 3D**). Combination further contributed to the proinflammatory and antitumor immunity effect of anti-PD1 with the highest enrichments in pathways of cytokine and chemokine signaling, T-cell activation and Th1-related responses, B-cell signaling, classically activated M1 macrophages, dendritic cells, antigen presentation, and features of response to nivolumab in melanoma (ref. 37; $P < 0.05$ vs. placebo; **Fig. 3D**; Supplementary Fig. S4D). Flow cytometry did not reveal significant changes in the immune infiltrate composition for B cells or dendritic cells, but showed a cabozantinib-related reduction in macrophage percentages (Supplementary Fig. S4G).

In terms of immune suppression features, IHC analysis revealed decreased infiltration of Tregs ($FOXP3^+$) in combination and anti-PD1 arms versus placebo ($P < 0.05$), with a clear trend for cabozantinib (**Fig. 3B**). In addition, combination and cabozantinib-treated tumors excluded Tregs from intratumoral areas, with mean 1.7% and 3.2% of the total $FOXP3^+$ positivity in the IHC sections being intratumoral ($P < 0.05$ vs. 15% in placebo; **Fig. 3C**). In parallel, gene expression data revealed that combination treatment also caused a significantly reduced enrichment in TGFβ and β-catenin signaling pathways, associated with immune exclusion features in HCC and resistance to immunotherapies (refs. 25, 38–40; $P < 0.05$ vs. placebo; **Fig. 3D**). Furthermore, cabozantinib and combination arms were also linked to the strongest PD-L1 expression in tumor cells and increased CTLA4 staining (Supplementary Fig. S4H), which could potentially be associated with the activation of feedback loops to negatively regulate T-cell activation. Overall, tumor molecular data suggest that combination enhanced antitumor immunity by stimulating both innate and adaptive components.

Combination treatment with cabozantinib promotes adaptive immune cell populations in blood

We then investigated treatment-related effects on systemic immunity in our Hepa1-6 model through flow cytometry and chemokine profiling in blood. In contrast to what was observed in tumor tissue, the proportions of circulating overall T lymphocytes ($CD45^+CD3^+$) as well as $CD4^+$ and $CD8^+$ subpopulations were significantly increased by cabozantinib and combination (mean 38% and 34% of $CD45^+$ cells) as compared with placebo and anti-PD1 (20% and 21%, $P < 0.05$; **Fig. 3E**). In addition, combination induced a significant increase in the proportions of proliferating $CD8^+$ T cells in blood ($P < 0.05$ vs. placebo; **Fig. 3E**), and the greatest enrichment in the subset of memory/effector T cells

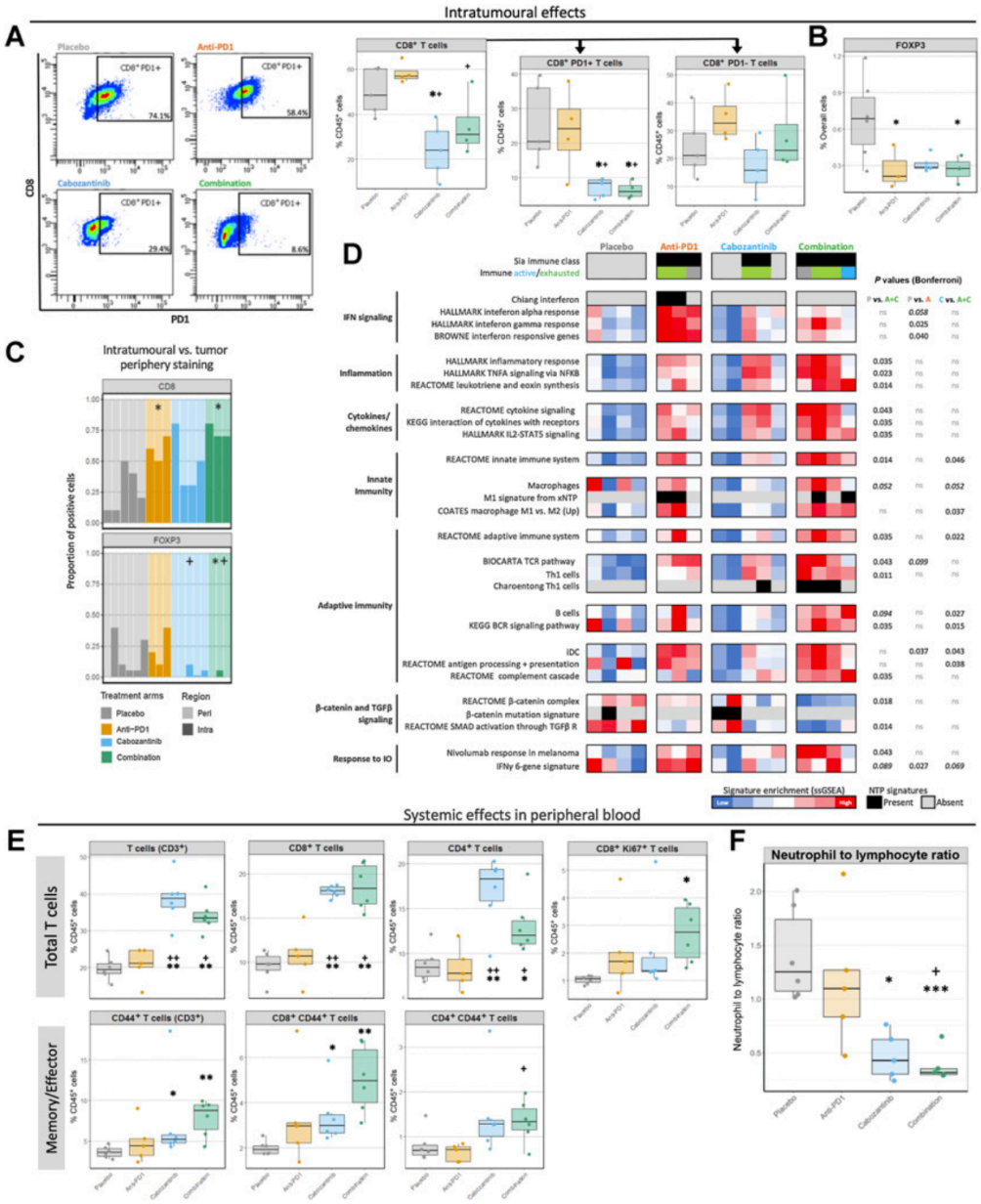

Figure 3.

Cabozantinib + anti-PD1 therapy induces a strong proinflammatory effect. **A,** Representative dot plots showing PD1 gating among $CD45^+CD3^+CD8^+$ cells (left), and proportions of intratumoral $CD8^+$ T lymphocytes and their $PD1^+$ and $PD1^-$ subsets as a percentage of $CD45^+$ cells, as determined by flow cytometry (right). **B,** Mean percentage of FOXP3-positive cells in tumor parenchyma as determined by IHC using QuPath, relative to all cells. **C,** The proportion of total CD8 and FOXP3 staining in intratumoral or peripheral areas. Each bar represents a mouse, and the darker color depicts which % of staining is intratumoral. **D,** Heatmap showing tumor immunity features. Gene signatures representing different states of inflammation, HCC subclasses, or distinct immune cell populations were tested using NTP and ssGSEA. Bonferroni-corrected *P* values from Dunn *post hoc* test. **E,** Overall populations of T lymphocytes ($CD3^+$), and specifically $CD8^+$ T cells, $CD4^+$ T cells, and proliferating $CD8^+$ T cells (defined as $CD8^+Ki67^+$) in peripheral blood after 14 days of treatment, and the proportions of the memory/effector subgroups within these populations (characterized by CD44 expression). **F,** The ratio of neutrophil to lymphocyte proportions in peripheral blood. *, $P < 0.05$ and FDR < 0.1 compared with placebo; $^+$, $P < 0.05$ and FDR < 0.1 compared with anti-PD1. Data obtained from the Hepa1-6 model.

(CD45$^+$CD3$^+$CD44$^+$), particularly memory/effector CD8$^+$ T cells ($P < 0.01$ vs. placebo), which were seen increased to a lesser extent by cabozantinib monotherapy ($P < 0.05$ vs. placebo; **Fig. 3E**). We also assessed the neutrophil-to-lymphocyte ratio (NLR), associated with poor prognosis in patients with HCC (41), as the rate between CD3$^+$ T cell and CD11b$^+$Ly6G$^+$ cell percentages. Cabozantinib and combination induced a significant reduction of the NLR as compared with placebo (mean 0.47 and 0.38 vs. 1.4, $P < 0.05$; **Fig. 3F**). Of note, no significant changes were observed for circulating Tregs, B cells, macrophages, or dendritic cells (Supplementary Fig. S5A). Finally, cytokine and chemokine profiling of peripheral blood revealed significantly increased levels of two chemoattractants in the combination arm: CTACK/CCL27 (chemotactic agent for T lymphocytes) and IL16 (leukocyte chemoattractant and modulator of T-cell activation; $P < 0.05$ vs. placebo; Supplementary Fig. S5B). Overall, cabozantinib and especially combination impacted systemic immunity by promoting an enrichment in adaptive immune cell subsets.

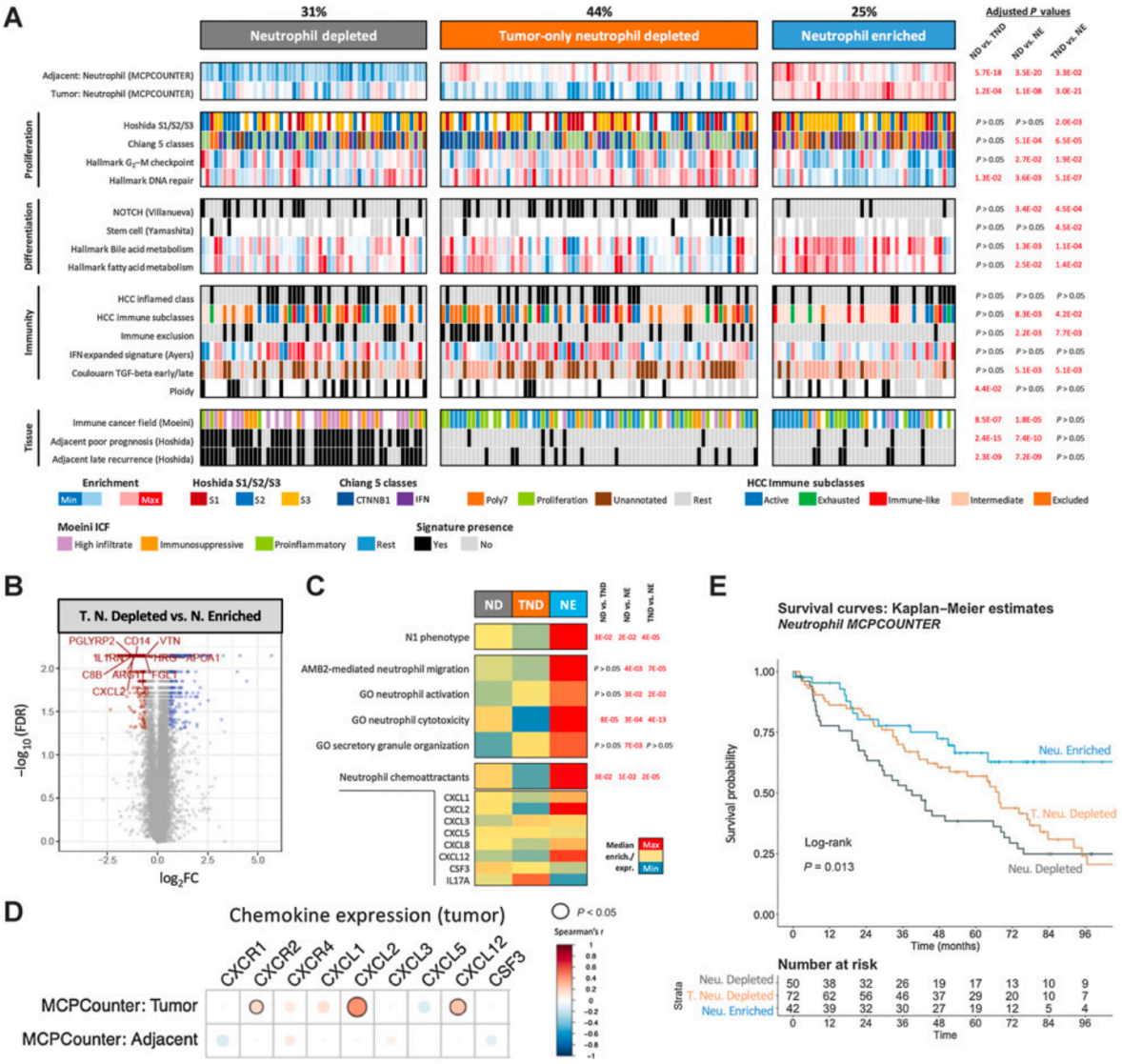

Figure 4.

Unsupervised clustering reveals distinct neutrophil profiles in human HCC. **A,** Heatmap displaying molecular features linked to the three neutrophil-related profiles: Neutrophil Depleted (ND), Tumor-only Neutrophil Depleted (TND), and Neutrophil Enriched (NE), with adjusted *P* values comparing between groups. **B,** Volcano plot displaying the top DEGs between the TND and NE groups. **C,** Heatmap representation of the median enrichment in neutrophil-related gene expression signatures across neutrophil-related clusters. Genes included in the neutrophil chemoattractants signature are depicted below. **D,** Correlation between the tumor expression of a set of neutrophil-attracting chemokines/chemokine receptors, and the enrichment in MCPCounter neutrophil signature in the tumor and adjacent tissues. **E,** Kaplan–Meier survival analysis (with log-rank *P* value). All data presented are from cohort 1 ($n = 167$).

Human HCCs with combination-like neutrophil features have favorable clinical outcomes and molecular profiles

We then elucidated whether these active neutrophil profiles were linked to any specific molecular or clinical features in human HCC, using two cohorts of patients (cohort 1: $n = 167$, and cohort 2: $n = 57$ including paired tissue and blood samples), and the MCPCounter (42) neutrophil signature which correlated strongly with the neutrophil infiltration and activation profile in combination-treated mice (Supplementary Fig. S6). Unsupervised clustering of human HCC based on enrichment of the neutrophil signature revealed three distinct clusters of samples—Neutrophil Enriched, Neutrophil Depleted, and Tumor-only Neutrophil Depleted (*TND*; Supplementary Fig. S7A and S7B).

The Neutrophil Enriched cluster, accounting for 25% (42/167) of patients, was characterized by high neutrophil enrichment both in the tumor and in the adjacent tissue. These samples exhibited significant enrichment in the S3 HCC molecular class (27) and liver metabolic pathways—capturing more differentiated tumors and suppression of TGFβ signaling (43), but a reduced activation of proliferation and DNA repair pathways (**Fig. 4A**). In terms of immunity, Neutrophil Enriched HCCs were neither associated with adaptive immunity pathways, the HCC Inflamed (44) or Immune Classes (25) nor their active or exhausted subclasses, and they lacked HCC immune exclusion features derived from β-catenin pathway activation (39).

The Neutrophil Depleted cluster captured 31% of cases (52/167) which presented low neutrophil enrichment in both the tumor and adjacent nontumor tissue. Finally, the *TND* cluster encompassed 44% of cases (73/167) displaying low neutrophil enrichment in the tumor but high enrichment in the adjacent tissue. Both the Neutrophil Depleted and *TND* groups presented pro-proliferative traits, with a higher prevalence of stem cell features and an enrichment in oncogenic TGFβ signaling (late TGFβ; **Fig. 4A**; ref. 43). In addition, Neutrophil Depleted HCCs were more polyploid (FDR < 0.05 vs. *TND*) and displayed a marked enrichment in poor prognosis signatures in the adjacent tissue (FDR < 0.05 vs. *TND* and Neutrophil Enriched). Furthermore, we observed a reduced proportion of hepatitis B and C virus infections in Neutrophil Enriched cases (Supplementary Fig. S8A) and a higher proportion of cirrhotic cases in the Neutrophil Depleted subgroup (FDR < 0.05). We also observed an overall lack of correlation between tumor and adjacent neutrophil enrichment values (Supplementary Fig. S7C and S7D).

To gain insight into the neutrophil phenotypes and potential molecular mechanisms driving neutrophil recruitment in the tumors, we analyzed the DEGs in tumor tissue among clusters (FDR < 0.05, fold change > 1.5). We identified 74 genes commonly upregulated in the Neutrophil Enriched group when compared with *TND*, some of which were linked to innate immune cells like the macrophage-related *CD14* and the neutrophil chemoattractant *CXCL2* (**Fig. 4B**; Supplementary Fig. S9B). In parallel, we confirmed that Neutrophil Enriched HCCs were significantly associated with transcriptomic features of anti-tumor activity like the N1 phenotype, neutrophil migration, activation, and cytotoxicity (**Fig. 4C**; Supplementary Fig. S9C). We also detected an enrichment in neutrophil chemokines mostly driven by *CXCL2* and *CXCL12* expression, which were more strongly correlated with MCPCounter tumor enrichment ($P < 0.05$; **Fig. 4D**; Supplementary Fig. S9D). In addition, following up on the absence of β-catenin–driven immune exclusion among Neutrophil Enriched tumors, we observed that β-catenin activation (assessed through the presence of the Chiang CTNNB1 subclass) was linked to lack of active neutrophil features and a reduced expression of neutrophil chemoattractants ($P < 0.05$ for *CXCL3* and *CXCL12* in the CTNNB1 subclass vs. rest; Supplementary Fig. S9E).

Importantly, and consistent with the favorable molecular features of Neutrophil Enriched tumors, patients of this cluster presented significantly longer survival as compared with the rest of the cohort [**Fig. 4E**; HR = 0.49 (95% CI, 0.28–0.85)], log-rank $P = 0.011$, which remained significant in a multivariate analysis (Cox proportional hazards model, $P = 0.025$; **Table 1**). On the other hand, the Neutrophil Depleted subgroup presented reduced survival in the univariate analysis [**Fig. 4E**; **Table 1**; log-rank $P = 0.02$, HR = 1.62 (95% CI, 1.07–2.45)]. Furthermore, we observed that tumors with the highest MCPCounter signature enrichment were associated with significantly better outcomes as compared with the rest [$n = 164$, HR = 0.45 (95% CI, 0.25–0.81), multivariate Cox $P = 0.007$] and these results were recapitulated in TCGA [$n = 319$, HR = 0.37 (95% CI, 0.21–0.66), multivariate Cox $P < 0.001$; Supplementary Fig. S10; Supplementary Table S9]. In addition, we confirmed all the above molecular findings in an independent cohort (cohort 2: $n = 57$; Supplementary Figs. S8B and S9A).

Overall, we identified that a subset of human HCC recapitulates the specific neutrophil-related molecular effect of cabozantinib and anti-

Table 1. Univariate and multivariate analysis of the three neutrophil clusters and key clinical features associated with survival in cohort 1 ($n = 167$).

	Univariate analysis		Multivariate analysis	
Variable	**HR (95% CI)**	***log-rank P* value**	**HR (95% CI)**	***Cox PH P* value**
MCPCounter clusters				
Neutrophil Depleted	**1.62 (1.07–2.45)**	**0.02**	(Reference)	
Tumor-only Neutrophil Depleted	1.04 (0.70–1.57)	0.8	0.79 (0.50–1.26)	0.329
Neutrophil Enriched	**0.49 (0.28–0.85)**	**0.011**	**0.50 (0.27–0.91)**	**0.025**
Age (≥65)	0.70 (0.47–1.05)	0.079		
Cirrhosis	1.20 (0.73–1.99)	0.5		
Poor differentiation	1.23 (0.74–2.03)	0.4		
Gender (male)	**0.60 (0.39–0.93)**	**0.022**	**0.55 (0.35–0.88)**	**0.012**
High AFP (≥400 ng/mL)	1.47 (0.82–2.62)	0.19		
Multinodularity (>1 nodule)	**2.22 (1.46–3.36)**	**<0.001**	**2.34 (1.50–3.65)**	**<0.001**
Satellites (yes/no)	**1.69 (1.10–2.60)**	**0.015**	1.52 (0.99–2.35)	0.056
Size (≥3.5 cm)	**1.60 (1.05–2.44)**	**0.027**	1.04 (0.99–1.10)	0.145
Vascular invasion (micro/macro)	**2.10 (1.40–3.15)**	**<0.001**	1.49 (0.97–2.30)	0.07

Note: Statistically significant values ($P < 0.05$) are in bold.

PD1 combination from our preclinical model, and these tumors of the Neutrophil Enriched cluster were linked to favorable molecular and clinical features.

Discussion

The recent approval of atezolizumab + bevacizumab has been a pivotal milestone in the treatment of advanced HCC and suggests that combination therapies with ICIs are the future for HCC treatment. However, responses are typically observed in a subset of patients, and there is currently a surge of research into broadening the spectrum of responders by overcoming potential tumor-intrinsic resistance to immune checkpoint blockade. The fact that recent reports suggest that immune therapies might be more effective in viral than nonviral-related HCCs (8, 45) also further highlights the need to understand the benefits of combining distinct agents with ICIs, because not all TKIs lead to equal immunomodulatory effects. In this study, we determined using preclinical models that the experimental combination of cabozantinib with anti-PD1 was associated with a greater proportion of antitumor responses in a shorter time, and enhanced molecular features of antitumor immunity including higher neutrophil recruitment and activation. To our knowledge, this is the first study reporting a dominant role of neutrophils, particularly of the N1 phenotype, in the immune effects associated with a TKI combined with anti-PD1 therapy in HCC. We also identified distinct subgroups of human HCCs based on neutrophil features with potential clinical relevance (**Fig. 5**).

The observed increase in neutrophil infiltration after cabozantinib administration in our murine models had only been previously reported in a prostate cancer model, where neutrophil recruitment proved to be essential for the antitumor effect of the drug (23). These results were also supported by the transcriptomic data from a human colorectal cancer PDX model (24), contributing to the notion that this effect of cabozantinib may not be limited to a specific cancer type. Our transcriptomic analysis revealed that cabozantinib could be driving neutrophil infiltration through the upregulation of ligands for the neutrophil receptor CXCR2 (CXCL3 in our subcutaneous tumors, CXCL1 in the colorectal cancer PDX model), and that the upregulation of CXCL12 could promote their retention in the tumor, as previously reported in prostate cancer (23). In light of the phenotypic plasticity attributed to neutrophils in cancer biology (46), we observed that cabozantinib in combination with anti-PD1 could further enhance a molecular phenotype of neutrophil activation, possibly due to a contributing proinflammatory effect of the immunotherapy. In fact, the combination had the greatest impact upregulating genes linked to N1 phenotype, neutrophil maturity and degranulation, as well as immunoglobulin-related genes, which could also contribute to an antitumor neutrophil phenotype through antibody-dependent cellular cytotoxicity (47). Moreover, combination treatment was linked to reduced β-catenin signaling, which is associated with immune exclusion in HCC (38, 39), as well as lower enrichment of TGFβ signaling, which has been demonstrated to polarize neutrophils toward a protumor N2 phenotype (35, 46). Overall, this demonstrates the potential of cabozantinib to trigger a neutrophil-mediated antitumor innate immune response, which is enhanced when combined with anti-PD1 therapy.

In addition, cabozantinib significantly reduced infiltrating $CD8^+PD1^+$ T cells, a clinically interesting effect given that the accumulation of a dysfunctional $CD8^+PD1^+$ T-cell subpopulation could be responsible for the reduced efficacy of ICIs in nonviral HCC, particularly NASH-HCC (8). Further studies are required to confirm whether cabozantinib and anti-PD1 combinations could improve NASH-HCC patient response by depleting this $CD8^+PD1^+$ T-cell subset while increasing neutrophil infiltration. Of note, the evaluation of this combination in preclinical NASH-HCC models (e.g., high-fat diet) and a subgroup analysis of the COSMIC-312 trial (21) could shed light on this question.

In parallel to these effects, the combination of cabozantinib and anti-PD1 had the most favorable impact on the tumor immune microenvironment out of the treatment arms investigated, such as a significant reduction of Tregs, enriched Th1 and M1 macrophage phenotypes, and enriched innate/adaptive immune pathways. The increased proportions of memory/effector T cells found in blood suggest that adaptive immunity was also activated with this treatment, a feature associated with a significant lowering of the NLR ($P < 0.001$ for combination). HCC progression is closely linked with inflammation, and the importance of this is underscored by the wealth of evidence linking inflammation-based scores such as the NLR with HCC prognosis (48). Finally, consistent with the inhibitory activity of cabozantinib against tyrosine kinases including VEGFR2 (19), our data indicate that at least part of the antitumor mechanism of action of

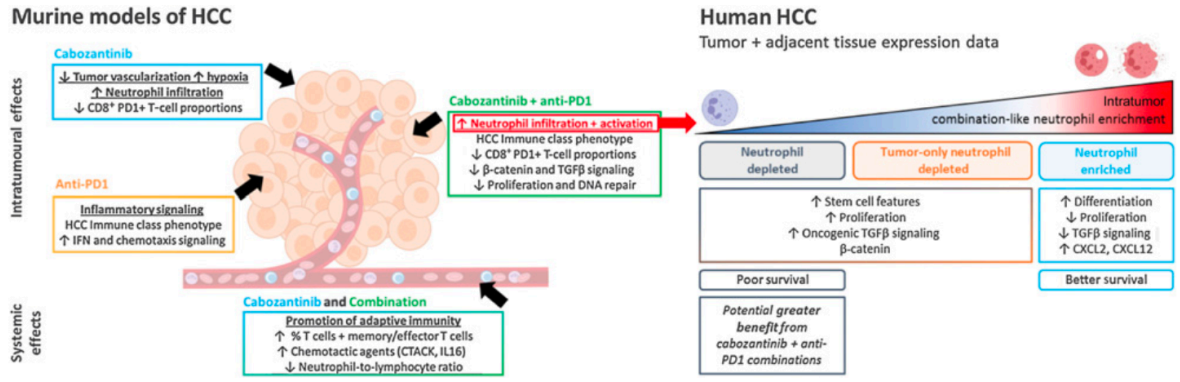

Figure 5.
Schematic summary of the study results.

cabozantinib is derived from its antiangiogenic properties (reduced endothelial cells and VEGF signaling, and absence of VETCs, which have been proposed as a predictor of aggressive HCC; ref. 48).

In patients with HCC, using MCPCounter (42) as a transcriptomic tool to evaluate active neutrophil infiltration in tumor and nontumor adjacent tissue, we confirmed that neutrophil enrichment in the adjacent tissue or in blood is not always linked to intratumor enrichment. This suggests that neutrophil recruitment mechanisms may be independent in liver adjacent and tumor tissues, and the circulating NLR associated with poor prognosis (41) may not reflect intratumoral neutrophil levels nor their phenotype. This finding has significance given we found that a high enrichment of active neutrophils in the tumor was linked to better outcomes in two independent cohorts, along with less proliferative and more differentiated molecular features, and no enrichment in inflammation profiles (HCC Immune Class; ref. 25). In addition, intratumor neutrophil enrichment was linked to the expression of the chemokines CXCL2 (a CXCR2 ligand like CXCL1 and CXCL3, upregulated by cabozantinib in mice) and CXCL12 (upregulated in our model and previously described as a cabozantinib effect in prostate cancer; ref. 23), suggesting that relevant mechanisms of neutrophil chemoattraction in human HCC were recapitulated in the preclinical models. Moreover, β-catenin pathway activation (39) may negatively influence the presence of this neutrophil phenotype in HCC as we observed it was linked to reduced enrichment in neutrophil signatures and expression of neutrophil chemokines; this may represent an additional immune exclusion effect of β-catenin activation that is worth further exploration.

Taken together, these observations suggest that cabozantinib, particularly in combination with anti-PD1 treatment, contributes to inducing neutrophil infiltration, decreasing an immune suppressive environment, and enhancing antitumor activity compared with the monotherapies in HCC. Those patients with a reduced enrichment of active neutrophil phenotypes in the tumor (∼30% of cases) could potentially gain the greatest benefits from this combination (**Fig. 5**), although the molecular assessment of tumor samples from patients with HCC exposed to cabozantinib in combination with PD1/PDL1 inhibitors will be necessary to test these hypotheses.

Overall, the combination of cabozantinib and anti-PD1 has the potential to bring together the activation of adaptive and innate immune responses against the tumor, and this provides a mechanistic rationale for combining cabozantinib and anti-PD1 therapy to render enhanced antitumor immune responses among patients with HCC.

Authors' Disclosures

J.M. Llovet reports grants and personal fees from Bayer HealthCare Pharmaceuticals, Eisai Inc, and Ipsen; grants from Boehringer Ingelheim; and personal fees from Eli Lilly, Merck, Bristol Myers Squibb, Glycotest, Nucleix, Genentech, Roche, AstraZeneca, Omega Therapeutics, Iylon, Mina Alpha, and Boston Scientific outside the submitted work. No disclosures were reported by the other authors.

Authors' Contributions

R. Esteban-Fabró: Conceptualization, data curation, formal analysis, validation, investigation, visualization, methodology, writing–original draft, writing–review and editing. **C.E. Willoughby:** Conceptualization, data curation, formal analysis, validation, investigation, visualization, methodology, writing–original draft, writing–review and editing. **M. Piqué-Gili:** Validation, investigation, visualization, writing–review and editing. **C. Montironi:** Formal analysis, investigation, methodology, writing–review and editing. **J. Abril-Fornaguera:** Formal analysis, investigation, writing–review and editing. **J. Peix:** Investigation, methodology, writing–review and editing. **L. Torrens:** Formal analysis, investigation, methodology, writing–review and editing. **A. Mesropian:** Investigation, writing–review and editing. **U. Balaseviciute:** Investigation, writing–review and editing. **F. Miró-Mur:** Formal analysis, methodology, writing–review and editing. **V. Mazzaferro:** Resources, writing–review and editing. **R. Pinyol:** Conceptualization, formal analysis, supervision, investigation, methodology, project administration, writing–review and editing. **J.M. Llovet:** Conceptualization, formal analysis, supervision, funding acquisition, investigation, methodology, writing–original draft, project administration, writing–review and editing.

Acknowledgments

This study was sponsored by Ipsen Pharmaceuticals. R. Esteban-Fabró is supported by a doctoral training grant (BES-2017-081286) from MCIN/AEI/10.13039/501100011033 and the European Social Fund (ESF) and a mobility grant from Fundació Universitària Agustí Pedro i Pons. C.E. Willoughby is supported by a Sara Borrell fellowship (CD19/00109) from the Instituto de Salud Carlos III (ISCIII) and ESF. M. Piqué-Gili is supported by a doctoral training grant (PRE2020-094716) from MCIN/AEI/10.13039/501100011033 and ESF, and a mobility grant from Fundació Universitària Agustí Pedro i Pons. C. Montironi is supported by a Rio Hortega fellowship (CM19/00039) from ISCIII and ESF. J. Abril-Fornaguera is supported by a doctoral training grant from the University of Barcelona (PREDOCS-UB 2020) and a mobility grant from Fundació Universitària Agustí Pedro i Pons. J. Peix is supported by a PERIS ICT-Suport grant from the Departament de Salut de la Generalitat de Catalunya (SLT017/20/000206). A. Mesropian is supported by a FI-SDUR pre-doctoral support grant (BDNS 550325) from the Agency for Management of University and Research Grants (AGAUR) and the Generalitat de Catalunya. U. Balaseviciute is supported by an EILF-EASL Juan Rodés PhD Studentship (EASL_JR_12_20) from the European Association for the Study of the Liver (EASL) and the EASL International Liver Foundation (EILF). J.M. Llovet is supported by grants from the European Commission (EC) Horizon 2020 Program (HEPCAR, proposal number 667273-2), the NIH (RO1DK56621 and RO1DK128289), the Samuel Waxman Cancer Research Foundation, the Spanish National Health Institute (MICINN, SAF-2016-76390 and PID2019-105378RB-I00), through an Accelerator award in partnership between Cancer Research UK, Fondazione AIRC and Fundación Científica de la Asociación Española Contra el Cáncer (HUNTER, ref. C9380/A26813), and by the Generalitat de Catalunya (AGAUR, SGR-1358). We are indebted to the Cytometry and Cell Sorting Core Facility of the Institut d'Investigacions Biomèdiques August Pi i Sunyer (IDIBAPS), particularly Dr. Isabel Crespo, for excellent flow cytometry technical assistance.

The costs of publication of this article were defrayed in part by the payment of page charges. This article must therefore be hereby marked *advertisement* in accordance with 18 U.S.C. Section 1734 solely to indicate this fact.

Received July 12, 2021; revised January 28, 2022; accepted March 16, 2022; published first March 18, 2022.

References

1. Sung H, Ferlay J, Siegel RL, Laversanne M, Soerjomataram I, Jemal A, et al. Global cancer statistics 2020: GLOBOCAN estimates of incidence and mortality worldwide for 36 cancers in 185 countries. CA Cancer J Clin 2021;71:209–49.
2. Llovet JM, Kelley RK, Villanueva A, Singal AG, Pikarsky E, Roayaie S, et al. Hepatocellular carcinoma. Nat Rev Dis Prim 2021;7:6.
3. Finn RS, Qin S, Ikeda M, Galle PR, Ducreux M, Kim T-Y, et al. Atezolizumab plus bevacizumab in unresectable hepatocellular carcinoma. N Engl J Med 2020;382:1894–905.
4. Finn RS, Qin S, Ikeda M, Galle PR, Ducreux M, Kim T-Y, et al. IMbrave150: Updated overall survival (OS) data from a global, randomized, open-label phase III study of atezolizumab (atezo) + bevacizumab (bev) versus sorafenib (sor) in patients (pts) with unresectable hepatocellular carcinoma (HCC). J Clin Oncol 39: 3s, 2021 (suppl; abstr 267).
5. Llovet JM, Ricci S, Mazzaferro V, Hilgard P, Gane E, Blanc JF, et al. Sorafenib for advanced hepatocellular carcinoma. N Engl J Med 2008;359:378–90.
6. El-Khoueiry AB, Sangro B, Yau T, Crocenzi TS, Kudo M, Hsu C, et al. Nivolumab in patients with advanced hepatocellular carcinoma (CheckMate 040): an open-label, non-comparative, phase 1/2 dose escalation and expansion trial. Lancet 2017;389:2492–502.

7. Zhu AX, Finn RS, Edeline J, Cattan S, Ogasawara S, Palmer D, et al. Pembrolizumab in patients with advanced hepatocellular carcinoma previously treated with sorafenib (KEYNOTE-224): a non-randomised, open-label phase 2 trial. Lancet Oncol 2018;19:940–52.
8. Pfister D, Núñez NG, Pinyol R, Govaere O, Pinter M, Szydlowska M, et al. NASH limits anti-tumour surveillance in immunotherapy-treated HCC. Nature 2021; 592:450–6.
9. Llovet JM, Montal R, Sia D, Finn RS. Molecular therapies and precision medicine for hepatocellular carcinoma. Nat Rev Clin Oncol 2018;15: 599–616.
10. Hegde PS, Karanikas V, Evers S. The where, the when, and the how of immune monitoring for cancer immunotherapies in the era of checkpoint inhibition. Clin Cancer Res 2016;22:1865–74.
11. Khan KA, Kerbel RS. Improving immunotherapy outcomes with anti-angiogenic treatments and vice versa. Nat Rev Clin Oncol 2018;15:310–24.
12. Huang Y, Yuan J, Righi E, Kamoun WS, Ancukiewicz M, Nezivar J, et al. Vascular normalizing doses of antiangiogenic treatment reprogram the immunosuppressive tumor microenvironment and enhance immunotherapy. Proc Natl Acad Sci U S A 2012;109:17561–6.
13. Voron T, Colussi O, Marcheteau E, Pernot S, Nizard M, Pointet AL, et al. VEGF-A modulates expression of inhibitory checkpoints on CD8++ T cells in tumors. J Exp Med 2015;212:139–48.
14. Allen E, Jabouille A, Rivera LB, Lodewijckx I, Missiaen R, Steri V, et al. Combined antiangiogenic and anti-PD-L1 therapy stimulates tumor immunity through HEV formation. Sci Transl Med 2017;9:eaak9679.
15. Wallin JJ, Bendell JC, Funke R, Sznol M, Korski K, Jones S, et al. Atezolizumab in combination with bevacizumab enhances antigen-specific T-cell migration in metastatic renal cell carcinoma. Nat Commun 2016;7:12624.
16. Hodi FS, Lawrence D, Lezcano C, Wu X, Zhou J, Sasada T, et al. Bevacizumab plus ipilimumab in patients with metastatic melanoma. Cancer Immunol Res 2014;2:632–42.
17. Abou-Alfa GK, Meyer T, Cheng A-L, El-Khoueiry AB, Rimassa L, Ryoo B-Y, et al. Cabozantinib in patients with advanced and progressing hepatocellular carcinoma. N Engl J Med 2018;379:54–63.
18. Zhou L, Liu XD, Sun M, Zhang X, German P, Bai S, et al. Targeting MET and AXL overcomes resistance to sunitinib therapy in renal cell carcinoma. Oncogene 2016;35:2687–97.
19. Xiang Q, Chen W, Ren M, Wang J, Zhang H, Deng DYB, et al. Cabozantinib suppresses tumor growth and metastasis in hepatocellular carcinoma by a dual blockade of VEGFR2 and MET. Clin Cancer Res 2014;20:2959–70.
20. Yau T, Zagonel V, Santoro A, Acosta-Rivera M, Choo SP, Matilla A, et al. Nivolumab (NIVO) + ipilimumab (IPI) + cabozantinib (CABO) combination therapy in patients (pts) with advanced hepatocellular carcinoma (aHCC): results from CheckMate 040. J Clin Oncol 38: 4s, 2020 (suppl; abstr 478).
21. Rimassa L, Cheng A-L, Braiteh F, Chaudhry A, Benzaghou F, Thuluvath P, et al. Phase III (COSMIC-312) study of cabozantinib (C) in combination with atezolizumab (A) vs sorafenib (S) in patients (pts) with advanced hepatocellular carcinoma (aHCC) who have not received previous systemic anticancer therapy. Ann Oncol 2019;30:v320.
22. Kelley RK, Yau T, Cheng A-L, Kaseb A, Qin S, Zhu AX, et al. VP10–2021: Cabozantinib (C) plus atezolizumab (A) versus sorafenib (S) as first-line systemic treatment for advanced hepatocellular carcinoma (aHCC): results from the randomized phase III COSMIC-312 trial. Ann Oncol 2022;33:114–6.
23. Patnaik A, Swanson KD, Csizmadia E, Solanki A, Landon-Brace N, Gehring MP, et al. Cabozantinib eradicates advanced murine prostate cancer by activating antitumor innate immunity. Cancer Discov 2017;7:750–65.
24. Song EK, Tai WM, Messersmith WA, Bagby S, Purkey A, Quackenbush KS, et al. Potent antitumor activity of cabozantinib, a c-MET and VEGFR2 inhibitor, in a colorectal cancer patient-derived tumor explant model. Int J Cancer 2015;136: 1967–75.
25. Sia D, Jiao Y, Martinez-Quetglas I, Kuchuk O, Villacorta-Martin C, Castro de Moura M, et al. Identification of an immune-specific class of hepatocellular carcinoma, based on molecular features. Gastroenterology 2017;153:812–26.
26. Chiang DY, Villanueva A, Hoshida Y, Peix J, Newell P, Minguez B, et al. Focal gains of VEGFA and molecular classification of hepatocellular carcinoma. Cancer Res 2008;68:6779–88.
27. Hoshida Y, Nijman SMB, Kobayashi M, Chan JA, Brunet JP, Chiang DY, et al. Integrative transcriptome analysis reveals common molecular subclasses of human hepatocellular carcinoma. Cancer Res 2009;69:7385–92.
28. Boyault S, Rickman DS, De Reyniès A, Balabaud C, Rebouissou S, Jeannot E, et al. Transcriptome classification of HCC is related to gene alterations and to new therapeutic targets. Hepatology 2007;45:42–52.
29. Reich M, Liefeld T, Gould J, Lerner J, Tamayo P, Mesirov JP. GenePattern 2.0. Nat Genet 2006;38:500–1.
30. Kuleshov MV, Jones MR, Rouillard AD, Fernandez NF, Duan Q, Wang Z, et al. Enrichr: a comprehensive gene set enrichment analysis web server 2016 update. Nucleic Acids Res 2016;44:W90–7.
31. Villanueva A, Portela A, Sayols S, Battiston C, Hoshida Y, Méndez-González J, et al. DNA methylation-based prognosis and epidrivers in hepatocellular carcinoma. Hepatology 2015;61:1945–56.
32. Ally A, Balasundaram M, Carlsen R, Chuah E, Clarke A, Dhalla N, et al. Comprehensive and integrative genomic characterization of hepatocellular carcinoma. Cell 2017;169:1327–41.
33. Yoshihara K, Shahmoradgoli M, Martínez E, Vegesna R, Kim H, Torres-Garcia W, et al. Inferring tumour purity and stromal and immune cell admixture from expression data. Nat Commun 2013;4:2612.
34. Torrens L, Montironi C, Puigvehí M, Mesropian A, Leslie J, Haber PK, et al. Immunomodulatory effects of lenvatinib plus anti–programmed cell death protein 1 in mice and rationale for patient enrichment in hepatocellular carcinoma. Hepatology 2021;74:2652–69.
35. Fridlender ZG, Sun J, Kim S, Kapoor V, Cheng G, Ling L, et al. Polarization of tumor-associated neutrophil phenotype by TGF-β: "N1" versus "N2" TAN. Cancer Cell 2009;16:183–94.
36. Grieshaber-Bouyer R, Radtke FA, Cunin P, Stifano G, Levescot A, Vijaykumar B, et al. The neutrotime transcriptional signature defines a single continuum of neutrophils across biological compartments. Nat Commun 2021;12:2856.
37. Riaz N, Havel JJ, Makarov V, Desrichard A, Urba WJ, Sims JS, et al. Tumor and microenvironment evolution during immunotherapy with nivolumab. Cell 2017;171:934–49.
38. de Galarreta MR, Bresnahan E, Molina-Sánchez P, Lindblad KE, Maier B, Sia D, et al. β-catenin activation promotes immune escape and resistance to anti–PD-1 therapy in hepatocellular carcinoma. Cancer Discov 2019;9:1124–41.
39. Pinyol R, Sia D, Llovet JM. Immune exclusion-WNT/CTNNB1 class predicts resistance to immunotherapies in HCC. Clin Cancer Res 2019; 25:2021–3.
40. Harding JJ, Nandakumar S, Armenia J, Khalil DN, Albano M, Ly M, et al. Prospective genotyping of hepatocellular carcinoma: Clinical implications of next-generation sequencing for matching patients to targeted and immune therapies. Clin Cancer Res 2019;25:2116–26.
41. Xiao WK, Chen D, Li SQ, Fu SJ, Peng BG, Liang LJ. Prognostic significance of neutrophil-lymphocyte ratio in hepatocellular carcinoma: a meta-analysis. BMC Cancer 2014;14:117.
42. Becht E, Giraldo NA, Lacroix L, Buttard B, Elarouci N, Petitprez F, et al. Estimating the population abundance of tissue-infiltrating immune and stromal cell populations using gene expression. Genome Biol 2016;17:218.
43. Coulouarn C, Factor VM, Thorgeirsson SS. Transforming growth factor-β gene expression signature in mouse hepatocytes predicts clinical outcome in human cancer. Hepatology 2008;47:2059–67.
44. Montironi C, Castet F, Haber PK, Pinyol R, Torres-Martin M, Torrens L, et al. Inflamed and non-inflamed classes of HCC: a revised immunogenomic classification. Gut 2022;gutjnl-2021-325918.
45. Haber PK, Puigvehí M, Castet F, Lourdusamy V, Montal R, Tabrizian P, et al. Evidence-based management of hepatocellular carcinoma: systematic review and meta-analysis of randomized controlled trials (2002–2020). Gastroenterology 2021;161:879–98.
46. Geh D, Leslie J, Rumney R, Reeves HL, Bird TG, Mann DA. Neutrophils as potential therapeutic targets in hepatocellular carcinoma. Nat Rev Gastroenterol Hepatol 2022 Jan 12 [Epub ahead of print].
47. Matlung HL, Babes L, Zhao XW, van Houdt M, Treffers LW, van Rees DJ, et al. Neutrophils kill antibody-opsonized cancer cells by trogoptosis. Cell Rep 2018; 23:3946–59.
48. Renne SL, Woo HY, Allegra S, Rudini N, Yano H, Donadon M, et al. Vessels encapsulating tumor clusters (VETC) is a powerful predictor of aggressive hepatocellular carcinoma. Hepatology 2020;71:183–95.

Study 3: CXCR2 inhibition enables NASH-HCC immunotherapy

Jack Leslie, John B G Mackey, Thomas Jamieson, Erik Ramon-Gil, Thomas M Drake, Frédéric Fercoq, William Clark, Kathryn Gilroy, Ann Hedley, Colin Nixon, Saimir Luli, Maja Laszczewska, Roser Pinyol, **Roger Esteban-Fabró**, Catherine E Willoughby, Philipp K Haber, Carmen Andreu-Oller, Mohammad Rahbari, Chaofan Fan, Dominik Pfister, Shreya Raman, Niall Wilson, Miryam Müller, Amy Collins, Daniel Geh, Andrew Fuller, David McDonald, Gillian Hulme, Andrew Filby, Xabier Cortes-Lavaud, Noha-Ehssan Mohamed, Catriona A Ford, Ximena L Raffo Iraolagoitia, Amanda J McFarlane, Misti V McCain, Rachel A Ridgway, Edward W Roberts, Simon T Barry, Gerard J Graham, Mathias Heikenwälder, Helen L Reeves, Josep M Llovet, Leo M Carlin, Thomas G Bird, Owen J Sansom, Derek A Mann

Gut, 2022 Apr;71(10):2093-2106. (IF: 31.84, Q1)

Summary

Hepatocellular carcinoma develops on a background of liver damage from persistent viral infection (HBV and HCV) or non-virological damage; in the Western countries, an increasing prevalence of obesity and metabolic syndrome is leading to a higher proportion of HCCs being attributed to non-alcoholic steatohepatitis (NASH)[2,8]. Of note, only a minority of advanced HCC patients (30%)[3] respond to immunotherapy, and it has been recently reported that NASH-HCC is less responsive to immunotherapy due to an expansion of a subset of exhausted infiltrating $CD8^+$ T cells[9]. Considering the growing evidence for pro- and anti-tumor functions of neutrophils in cancer and HCC[10], we investigated whether modulating neutrophil phenotype targeting CXCR2 (a chemoreceptor for interleukin 8) could influence the resistance of NASH-HCC to immunotherapy.

In light of the above, we hypothesized that **targeting neutrophils with a small CXCR2 inhibitor could sensitize NASH to immune checkpoint inhibitor therapy**. We aimed (1) to assess the presence of $CXCR2^+$ neutrophils in mouse models of NASH-HCC and in patients; (2) to evaluate the capacity of a CXCR2 inhibitor (AZD5069) to re-sensitize NASH-HCC to anti-PD1 therapy in preclinical models; and (3) to determine the immunomodulatory mechanisms that characterize CXCR2 inhibition in combination with anti-PD1.

In this study, neutrophil infiltration was characterized in human HCC and in three mouse models of NASH-HCC: an orthotopic on Western diet model, a DEN/ALIOS model and a choline-deficient high-fat diet model. Animals from the first two models were administered anti-PD1, AZD5069, the combination or vehicle, and the molecular effects of the therapies on the tumor immune microenvironment were evaluated by imaging mass cytometry, RNA-seq and flow cytometry. Anti-CD8a was administered for $CD8^+$ T cell depletion, iCCR mice (CCR1, 2, 3 and 5 knockout) with DEN/ALIOS treatment was used to impair dendritic cell (DC) recruitment, anti-XCL1 was used to block cDC-$CD8^+$ T cell interactions and neutrophil transfusions were performed in the orthotopic NASH-HCC model.

The findings of the study were:

1. **$CXCR2^+$ expression** was detected specifically among **infiltrating neutrophils** in human **NASH** and within the **tumor** of both human and mouse models of **NASH-HCC**. In mouse models, tumor-associated neutrophils (TANs) express inflammatory and pro-tumor neutrophil genes.

2. Using **preclinical models of NASH-HCC** that are **resistant to anti-PD1 therapy**, we observed that such **resistance is overcome** by co-treatment with the **CXCR2 small molecule inhibitor** AZD5069, which can extend survival, reduce tumor burden and impair tumor cell proliferation.

3. The **combination** of anti-PD1 and CXCR2 inhibitor **increased CD8+ T cell infiltration** and induced a higher number of **Granzyme B^+ T cell clusters**. These clusters were also enriched in **conventional $XCR1^+$ dendritic cells** and **immature proliferating neutrophils**.

4. The combination, which increased the number of TANs, also induced a **TAN re-programming** from a pro- to an anti-tumor phenotype: combination-treated TANs were enriched in cell cycle, phagocytosis, antigen presentation and degranulation processes.

5. The treatment based on the **transfusion** of **immature inflammatory neutrophils** in **combination with anti-PD1** had a **similar anti-tumor effect** than the combination with the CXCR2 inhibitor. It also increased intratumor CD8 T cells and conventional dendritic cells. In parallel, **depletion of CD8+ T cells**, **of cDC1s** and **blockade of cDC-CD8+ T cell**

interactions impaired the anti-tumor activity of the combination. Therefore, our results suggest that these cells are required for the therapeutic benefit of the combination.

In conclusion, we observed that TANs can be selectively manipulated through CXCR2 inhibition to adopt an anti-tumor phenotype. The combination of CXCR2 antagonism with anti-PD1 therapy enhances the efficacy of anti-PD1 in preclinical models of NASH-HCC and is a promising candidate for clinical testing.

Hepatology

OPEN ACCESS

Original research

CXCR2 inhibition enables NASH-HCC immunotherapy

Jack Leslie ,[1,2] John B G Mackey,[3] Thomas Jamieson,[3] Erik Ramon-Gil,[1,2] Thomas M Drake,[3,4,5] Frédéric Fercoq ,[3] William Clark,[3] Kathryn Gilroy,[3] Ann Hedley,[3] Colin Nixon,[3] Saimir Luli,[1,2,6] Maja Laszczewska,[1,2] Roser Pinyol ,[7] Roger Esteban-Fabró,[7,8] Catherine E Willoughby ,[7] Philipp K Haber,[8] Carmen Andreu-Oller,[7,8] Mohammad Rahbari ,[9] Chaofan Fan,[9] Dominik Pfister,[9] Shreya Raman,[10] Niall Wilson,[1,2] Miryam Müller ,[3] Amy Collins,[1,2] Daniel Geh ,[1,2] Andrew Fuller,[11] David McDonald,[11] Gillian Hulme,[11] Andrew Filby,[11,12] Xabier Cortes-Lavaud,[3] Noha-Ehssan Mohamed,[3] Catriona A Ford,[3] Ximena L Raffo Iraolagoitia,[3] Amanda J McFarlane,[3] Misti V McCain,[2] Rachel A Ridgway,[3] Edward W Roberts,[3] Simon T Barry,[13] Gerard J Graham,[14] Mathias Heikenwälder,[9,15] Helen L Reeves,[2,16] Josep M Llovet,[7,8,17] Leo M Carlin,[3,5] Thomas G Bird ,[3,4] Owen J Sansom,[3,5,18] Derek A Mann[1,2,19,20]

► Additional supplemental material is published online only. To view, please visit the journal online (http://dx.doi.org/10.1136/gutjnl-2021-326259).

For numbered affiliations see end of article.

Correspondence to
Dr Derek A Mann, Newcastle Fibrosis Research Group, Biosciences Institute, Faculty of Medical Sciences, Newcastle University, Newcastle upon Tyne, Newcastle upon Tyne, UK; derek.mann@newcastle.ac.uk

JL, JBGM and TJ are joint first authors.
JML, LMC, TGB, OJS and DAM are joint senior authors.

Received 5 October 2021
Accepted 17 March 2022
Published Online First 27 April 2022

Linked

► http://dx.doi.org/10.1136/gutjnl-2022-327396

Check for updates

To cite: Leslie J, Mackey JBG, Jamieson T, *et al*. *Gut* 2022;**71**:2093–2106.

ABSTRACT

Objective Hepatocellular carcinoma (HCC) is increasingly associated with non-alcoholic steatohepatitis (NASH). HCC immunotherapy offers great promise; however, recent data suggests NASH-HCC may be less sensitive to conventional immune checkpoint inhibition (ICI). We hypothesised that targeting neutrophils using a CXCR2 small molecule inhibitor may sensitise NASH-HCC to ICI therapy.

Design Neutrophil infiltration was characterised in human HCC and mouse models of HCC. Late-stage intervention with anti-PD1 and/or a CXCR2 inhibitor was performed in murine models of NASH-HCC. The tumour immune microenvironment was characterised by imaging mass cytometry, RNA-seq and flow cytometry.

Results Neutrophils expressing CXCR2, a receptor crucial to neutrophil recruitment in acute-injury, are highly represented in human NASH-HCC. In models of NASH-HCC lacking response to ICI, the combination of a CXCR2 antagonist with anti-PD1 suppressed tumour burden and extended survival. Combination therapy increased intratumoural XCR1$^+$ dendritic cell activation and CD8$^+$ T cell numbers which are associated with anti-tumoural immunity, this was confirmed by loss of therapeutic effect on genetic impairment of myeloid cell recruitment, neutralisation of the XCR1-ligand XCL1 or depletion of CD8$^+$ T cells. Therapeutic benefit was accompanied by an unexpected increase in tumour-associated neutrophils (TANs) which switched from a protumour to anti-tumour progenitor-like neutrophil phenotype. Reprogrammed TANs were found in direct contact with CD8$^+$ T cells in clusters that were enriched for the cytotoxic anti-tumoural protease granzyme B. Neutrophil reprogramming was not observed in the circulation indicative of the combination therapy selectively influencing TANs.

Conclusion CXCR2-inhibition induces reprogramming of the tumour immune microenvironment that promotes ICI in NASH-HCC.

Significance of this study

What is already known on this subject?

⇒ Immune checkpoint inhibition (ICI) therapy is emerging as a promising new therapy for the treatment of advanced hepatocellular carcinoma (HCC).

⇒ Only a minority of HCC patients will respond to ICI therapy and recent data suggest that HCC on the background of non-alcoholic steatohepatitis (NASH) may have reduced sensitivity to this treatment strategy.

⇒ Neutrophils are a typical myeloid component of the liver in NASH and are found either within the HCC tumour microenvironment or in a peritumoural location.

⇒ Neutrophils have considerable phenotypic plasticity and can exist in both tumour promoting and tumour suppressing states.

⇒ Neutrophils may have the ability to influence ICI therapy.

INTRODUCTION

Primary liver cancer is emerging globally as one of the most common and deadly malignancies with 905 000 new diagnosed cases and 830 000 deaths recorded in 2020.[1] Hepatocellular carcinoma (HCC) accounts for up to 85% of primary liver cancers and develops on the background of chronic liver disease caused by persistent virological (hepatitis B virus (HBV) and hepatitis C virus (HCV)) or non-virological liver damage. Due to the increasing prevalence of obesity and the metabolic syndrome a high proportion of HCC is now attributed to non-alcoholic steatohepatitis (NASH), identified as the most common risk factor for HCC in UK and USA.[2 3]

Significance of this study

What are the new findings?

⇒ CXCR2$^+$ neutrophils are found in human NASH and within the tumour of both human and mouse models of NASH-HCC.
⇒ The resistance of NASH-HCC to anti-PD1 therapy is overcome by co-treatment with a CXCR2 small molecule inhibitor, with evidence of reduced tumour burden and extended survival.
⇒ Anti-PD1 and CXCR2 inhibitor combine to selectively reprogramme tumour-associated neutrophils (TANs) from a protumour to an anti-tumour phenotype.
⇒ Reprogrammed TANs proliferate locally within Granzyme B$^+$ immune clusters that contain physically associating CD8$^+$ T cells and antigen presenting cells.
⇒ Conventional XCR1$^+$ dendritic cells are found to be elevated in anti-PD1 and CXCR2 inhibitor treated HCCs and together with CD8$^+$ T cells are required for therapeutic benefit.

How might it impact on clinical practice in the foreseeable future?

⇒ TANs can be selectively manipulated to adopt an anti-tumour phenotype which unlocks their potential for cancer therapy. The ability of CXCR2 antagonism to combine with ICI therapy to bring about enhanced therapeutic benefit in NASH-HCC (and potentially in HCC of other aetiologies) warrents clinical investigation.

Possible curative options for HCC such as tumour resection, liver transplant or ablation are at present limited to a minority of patients who are diagnosed at an early stage of the disease.[4] For more advanced HCC, approved systemic therapies include multikinase inhibitors and agents targeting vascular endothelial growth factor (VEGF) . More recently, immune checkpoint inhibition (ICI) has emerged as a therapeutic modality in HCC with PD1 antibodies (nivolumab and pembrolizumab) being approved, and a combination of anti-PDL1 (atezolizumab) with anti-VEGF (bevacizumab) now being first-line treatment for advanced HCC.[5–7] However, only a minority (up to 30%) of HCC patients respond to immunotherapy.[5–8] Moreover, it was recently reported that HCC on the background of NASH is less responsive to immunotherapy due to a NASH-induced alteration in the immune components of the liver and in particular an expansion in numbers of exhausted CD8$^+$PD1$^+$ T cells, that appear to promote, rather than suppress, NASH-HCC.[9 10] Therefore, advanced therapeutic strategies for HCC will require a deeper appreciation of the complex immune landscape of the tumour microenvironment, and in particular, should also take into account the influence that the background liver pathology may have on the numbers, regional distributions, phenotypes and activities of key immune cell types of relevance to cancer growth.

Recent use of imaging mass cytometry (IMC) and single cell sequencing to probe the cellular constituents of human HCC revealed considerable heterogeneity within the tumour microenvironment with intratumoural region-specific distributions of immune cells.[11] Regions with evidence of less aggressive cancer and ongoing liver damage (fibrogenesisis) were enriched for CD8$^+$ T cells, B cells and CD11b$^+$CD15$^+$GranzymeB$^+$ neutrophils. When considering the growing evidence for both pro-tumour and anti-tumour functions for neutrophils in a variety of cancers[12 13] including HCC[14] we were interested to determine if modulation of neutrophil biology within the tumour microenvironment would influence the resistance of NASH-HCC to anti-PD1 immunotherapy.

Here, we determined that the CXC chemokine receptor, CXCR2 is almost exclusively located on neutrophils in human and mouse NASH-HCC. This finding led us to ask if antagonism of CXCR2 can combine with anti-PD1 to overcome resistance of NASH-HCC to immunotherapy. Our findings suggest that this combination therapy reprogrammes the phenotype of tumour neutrophils and enhances their association with CD8$^+$ T cells and conventional dendritic cells (cDC). Reshaping the tumour immune microenvironment was associated with a T cell- and DC-dependent reduction in tumour burden and increased survival. We propose that combined neutrophil phenotype modification and ICI may achieve improved outcomes in NASH-HCC.

Protumour CXCR2$^+$ neutrophils associate with NASH-HCC resistance to anti-PD1 immunotherapy

To investigate the immunological determinants of unresponsiveness of NASH-HCC to anti-PD1 therapy we designed an orthotopic mouse model using the Hep-53.4 HCC cell line, which was selected due to its high mutational burden (online supplemental figure 1A–C). On the background of steatosis induced by a modified diet of high sugar and fat, we observed weight gain and larger tumours compared with non-steatotic controls (online supplemental figure 1D,E). Tumours in non-steatotic controls were responsive to anti-PD1 therapy, however, anti-PD1 showed no benefit on tumour burden, survival, steatosis, proliferation or immune cell infiltration in steatotic mice (figure 1A–F and online supplemental figure 1H,K). For an additional autochthonous model, we employed either Diethylnitrosamine (DEN) alone or in combination with the American lifestyle induced obesity syndrome diet (DEN/ALIOS), the latter to establish HCC on a background of NASH[15 16] (online supplemental figure 1I–O). Anti-PD1 responsiveness was observed in DEN mice fed a control diet, whereas anti-PD1 therapy had no effect on tumour burden, proliferation, or steatosis and animal survival when mice were fed the ALIOS diet (figure 1G–L and online supplemental figure 1P,Q). However, F4/80$^+$ and CD3$^+$ immune cell infiltrates were increased in anti-PD1 treated ALIOS fed mice (online supplemental figure 1R,S) indicative of anticipated alterations in tumour immunity.

Although elevated numbers of circulating neutrophils are associated with reduced HCC survival,[17] by contrast an enrichment of tumour-associated neutrophils (TANs) is reported to correlate with improved survival.[18] This latter observation indicates a potential for TANs to influence the progression of HCC and raises the question of whether immunotherapy is influencing TANs (and vice versa). Ly6G$^+$ neutrophils were found to be present in both tumour and non-tumour tissue of orthotopic-HCC mice and were significantly elevated in both compartments in the presence of NASH and remained high with anti-PD1 therapy (figure 2A and online supplemental figure 2A). Increased numbers of TANs were also a feature in the DEN/ALIOS model and the increase reached significance with anti-PD1 treatment (figure 2B and online supplemental figure 2A). In addition, TANs were elevated in choline deficient-high fat diet (CD-HFD) spontaneous NASH-HCC model, and were retained with anti-PD1 therapy which is reported to also fail in this model[9] (online supplemental figure 2B,C). Thus, we consistently observe TANs to accumulate in NASH-HCC, independent of the model examined, and they are retained in the tumour with anti-PD1 therapy. TANs display functional heterogeneity including

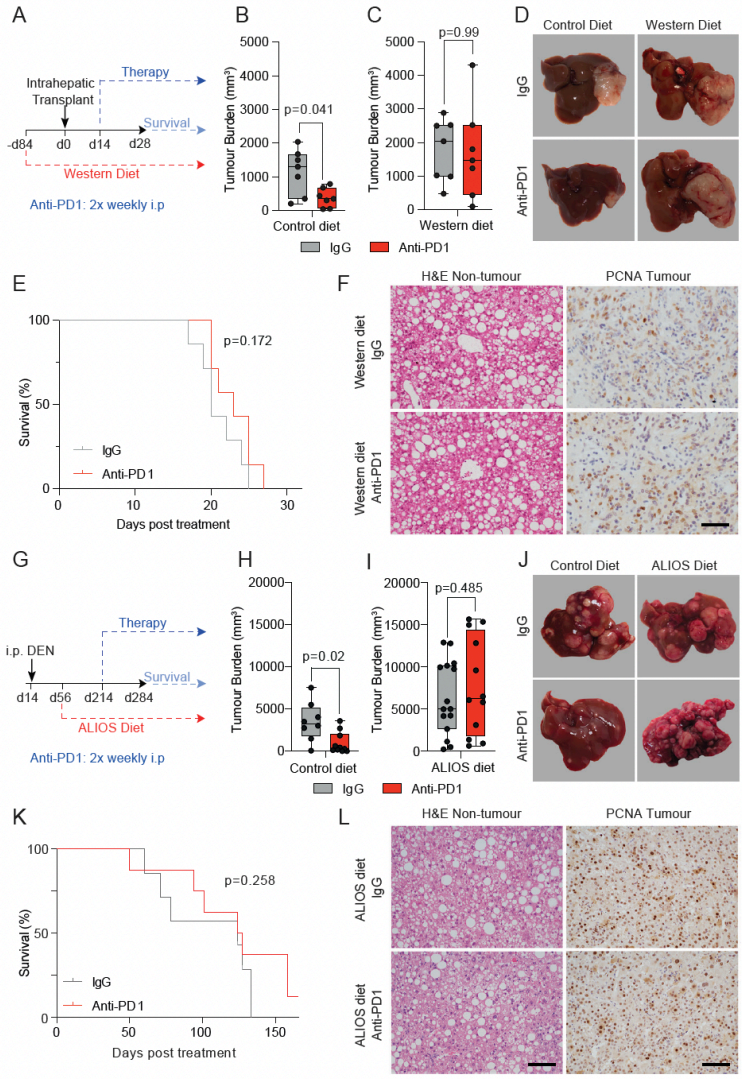

Figure 1 NASH-HCC is resistant to anti-PD1 immunotherapy. (A) Timeline schematic of the NASH-HCC model. (B-D) Quantification and representative images of tumour burden at day 28 post-intrahepatic injection for orthotopic HCC mice fed a control diet or western diet and treated with IgG-control or anti-PD1. (E) Survival plot in orthotopic NASH-HCC mice fed a Western diet and treated with IgG-control or anti-PD1. (F) Representative images of H&E-stained non-tumour livers and PCNA-stained tumours from orthotopic NASH-HCC mice fed a Western diet and treated with IgG-control or anti-PD1. Scale bar = 100 µm. (G) Timeline schematic for the DEN/ALIOS NASH-HCC model. (H-J) Quantification and representative images of tumour burden at day 284 for DEN mice fed a control diet or ALStreated with IgG-control or anti-PD1. (K) Survival plot in DEN/ALIOS mice treated with IgG-control or anti-PD1 (censored at day 165 post-treatment). (L) Representative images of H&E-stained non-tumour livers and PCNA-stained tumours from DEN/ALIOS mice treated with IgG-control or anti-PD1 at day 284. Scale bar = 100 µm. Dots in (B, C, H, I) represent individual mice. Significance tested using: Mann-Whitney*U*-test (A, B, H, L) and Log-rank (Mantel-Cox) test (E, K). Exact p-values indicated on graph. HCC, hepatocellular carcinoma; NASH, non-alcoholic steatohepatitis; PCNA, proliferating cell nuclear antigen.

anti-tumour or protumour phenotypes that impact on tumour growth.[19] Using transcriptomic profiling of tumour-isolated Ly6G$^+$ cells, we determined the phenotype of TANs from DEN/ALIOS tumours. To account for environmentally induced differences in gene expression,[20] we compared TANs with peripheral blood and liver neutrophils. DEGs with increased expression were enriched for process networks associated with inflammatory (eg, *Nfkb1*/*Rel*, *Mapk8*/*Jnk1*, *Mapk9*/*Jnk2*, *Icam1*) and calcium (eg, *Itpr1*, *Plcb1*, *Plcg1*) signalling (figure 2C and online supplemental figure 2D). Genes associated with a protumour neutrophil phenotype, including *Csf1*, *Ccl3*, *Vegfa* and *Ptgs2*[19–21] were also significantly upregulated in TANs (online supplemental figure 2E).

Transcriptomic analysis of DEN/ALIOS tumours identified an upregulation of myeloid associated cytokine and chemokine gene expression compared with normal liver (figure 2D). Notably, ligands (*Cxcl1*, *Cxcl2*, *Cxcl3*, *Cxcl5*) for the chemokine receptor CXCR2, the latter identified as being predominantly expressed by Ly6G$^+$ neutrophils, were all increased in tumour tissue (figure 2D,E and online supplemental figure 2F).

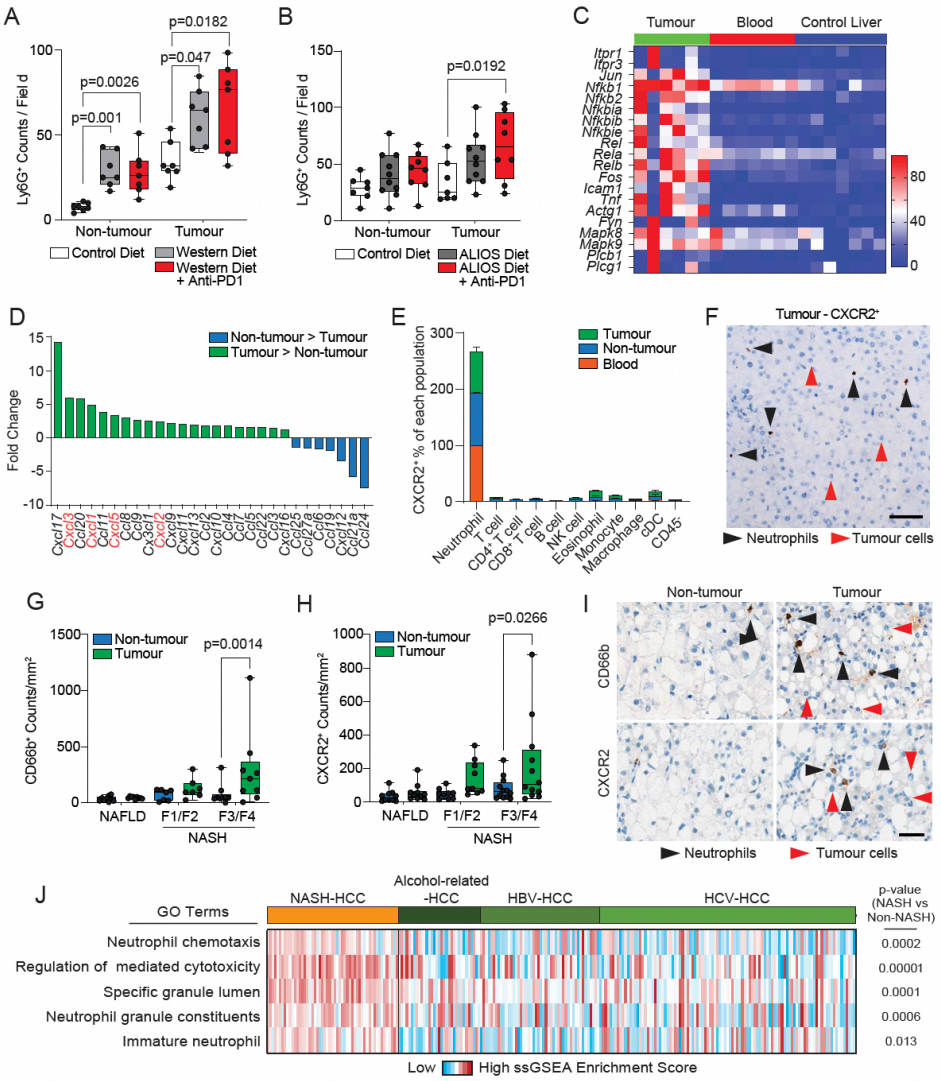

Figure 2 NASH-HCC and anti-PD1 resistance is associated with CXCR2$^+$ neutrophils. (A) Quantification of Ly6G$^+$ counts/field in non-tumour liver and tumours from IgG-control or anti-PD1 treated orthotopic NASH-HCC mice. (B) Quantification of Ly6G$^+$ counts/field in non-tumour liver and tumours from IgG-control or anti-PD1 treated DEN/ALIOS mice. (C) Heatmap showing row-scaled expression of DEGs associated with a pro-tumour neutrophil phenotype upregulated in DEN/ALIOS TANs compared with peripheral blood and control liver neutrophils. (D) Quantification of fold change for *Cxcl* and *Ccl* chemokine transcripts between DEN/ALIOS non-tumour liver and tumour. (E) Flow cytometric quantification of CXCR2$^+$ as a percentage of cell populations in the peripheral blood, non-tumour liver and tumour in DEN/ALIOS mice. Error bars represent Mean ± SEM. (F) Representative image of RNAscope *in situ* hydrisation staining of CXCR2 in DEN/ALIOS mouse tumours. Black arrowheads indicate positive infiltrating non-parenchymal cells and red arrows indicate negative tumour cells. (G-I) Quantification and representative images of CD66b$^+$ and CXCR2$^+$ cell counts/mm^2 in non-tumour liver and tumour by IHC of non-alcoholic fatty liver disease (NAFLD)-HCC and NASH-HCC patient resected tissue. (J) Heatmap showing row-scaled expression of neutrophil-associated process networks for human NASH-HCC compared with HBV, HCV and alcohol-related HCC (non-NASH-HCC). Scale bar = 100 µm. Data are from; bulk Ly6G$^+$ neutrophil RNA-Seq (C), bulk tissue RNA-Seq (D), bulk tumour microarray (J). Dots in (A, B, G, H) represent individual mice. Significance tested using: Two-way ANOVA with Sidak's multiple comparisons test (A, B, G, H). Exact p-values indicated on graph. ALIOS, American lifestyle induced obesity syndrome diet; ANOVA, analysis of variance; DEN, Diethylnitrosamine; GO, gene ontology; HBV, hepatitis B virus; HCC, hepatocellular carcinoma; HCV, hepatitis C virus; IHC, immunohistochemistry; NASH, non-alcoholic steatohepatitis; TANs, tumour-associated neutrophils.

In situ hybridation analysis of *Cxcr2* expression in DEN/ALIOS mouse tumours confirmed expression of *Cxcr2* to be specifically associated with morphologically identified infiltrating neutrophils and absent in parenchymal and tumour cells (figure 2F). This identifies CXCR2 as a neutrophil chemokine receptor that could be targeted to manipulate TANs in models of HCC-NASH.[14] In humans, the CXCR2 ligands *CXCL1* and *CXCL8* were significantly upregulated in NASH-HCC compared with NASH (online supplemental figure 2G). Neutrophil chemotaxis/migratory gene ontology terms were enriched in advanced

human NASH (F4 fibrosis)[22] and numbers of hepatic CD66b$^+$ neutrophils increased with severity of NASH (online supplemental figure 2H,I). Moreover, in HCC patient tissue, CD66b$^+$ neutrophils and CXCR2$^+$ cells predominantly localised to NASH-HCC tumours with expression of the two markers correlating, and furthermore being demonstrated to be colocalised at the cellular level (figure 2G,H and online supplemental figure 2J,K). Similar to the mouse models, CXCR2 expression was limited to infiltrating immune cells and was absent on tumour epithelium within HCC in patients (figure 2I). We additionally noted that neutrophil expression signatures were enriched in human NASH-HCC compared with HBV-HCC, HCV-HCC and alcohol-related-HCC[23] (figure 2J). Thus, tumour infiltration of CXCR2-expressing neutrophils is characteristic of both murine models and human NASH-HCC and associates with resistance to anti-PD1 therapy in experimental models of NASH-HCC.[9]

CXCR2 antagonism resensitises NASH-HCC to immunotherapy

We next determined the effects of a CXCR2 small molecule inhibitor (AZD5069)[24] in experimental NASH-HCC either administered alone or in combination with anti-PD1. We hypothesised that AZD5069 would suppress hepatic neutrophil recruitment. This was confirmed in the context of DEN-induced acute liver damage (online supplemental figure 3A–C). We also observed no change in F4/80$^+$ macrophages and CD3$^+$ T cells (online supplemental figure 3D,E). These data are consistent with previous studies showing that in acute inflammatory settings CXCR2 inhibition selectively reduces neutrophil recruitment.[24]

Treatments using either or both AZD5069/anti-PD1 were then investigated for their ability to suppress tumour growth in the DEN-ALIOS model (figure 3A). Tumour burden at day 284 was reduced for AZD5069 monotherapy and with combined AZD5069/anti-PD1 treatment compared with vehicle and anti-PD1 monotherapy, however, no change in tumour number was identified suggesting a suppression of cancer progression (figure 3B and online supplemental figure 3F,G). Examination of tumours revealed reduced numbers of epithelial mitotic bodies and a lower tumour-stage grading for the AZD5069/anti-PD1 group compared with other treatment arms including AZD5069 monotherapy without significantly altering the underlying NASH pathology (figure 3C–F and online supplemental figure 3H). This is clinically relevant as a high mitotic index in human HCC is a predictor of shorter disease-specific survival.[25] It was therefore noteworthy that the combination of AZD5069/anti-PD1 improved survival relative to monotherapies (figure 3G) Importantly, the benefits of AZD5069/anti-PD1 therapy were recapitulated in the orthotopic NASH-HCC model (figure 3H–J). In contrast to the DEN/ALIOS model, a lack of therapeutic effect was observed with either AZD5069 or anti-PD1 monotherapy (figure 3I,J). However, AZD5069/anti-PD1 combination therapy reduced tumour burden at day 28 and extended survival relative to vehicle control and monotherapies (figure 3I,J and online supplemental figure 3I). Notably, the treatments had no influence on steatosis or body weight (online supplemental figure 3J,K). AZD5069/anti-PD1 treated mice reached clinical endpoint later, at which point tumour burden was similar between treatment arms, this being consistent with suppression of tumour growth (online supplemental figure 3L). Hence, although CXCR2 antagonism alone delivered modest model-dependant antitumour benefit, similar to observations made in models of non-hepatic cancers,[26–31] we show that CXCR2 inhibition sensitises to anti-PD1 immunotherapy in models of NASH-HCC that are otherwise resistant to anti-PD1 monotherapy.

AZD5069/anti-PD1 therapy promotes an antitumour immune microenvironment

To further examine the concept that CXCR2 antagonism sensitises NASH-HCC to anti-PD1 therapy we asked if combination therapy activates classic T-cell mediated anti-tumour immunity. Characterisation of intratumoural T cells revealed intratumoural CD8$^+$ T cells were significantly increased in both anti-PD1 and AZD5069/anti-PD1 therapy groups, with only anti-PD1 monotherapy significantly affecting CD4$^+$ T cells (figure 4A and online supplemental figure 4A). Combination therapy also enhanced intratumoural CD8$^+$ T cell numbers in the orthotopic model (online supplemental figure 4B) Flow cytometric analysis revealed no gross phenotypic changes in early effector CD8$^+$CD44^{Hi} T cells across treatment groups. However, anti-PD1 treatment alone significantly increased numbers of CD8$^+$PD1$^+$ T cells, this effect being recently reported by Pfister *et al*[9] who suggested this T cell phenotype compromises the efficacy of anti-PD1 treatment in NASH-HCC (online supplemental figure 4C). The percentage of CD4$^+$PD1$^+$ T cells was also higher in the context of anti-PD1 monotherapy relative to other treatment groups (online supplemental figure 4D). RNAseq on isolated CD3$^+$ cells revealed enhanced expression of the recently identified T cell ageing markers *Gzmk* and *Eomes* following anti-PD1 therapy, both of which were suppressed when AZD5069 was combined with anti-PD1 (figure 4B). Alongside these changes, AZD5069/anti-PD1 therapy enhanced the expression of Granzyme B (Gzmb), a cytotoxic serine protease expressed by neutrophils, NK cells and by recently activated CD8$^+$ T cells and for which expression correlates with clinical outcome in PD1 immunotherapy.[32–35] Immunostaining of DEN/ALIOS tumours revealed that Gzmb was detected at low levels in vehicle and monotherapy groups yet in the context of AZD5069/anti-PD1 combination therapy was highly expressed and was localised within discrete immune cell clusters containing banded immature neutrophils and lymphocytes (figure 4C and online supplemental figure 4E). Enhanced Gzmb protein expression was also achieved with combination therapy in orthotopic tumours where we also noted that anti-PD1 monotherapy depressed expression of the protease relative to vehicle control (online supplemental figure 4F). These data led us to ask if depletion of CD8$^+$ T cells would modulate the anti-tumour effects of AZD5069/anti-PD1 therapy. Depletion of CD8$^+$ T cells was carried out by administration of anti-CD8α to mice bearing an orthotopic NASH-HCC tumour and alongside AZD5069/anti-PD1 treatment (figure 4D). Succesful depletion of CD8$^+$ T cells was confirmed by an increase in the proportion of CD4$^+$ cells relative to the total CD3$^+$ population (online supplemental figure 4G–I) and resulted in a higher orthotopic tumour burden compared with IgG controls (figure 4E). The requirement for CD8$^+$ T cells for the anti-tumour effect of combination therapy was additionally confirmed by performing anti-CD8α-mediated depletion in tumour-bearing DEN/ALIOS mice treated with combination AZD5069/anti-PD1 (online supplemental figure 4J–M).

As recruitment and activation of XCR1$^+$ cDC1 in tumours is considered critical for activation of cytotoxic CD8$^+$ T cells and immunotherapy[36] we next assessed CD86 surface expression as a marker of cDC1 activation in mice treated with AZD5069/anti-PD1 therapy. Anti-PD1 alone had no effect on activation of intratumour XCR1$^+$ cDC1 cells compared with vehicle controls in the DEN/ALIOS model (figure 4F). AZD5069 alone also had

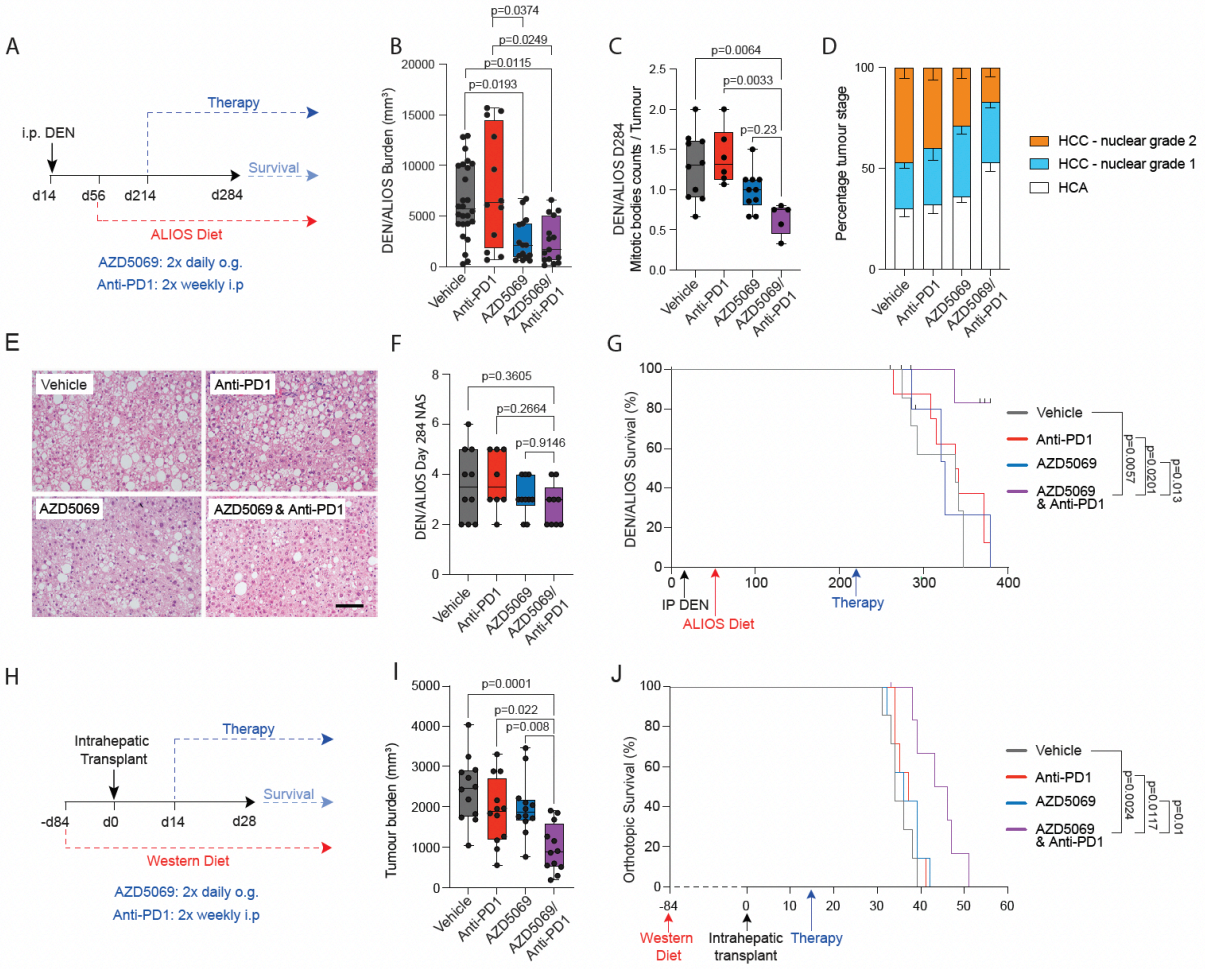

Figure 3 Inhibition of CXCR2$^+$ protumour neutrophils resensitises NASH-HCC to anti-PD1 therapy. (A) Schematic for DEN/ALIOS model treatment regime. (B) Quantification of tumour burden for DEN/ALIOS mice at day 284 for each treatment arm. (C) Quantification of average mitotic body counts per tumour for DEN/ALIOS mice at day 284. (D) Quantification of tumour stage based on nuclear grading for DEN/ALIOS mice at day 284 for each treatment arm. Mean ± SEM. (E) Representative images of non-tumour liver H&E for DEN/ALIOS mice. Scale bar = 100 µm. (F) Quantification of NAFLD activity score (NAS) in the livers for DEN/ALIOS mice at day 284. **G)** Survival plot for DEN/ALIOS mice (censored at day 365). (H) Schematic for orthotopic NASH-HCC model treatment regime. (I) Quantification of tumour burden for the orthotopic NASH-HCC mice at day 28. (J) Survival plot in orthotopic NASH-HCC mice. One mouse censored due to non-liver related medical issue. Dots in (B, C, F, I) represent individual mice.Significance tested using: Kruskal-Wallis test with Dunn's multiple comparisons test (B), One-Way ANOVA with Tukey multiple comparisons test (C, F, I), Log-rank (Mantel-Cox) test (G, J). Exact p-values indicated on graph. ALIOS, American lifestyle induced obesity syndrome diet; ANOVA, analysis of variance; DEN, Diethylnitrosamine; HCC, hepatocellular carcinoma; NAFLD, non-alcoholic fatty liver disease; NASH, non-alcoholic steatohepatitis.

no effect on activation of intratumour XCR1$^+$ cDC1 cells, likely due to the limited expression of CXCR2 on cDCs (figure 2E). However, combined AZD5069/anti-PD1 therapy substantially increased the activation of intratumoural cDC1 cells (figure 4F). As several CC chemokines associated with DC recruitment were expressed in mouse NASH-HCC tumours responding to mono and dual therapies (online supplemental figure 5A) we next determine the effects of perturbing DC recruitment employing mice that are deficient for *Ccr1*, *Ccr2*, *Ccr3* and *Ccr5*, termed iCCR.[37] These mice were treated as per the DEN/ALIOS model and AZD5069/anti-PD1 or control therapy administered (figure 4G). The number of cDC1 and cDC2 cells, and to a lesser extent F4/80$^+$ macrophages but not neutrophils, were decreased in the tumours of iCCR mice (online supplemental figure 5B–D). Importantly, loss of myeloid recruitment alone in iCCR mice had no impact on tumour burden in the DEN/ALIOS model (figure 4H). However, unlike in wild-type mice, AZD5069/anti-PD1 therapy failed to reduce tumour burden in iCCR mice (figure 4H). This loss of effect was associated both with a reduction in tumour associated CD3$^+$CD8$^+$ T cells and loss of granzyme B$^+$ immune clusters (figure 4I,J). To corroborate these data and to more specifically address the role of XCR1$^+$ cDC1 cells we determined if AZD5069/anti-PD1 therapy of orthotopic NASH-HCC would be affected by anti-XCL1-mediated blockade of XCL1, a major chemokine involved in mediating cDC1 and CD8 T cell interactions (figure 4K).[38] AZD5069/anti-PD1 therapy resulted in an increase in activated intratumoural XCR1$^+$ cDC1 cells in line with observations in DEN/ALIOS mice, but with cDC1 activation being selectively suppressed on treatment with anti-XCL1 (online supplemental figure 5E,F).

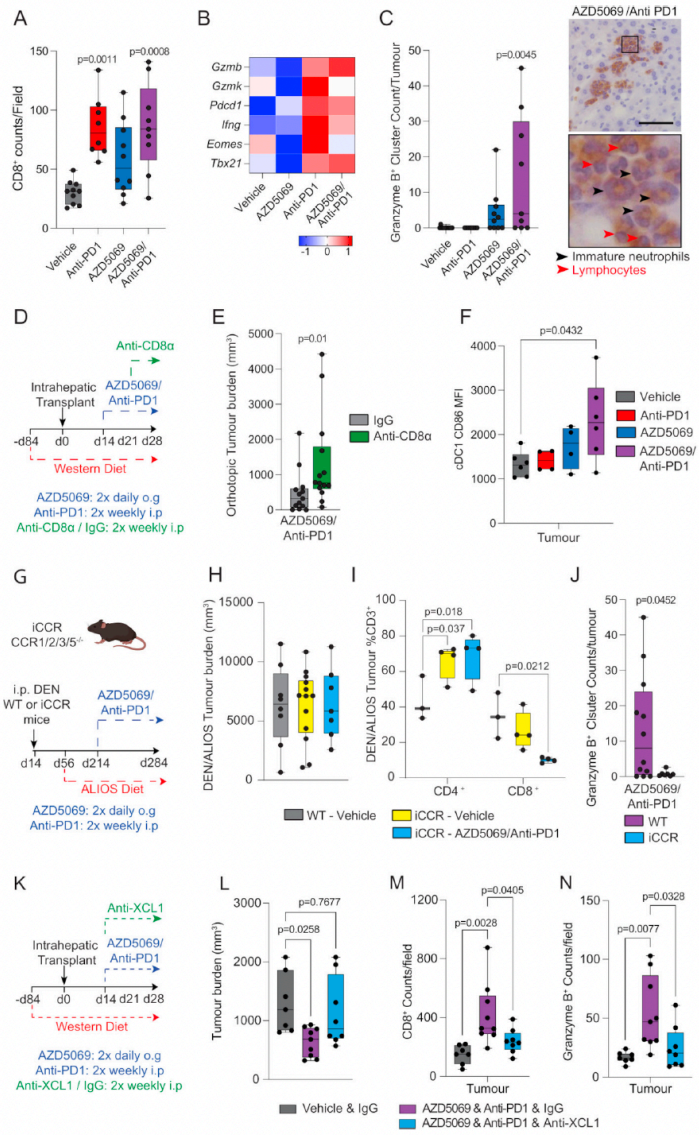

Figure 4 AZD5069/anti-PD1 therapy promotes an anti-tumour immune microenvironment. (A) Quantification of $CD8^+$ counts/field in tumours DEN/ALIOS model from each treatment arm. (B) Heatmap showing row-scaled expression of genes associated with $CD8^+$ T cell activation and exhaustion for DEN/ALIOS treatment groups. Data are from bulk $CD3^+$ Tumour associated T cells analysed by RNA-Seq. (C) Quantification of granzyme B^+clusters in the tumours for DEN/ALIOS mice from each treatment arm at day 284 and representative images of granzyme B^+ clusters in AZD5069/anti-PD1 treated mice (black arrow heads = banded neutrophils; blue arrow heads = lymphocytes). Scale bar = 100 µm. (D) Timeline schematic for the anti-CD8a depletion regime in the orthotopic NASH-HCC model. (E) Quantification of tumour burden in orthotopic NASH-HCC mice treated with AZD5069/anti-PD1 and IgG-control or anti-CD8α at day 28 post-intrahepatic injection. (F) Flow cytometric quantification of CD86 median fluorescence intensity (MFI) of intratumoural $XCR1^+$ cDC1 cells from DEN/ALIOS mice treatment arms at day 284. (G) Timeline schematic for the DEN/ALIOS regimen and targeted therapies in mice with compound deletion of *Ccr1, 2, 3, 5* knockout mice, designated iCCR. (H) Quantification of tumour burden for DEN/ALIOS mice Vehicle-treated WT and iCCR, and AZD5069/anti-PD1 treated iCCR mice at day 284. (I) Flow cytometric quantification of $CD4^+$ and $CD8^+$ cells as a percentage of $CD3^+$ T cells in tumours from WT-Vehicle, iCCR-Vehicle and iCCR-AZD5069/anti-PD1 treated DEN/ALIOS mice at day 284. (J) Quantification of granzyme B^+ clusters in WT and iCCR DEN/ALIOS mice treated with AZD5069/Anti-PD1 at day 284. (K) Timeline schematic for the anti-XCL1 neutralisation regime in the orthotopic NASH-HCC model. (L) Quantification of tumour burden in orthotopic NASH-HCC mice treated with vehicle control and IgG-control or AZD5069/anti-PD1 and either IgG-control or anti-XCL1 at day 28 post-intrahepatic injection. (M, N) Quantification of $CD8^+$ and granzyme B^+ counts/field in tumours of orthotopic NASH-HCC mice treated with vehicle control and IgG-control or AZD5069/anti-PD1 and either IgG-control or anti-XCL1 at day 28 post-intrahepatic injection. Dots in (A, C, E, F, H-J, L-N) represent individual mice. Significance tested using: One-Way ANOVA with Tukey multiple comparisons test (A, C, F, L, M, N), Mann-Whitney *U*-test (E), Two-way ANOVA with Tukey's multiple comparisons test (I), Unpaired T-test (J). Exact p-values indicated on graph. ALIOS, American lifestyle induced obesity syndrome diet; ANOVA, analysis of variance; DEN, Diethylnitrosamine; HCC, hepatocellular carcinoma; ; IHC, immunohistochemistry, NASH, non-alcoholic steatohepatitis; WT, wild-type.

This effect was associated with loss of the anti-tumoural action of AZD5069/anti-PD1 therapy; demonstrated by increased tumour burden in anti-XCL1 treated mice compared with IgG controls (figure 4L). Confirming an associated impact on cytotoxic T cells, AZD5069/anti-PD1-induced increases in intratumoural cytotoxic $CD8^+$ and $GzmB^+$ cells which was suppressed when cDC1 activation was selectively blocked by anti-XCL1 (figure 4M,N). We conclude that combined suppression of CXCR2 and PD1 stimulates both intratumoural recruitment and activation of cDC1 cells enabling T cell-mediated cytotoxicity.

AZD5069/anti-PD1 therapy promotes tumour neutrophil accumulation and the formation of intratumoural immunological hubs

Given that CXCR2 is almost exclusively expressed on neutrophils (figure 2E), we were curious as to their role in AZD5069/anti-PD1 therapy and its associated tumour immune cell remodelling. Unexpectedly, we observed that combination therapy in both models of NASH-HCC was associated with a dramatic increase in TANs, whereas AZD5069 monotherapy brought about the anticipated reduction in TANs (figure 5A,B and online supplemental figure 6A). Real-time analysis of tumour neutrophil infiltration was not possible across the therapy time-course, so instead we examined circulating neutrophils sampled weekly from peripheral blood. Anti-PD1 alone had no demonstrable effects on circulating neutrophil numbers across the treatment period, whereas AZD5069 stimulated a transient increase in circulating $Ly6G^+$ neutrophils peaking at 4 weeks after start of treatment (online supplemental figure 6B). A similar transient increase in circulating neutrophils was observed in AZD5069/anti-PD1 treated mice, however, this effect was delayed peaking at 6 weeks from start of treatment. These peripheral blood data indicated a change in neutrophil behaviour in response to dual long-term targeting of CXCR2 and PD1.

Immunohistochemical analysis of tumours identified clusters of TANs that were unique to AZD5069/anti-PD1 treatment and comprising a mixed population of banded and segmented neutrophil populations (figure 5B,C and online supplemental figure 6C). The presence of these clustered TANs in AZD5069/anti-PD1 treated HCCs was intriguing and suggestive of local proliferation. Zhu *et al*[39] recently described early unipotent neutrophil progenitors (NeP) that produce neutrophils from adult bone marrow (BM). Conspicuously, NePs were significantly increased not only in the BM but also in tumours of AZD5069/anti-PD1 treated mice (figure 5D and online supplemental figure 6D,E). AZD5069/anti-PD1 treatment, therefore, alters granulopoiesis, while intratumour NePs may locally generate neutrophils, thus offering an explanation for the unexpectedly elevated numbers of TANs observed in mice receiving combination therapy.

To validate the presence of immature neutrophils in combined AZD5069/anti-PD1 treated tumours we used IMC of tumour sections from DEN/ALIOS treatment arms (online supplemental figure 6F–J). Neutrophils, both immature and mature, were identified as expressing the primary granule protein MPO. We confirmed intratumoural clusters of proliferating MPO^+Ki67^+ neutrophils to be significantly increased in AZD5069/anti-PD1 treated mice compared with monotherapies and vehicle controls (figure 5E,F). IMC neighbourhood analysis revealed intimate associations of MPO^+Ki67^+ neutrophils with $CD8^+$ T cells and MHC Class II^+ ($MHCII^+$) antigen presenting cells (APCs) that were found in the regions of interest with six out of seven AZD5069/anti-PD1 treated tumours that were examined by IMC (figure 5G–I). In contrast, for anti-PD1 and AZD5069 monotherapies, IMC only detected these mixed immune cell hubs in one tumour for each type of treatment (figure 5I).

Intravital microscopy confirmed the presence of stable tumour-associated $Ly6G^+$ clusters, in vivo, in AZD5069/anti-PD1 treated mice (online supplemental figure 6K,L). Directly interacting $Ly6G^+$ TANs and $CD3^+CD8^+$ T cells that maintained physical contact over several minutes or more were also observed (online supplemental figure 6M).

Longitudinal imaging of ex vivo precision cut liver slices (PCLS) was then performed to further interrogate $Ly6G^+$ cell (neutrophil), $CD8^+$ cell (T cell) and $CD11c^+$ cell (DC and a subset of macrophages) dynamics within the tumours of DEN/ALIOS mice (online supplemental figure 6N,O and video). PCLS from AZD5069/anti-PD1 treated mice had the expected, elevated numbers of neutrophils, $CD11c^+$ cells and $CD8^+$ T cells (online supplemental figure 6P–R). Although T cell speeds remained low in PCLS from all groups, neutrophil speed was increased in AZD5069/anti-PD1 treated tumours suggesting a more actively migrating phenotype for these neutrophils (online supplemental figure 6S,T). Neutrophil-$CD11c^+$ cell interactions were high in tumours irrespective of treatment, however, neutrophil-$CD8^+$ T cell and $CD11c^+$-$CD8^+$ T cell interactions were elevated in AZD5069/anti-PD1 treated tumours compared with vehicle controls (online supplemental figure 6U–Y, video). These data provide evidence that combined therapeutic targeting of $CXCR2^+$ neutrophils and the PD1-PDL1 immune checkpoint remodels the NASH-HCC tumour immune microenvironment, including the generation of locally proliferating immature NeP in close physical association with cytotoxic T cells.

AZD5069/anti-PD1 combination therapy reprogrammes the TAN phenotype

Given that our observations were consistent with intratumoural granulopoiesis in response to combination AZD5069/anti-PD1 therapy, we more closely characterised the TAN phenotype under these conditions. Grieshaber-Bouyer *et al*[40] recently reported a chronologically ordered developmental path for neutrophils termed 'neutrotime'. This extends from immature preneutrophils (early neutrotime) that are predominantly found in BM to fully mature neutrophils (late neutrotime) mainly located in the circulation and spleen (online supplemental figure 7A). TAN transcriptome analysis revealed that AZD5069/anti-PD1 therapy induced neutrotime reprogramming along this neutrotime spectrum (figure 6A and online supplemental figure 7B). TANs in vehicle, anti-PD1 and AZD5069 treated tumours phenotypically resembled mature neutrophils, expressing genes characteristic of the late neutrotime (eg, *Jund, Csf3r, Rps27*) (figure 6A and online supplemental figure 7B). However, late neutrotime genes were comprehensively downregulated in TANs from AZD5069/anti-PD1 treated mice, with a corresponding upregulation of transcripts characteristic of the early neutrotime (eg, *Mmp8, Retnlg, Ltf, Lcn2, Camp, Chil3, Tuba1b, Fcnb*). Lactoferrin (Ltf) was of particular interest among the early neutrotime genes as its protein has well documented anticancer activities; including the activation of DCs and macrophages and enhancing the cytotoxic properties of natural killer cells.[41–43] Staining for Lactoferrin in DEN/ALIOS tumours was elevated in AZD5069/anti-PD1 treated mice where the protein was localised to the neutrophil-rich immune clusters that included banded immature neutrophils (figure 6B,C). These observations indicate a potential mechanism by which reprogrammed TANs may network with other immune cells to enact antitumoural effects.

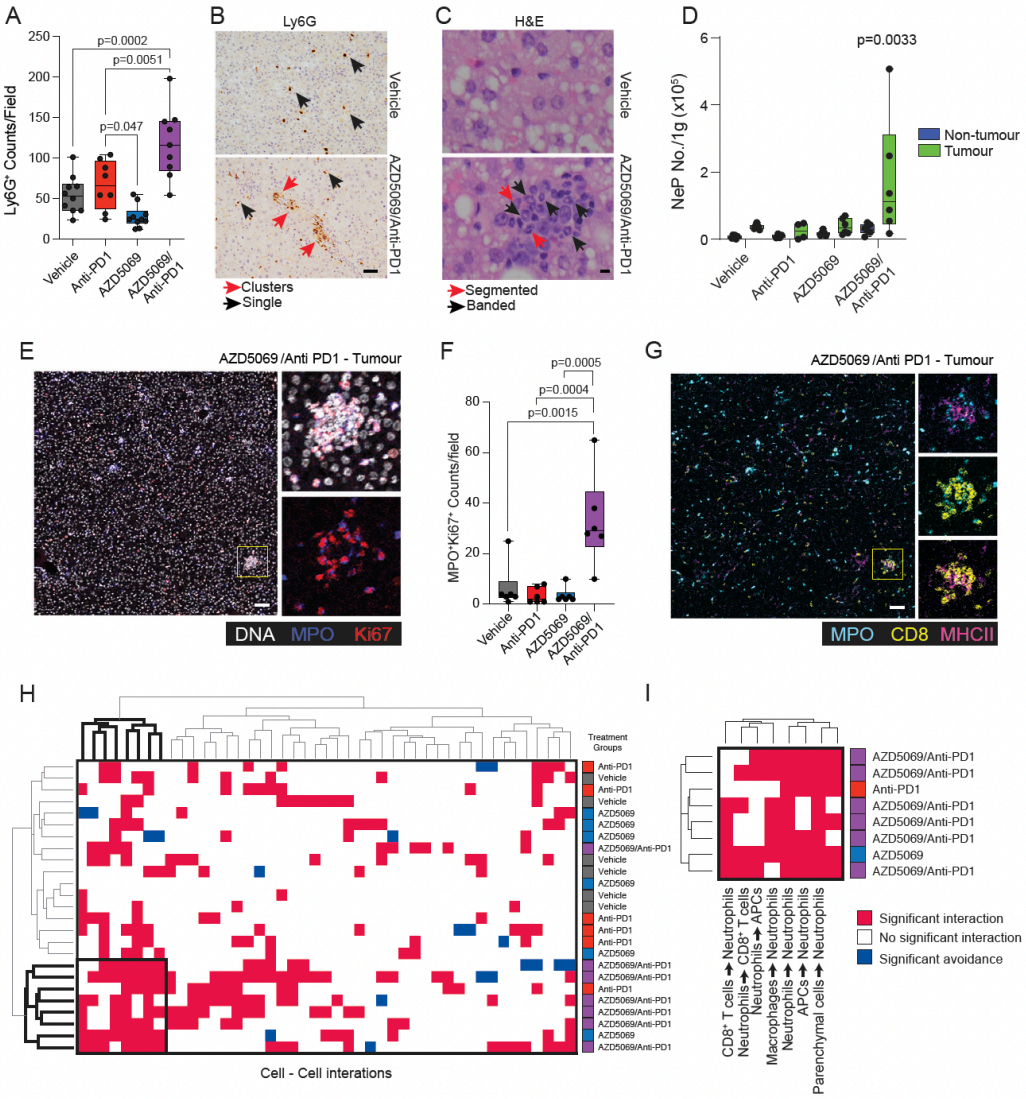

Figure 5 AZD5069/anti-PD1 therapy promotes tumour neutrophil accumulation and the formation of intratumoural immunological hubs. (A) Quantification of Ly6G$^+$ counts/field by IHC for DEN/ALIOS mice tumours at day 284. (B) Representative images of Ly6G$^+$ staining for DEN/ALIOS tumours in mice treated with vehicle or AZD5069/Anti-PD1. Black arrows indicate single Ly6G$^+$ neutrophils; red arrows indicate clusters of Ly6G$^+$ neutrophils. Scale bar = 100 µm. (C) Representative H&E from Vehicle-control and AZD5069/anti-PD1 treated mouse tumours identifying clusters of neutrophils with banded (blue arrows) and segmented (black arrows) nuclear morphology. Scale bar = 10 µm. (D) Flow cytometric quantification of NeP count/gram in non-tumour liver and tumour tissues for DEN/ALIOS mice for each treatment arm at day 284. (E) Representative intra-tumour IMC image for DEN/ALIOS mice treated with AZD5069/anti-PD1. DNA = white; MPO = blue; Ki-67 = red. n=6 mice. Scale bar = 100 µm. (F) Quantification of MPO$^+$Ki-67$^+$ counts/field for DEN/ALIOS tumours from IMC analysis. (G) Representative intra-tumour IMC image for DEN/ALIOS mice treated with AZD5069/anti-PD1. MPO = cyan; CD3 = yellow; MHCII = purple. Scale bar = 100 µm. (H) HistoCAT neighbourhood clustering analysis performed using phonograph clustered cell populations across all four treatment arms where red indicated a significant interaction, blue indicates a significant avoidance and white indicated no significant interaction. Each column represents the interaction of two cell types. Each row represents an individual mouse. (I) Magnified image of HistoCAT neighbourhood clustering analysis. Cluster showing specifically enriched cell-cell interactions. 7/8 cell-cell interactions characterised by antibodies used. Dots in (A, D, F) represent individual mice. Significance tested using: One-Way ANOVA with Tukey's multiple comparisons test (A, F), Two-way ANOVA with Sidak's multiple comparisons test (D). Exact p-values indicated on graph. ALIOS, American lifestyle induced obesity syndrome diet; ANOVA, analysis of variance; APC, antigen presenting cell; DEN, Diethylnitrosamine; HCC, hepatocellular carcinoma; ; IHC, immunohistochemistry, IMC, imaging mass cytometry; NASH, non-alcoholic steatohepatitis.

Interrogation of transcriptome data from NASH-related and non-NASH-related HCC patients identified the late neutrotime signature to be significantly enriched in NASH-HCC when compared with HCCs of other aetiologies[44] (figure 6D). Moreover, the late neutrotime profile was specifically associated with human HCCs that are stratified by gene expression to the immune class and specifically within this group to the exhausted immune class which are typically resistant to immunotherapy

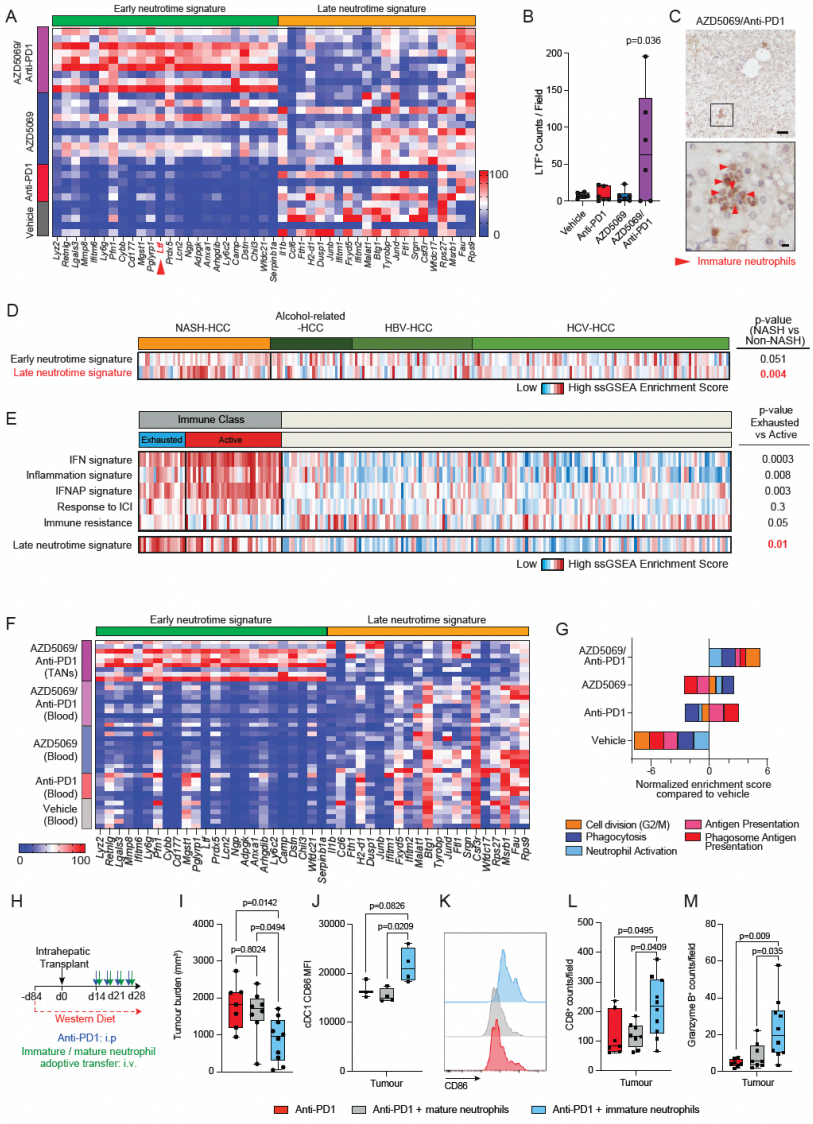

Figure 6 AZD5069/anti-PD1 combination therapy reprogrammes the TAN phenotype. (A) Heatmap showing row-scaled expression of genes associated with late and early neutrotime for DEN/ALIOS mice TANs. (B) Quantification of LTF$^+$ counts/field by IHC for DEN/ALIOS mice tumours at day 284. (C) Represenative image of LTF positive neutrophils (red arrow) in the tumour of AZD5069/anti-PD1 treated DEN/ALIOS mice at day 284. Scale bar top = 100 µm, bottom = 10 µm. (D) Heatmap showing row-scaled expression of early and late neutrotime signatures for human NASH-HCC compared with HBV, HCV and alcohol-related HCC (non-NASH-HCC). In total n=237 patients analysed. (E) Heatmap showing row-scaled expression of published HCC immune class signatures; IFN, inflammation, IFNAP, Response to ICI and immune resistance as well as the late neutrotime signature for human HCC active and exhausted immune subsets. In total n=228 patients analysed. (F) Heatmap showing row-scaled expression of genes associated with late and early neutrotime signatures for DEN/ALIOS peripheral blood neutrophils and AZD5069/Anti-PD1 treated TANs. (G) Gene set enrichment analysis (GSEA) showing normalised enrichment scores for TAN process networks highly enriched in; Anti-PD1 vs Vehicle (Phagosome Antigen Presentation and Antigen Presentation), AZD5069 vs Vehicle (Neutrophil Activation and Phagocytosis), and AZD5069/Anti-PD1 vs Vehicle (G2-M). (H) Timeline schematic for neutrophil based therapy treatment regime in the orthotopic NASH-HCC model. (I) Quantification of tumour burden in orthotopic NASH-HCC mice treated with anti-PD1 and immature or mature neutrophils at day 28 post-intrahepatic injection. (J, K) Flow cytometric quantification and representative histogram plot of CD86 median fluorscent intensity (MFI) of intraturmoural XCR1$^+$ cDC1 cells from orthotopic NASH-HCC neutrophil/anti-PD1 therapy mice at day 28. (L, M) Quantification of intratumoural CD8$^+$ and gramzyme B$^+$ counts/field in the tumours of orthotopic NASH-HCC neutrophil/anti-PD1 therapy mice at day 28. Data are from: Bulk DEN/ALIOS Ly6G$^+$ TAN RNA-Seq data in (A, F, G) and bulk tumour microarray in (D, E). Dots in (B, I, J, L, M) represent individual mice. Significance tested using: One-Way ANOVA with Tukey's multiple comparisons test (B, I, J, L, M). Exact p-values indicated on graph. ALIOS, American lifestyle induced obesity syndrome diet; ANOVA, analysis of variance; DEN, Diethylnitrosamine; HCC, hepatocellular carcinoma; IHC, immunohistochemistry; ICI, immune checkpoint inhibition; NASH, non-alcoholic steatohepatitis; TANs, tumour-associated neutrophils.

(figure 6E).[44–47] This suggests that TANs in human NASH-HCC resemble the mature phenotype of TANs in mouse NASH-HCC and may play a role in preventing ICI responses in patients, and as such we speculate they may be susceptible to similar therapeutic neutrotime reprogramming with AZD5069/anti-PD1 treatment. To examine the stage at which neutrophils are reprogrammed we compared intratumoural to circulating neutrophil profiles in the treatment groups in the DEN/ALIOS model. Neutrotime reprogramming was specific to the intratumoural population of AZD5069/anti-PD1 treated mice and noteably without an associated neutrotime change in circulating neutrophils of this treatment group (figure 6F), this observation being consistent with tumour-selective neutrophil reprogramming. Hence, while the combination therapy brings about reprogramming of TAN maturity, it leaves intact the mature phenotype of circulating neutrophils required for their classic anti-microbial surveillance functions.[48 49]

RNA-Seq of purified Ly6G$^+$ neutrophils revealed that TANs from AZD5069/anti-PD1 treatment mice were enriched for process networks associated with cell cycle, phagocytosis and antigen presentation when compared with vehicle controls (figure 6G and online supplemental figure 7C). AZD5069 monotherapy modestly enhanced the expression of signatures associated with cell division, phagocytosis, and degranulation while also eliciting a reduction in protumour gene expression, with all of these effects being accentuated when AZD5069 was combined with anti-PD1 (figure 6G and online supplemental figure 7C–E). Anti-PD1 treatment promoted antigen presentation and processing signatures, which were also enriched in combined AZD5069/anti-PD1 treatment but not with AZD5069 monotherapy (figure 6G). These findings were again indicative of the combinatorial effects of AZD5069/anti-PD1 therapy on TAN phenotype. AZD5069 monotherapy (but not anti-PD1 monotherapy) suppressed the expression of key immune checkpoint molecules in TANs, including downregulation of *Cd80, Pvr, Sirpa, Pdl1* and *Pdl2*. This loss of immune checkpoint gene expression was maintained in the context of combination therapy and for some genes (eg, *Pvr* and *Srpa*) we noted more pronounced suppressive effects when compared with the AZD5069 montherapy alone (online supplemental figure 7F). Hence, TAN-enriched immune hubs observed in AZD5069/anti-PD1 treated tumours are able to avoid ICI signals that might otherwise cause immune exhaustion. AZD5069/anti-PD1 TANs also displayed a strong correlation with transcriptional changes seen in neutrophils during an acute systemic inflammatory response,[50] including expression of genes involved in exocytosis, myeloid cell activation and degranulation (online supplemental figure 7G,H). Finally, these AZD5069/anti-PD1 TANs closely resembled a recently objectively characterised acute-inflammatory immature-Ly6G^{Int} neutrophil population isolated from lipopolysaccharide-(LPS)-treated mice[50] (online supplemental figure 7I). In summary, AZD5069/anti-PD1 combination therapy brings about reprogramming of HCC-NASH TANs to exhibit immature, proliferative and inflammatory characteristics.

From these data we hypothesised that activated early neutrotime TANs have anti-tumoural properties. Due to their relatively low numbers and lack of specific surface markers it was not possible to isolate reprogrammed TANs from tumours in order to formally test this hypothesis. Instead, as proof-of-principle, we isolated inflammatory immature neutrophils enriched in the BM of LPS-treated mice and a pool of mature BM neutrophils isolated from control PBS treated mice. Adoptively transferring these cells to orthotopic NASH-HCC mice, we asked whether they would bring about an anti-tumoural effect in combination with anti-PD1 treatment (figure 6H and online supplemental figure 7J,K). Transfer of inflammatory immature neutrophils lead to a significant increase in circulating immature CXCR2^{Lo} neutrophils in the blood and resulted in a significant reduction in tumour burden (figure 6I and online supplemental figure 7L). In contrast transfer of mature neutrophils had no effect on tumour burden (figure 6I). To investigate underlying mechanism we examined intratumoural cDC1 and CD8$^+$ T cells. Similar to treatment of mice with AZD5069/anti-PD1, we noted transfused immature neutrophils caused increased activation (CD86$^+$) of intratumoural XCR1$^+$ cDC1 cells and elevated CD8$^+$ T cells in tumours, unlike mice transfused with equal numbers of mature neutrophils (figure 6J–L). Moreover, the adoptive transfer of neutrophils from LPS treated was associated with increased intratumoural Gzmb expression indicative of stimulation of cytotoxic activity within the tumour (figure 6M). Hence, we conclude that BM derived immature inflammatory neutrophils which have phenotypic similarities to AZD5069/anti-PD1 reprogrammed TANs are able to stimulate immune remodelling within HCC tumours and promote anti-tumoural effects.

DISCUSSION

Immune-based therapies hold considerable promise for the treatment of advanced HCC, however at present response rates are low and according to recent reports this is at least in-part determined by the immune cell composition of the tumour.[45 51 52] HCC on the background of NASH presents additional considerations because of the crosstalk occurring between inflammatory cells and various metabolic adaptions manifest in the disease such as insulin resistance, steatosis, oxidative stress and altered mitochondrial function.[53] Pfister and colleagues have reported that immunotherapy in NASH-HCC may be compromised due to high numbers of protumour CD8$^+$PD1$^+$ T cells in the tumour microenvironment.[9] Here we show that selective targeting of neutrophils with a CXCR2 antagonist promotes the anti-tumour effects of anti-PD1 therapy in NASH-HCC, this effect being mechanistically associated with activation of classic CD8$^+$ T cell and DC mediated anti-tumour immunity, but also with intratumoural reprogramming of TAN maturation and phenotype. Based on IMC we propose that the reprogrammed TANs, which are characterised by their proliferative and inflammatory characteristics, associate in tight clusters with CD8$^+$ T cells and APCs to form anti-tumour Gzmb-secreting immune hubs within the NASH-HCC tumour microenvironment. Our work therefore emphasises the strong potential for targeted therapeutic manipulation of the innate immune system in cancer, but also uncovers a previously unrecognised crosstalk between the C-X-C chemokine/CXCR2 and PD1/PDL1 signalling systems that may be exploited to improve immunotherapy responses not only in NASH-HCC but also in other types of cancer that exhibit immunotherapy resistance.[54 55]

Neutrophil infiltration is a key pathological feature of human NASH that may result from upregulation of hepatic CXCL8 (IL-8) and CXCL1,[56 57] which we also report here to be enriched in human NASH-HCC. In addition, expression of CXCR2 on neutrophils in NASH is selectively enhanced through an auto-stimulation mechanism involving the upregulation of neutrophil-derived lipocalin 2.[58] Once present in the NASH and NASH-HCC microenvironments neutrophils are exposed to high levels of TGF-β which, as reported with other cancers,[19–21] can polarise TANs towards a so-called 'N2' tumour-promoting state.[14] It is also pertinent to address the relationship between TANs and myeloid-derived suppressor cells (MDSC), the latter

being a heterogeneous population comprising polymorphonuclear granulocytic $Ly6G^{+}Ly6C^{Lo}$ (PMN-MDSC) and monocytic $Ly6G^{-}Ly6C^{Hi}$ (M-MDSC) cells. Accumulating evidence suggests that PMN-MDSC are immunosuppressive neutrophils and may be functionally very similar to the TANs that have been termed 'N2', with shared protumour properties.[14 59] In the mouse there are no markers to distinguish between PMN-MDSCs and neutrophils and as such we cannot rule out that TANs in mouse models of NASH-HCC include PMN-MDSCs which may also be susceptible to reprogramming in response to combined CXCR2 antagonism and anti-PD1 therapy. However, the typical inhibitory effects on DC and $CD8^{+}$ T cell functions associated with the activities of PMN-MDSCs and immunosuppressive neutrophils were clearly overcome by combined AZD5069/anti-PD1 therapy.

A growing body of evidence suggests that CXCR2 inhibition may be therapeutically beneficial in many human cancers including; pancreatic, lung, ovarian, prostate, colon and now the liver.[26–30 60] Furthermore, in genetic murine models of lung cancer, inhibition of CXCR1 and 2 receptors in combination with anti-PD1 amplified anti-tumour responses.[61 62] The proposed mechanism of action, until now, however, was thought to rely on reprogramming of the tumour immune microenvironment, primarily as a result of impaired myeloid recruitment. The most remarkable immunobiological finding of our study was that, paradoxically, when combined with anti-PD1, CXCR2 inhibition leads to an increase in tumour neutrophils and a selective reprogramming of the TAN neutrotime, with no evidence for a similar systemic effect on circulating neutrophils. The immature proliferative phenotype of the reprogrammed TANs evokes extramedullary granulopoiesis which can be seen in mice following antibody-mediated depletion of $Ly6G^{+}$ cells and that is due to survival and expansion of residual tissue neutrophils driven by high systemic levels of granulocyte colony-stimulating factor,[63] indeed this rebound effect meant that we were unable to exploit this protocol to directly interrogate the function of reprogrammed TANs. However, as proof-of-principle we were able to establish that adoptive transfer of immature activated neutrophils isolated from BM of LPS-treated mice has antitumour activity in NASH-HCC and this effect was accompanied by remodelling of tumour immunity including the activation of cDC1 cells, elevated $CD8^{+}$ T cell counts and induction of antitumoural Gzmb; these being changes that were also noted with AZD506/anti-PD1 therapy. In future work it will be important to identify selective markers of the reprogrammed TANs that might be exploited for detailed functional characterisation, as well as for enabling their selective experimental manipulation which at present is not possible. Also, it will be important to determine precisely how and why combined CXCR2 antagonism and anti-PD1 treatment selectively induces proliferative immature neutrophils in the tumour. Clinically the ability to selectively reprogramme TANs while retaining mature antimicrobial neutrophils in the circulation may be very relevant in HCC since bacterial infections and septic shock are common clinical challenges in cirrhotic patients (in whom 90% of HCC develops).[64]

In summary, we present a novel combination immunotherapy that enhances the efficacy of anti-PD1 in NASH-HCC. As the CXCR2 antagonist AZD5069 has been demonstrated to be safe for use in humans it is timely to determine if HCC patients would benefit from a similar therapy.

METHODS

Mice ethical approval

All animal experiments using the orthotopic NASH-HCC model and DEN/ALIOS model were performed in accordance with a UK Home Office licence (PP8854860, PP390857 and PP0604995), adhered to ARRIVE guidelines (https://www.nc3rs.org.uk/arrive-guidelines), and in accordance with the UK Animal (Scientific Procedures) Act 1986, and were subject to review by the animal welfare and ethical review board of the University of Glasgow and Newcastle University. All mice were housed in specific pathogen free conditions with unrestricted access to food and water and maintained on a constant 12 hours light-dark cycle under controlled climate (19°C–22°C, 45%–65% humidity). All animal experiments using the CD-HFD were performed in accordance with German law and the governmental bodies, and with approval from the Regierungspräsidium Karlsruhe (G11/16, G129/16, G7/17). Male mice were housed at the German Cancer Research Centre (DKFZ) (constant temperature of 20°C–24°C and 45%–65% humidity with a 12 hours light-dark cycle and were maintained under specific pathogen-free conditions.

Quantification and statistical analysis

Statistical analyses were performed using GraphPad Prism software (V.9 GraphPad Software, La Jolla, CA, USA) and R (V.3.5.1) performing tests as indicated and were considered statistically significant. P values are included in figures.

Additional methods are described in online supplemental materials.

Author affiliations
[1]Newcastle Fibrosis Research Group, Biosciences Institute, Faculty of Medical Sciences, Newcastle University, Newcastle Upon Tyne, UK
[2]The Newcastle University Centre for Cancer, Newcastle University, Newcastle upon Tyne, UK
[3]Cancer Research UK Beatson Institute, Glasgow, UK
[4]MRC Centre for Inflammation Research, The Queen's Medical Research Institute, University of Edinburgh, Edinburgh, UK
[5]Institute of Cancer Sciences, University of Glasgow, Glasgow, UK
[6]Preclinical In Vivo Imaging Facility, Faculty of Medical Sciences, Newcastle University, Newcastle upon Tyne, UK
[7]Translational Research in Hepatic Oncology, Liver Unit, IDIBAPS, Hospital Clínic, University of Barcelona, Barcelona, Spain
[8]Mount Sinai Liver Cancer Program, Division of Liver Diseases, Tisch Cancer Institute, Icahn School of Medicine at Mount Sinai, New York, New York, USA
[9]Division of Chronic Inflammation and Cancer, German Cancer Research Centre, Heidelberg, Germany
[10]Department of Pathology, Newcastle Upon Tyne Hospitals NHS Foundation Trust, Newcastle Upon Tyne, UK
[11]Flow Cytometry Facility, Biosciences Institute, Faculty of Medical Sciences, Newcastle University, Newcastle Upon Tyne, UK
[12]Innovation, Methodology and Innovation (IMA) theme, Biosciences Institute, Faculty of Medical Sciences, Newcastle University, Newcastle upon Tyne, UK
[13]Bioscience, Early Oncology, AstraZeneca, Macclesfield, UK
[14]Chemokine Research Group, Institute of Infection, Immunity and Inflammation, University of Glasgow, Glasgow, UK
[15]Department of Surgery, University Hospital Mannheim, Medical Faculty Mannheim, University of Heidelberg, Heidelberg, Germany
[16]Translational and Clinical Research Institute, Faculty of Medical Sciences, Newcastle University, Newcastle upon Tyne, UK
[17]Institució Catalana de Recerca i Estudis Avançats (ICREA), Barcelona, Spain
[18]Beatson Institute for Cancer Research, Glasgow, UK
[19]Fibrofind Ltd, William Leech Building, Medical School, Newcastle University, Newcastle upon Tyne, UK
[20]Department of Gastroenterology and Hepatology, School of Medicine, Koç University, Istanbul, Turkey

Correction notice This article has been corrected since it published Online First. The joint senior shared author statement has been added and the corresponding author's address updated.

Twitter Frédéric Fercoq @FFERCOQ, Roger Esteban-Fabró @ef_roger, Catherine E Willoughby @DrCEWilloughby and Miryam Müller @mimue_lab

Acknowledgements We would like to that the core services and advanced technologies at the CRUK Beatson Institute with particular thanks to the Biological Services Unit, Molecular Services, Bioinformatics, Histology Department and the Beatson Advanced Imaging Resource. We would like to thank Danijela Heide, Jenny Hetzer for technical support for the CD-HFD NASH-HCC model. We would like to thank Catherine Winchester and Nathalie Sphyris for critical reading of the manuscript. We would like to thank the Newcastle University Comparative Biology Centre, Newcastle University Bioimaging Unit and the Newcastle University Flow cytometry core facility for technical assistance.

Contributors JL, JM and TJ performed the majority of the laboratory-based work and analyses presented in the manuscript. ER, TD, FF, WC, KG, AH, CN, SL, ML, RP, PH, RE, CEW, MR, CAF, DP, SR, NW, MVM, AC, DG, AF, DM, AF, XC-L, N-EM, CAF, XLRI, AJM, MVM and RAR performed a portion of the laboratory experiments and their related analyses. ER, SB, JML, MFH and GG provided advice and/or contributed to the experimental design and writing. JL, JM, HR, LC, TB, OJS and DAM conceived the studies, designed the experiments and wrote the manuscript. All authors read and commented on the final manuscript. DAM, OJS, HR, LC and TB provided funding. DAM acts as guarantor for the study.

Funding DM, OJS, HR and TB were supported by program grant funding from CRUK (C9380/A26813). DM was supported by MRC program Grants MR/K0019494/1 and MR/R023026/1. DM, OJS, HR, TB, JM and JML are supported by a CRUK programme grant (C18342/A23390). OJS is funded by a CRUK grant (CRUK A21339). LC is funded by a CRUK grant (CRUK A23983). TB receives research funding support from AstraZeneca. TB and MM were funded by the Wellcome Trust (WT107492Z). HR was funded by CRUK Newcastle Experimental Cancer Medicine Centre award (C9380/A18084). JM and TJ were supported by CRUK core funding (A17196 and A31287). JL was supported by funding from the Faculty of Medical Sciences, Newcatle University. DG is supported by the Newcastle CRUK Clinical Academic Training Programme. AC is funded by the WE Harker Foundation. RE is supported by a doctoral training grant from MICINN/MINECO (BES-2017-081286) and a mobility grant from Fundació Universitària Agustí Pedro i Pons. CEW is supported by a Sara Borrell fellowship (CD19/00109) from the Instituto de Salud Carlos III (ISCIII) and the European Social Fund. PH is supported by a fellowship grant from the German Research Foundation (DFG, HA 8754/1-1). CA-O is supported by a predoctoral research scholarship from Fulbright España. JL is supported by grants from the NIH (RO1DK56621 and RO1DK128289), the Samuel Waxman Cancer Research Foundation, the Spanish National Health Institute (PID2019-105378RB-I00), through an Accelerator award in partnership between Cancer Research UK, Fondazione AIRC and Fundación Científica de la Asociación Española Contra el Cáncer (HUNTER, C9380/A26813), and by the Generalitat de Catalunya (AGAUR, SGR-1358).

Competing interests DM is a director of Fibrofind. JL and DM are shareholders in Fibrofind limited. SB owns shares in AstraZeneca. OJS receives funding from AstraZeneca and Novartis. TGB receives research funding support from AstraZeneca. JML receives research support from Bayer HealthCare Pharmaceuticals, Eisai Inc, Bristol-Myers Squibb, Boehringer-Ingelheim and Ipsen, and consulting fees from Eli Lilly, Bayer HealthCare Pharmaceuticals, Bristol-Myers Squibb, Eisai Inc, Celsion Corporation, Exelixis, Merck, Ipsen, Genentech, Roche, Glycotest, Nucleix, Sirtex, Mina Alpha and AstraZeneca.

Patient and public involvement Patients and/or the public were not involved in the design, or conduct, or reporting, or dissemination plans of this research.

Patient consent for publication Not applicable.

Ethics approval Collection and use of human tissue were ethically approved by the North East – Newcastle and North Tyneside 1 Research Ethics Committee. Human liver tissue from surgical resections was obtained under full ethical approval (H10/H0906/41) and through the CEPA biobank (17/NE/0070) and used subject to patients written consent. HCC tumour and non-tumour biopsy tissue was obtained under full ethical approval as approved by the Newcastle and North Tyneside Regional Ethics Committee, the Newcastle Academic Health Partners Bioresource (NAHPB) and the Newcastle upon Tyne NHS Foundation Trust Research and Development (R&D) department. (Reference numbers: 10/H0906/41; NAHPB Project 48; REC 12/NE/0395; R&D 6579; Human Tissue Act licence 12534).

Provenance and peer review Not commissioned; externally peer reviewed.

Data availability statement Data are available in a public, open access repository. All data will be deposited with accession codes, unique identifiers or web links for publicly available datasets provided before publication.

ORCID iDs
Jack Leslie http://orcid.org/0000-0001-6443-2396
Frédéric Fercoq http://orcid.org/0000-0002-4825-024X
Roser Pinyol http://orcid.org/0000-0002-0288-6314
Catherine E Willoughby http://orcid.org/0000-0002-0617-8833
Mohammad Rahbari http://orcid.org/0000-0003-1133-2134
Miryam Müller http://orcid.org/0000-0002-0751-1407
Daniel Geh http://orcid.org/0000-0002-3592-7469
Thomas G Bird http://orcid.org/0000-0002-6120-1581

REFERENCES

1 Sung H, Ferlay J, Siegel RL, *et al*. Global cancer statistics 2020: GLOBOCAN estimates of incidence and mortality worldwide for 36 cancers in 185 countries. *CA Cancer J Clin* 2021;71:209–49.
2 Younossi Z, Stepanova M, Ong JP, *et al*. Nonalcoholic steatohepatitis is the fastest growing cause of hepatocellular carcinoma in liver transplant candidates. *Clin Gastroenterol Hepatol* 2019;17:748–55.
3 Dyson J, Jaques B, Chattopadyhay D, *et al*. Hepatocellular cancer: the impact of obesity, type 2 diabetes and a multidisciplinary team. *J Hepatol* 2014;60:110–7.
4 Gallage S, García-Beccaria M, Szydlowska M, *et al*. The therapeutic landscape of hepatocellular carcinoma. *Med* 2021;2:505–52.
5 Finn RS, Qin S, Ikeda M, *et al*. Atezolizumab plus bevacizumab in unresectable hepatocellular carcinoma. *N Engl J Med* 2020;382:1894–905.
6 Yau T, Kang Y-K, Kim T-Y, *et al*. Efficacy and safety of nivolumab plus ipilimumab in patients with advanced hepatocellular carcinoma previously treated with sorafenib: the CheckMate 040 randomized clinical trial. *JAMA Oncol* 2020;6:e204564.
7 Finn RS, Ryoo B-Y, Merle P, *et al*. Pembrolizumab as second-line therapy in patients with advanced hepatocellular carcinoma in KEYNOTE-240: a randomized, double-blind, phase III trial. *J Clin Oncol* 2020;38:193–202.
8 Yau T, Park J-W, Finn RS, *et al*. Nivolumab versus sorafenib in advanced hepatocellular carcinoma (CheckMate 459): a randomised, multicentre, open-label, phase 3 trial. *Lancet Oncol* 2022;23:77–90.
9 Pfister D, Núñez NG, Pinyol R, *et al*. NASH limits anti-tumour surveillance in immunotherapy-treated HCC. *Nature* 2021;592:450–6.
10 Haber PK, Puigvehí M, Castet F, *et al*. Evidence-based management of hepatocellular carcinoma: systematic review and meta-analysis of randomized controlled trials (2002-2020). *Gastroenterology* 2021;161:879–98.
11 Sheng J, Zhang J, Wang L, *et al*. Topological analysis of hepatocellular carcinoma tumour microenvironment based on imaging mass cytometry reveals cellular neighbourhood regulated reversely by macrophages with different ontogeny. *Gut* 2022;71:1176–91.
12 Shaul ME, Fridlender ZG. Tumour-associated neutrophils in patients with cancer. *Nat Rev Clin Oncol* 2019;16:601–20.
13 Coffelt SB, Wellenstein MD, de Visser KE. Neutrophils in cancer: neutral no more. *Nat Rev Cancer* 2016;16:431–46.
14 Geh D, Leslie J, Rumney R. Neutrophils as potential therapeutic targets in hepatocellular carcinoma. *Nat Rev Gastroenterol Hepatol* 2022:1–17.
15 Tetri LH, Basaranoglu M, Brunt EM, *et al*. Severe NAFLD with hepatic necroinflammatory changes in mice fed trans fats and a high-fructose corn syrup equivalent. *Am J Physiol Gastrointest Liver Physiol* 2008;295:987–95.
16 Zaki MYW, Mahdi AK, Patman GL, *et al*. Key features of the environment promoting liver cancer in the absence of cirrhosis. *Sci Rep* 2021;11:16727.
17 Margetts J, Ogle LF, Chan SL, *et al*. Neutrophils: driving progression and poor prognosis in hepatocellular carcinoma? *Br J Cancer* 2018;118:248–57.
18 Esteban-Fabró R, Willoughby CE, Piqué-Gili M, *et al*. Cabozantinib enhances the efficacy and immune modulatory activity of anti-PD1 therapy in a syngeneic mouse model of hepatocellular carcinoma. *J Hepatol* 2020;73:S40. doi:10.1016/S0168-8278(20)30632-2
19 Shaul ME, Levy L, Sun J, *et al*. Tumor-associated neutrophils display a distinct N1 profile following TGFβ modulation: a transcriptomics analysis of pro- vs. antitumor TANs. *Oncoimmunology* 2016;5:e1232221.
20 Fridlender ZG, Albelda SM. Tumor-associated neutrophils: friend or foe? *Carcinogenesis* 2012;33:949–55.
21 Fridlender ZG, Sun J, Kim S, *et al*. Polarization of tumor-associated neutrophil phenotype by TGF-beta: "N1" versus "N2" TAN. *Cancer Cell* 2009;16:183–94.

22 Govaere O, Cockell S, Tiniakos D, *et al*. Transcriptomic profiling across the nonalcoholic fatty liver disease spectrum reveals gene signatures for steatohepatitis and fibrosis. *Sci Transl Med* 2020;12:aba4448. doi:10.1126/scitranslmed.aba4448
23 Pinyol R, Torrecilla S, Wang H, *et al*. Molecular characterisation of hepatocellular carcinoma in patients with non-alcoholic steatohepatitis. *J Hepatol* 2021;75:865–78.
24 Jamieson T, Clarke M, Steele CW, *et al*. Inhibition of CXCR2 profoundly suppresses inflammation-driven and spontaneous tumorigenesis. *J Clin Invest* 2012;122:3127–44.
25 Ha SY, Choi M, Lee T, *et al*. The prognostic role of mitotic index in hepatocellular carcinoma patients after curative hepatectomy. *Cancer Res Treat* 2016;48:180–9.
26 Yang G, Rosen DG, Liu G, *et al*. CXCR2 promotes ovarian cancer growth through dysregulated cell cycle, diminished apoptosis, and enhanced angiogenesis. *Clin Cancer Res* 2010;16:3875–86.
27 Steele CW, Karim SA, Leach JDG, *et al*. CXCR2 inhibition profoundly suppresses metastases and augments immunotherapy in pancreatic ductal adenocarcinoma. *Cancer Cell* 2016;29:832–45.
28 Li Y, He Y, Butler W, *et al*. Targeting cellular heterogeneity with CXCR2 blockade for the treatment of therapy-resistant prostate cancer. *Sci Transl Med* 2019;11:aax0428.
29 Cheng Y, Mo F, Li Q, *et al*. Targeting CXCR2 inhibits the progression of lung cancer and promotes therapeutic effect of cisplatin. *Mol Cancer* 2021;20:62.
30 Katoh H, Wang D, Daikoku T, *et al*. CXCR2-expressing myeloid-derived suppressor cells are essential to promote colitis-associated tumorigenesis. *Cancer Cell* 2013;24:631–44.
31 Tang KH, Li S, Khodadadi-Jamayran A, *et al*. Combined inhibition of SHP2 and CXCR1/2 promotes antitumor T-cell response in NSCLC. *Cancer Discov* 2022;12:47–61.
32 Hurkmans DP, Basak EA, Schepers N, *et al*. Granzyme B is correlated with clinical outcome after PD-1 blockade in patients with stage IV non-small-cell lung cancer. *J Immunother Cancer* 2020;8.
33 Rousalova I, Krepela E. Granzyme B-induced apoptosis in cancer cells and its regulation (review). *Int J Oncol* 2010;37:1361–78.
34 Wagner C, Iking-Konert C, Denefleh B, *et al*. Granzyme B and perforin: constitutive expression in human polymorphonuclear neutrophils. *Blood* 2004;103:1099–104.
35 Nowacki TM, Kuerten S, Zhang W, *et al*. Granzyme B production distinguishes recently activated CD8(+) memory cells from resting memory cells. *Cell Immunol* 2007;247:36–48.
36 Gardner A, de Mingo Pulido Álvaro, Ruffell B. Dendritic cells and their role in immunotherapy. *Front Immunol* 2020;11:924.
37 Dyer DP, Medina-Ruiz L, Bartolini R, *et al*. Chemokine receptor redundancy and specificity are context dependent. *Immunity* 2019;50:378–89.
38 Deczkowska A, David E, Ramadori P, *et al*. XCR1^{+} type 1 conventional dendritic cells drive liver pathology in non-alcoholic steatohepatitis. *Nat Med* 2021;27:1043–54.
39 Zhu YP, Padgett L, Dinh HQ, *et al*. Identification of an early Unipotent neutrophil progenitor with pro-tumoral activity in mouse and human bone marrow. *Cell Rep* 2018;24:2329–41.
40 Grieshaber-Bouyer R, Radtke FA, Cunin P, *et al*. The neutrotime transcriptional signature defines a single continuum of neutrophils across biological compartments. *Nat Commun* 2021;12:2856.
41 Actor JK, Hwang S-A, Kruzel ML. Lactoferrin as a natural immune modulator. *Curr Pharm Des* 2009;15:1956–73.
42 Spadaro M, Montone M, Arigoni M, *et al*. Recombinant human lactoferrin induces human and mouse dendritic cell maturation via Toll-like receptors 2 and 4. *Faseb J* 2014;28:416–29.
43 Cutone A, Rosa L, Ianiro G, *et al*. Lactoferrin's anti-cancer properties: safety, selectivity, and wide range of action. *Biomolecules* 2020;10:10030456. doi:10.3390/biom10030456
44 Villanueva A, Portela A, Sayols S, *et al*. DNA methylation-based prognosis and epidrivers in hepatocellular carcinoma. *Hepatology* 2015;61:1945–56.
45 Sia D, Jiao Y, Martinez-Quetglas I, *et al*. Identification of an immune-specific class of hepatocellular carcinoma, based on molecular features. *Gastroenterology* 2017;153:812–26.
46 Ayers M, Lunceford J, Nebozhyn M, *et al*. IFN-γ-related mRNA profile predicts clinical response to PD-1 blockade. *J Clin Invest* 2017;127:2930–40.
47 Sangro B, Melero I, Wadhawan S, *et al*. Association of inflammatory biomarkers with clinical outcomes in nivolumab-treated patients with advanced hepatocellular carcinoma. *J Hepatol* 2020;73:1460–9.
48 Mayadas TN, Cullere X, Lowell CA. The multifaceted functions of neutrophils. *Annu Rev Pathol* 2014;9:181–218.
49 Amulic B, Cazalet C, Hayes GL, *et al*. Neutrophil function: from mechanisms to disease. *Annu Rev Immunol* 2012;30:459–89.
50 Mackey JBG, McFarlane AJ, Jamieson T. Maturation, developmental site, and pathology dictate murine neutrophil function. *bioRxiv*.
51 Kurebayashi Y, Ojima H, Tsujikawa H, *et al*. Landscape of immune microenvironment in hepatocellular carcinoma and its additional impact on histological and molecular classification. *Hepatology* 2018;68:1025–41.
52 Yarchoan M, Xing D, Luan L, *et al*. Characterization of the immune microenvironment in hepatocellular carcinoma. *Clin Cancer Res* 2017;23:7333–9.
53 Anstee QM, Reeves HL, Kotsiliti E, *et al*. From NASH to HCC: current concepts and future challenges. *Nat Rev Gastroenterol Hepatol* 2019;16:411–28.
54 Boi SK, Orlandella RM, Gibson JT, *et al*. Obesity diminishes response to PD-1-based immunotherapies in renal cancer. *J Immunother Cancer* 2020;8:e000725.
55 An Y, Wu Z, Wang N, *et al*. Association between body mass index and survival outcomes for cancer patients treated with immune checkpoint inhibitors: a systematic review and meta-analysis. *J Transl Med* 2020;18:235.
56 Pan X, Chiwanda Kaminga A, Liu A, *et al*. Chemokines in non-alcoholic fatty liver disease: a systematic review and network meta-analysis. *Front Immunol* 2020;11:01802.
57 Liu K, Wang F-S, Xu R. Neutrophils in liver diseases: pathogenesis and therapeutic targets. *Cell Mol Immunol* 2021;18:38–44.
58 Ye D, Yang K, Zang S, *et al*. Lipocalin-2 mediates non-alcoholic steatohepatitis by promoting neutrophil-macrophage crosstalk via the induction of CXCR2. *J Hepatol* 2016;65:988–97.
59 Zhou J, Nefedova Y, Lei A, *et al*. Neutrophils and PMN-MDSC: their biological role and interaction with stromal cells. *Semin Immunol* 2018;35:19–28.
60 Tang KH, Li S, Khodadadi-Jamayran A. Combined inhibition of SHP2 and CXCR1/2 promotes anti-tumor T cell response in NSCLC. *Cancer Discov* 2021.
61 Kargl J, Zhu X, Zhang H, *et al*. Neutrophil content predicts lymphocyte depletion and anti-PD1 treatment failure in NSCLC. *JCI Insight* 2019;4:130850. doi:10.1172/jci.insight.130850
62 Sun L, Clavijo PE, Robbins Y, *et al*. Inhibiting myeloid-derived suppressor cell trafficking enhances T cell immunotherapy. *JCI Insight* 2019;4:126853. doi:10.1172/jci.insight.126853
63 Moses K, Klein JC, Männ L, *et al*. Survival of residual neutrophils and accelerated myelopoiesis limit the efficacy of antibody-mediated depletion of Ly-6G+ cells in tumor-bearing mice. *J Leukoc Biol* 2016;99:811–23.
64 Bajaj JS, Kamath PS, Reddy KR. The evolving challenge of infections in cirrhosis. *N Engl J Med* 2021;384:2317–30.

Discussion

Hepatocellular carcinoma (HCC) is a devastating disease and a major cause of cancer-related death globally, with incidence numbers currently on the rise. A high proportion of cases are diagnosed or progressing to advanced stages, where systemic therapies are the treatment of choice[2,91]. Recently, the combination of atezolizumab and bevacizumab, which has become the standard-of-care in first line[3], has revolutionized the landscape of systemic therapies for advanced HCC[2]. However, the primary resistance rates around 70% highlight the need for a deeper comprehension of the mechanisms behind antitumor immunity and for biomarkers of response to molecular agents; they also leave room for the investigation of novel combinatorial approaches. The studies presented in this doctoral thesis represent a step in that direction.

Copy-number alterations and the molecular and immune profiles of HCC

Genomic instability and the resulting CNAs are considered a cancer enabling characteristic[16]. Recent pan-cancer studies have linked the CNA burdens to tumor immune infiltration and exclusion in several cancer types[4,5], although the strength and direction of these correlations may not be common across all cancer types, which have specific contexts[155].

In HCC, microsatellite instability-high (MSI-H) tumors, which are reported to respond to ICI in a cancer-agnostic manner, represent a minority of cases (<3%)[156]. In addition, the impact of CNA genomic burdens on antitumor immunity had not been comprehensively assessed. In our study we used data from a high-resolution whole-genome SNP array to understand the immune and molecular impact of genomic CNA burdens in HCC, using the scores determined by the CNApp tool for that purpose[11]. We observed, similarly to other cancers[5], that broad CNA landscapes were linked to specific immune profiles, while focal CNA profiles did not. Specifically, low broad CNA tumors displayed features of an immunologically “hot” microenvironment with higher immune infiltration and cytolytic activity, as well as upregulation of proinflammatory cues. This pre-existing immune infiltrate may be harnessed by immunotherapy to trigger an antitumor immune response. Thus, as described in melanoma[5], we hypothesized that low-BS tumors might represent potential responders to immunotherapy. Such hypothesis is further sustained by (i) the transcriptomic similarity between low-BS tumors and tumors responding to immunotherapy from an external cohort

and (ii) the upregulation of genes and pathways linked to response to immunotherapy in HCC found among low-BS HCCs[66]. Conversely, high CNA burdens, linked to immune "cold" microenvironments with immune exclusion and enrichment in DNA repair and proliferation signatures, may identify primary resistant patients where the genetic variability induced by aneuploidy may provide tumor cells with an advantage to avoid immunologic recognition. In these cases, combinatorial approaches of immunotherapies with agents that enhance immune infiltration might be needed to obtain a clinical benefit. Overall, in our study we propose a strategy to classify HCC into immune/inflamed and excluded/noninflamed tumors based on CNAs, regardless of the mutational load. This classification would expand on our previously proposed immune classification of HCC[107,108], and in fact these observations have been subsequently confirmed in a thorough revision of HCC immune-based subclasses[109]. Specifically, we found BS ≤ 4 (low BS) to identify patients with inflamed HCC profiles, and BS ≥ 11 (high BS) to capture HCCs lacking immune-related features. The fact that in HCC only broad CNAs can predict immune profiles aligns with the evidence in melanoma mentioned above[5]. The reason behind this could be that broad CNAs have large phenotypic impacts through the alteration of the expression of many genes[63] and can increase intratumor heterogeneity. Given that the immune system exerts a selective pressure on tumor cells, increased intratumor heterogeneity could facilitate the selection of subclones with specific alterations in immune-related genes or with deletions in immunogenic neoantigens[64,65]. Hypothetically, this may render HCCs with high BS less responsive to immunotherapies. However, because no molecular data allowing to extract CNA profiles of HCC patients treated with immunotherapies are publicly available to date, the predictive value of the scores warrants further validation.

In terms of focal copy-number events, HCCs with a high burden of focal CNAs were characterized by pro-proliferative and more aggressive features and exhibited no *CTNNB1* mutations. The fact that high-FS HCCs were more proliferative is consistent with data from other tumor types[5], and has been demonstrated experimentally in human cell lines with depletion of CDKN2A[157].

The connection of broad CNAs with anti-tumor immunity

We also analyzed the potential mechanisms by which an increase in broad CNA burdens might be associated with exclusion of immune infiltration (**Figure 14**). On one hand, the ratio of observed/expected neoepitopes was lower among high-BS tumors, suggesting that the accumulation of broad CNAs would be linked to an enhanced pruning of neoantigenic mutations, regardless of overall mutation burden (which was higher in the high-BS group); such effect may reduce functional presentation of antigens among high-BS cases, reducing cytolytic activity in those tumors[158]. Another reason would be the reduced antigenicity of neoantigenic mutations among high-BS tumors: in other cancer types, not only the amount of neoantigens has been reported as a determinant of the tumor immune status, but also the ability of neoantigens to induce an immune response[159,160].

In addition, we identified specific CNAs involving genes that could impact antitumor immunity features. For example, gene losses involved in antigen presentation (i.e.,HLA-DQB1), found enriched among high-BS HCCs, could explain the failure in attracting effector T cells in these tumors. Enrichment in arginine degradation pathways among high-BS tumors also point towards an evasion of immune destruction by impairment of the MHC-mediated antigen presentation[161]. Overall, our findings are in concordance with recent studies on NSCLC (TRACERx): tumors sparsely infiltrated exhibited decreased neoantigen editing indicative of copy-number losses of clonal neoantigens, and dysfunction in the neoantigen-presenting machinery, among the mechanisms of immune evasion[161,162].

In parallel, we observed a correlation between broad CNA burden and widespread hypomethylation, in line with previous evidence correlating genomic hypomethylation with immune escape signatures[12]. A higher cell division rate (found in BS-high HCCs) involves methylation loss of late-replicating partial methylation domains, which are enriched in immunomodulatory pathway genes; such effect has been proposed as a mechanism to counteract the contribution of high mutation burden and promote resistance to immunotherapy[12].

Our findings in HCC were found to be extensible to preneoplastic lesions and very early HCCs: the presence of broad CNAs in those samples was linked to reduced cytotoxic activity and immune infiltration features. Although further confirmatory studies with larger cohorts would be required, these data align with the idea that CNAs may contribute to the escape from antitumor immune pressure throughout the hepatocarcinogenic process[5,163].

Even though our data suggest potential explanations for the link between tumor CNA burden and antitumor immunity, further mechanistic studies will be required to determine the causality. Studies in other cancer types have proposed the use of diverse i*n vivo* and *in vitro* models to evaluate the molecular consequences of aneuploidy in cancer cells[152,155,164].

Overall, we observed differential associations between broad and focal genomic CNA burdens and several molecular features of HCC (**Figure 14**). Most importantly, our data reinforce the evidence supporting a differential role for broad CNAs in determining antitumor immune profiles in HCC and provide evidence in favor of chromosomal stability as a hallmark of tumor immunogenicity, and consequently, patient response to immunotherapies.

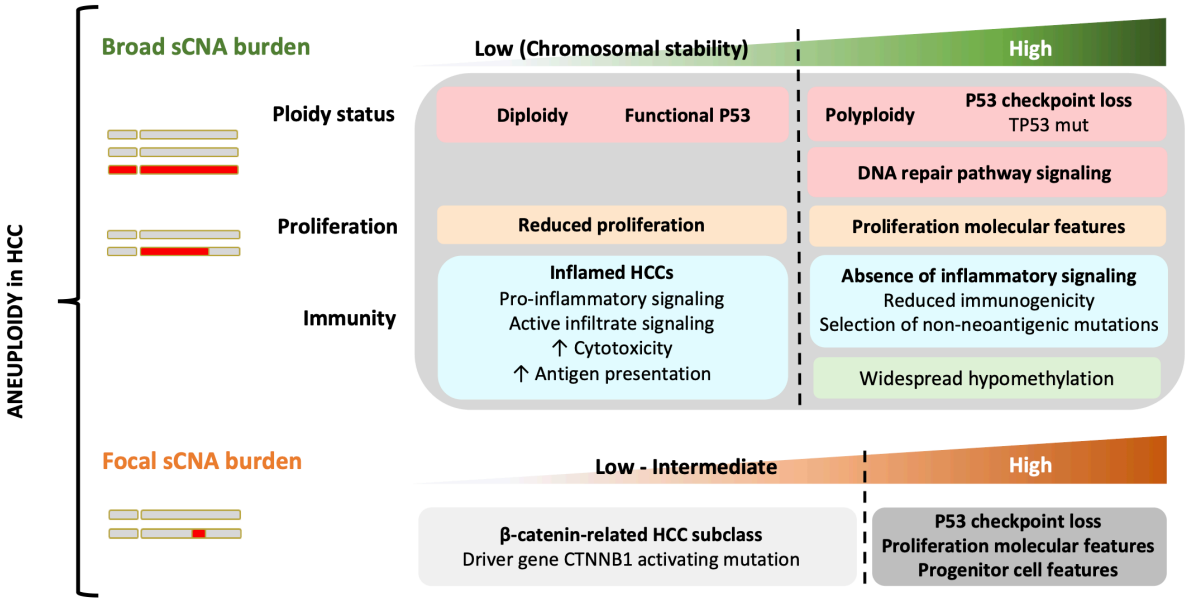

Figure 14 | Differential associations found in HCC for broad and focal CNA burdens. Summary of the findings found in Study 1, where broad CNA burdens were correlated with lack of immune features, while the accumulation of focal CNAs in HCC genomes was linked to proliferative and aggressive tumor features.

Novel combination therapies to overcome primary resistance to immunotherapy in HCC

The recent approval of atezolizumab and bevacizumab has been a pivotal milestone in the treatment of advanced HCC and exposed that combination therapies with ICIs are the future for HCC treatment, although the rates of primary resistance are high. Given the need to broaden the spectrum of responders in HCC by overcoming primary resistance mechanisms[3,127], in the present thesis we described the enhanced antitumor effects of two novel combinatorial approaches: cabozantinib plus anti-PD1 and a CXCR2 inhibitor plus anti-PD1. Both combinations had immunomodulatory activity converging into antitumor neutrophil activity. Thus, we fulfilled our aim to identify therapies triggering antitumor immunity mechanisms that may overcome primary resistance to the available immunotherapeutic strategies in HCC.

The increased anti-tumor effects combining cabozantinib and anti-PD1

We assessed the efficacy and immune modulatory effects of anti-PD1 in combination with cabozantinib, resulting in a greater proportion of antitumor responses in a shorter time, and enhanced molecular features of antitumor immunity including higher neutrophil recruitment and activation. To our knowledge, this is the first study reporting a dominant role of neutrophils, particularly of the N1 phenotype, in the immune effects associated with a TKI combined with anti-PD1 therapy in HCC. We also identified distinct subgroups of human HCCs based on neutrophil features with potential clinical relevance (**Figure 15**).

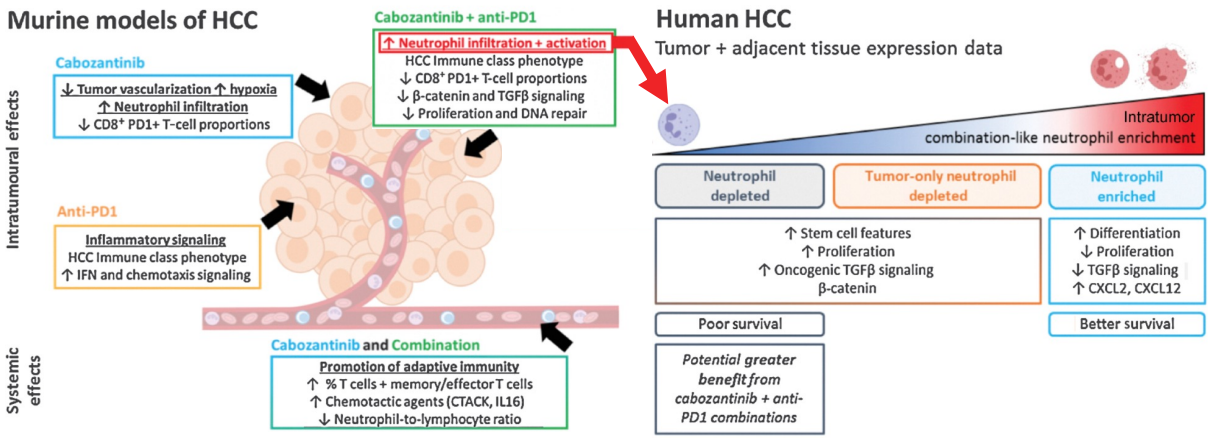

Figure 15 | Schematic summary of the results from Study 2. Adapted from Esteban-Fabró *et al.* Clin Cancer Res 2022.

Previous results in prostate cancer[150] and the transcriptomic data analyzed from colorectal cancer[165] suggest that neutrophil infiltration induced by cabozantinib may be an effect seen in multiple tumor types. Aligned with the results in prostate cancer[150], upregulation of neutrophil chemoattractants binding to the neutrophil receptors CXCR2 (ligands CXCL1, CXCL2) and CXCR4 (ligand CXCL12) could promote neutrophil infiltration and retention in the tumor tissue. Considering the phenotypic plasticity attributed to neutrophils[10], we observed that the combination treatment was able to induce neutrophil activation, possibly due to a contributing pro-inflammatory effect of the immunotherapy. The upregulation of N1 phenotype genes, pathways of neutrophil maturity and degranulation and upregulation of immunoglobulin-related genes linked to antibody-dependent cellular cytotoxicity[166] are evidence in favor of a polarization of neutrophils towards an anti-tumor phenotype. Moreover, combination also decreased β-catenin signaling, which has proven to drive immune exclusion in HCC[107,112], and attenuated TGF-β signaling, which polarizes neutrophils towards the pro-tumor N2 phenotype[81]. Overall, this demonstrates the potential of cabozantinib to trigger a neutrophil-mediated antitumor innate immune response, which is enhanced when combined with anti-PD1 therapy.

In addition, cabozantinib reduced infiltrating $CD8^+PD1^+$ T cells, a clinically interesting effect given that the accumulation of a dysfunctional $CD8^+PD1^+$ T-cell subpopulation could be responsible for the reduced efficacy of ICIs in nonviral HCC, particularly NASH-HCC[9]. Further studies are required to confirm whether this effect could improve NASH-HCC patient response; evaluating this combination in preclinical NASH-HCC models and a subgroup analysis of the COSMIC-312 trial could contribute to answer this question (discussed below).

In parallel to these effects, a wider range of anti-tumor immunity pathways were stimulated by the combination of cabozantinib and anti-PD1 (e.g. reduced Tregs, enriched Th1 and M1 macrophage phenotypes and adaptive and innate immune pathways). The increased proportions of memory/effector T cells found in blood suggest that adaptive immunity was also activated with this treatment, a feature associated with a significant lowering of the neutrophil-to-lymphocyte ratio (NLR) and linked to better prognosis[167].

Finally, consistent with the inhibitory activity of cabozantinib against tyrosine kinases including VEGFR2[149], our data indicate that at least part of the antitumor mechanism of action

of cabozantinib is derived from its antiangiogenic properties (reduced endothelial cells and VEGF signaling, and absence of vessels encapsulating tumor clusters).

In patients with HCC, using MCPCounter[168] as a transcriptomic tool to evaluate active neutrophil infiltration in tumor and nontumor adjacent tissue, we confirmed that neutrophil enrichment in the adjacent tissue or in blood is not always linked to intratumor enrichment. This suggests that neutrophil recruitment mechanisms may be independent in liver adjacent and tumor tissues, and the circulating NLR associated with poor prognosis[167] may not reflect intratumoral neutrophil levels nor their phenotype. This finding has significance given we found that a high enrichment of active neutrophils in the tumor was linked to better outcomes in two independent cohorts, along with less proliferative and more differentiated molecular features, and no enrichment in inflammation profiles (HCC Immune Class[108]). In addition, intratumor neutrophil enrichment was linked to the expression of the chemokines CXCL2 (a CXCR2 ligand like CXCL1 and CXCL3, upregulated by cabozantinib in mice) and CXCL12 (upregulated in our model and previously described as a cabozantinib effect in prostate cancer[150]), suggesting that relevant mechanisms of neutrophil chemoattraction in human HCC were recapitulated in the preclinical models. Moreover, β-catenin pathway activation[107] may negatively influence the presence of this neutrophil phenotype in HCC as we observed it was linked to reduced enrichment in neutrophil signatures and expression of neutrophil chemokines; this may represent an additional immune exclusion effect of β-catenin activation that is worth further exploration.

Taken together, these observations suggest that cabozantinib, particularly in combination with anti-PD1 treatment, contributes to inducing neutrophil infiltration, decreasing an immune suppressive environment, and enhancing antitumor activity compared with the monotherapies in HCC.

Recent evidence from the phase III study COSMIC-312 assessing the combination of cabozantinib plus atezolizumab (anti-PD-L1) versus sorafenib in advanced HCC revealed that the combination significantly improved progression-free survival (median of 6.8 months vs. 4.2 months, HR = 0.63, p=0.0012) and showed increased disease control and lower primary progression compared to sorafenib[169]. However, there was a lack of improvement in overall survival. These data may reflect the need to identify predictive biomarkers for this therapy

and to further explore antitumor immunity mechanisms triggered in the preclinical models that can be extrapolated to human HCC.

In our study, we hypothesized that patients with a reduced enrichment of active neutrophil phenotypes in the tumor (~30% of cases) could potentially gain the greatest benefits from the combination of cabozantinib with anti-PD1 (**Figure 15**). However, given the phenotypic plasticity exhibited by neutrophils and their susceptibility to molecular cues from diseased livers and the tumor microenvironment[10], the molecular assessment of tumor samples from HCC patients exposed to cabozantinib in combination with PD1/PDL1 inhibitors will be necessary to validate these hypotheses.

Overall, we report that the combination of cabozantinib and anti-PD1 has the potential to bring together the activation of adaptive and innate immune responses against the tumor, and this provides a mechanistic rationale for combining these agents to render enhanced antitumor immunity in patients with HCC.

CXCR2 inhibition and anti-PD1 enhance anti-tumor immunity in NASH-HCC

HCC on a NASH background is characterized by a crosstalk between infiltrating immune cells and diverse metabolic adaptations such as insulin resistance, steatosis, oxidative stress and an altered mitochondrial function[170]. In fact, it has been reported that immunotherapy in NASH-HCC may be compromised due to high numbers of exhausted tumor-specific $CD8^+PD1^+$ T cells in the tumor microenvironment[9] and tissue-damaging auto-aggressive $CXCR6^+$ $CD8^+PD1^+$ T cells[171]. Thus, optimized immunotherapeutic strategies may be required to reinvigorate tumor-specific $CD8^+$ T cells to promote antitumor immunity[172].

Here, we show that selective targeting of neutrophils with a CXCR2 antagonist promotes the anti-tumor effects of anti-PD1 therapy in NASH-HCC, this effect being mechanistically associated with activation of classic $CD8^+$ T cells and DC-mediated anti-tumor immunity, but also with intratumoral reprogramming of TAN maturation and phenotype (**Figure 16**). These results therefore emphasize the potential for therapeutic manipulation of the innate immune system in cancer and uncover a crosstalk between the C-X-C chemokine/CXCR2 and PD1/PDL1 signaling that can also be therapeutically exploited.

In NASH, neutrophil recruitment can happen due to upregulation of hepatic CXCL8 and CXCL1[173]. Here, we showed evidence in favor of the same mechanisms in NASH-HCC. Also, CXCR2 expression on neutrophils is increased through an auto-stimulation mechanism involving lipocalin-2[174]. Once infiltrated in the NASH and NASH-HCC microenvironments, exposure to high TGF-β levels may induce neutrophil polarization towards an 'N2' or pro-tumor state[81].

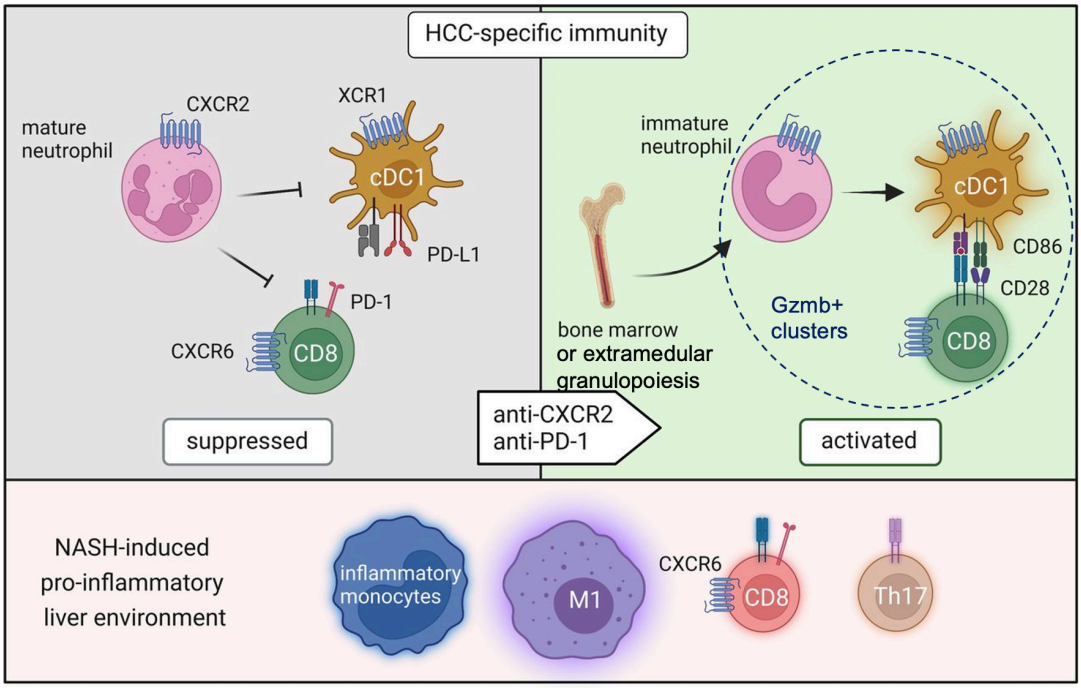

Figure 16 |The blockade of CXCR2 and PD1 in NASH-HCC can reinvigorate HCC-specific immunity. In NASH-HCC, the immune landscape consists of immune cells that contribute to a proinflammatory or to an immune suppressive milieu. Proinflammatory myeloid cells, auto aggressive CXCR6$^+$ CD8 T cells and Th17 cells promote constant liver inflammation, and immune cells like mature neutrophils favor immune suppression near tumor cells. The combination of anti-CXCR2 and anti-PD-1 in preclinical models of NASH-HCC led to a higher number of immature neutrophils in the tumor, promoting efficient priming of tumor-specific CD8 T cells by activated XCR1$^+$ cDC1. XCR1, X-C motif chemokine receptor 1; cDC, conventional dendritic cells; CXCR2, CXC chemokine receptor 2; PD-1, programmed cell death-1; CXCR6, CXC chemokine receptor 6; Th17 cells, T helper 17 cells. HCC, hepatocellular carcinoma; NASH, non-alcoholic steatohepatitis. Figure adapted from Dudek *et al* Gut 2022[172].

Of note, although the current work described these CXCR2$^+$ cells as pro-tumor neutrophils, the TANs named 'N2' may be transcriptomically very similar to the immunosuppressive subset of polymorphonuclear granulocytic myeloid-derived suppressor cells (PMN-MDSCs)[10]. Since there are no markers to differentiate PMN-MDSCs and N2 TANs in mice, it is not possible to rule out that the TANs described in our models include PMN-MDSCs or that PMN-MDSCs are also reprogrammed by the combination therapy proposed here.

An increasing amount of data suggest that CXCR2 inhibition could be therapeutically beneficial in many human cancers including pancreatic, lung, ovarian, prostate, colon and now the liver[10]. Until the present study, the mechanism of action of CXCR2 inhibition combined with PD-1 blockade was thought to be the impairment of myeloid cell recruitment leading to the reprogramming of the tumor immune microenvironment[175]. In our study, paradoxically, the most remarkable immunobiological finding was that CXCR2 inhibition combined with anti-PD1 leads to a selective increase in the recruitment of TANs and their phenotype reprogramming: they become more immature, proliferative and inflammatory (or activated). This effect resembles the extramedullary granulopoiesis in mice following antibody-mediated depletion of $Ly6G^+$ cells and that is due to survival and expansion of residual tissue neutrophils driven by high systemic levels of granulocyte colony-stimulating factor (G-CSF)[176]. As a proof-of-principle of the relevance of reprogrammed TANs for antitumor immunity, we performed adoptive transfer of immature activated neutrophils isolated from the bone marrow of LPS-treated mice and combined it with anti-PD1 therapy in NASH-HCC mice. Consistently, the experiments recapitulated the antitumor activity and the remodeling of tumor immunity of AZD506/anti-PD1 therapy (cDC1 cell activation, elevated $CD8^+$ T cells and induction of Gzmb-positive immune clusters), therefore corroborating this new mechanism of action.

In future work it will be important to perform detailed functional characterization of the reprogrammed TANs by identifying specific markers and to determine precisely how and why this combination selectively induces neutrophil reprogramming in the tumor. Clinically, this selective effect on TANs while retaining mature anti-microbial neutrophils in the circulation may be very relevant in HCC since bacterial infections and septic shock are common clinical challenges in cirrhosis (the background of 90% of HCCs)[177].

In summary, a novel combination immunotherapy that enhances the efficacy of anti-PD1 in NASH-HCC was described. As the CXCR2 antagonist AZD5069 has been demonstrated to be safe for use in humans it is timely to determine if HCC patients would benefit from a similar therapy.

Activating neutrophil anti-tumor immunity in HCC

In general, neutrophils are believed to contribute to the pathogenesis of HCC and to have a role in tumorigenesis, local tumor progression and metastasis via immunosuppression, enhancement of tumor cell survival, invasiveness, extracellular matrix remodeling and angiogenesis[10]. However, the combination therapies of anti-PD1 plus cabozantinib/CXCR2 inhibitor that were tested in preclinical models of HCC successfully modulated neutrophil function: they increased the presence of neutrophils (via enhanced recruitment or local proliferation) and unlocked their anti-tumor potential. Together with the enhanced anti-tumor efficacy results, the data presented here constitutes rationale in favor of targeting this innate immune subset to enhance antitumor immunity and render the HCC immune microenvironment more permissive to systemic immunotherapies. This aligns with preclinical evidence available from prostate cancer, where cabozantinib has shown similar neutrophil-recruiting antitumor activity[150]. Although demonstrating an efficacy and immunomodulatory benefit, we tested therapeutic approaches with a limited specificity for pro-tumor neutrophils; this highlights the need for a deeper understanding of TAN phenotypes. Further research may lead to an improved definition of TAN subpopulations with unique markers and functions that enable more refined strategies to exploit the therapeutic modulation of their phenotypes[10].

Conclusions

The main conclusions arising from the work in this thesis are the following:

- **Broad and focal CNA landscapes** distinguish **specific molecular features of HCC** that can be captured with scores (BS and FS). **Low Broad CNA burdens** (Low BS) are associated with a **pro-inflammatory state**, cytolytic immune responses and a transcriptomic profile like immunotherapy responders. **High Broad CNA loads** (High BS) are linked to a lack of immune-related features and potential mechanisms of resistance like a negative neoantigen selection, impaired mechanisms of antigen presentation and altered methylation patterns.

- **Cabozantinib combined with anti-PD1** enhance anti-tumor immunity bringing together **innate neutrophil-driven** and **adaptive immune responses** in preclinical models of HCC. Combination-treated tumors benefited from the anti-angiogenic and neutrophil-recruiting effects of cabozantinib and the inflammatory signaling promoted by anti-PD1, inducing the strongest antitumor immunity with neutrophil activation, enhanced pro-inflammatory pathways, reduction of immunosuppressive features and the promotion of systemic adaptive immunity.

- **Human HCC** tumors enriched in **neutrophil features** from mice treated with **cabozantinib and anti-PD1-** display a **favorable molecular and clinical profile**, suggesting the benefit of this combination for HCC treatment.

- The novel **combination immunotherapy of CXCR2 inhibition and anti-PD1 enhances the efficacy** of anti-PD1 in preclinical models of **NASH-HCC** and is a promising **candidate for clinical testing**, as $CXCR2^{+}$ neutrophils are found in human NASH and within NASH-HCC tumors.

- **Anti-PD1 and CXCR2 inhibitor** combine to **selectively reprogram tumor-associated neutrophils** (TANs) from a pro- to an **anti-tumor phenotype**. Reprogrammed TANs proliferate locally within Granzyme B^{+} clusters that contain physically associating cytotoxic lymphocytes and antigen presenting dendritic cells, both of which are required for therapeutic benefit.

- The identification of **new molecular features linked to antitumor immunity in HCC** can **broaden our understanding** of the **immunotherapy response and resistance mechanisms** and provide **new candidate predictive biomarkers**.

- The preclinical assessment of **novel combinatorial agents in HCC** can reveal **new mechanisms of immunomodulation** to **enhance immunotherapy response** with the goal to identify promising therapeutic strategies for patients.

References

1. Sung H, Ferlay J, Siegel RL, Laversanne M, Soerjomataram I, Jemal A, & Bray F. Global cancer statistics 2020: GLOBOCAN estimates of incidence and mortality worldwide for 36 cancers in 185 countries. CA: A Cancer Journal for Clinicians 2021;71:209–49.

2. Llovet JM, Kelley RK, Villanueva A, Singal AG, Pikarsky E, Roayaie S, Lencioni R, et al. Hepatocellular carcinoma. Nature Reviews Disease Primers 2021;7.

3. Finn RS, Qin S, Ikeda M, Galle PR, Ducreux M, Kim T-Y, Kudo M, et al. Atezolizumab plus bevacizumab in unresectable hepatocellular carcinoma. New England Journal of Medicine 2020;382:1894–905.

4. Thorsson V, Gibbs DL, Brown SD, Wolf D, Bortone DS, Ou Yang T-H, Porta-Pardo E, et al. The immune landscape of cancer. Immunity 2018:1–19.

5. Davoli T, Uno H, Wooten EC, & Elledge SJ. Tumor aneuploidy correlates with markers of immune evasion and with reduced response to immunotherapy. Science 2017;355.

6. Hegde PS, Karanikas V, & Evers S. The where, the when, and the how of immune monitoring for cancer immunotherapies in the era of checkpoint inhibition. Clinical Cancer Research 2016;22:1865–74.

7. Khan KA, & Kerbel RS. Improving immunotherapy outcomes with anti-angiogenic treatments and vice versa. Nature Reviews Clinical Oncology 2018;15:310–24.

8. Younossi Z, Stepanova M, Ong JP, Jacobson IM, Bugianesi E, Duseja A, Eguchi Y, et al. Nonalcoholic steatohepatitis is the fastest growing cause of hepatocellular carcinoma in liver transplant candidates. Clinical Gastroenterology and Hepatology 2019;17:748-755.e3.

9. Pfister D, Núñez NG, Pinyol R, Govaere O, Pinter M, Szydlowska M, Gupta R, et al. NASH limits anti-tumour surveillance in immunotherapy-treated HCC. Nature 2021;592:450–6.

10. Geh D, Leslie J, Rumney R, Reeves HL, Bird TG, & Mann DA. Neutrophils as potential therapeutic targets in hepatocellular carcinoma. Nature Reviews Gastroenterology Hepatology 2022;19:257–73.

11. Franch-Expósito S, Bassaganyas L, Vila-Casadesús M, Hernández-Illán E, Esteban-Fabró R, Díaz-Gay M, Lozano JJ, et al. CNApp, a tool for the quantification of copy number alterations and integrative analysis revealing clinical implications. Elife 2020;9.

12. Jung H, Kim HS, Kim JY, Sun J-M, Ahn JS, Ahn M-J, Park K, et al. DNA methylation loss promotes immune evasion of tumours with high mutation and copy number load. Nature Communications 2019;10:4278.

13. Roh W, Chen PL, Reuben A, Spencer CN, Prieto PA, Miller JP, Gopalakrishnan V, et al. Integrated molecular analysis of tumor biopsies on sequential CTLA-4 and PD-1 blockade reveals markers of response and resistance. Science Translational Medicine 2017;9.

14. National Cancer Institute. What is cancer? 2021. cancer.gov (accessed December 6, 2022).

15. Torrens L, Pinyol R, Jimenez W, & Llovet JM. Overview of Translational Medicine. In: Llovet JM, editor. Handbook of Translational Medicine, Barcelona: UBe; 2016, p. 21–30.

16. Hanahan D, & Weinberg RA. Hallmarks of cancer: the next generation. Cell 2011;144:646–74.

17. Hanahan D, & Weinberg RA. The hallmarks of cancer. Cell 2000;100:57–70.

18. Hanahan D. Hallmarks of cancer: new dimensions. Cancer Discovery 2022;12:31–46.

19. Jackson SP, & Bartek J. The DNA-damage response in human biology and disease. Nature 2009;461:1071–8.

20. Negrini S, Gorgoulis VG, & Halazonetis TD. Genomic instability--an evolving hallmark of cancer. Nature Reviews Molecular Cell Biology 2010;11:220–8.

21. Stratton MR, Campbell PJ, & Futreal PA. The cancer genome. Nature 2009;458:719–24.

22. Vogelstein B, & Kinzler KW. The path to cancer — three strikes and you're out. New England Journal of Medicine 2015;373:1895–8.

23. Martínez-Jiménez F, Muiños F, Sentís I, Deu-Pons J, Reyes-Salazar I, Arnedo-Pac C, Mularoni L, et al. A compendium of mutational cancer driver genes. Nature Reviews Cancer 2020;20:555–72.

24. Krebs JE, Goldstein ES, & Kilpatrick SE. Genes are DNA. Lewin's Genes XI. 11th ed., Jones and Bartlett Publishers, Inc; 2013, p. 2–25.

25. Vogelstein B, Papadopoulos N, Velculescu VE, Zhou S, Diaz LA, & Kinzler KW. Cancer genome landscapes. Science 2013;340:1546–58.

26. Holland AJ, & Cleveland DW. Losing balance: the origin and impact of aneuploidy in cancer. EMBO Reports 2012;13:501.

27. Pfau SJ, & Amon A. Chromosomal instability and aneuploidy in cancer: from yeast to man. EMBO Reports 2012;13:515–27.

28. Sansregret L, Patterson JO, Dewhurst S, López-García C, Koch A, McGranahan N, Chao WCH, et al. APC/C dysfunction limits excessive cancer chromosomal instability. Cancer Discovery 2017;7:218–33.

29. Schukken KM, & Foijer F. CIN and Aneuploidy: Different Concepts, Different Consequences. BioEssays 2018;40:1700147.

30. Tang Y-C, & Amon A. Gene copy-number alterations: a cost-benefit analysis. Cell 2013;152:394–405.

31. Weiler SME, Pinna F, Wolf T, Lutz T, Geldiyev A, Sticht C, Knaub M, et al. Induction of chromosome instability by activation of Yes-associated protein and Forkhead Box M1 in liver cancer. Gastroenterology 2017;152:2037-2051.e22.

32. Carloni V, Lulli M, Madiai S, Mello T, Hall A, Luong TV, Pinzani M, et al. CHK2 overexpression and mislocalisation within mitotic structures enhances chromosomal instability and hepatocellular carcinoma progression. Gut 2018;67:348–61.

33. Sansregret L, Vanhaesebroeck B, & Swanton C. Determinants and clinical implications of chromosomal instability in cancer. Nature Reviews Clinical Oncology 2018;15:139–50.

34. Burrell RA, McClelland SE, Endesfelder D, Groth P, Weller M-C, Shaikh N, Domingo E, et al. Replication stress links structural and numerical cancer chromosomal instability. Nature 2013;494:492–6.

35. Gordon DJ, Resio B, & Pellman D. Causes and consequences of aneuploidy in cancer. Nature Reviews Genetics 2012;13:189–203.

36. Guichard C, Amaddeo G, Imbeaud S, Ladeiro Y, Pelletier L, Maad I ben, Calderaro J, et al. Integrated analysis of somatic mutations and focal copy-number changes identifies key genes and pathways in hepatocellular carcinoma. Nature Genetics 2012;44:694–8.

37. Krijgsman O, Carvalho B, Meijer GA, Steenbergen RDM, & Ylstra B. Focal chromosomal copy number aberrations in cancer—needles in a genome haystack. Biochimica et Biophysica Acta (BBA) - Molecular Cell Research 2014;1843:2698–704.

38. Beroukhim R, Mermel CH, Porter D, Wei G, Raychaudhuri S, Donovan J, Barretina J, et al. The landscape of somatic copy-number alteration across human cancers. Nature 2010;463:899–905.

39. Zack TI, Schumacher SE, Carter SL, Cherniack AD, Saksena G, Tabak B, Lawrence MS, et al. Pan-cancer patterns of somatic copy number alteration. Nature Genetics 2013;45:1134–40.

40. Totoki Y, Tatsuno K, Covington KR, Ueda H, Creighton CJ, Kato M, Tsuji S, et al. Trans-ancestry mutational landscape of hepatocellular carcinoma genomes. Nature Genetics 2014;46:1267–73.

41. Bakhoum SF, & Compton DA. Chromosomal instability and cancer: a complex relationship with therapeutic potential. Journal of Clinical Investigation 2012;122:1138–43.

42. Anderson NM, & Simon MC. The tumor microenvironment. Current Biology 2020;30:R921–5.

43. Zhang Y, & Zhang Z. The history and advances in cancer immunotherapy: understanding the characteristics of tumor-infiltrating immune cells and their therapeutic implications. Cell Molecular Immunology 2020;17:807–21.

44. Lei X, Lei Y, Li JK, Du WX, Li RG, Yang J, Li J, et al. Immune cells within the tumor microenvironment: Biological functions and roles in cancer immunotherapy. Cancer Letters 2020;470:126–33.

45. Demaria O, Cornen S, Daëron M, Morel Y, Medzhitov R, & Vivier E. Harnessing innate immunity in cancer therapy. Nature 2019;574:45–56.

46. Balkwill FR, Capasso M, & Hagemann T. The tumor microenvironment at a glance. Journal of Cell Science 2012;125:5591–6.

47. Alderton GK, & Bordon Y. Tumour immunotherapy--leukocytes take up the fight. Nature Reviews Immunology 2012;12:237.

48. Vesely MD, Kershaw MH, Schreiber RD, & Smyth MJ. Natural innate and adaptive immunity to cancer. Annual Review of Immunology 2011;29:235–71.

49. Greten FR, & Grivennikov SI. Inflammation and cancer: triggers, mechanisms, and consequences. Immunity 2019;51:27–41.

50. Chen DS, & Mellman I. Oncology meets Immunology: the cancer-immunity cycle. Immunity 2013;39:1–10.

51. Schreiber RD, Old LJ, & Smyth MJ. Cancer immunoediting: integrating immunity's roles in cancer suppression and promotion. Science 2011;331:1565–70.

52. Motz GT, & Coukos G. Deciphering and reversing tumor immune suppression. Immunity 2013;39:61–73.

53. Harlin H, Meng Y, Peterson AC, Zha Y, Tretiakova M, Slingluff C, McKee M, et al. Chemokine expression in melanoma metastases associated with CD8+ T-cell recruitment. Cancer Research 2009;69:3077–85.

54. Bouzin C, Brouet A, Vriese J de, DeWever J, & Feron O. Effects of vascular endothelial growth factor on the lymphocyte-endothelium interactions: identification of caveolin-1 and nitric oxide as control points of endothelial cell anergy. The Journal of Immunology 2007;178:1505–11.

55. Dirkx AEM, Oude Egbrink MGA, Kuijpers MJE, van der Niet ST, Heijnen VVT, Bouma-ter Steege JCA, Wagstaff J, et al. Tumor angiogenesis modulates leukocyte-vessel wall interactions in vivo by reducing endothelial adhesion molecule expression. Cancer Research 2003;63:2322–9.

56. Facciabene A, Motz GT, & Coukos G. T-regulatory cells: key players in tumor immune escape and angiogenesis. Cancer Research 2012;72:2162–71.

57. Gabrilovich DI, & Nagaraj S. Myeloid-derived suppressor cells as regulators of the immune system. Nature Reviews Immunology 2009;9:162–74.

58. Whiteside TL. Tumor-induced death of immune cells: its mechanisms and consequences. Seminars in Cancer Biology 2002;12:43–50.

59. Mendler AN, Hu B, Prinz PU, Kreutz M, Gottfried E, & Noessner E. Tumor lactic acidosis suppresses CTL function by inhibition of p38 and JNK/c-Jun activation. International Journal of Cancer 2012;131:633–40.

60. Palazón A, Aragonés J, Morales-Kastresana A, Ortiz De Landázuri M, & Melero I. Molecular pathways: Hypoxia response in immune cells fighting or promoting cancer. Clinical Cancer Research 2012;18:1207–13.

61. Chang CC, Campoli M, & Ferrone S. Classical and nonclassical HLA class I antigen and NK cell–activating ligand changes in malignant cells: current challenges and future directions. Advances in Cancer Research 2005;93:189–234.

62. Topalian SL, Taube JM, Anders RA, & Pardoll DM. Mechanism-driven biomarkers to guide immune checkpoint blockade in cancer therapy. Nature Reviews Cancer 2016;16:275–87.

63. Bhattacharya A, Bense RD, Urzúa-Traslaviña CG, de Vries EGE, van Vugt MATM, & Fehrmann RSN. Transcriptional effects of copy number alterations in a large set of human cancers. Nature Communications 2020;11:715.

64. Rosenthal R, Swanton C, & McGranahan N. Understanding the impact of immune-mediated selection on lung cancer evolution. British Journal of Cancer 2021;124:1615–7.

65. Anagnostou V, Smith KN, Forde PM, Niknafs N, Bhattacharya R, White J, Zhang T, et al. Evolution of neoantigen landscape during immune checkpoint blockade in non-small cell lung cancer. Cancer Discovery 2017;7:264–76.

66. Chan TA, Wolchok JD, & Snyder A. Genetic basis for clinical response to CTLA-4 blockade in melanoma. New England Journal of Medicine 2015;373:1984–1984.

67. van Allen EM, Miao D, Schilling B, Shukla SA, Blank C, Zimmer L, Sucker A, et al. Genomic correlates of response to CTLA-4 blockade in metastatic melanoma. Science 2015;350:207–11.

68. Khong HT, & Restifo NP. Natural selection of tumor variants in the generation of "tumor escape" phenotypes. Nature Immunology 2002;3:999–1005.

69. Borregaard N. Neutrophils, from marrow to microbes. Immunity 2010;33:657–70.

70. Ballesteros I, Rubio-Ponce A, Genua M, Lusito E, Kwok I, Fernández-Calvo G, Khoyratty TE, et al. Co-option of neutrophil fates by tissue environments. Cell 2020;183:1282-1297.e18.

71. Shaul ME, & Fridlender ZG. Tumour-associated neutrophils in patients with cancer. Nature Reviews Clinical Oncology 2019;16:601–20.

72. Takakura K, Ito Z, Suka M, Kanai T, Matsumoto Y, Odahara S, Matsudaira H, et al. Comprehensive assessment of the prognosis of pancreatic cancer: peripheral blood neutrophil-lymphocyte ratio and immunohistochemical analyses of the tumour site. Scandinavian Journal of Gastroenterology 2016;51:610–7.

73. Gentles AJ, Newman AM, Liu CL, Bratman S v, Feng W, Kim D, Nair VS, et al. The prognostic landscape of genes and infiltrating immune cells across human cancers. Nature Medicine 2015;21:938–45.

74. Wikberg ML, Ling A, Li X, Öberg Å, Edin S, & Palmqvist R. Neutrophil infiltration is a favorable prognostic factor in early stages of colon cancer. Human Pathology 2017;68:193–202.

75. Ilie M, Hofman V, Ortholan C, Bonnetaud C, Coëlle C, Mouroux J, & Hofman P. Predictive clinical outcome of the intratumoral CD66b-positive neutrophil-to-CD8-positive T-cell ratio in patients with resectable nonsmall cell lung cancer. Cancer 2012;118:1726–37.

76. Li YW, Qiu SJ, Fan J, Zhou J, Gao Q, Xiao YS, & Xu YF. Intratumoral neutrophils: A poor prognostic factor for hepatocellular carcinoma following resection. Journal of Hepatology 2011;54:497–505.

77. Patel S, Fu S, Mastio J, Dominguez GA, Purohit A, Kossenkov A, Lin C, et al. Unique pattern of neutrophil migration and function during tumor progression. Nature Immunology 2018;19:1236–47.

78. Jaillon S, Ponzetta A, di Mitri D, Santoni A, Bonecchi R, & Mantovani A. Neutrophil diversity and plasticity in tumour progression and therapy. Nature Reviews Cancer 2020;20:485–503.

79. van Wyk HC, Park JH, Edwards J, Horgan PG, McMillan DC, & Going JJ. The relationship between tumour budding, the tumour microenvironment and survival in patients with primary operable colorectal cancer. British Journal of Cancer 2016;115:156–63.

80. He G, Zhang H, Zhou J, Wang B, Chen Y, Kong Y, Xie X, et al. Peritumoural neutrophils negatively regulate adaptive immunity via the PD-L1/PD-1 signalling pathway in hepatocellular carcinoma. Journal of Experimental and Clinical Cancer Research 2015;34:1–11.

81. Fridlender ZG, Sun J, Kim S, Kapoor V, Cheng G, Ling L, Worthen GS, et al. Polarization of tumor-associated neutrophil phenotype by TGF-β: "N1" versus "N2" TAN. Cancer Cell 2009;16:183–94.

82. López-Lago MA, Posner S, Thodima VJ, Molina AM, Motzer RJ, & Chaganti RSK. Neutrophil chemokines secreted by tumor cells mount a lung antimetastatic response during renal cell carcinoma progression. Oncogene 2013;32:1752–60.

83. Andzinski L, Kasnitz N, Stahnke S, Wu CF, Gereke M, von Köckritz-Blickwede M, Schilling B, et al. Type I IFNs induce anti-tumor polarization of tumor associated neutrophils in mice and human. International Journal of Cancer 2016;138:1982–93.

84. Zhou SL, Zhou ZJ, Hu ZQ, Huang XW, Wang Z, Chen EB, Fan J, et al. Tumor-associated neutrophils recruit macrophages and T-regulatory cells to promote progression of hepatocellular carcinoma and resistance to sorafenib. Gastroenterology 2016;150:1646-1658.e17.

85. Munder M, Schneider H, Luckner C, Giese T, Langhans CD, Fuentes JM, Kropf P, et al. Suppression of T-cell functions by human granulocyte arginase. Blood 2006;108:1627–34.

86. Kuang DM, Zhao Q, Wu Y, Peng C, Wang J, Xu Z, Yin XY, et al. Peritumoral neutrophils link inflammatory response to disease progression by fostering angiogenesis in hepatocellular carcinoma. Journal of Hepatology 2011;54:948–55.

87. Rahib L, Smith BD, Aizenberg R, Rosenzweig AB, Fleshman JM, & Matrisian LM. Projecting cancer incidence and deaths to 2030: the unexpected burden of thyroid, liver, and pancreas cancers in the United States. Cancer Research 2014;74:2913–21.

88. Wang J, Chenivesse X, Henglein B, & Bréchot C. Hepatitis B virus integration in a cyclin A gene in a hepatocellular carcinoma. Nature 1990;343:555–7.

89. Matsushita H, & Takaki A. Alcohol and hepatocellular carcinoma. BMJ Open Gastroenterology 2019;6:e000260.

90. Galle PR, Forner A, Llovet JM, Mazzaferro V, Piscaglia F, Raoul J-L, Schirmacher P, et al. EASL clinical practice guidelines: management of hepatocellular carcinoma. Journal of Hepatology 2018;69:182–236.

91. Llovet JM, Pinyol R, Kelley RK, El-Khoueiry A, Reeves HL, Wang XW, Gores GJ, et al. Molecular pathogenesis and systemic therapies for hepatocellular carcinoma. Nature Cancer 2022;3:386–401.

92. Llovet JM, Zucman-Rossi J, Pikarsky E, Sangro B, Schwartz M, Sherman M, & Gores G. Hepatocellular carcinoma. Nature Reviews Disease Primers 2016;2:16018.

93. Védie A-L, Sutter O, Ziol M, & Nault J-C. Molecular classification of hepatocellular adenomas: impact on clinical practice. Hepatic Oncology 2018;5:HEP04.

94. Michalopoulos GK, & Bhushan B. Liver regeneration: biological and pathological mechanisms and implications. Nature Reviews Gastroenterology Hepatology 2021;18:40–55.

95. Schulze K, Imbeaud S, Letouzé E, Alexandrov LB, Calderaro J, Rebouissou S, Couchy G, et al. Exome sequencing of hepatocellular carcinomas identifies new mutational signatures and potential therapeutic targets. Nature Genetics 2015;47:505–11.

96. Torrecilla S, Sia D, Harrington AN, Zhang Z, Cabellos L, Cornella H, Moeini A, et al. Trunk mutational events present minimal intra- and inter-tumoral heterogeneity in hepatocellular carcinoma. Journal of Hepatology 2017;67:1222–31.

97. Nault JC, Mallet M, Pilati C, Calderaro J, Bioulac-Sage P, Laurent C, Laurent A, et al. High frequency of telomerase reverse-transcriptase promoter somatic mutations in hepatocellular carcinoma and preneoplastic lesions. Nature Communications 2013;4.

98. Ally A, Balasundaram M, Carlsen R, Chuah E, Clarke A, Dhalla N, Holt RA, et al. Comprehensive and integrative genomic characterization of hepatocellular carcinoma. Cell 2017;169:1327-1341.e23.

99. Ahn S-M, Jang SJ, Shim JH, Kim D, Hong S-M, Sung CO, Baek D, et al. Genomic portrait of resectable hepatocellular carcinomas: Implications of *RB1* and *FGF19* aberrations for patient stratification. Hepatology 2014;60:1972–82.

100. Martinez-Quetglas I, Pinyol R, Dauch D, Torrecilla S, Tovar V, Moeini A, Alsinet C, et al. IGF2 is up-regulated by epigenetic mechanisms in hepatocellular carcinomas and is an actionable oncogene product in experimental models. Gastroenterology 2016;151:1192–205.

101. Kim RD, Sarker D, Meyer T, Yau T, Macarulla T, Park JW, Choo SP, et al. First-in-human phase i study of fisogatinib (BLU-554) validates aberrant FGF19 signaling as a driver event in hepatocellular carcinoma. Cancer Discovery 2019;9:1696–707.

102. Sawey ET, Chanrion M, Cai C, Wu G, Zhang J, Zender L, Zhao A, et al. Identification of a therapeutic strategy targeting amplified FGF19 in liver cancer by oncogenomic screening. Cancer Cell 2011;19:347–58.

103. Letouzé E, Shinde J, Renault V, Couchy G, Blanc JF, Tubacher E, Bayard Q, et al. Mutational signatures reveal the dynamic interplay of risk factors and cellular processes during liver tumorigenesis. Nature Communications 2017;8.

104. Alexandrov LB, Kim J, Haradhvala NJ, Huang MN, Tian Ng AW, Wu Y, Boot A, et al. The repertoire of mutational signatures in human cancer. Nature 2020;578:94–101.

105. Hoshida Y, Nijman SMB, Kobayashi M, Chan JA, Brunet JP, Chiang DY, Villanueva A, et al. Integrative transcriptome analysis reveals common molecular subclasses of human hepatocellular carcinoma. Cancer Research 2009;69:7385–92.

106. Chiang DY, Villanueva A, Hoshida Y, Peix J, Newell P, Minguez B, LeBlanc AC, et al. Focal gains of VEGFA and molecular classification of hepatocellular carcinoma. Cancer Research 2008;68:6779–88.

107. Pinyol R, Sia D, & Llovet JM. Immune exclusion-WNT/CTNNB1 class predicts resistance to immunotherapies in HCC. Clinical Cancer Research 2019;25:2021–3.

108. Sia D, Jiao Y, Martinez-Quetglas I, Kuchuk O, Villacorta-Martin C, Castro de Moura M, Putra J, et al. Identification of an immune-specific class of hepatocellular carcinoma, based on molecular features. Gastroenterology 2017;153:812–26.

109. Montironi C, Castet F, Haber PK, Pinyol R, Torres-Martin M, Torrens L, Mesropian A, et al. Inflamed and non-inflamed classes of HCC: a revised immunogenomic classification. Gut 2022:gutjnl-2021-325918.

110. Boyault S, Rickman DS, de Reyniès A, Balabaud C, Rebouissou S, Jeannot E, Hérault A, et al. Transcriptome classification of HCC is related to gene alterations and to new therapeutic targets. Hepatology 2007;45:42–52.

111. Calderaro J, Ziol M, Paradis V, & Zucman-Rossi J. Molecular and histological correlations in liver cancer. Journal of Hepatology 2019;71:616–30.

112. de Galarreta MR, Bresnahan E, Molina-Sánchez P, Lindblad KE, Maier B, Sia D, Puigvehi M, et al. β-catenin activation promotes immune escape and resistance to anti–PD-1 therapy in hepatocellular carcinoma. Cancer Discovery 2019;9:1124–41.

113. Bruni D, Angell HK, & Galon J. The immune contexture and Immunoscore in cancer prognosis and therapeutic efficacy. Nature Reviews Cancer 2020;20:662–80.

114. Pfister D, Núñez NG, Pinyol R, Govaere O, Pinter M, Szydlowska M, Gupta R, et al. NASH limits anti-tumour surveillance in immunotherapy-treated HCC. Nature 2021;592:450–6.

115. Magen A, Hamon P, Fiaschi N, Troncoso L, Humblin E, D'souza D, Dawson T, et al. Intratumoral mregDC and CXCL13 T helper niches enable local differentiation of CD8 T cells following PD-1 blockade. BioRxiv 2022:2022.06.22.497216.

116. Prieto J, Melero I, & Sangro B. Immunological landscape and immunotherapy of hepatocellular carcinoma. Nature Reviews Gastroenterology Hepatology 2015;12:681–700.

117. Zhu AX, Abbas AR, de Galarreta MR, Guan Y, Lu S, Koeppen H, Zhang W, et al. Molecular correlates of clinical response and resistance to atezolizumab in combination with bevacizumab in advanced hepatocellular carcinoma. Nature Medicine 2022;28:1599–611.

118. Lavin Y, Mortha A, Rahman A, & Merad M. Regulation of macrophage development and function in peripheral tissues. Nature Reviews Immunology 2015;15:731–44.

119. Llovet JM, Castet F, Heikenwalder M, Maini MK, Mazzaferro V, Pinato DJ, Pikarsky E, et al. Immunotherapies for hepatocellular carcinoma. Nature Reviews Clinical Oncology 2022;19:151–72.

120. Arihara F, Mizukoshi E, Kitahara M, Takata Y, Arai K, Yamashita T, Nakamoto Y, et al. Increase in CD14+HLA-DR-/low myeloid-derived suppressor cells in hepatocellular carcinoma patients and its impact on prognosis. Cancer Immunology, Immunotherapy 2013;62:1421–30.

121. Hoechst B, Ormandy LA, Ballmaier M, Lehner F, Krüger C, Manns MP, Greten TF, et al. A new population of myeloid-derived suppressor cells in hepatocellular carcinoma patients induces CD4+CD25+Foxp3+ T cells. Gastroenterology 2008;135:234–43.

122. Zhou SL, Dai Z, Zhou ZJ, Wang XY, Yang GH, Wang Z, Huang XW, et al. Overexpression of CXCL5 mediates neutrophil infiltration and indicates poor prognosis for hepatocellular carcinoma. Hepatology 2012;56:2242–54.

123. Fukumura D, Kloepper J, Amoozgar Z, Duda DG, & Jain RK. Enhancing cancer immunotherapy using antiangiogenics: Opportunities and challenges. Nature Reviews Clinical Oncology 2018;15:325–40.

124. Ziogas AC, Gavalas NG, Tsiatas M, Tsitsilonis O, Politi E, Terpos E, Rodolakis A, et al. VEGF directly suppresses activation of T cells from ovarian cancer patients and healthy individuals via VEGF receptor type 2. International Journal of Cancer 2012;130:857–64.

125. Haber PK, Castet F, Torres-Martin M, Andreu-Oller C, Puigvehí M, Miho M, Radu P, et al. Molecular markers of response to anti-PD1 therapy in advanced hepatocellular carcinoma. Gastroenterology 2022.

126. Pinyol R, Torrecilla S, Wang H, Montironi C, Piqué-Gili M, Torres-Martin M, Wei-Qiang L, et al. Molecular characterisation of hepatocellular carcinoma in patients with non-alcoholic steatohepatitis. Journal of Hepatology 2021;75:865–78.

127. Llovet JM, Montal R, Sia D, & Finn RS. Molecular therapies and precision medicine for hepatocellular carcinoma. Nature Reviews Clinical Oncology 2018;15:599–616.

128. Haber PK, Puigvehí M, Castet F, Lourdusamy V, Montal R, Tabrizian P, Buckstein M, et al. Evidence-based management of hepatocellular carcinoma: systematic review and meta-analysis of randomized controlled trials (2002–2020). Gastroenterology 2021;161:879–98.

129. Llovet J, Ricci S, Mazzaferro V, Hilgard P, Gane E, Blanc J-FJJ, de Oliveira ACAACA, et al. Sorafenib in advanced hepatocellular carcinoma. New England Journal of Medicine 2008;359:378–90.

130. Kudo M, Finn RS, Qin S, Han K-H, Ikeda K, Piscaglia F, Baron A, et al. Lenvatinib versus sorafenib in first-line treatment of patients with unresectable hepatocellular carcinoma: a randomised phase 3 non-inferiority trial. The Lancet 2018;391:1163–73.

131. Bruix J, Qin S, Merle P, Granito A, Huang YH, Bodoky G, Pracht M, et al. Regorafenib for patients with hepatocellular carcinoma who progressed on sorafenib treatment (RESORCE): a randomised, double-blind, placebo-controlled, phase 3 trial. The Lancet 2017;389:56–66.

132. Abou-Alfa GK, Meyer T, Cheng A-L, El-Khoueiry AB, Rimassa L, Ryoo B-Y, Cicin I, et al. Cabozantinib in patients with advanced and progressing hepatocellular carcinoma. New England Journal of Medicine 2018;379:54–63.

133. Zhu AX, Kang Y-K, Yen C-J, Finn RS, Galle PR, Llovet JM, Assenat E, et al. Ramucirumab after sorafenib in patients with advanced hepatocellular carcinoma and increased α-fetoprotein concentrations (REACH-2): a randomised, double-blind, placebo-controlled, phase 3 trial. Lancet Oncology 2019;20:282–96.

134. Abou-Alfa GK, Chan SL, Kudo M, Lau G, Kelley RK, Furuse J, Sukeepaisarnjaroen W, et al. Phase 3 randomized, open-label, multicenter study of tremelimumab (T) and durvalumab (D) as first-line therapy in patients (pts) with unresectable hepatocellular carcinoma (uHCC): HIMALAYA. Journal of Clinical Oncology 2022;40:379–379.

135. Yau T, Kang YK, Kim TY, El-Khoueiry AB, Santoro A, Sangro B, Melero I, et al. Efficacy and safety of nivolumab plus ipilimumab in patients with advanced hepatocellular carcinoma previously treated with sorafenib: the CheckMate 040 randomized clinical trial. JAMA Oncology, vol. 6, 2020.

136. Zhu AX, Finn RS, Edeline J, Cattan S, Ogasawara S, Palmer D, Verslype C, et al. Pembrolizumab in patients with advanced hepatocellular carcinoma previously treated with sorafenib (KEYNOTE-224): a non-randomised, open-label phase 2 trial. Lancet Oncology 2018;19:940–52.

137. Kelley RK, Rimassa L, Cheng AL, Kaseb A, Qin S, Zhu AX, Chan SL, et al. Cabozantinib plus atezolizumab versus sorafenib for advanced hepatocellular carcinoma (COSMIC-312): a multicentre, open-label, randomised, phase 3 trial. Lancet Oncology 2022;23:995–1008.

138. Losic B, Craig AJ, Villacorta-Martin C, Martins-Filho SN, Akers N, Chen X, Ahsen ME, et al. Intratumoral heterogeneity and clonal evolution in liver cancer. Nature Communications 2020;11.

139. Huang A, Zhao X, Yang XR, Li FQ, Zhou XL, Wu K, Zhang X, et al. Circumventing intratumoral heterogeneity to identify potential therapeutic targets in hepatocellular carcinoma. Journal of Hepatology 2017;67:293–301.

140. El-Khoueiry AB, Sangro B, Yau T, Crocenzi TS, Kudo M, Hsu C, Kim TY, et al. Nivolumab in patients with advanced hepatocellular carcinoma (CheckMate 040): an open-label, non-comparative, phase 1/2 dose escalation and expansion trial. The Lancet 2017;389:2492–502.

141. Calderaro J, Ziol M, Paradis V, & Zucman-Rossi J. Molecular and histological correlations in liver cancer. Journal of Hepatology 2019;71:616–30.

142. Sangro B, Melero I, Wadhawan S, Finn RS, Abou-Alfa GK, Cheng AL, Yau T, et al. Association of inflammatory biomarkers with clinical outcomes in nivolumab-treated patients with advanced hepatocellular carcinoma. Journal of Hepatology 2020;73:1460–9.

143. Finn RS, Ryoo B-Y, Merle P, Kudo M, Bouattour M, Lim HY, Breder V, et al. pembrolizumab as second-line therapy in patients with advanced hepatocellular carcinoma in KEYNOTE-240: a randomized, double-blind, phase III trial. Journal of Clinical Oncology 2019:JCO1901307.

144. Yau T, Park JW, Finn RS, Cheng A-L, Mathurin P, Edeline J, Kudo M, et al. CheckMate 459: A randomized, multi-center phase III study of nivolumab (NIVO) vs sorafenib (SOR) as first-line (1L) treatment in patients (pts) with advanced hepatocellular carcinoma (aHCC). Annals of Oncology 2019;30:v874–5.

145. Huang Y, Yuan J, Righi E, Kamoun WS, Ancukiewicz M, Nezivar J, Santosuosso M, et al. Vascular normalizing doses of antiangiogenic treatment reprogram the immunosuppressive tumor microenvironment and enhance immunotherapy. Proceedings of the National Academy of Sciences 2012;109:17561–6.

146. Shigeta K, Matsui A, Kikuchi H, Klein S, Mamessier E, Chen IX, Aoki S, et al. Regorafenib combined with PD1 blockade increases CD8 T-cell infiltration by inducing CXCL10 expression in hepatocellular carcinoma. Journal of Immunotherapy in Cancer 2020;8:1435.

147. Torrens L, Montironi C, Puigvehí M, Mesropian A, Leslie J, Haber PK, Maeda M, et al. Immunomodulatory effects of lenvatinib plus anti–programmed cell death protein 1 in mice and rationale for patient enrichment in hepatocellular carcinoma. Hepatology 2021;74:2652–69.

148. Zhou L, Liu XD, Sun M, Zhang X, German P, Bai S, Ding Z, et al. Targeting MET and AXL overcomes resistance to sunitinib therapy in renal cell carcinoma. Oncogene 2016;35:2687–97.

149. Xiang Q, Chen W, Ren M, Wang J, Zhang H, Deng DYB, Zhang L, et al. Cabozantinib suppresses tumor growth and metastasis in hepatocellular carcinoma by a dual blockade of VEGFR2 and MET. Clinical Cancer Research 2014;20:2959–70.

150. Patnaik A, Swanson KD, Csizmadia E, Solanki A, Landon-Brace N, Gehring MP, Helenius K, et al. Cabozantinib eradicates advanced murine prostate cancer by activating antitumor innate immunity. Cancer Discovery 2017;7:750–65.

151. Wei SC, Levine JH, Cogdill AP, Zhao Y, Anang NAAS, Andrews MC, Sharma P, et al. Distinct cellular mechanisms underlie anti-CTLA-4 and anti-PD-1 checkpoint blockade. Cell 2017;170:1120-1133.e17.

152. Taylor AM, Shih J, Ha G, Gao GF, Zhang X, Berger AC, Schumacher SE, et al. Genomic and functional approaches to understanding cancer aneuploidy. Cancer Cell 2018;33:676-689.e3.

153. Jiménez-Sánchez A, Cybulska P, Mager KL, Koplev S, Cast O, Couturier D-L, Memon D, et al. Unraveling tumor–immune heterogeneity in advanced ovarian cancer uncovers immunogenic effect of chemotherapy. Nature Genetics 2020;52:582–93.

154. Braun DA, Hou Y, Bakouny Z, Ficial M, Sant' Angelo M, Forman J, Ross-Macdonald P, et al. Interplay of somatic alterations and immune infiltration modulates response to PD-1 blockade in advanced clear cell renal cell carcinoma. Nature Medicine 2020;26:909–18.

155. Ben-David U, & Amon A. Context is everything: aneuploidy in cancer. Nature Reviews Genetics 2020;21:44–62.

156. Hause RJ, Pritchard CC, Shendure J, & Salipante SJ. Classification and characterization of microsatellite instability across 18 cancer types. Nature Medicine 2016;22:1342–50.

157. Bou-Nader M, Caruso S, Donne R, Celton-Morizur S, Calderaro J, Gentric G, Cadoux M, et al. Polyploidy spectrum: a new marker in HCC classification. Gut 2020;69:355–64.

158. Rooney MS, Shukla SA, Wu CJ, Getz G, & Hacohen N. Molecular and genetic properties of tumors associated with local immune cytolytic activity. Cell 2015;160:48–61.

159. McGranahan N, Furness AJS, Rosenthal R, Ramskov S, Lyngaa R, Saini SK, Jamal-Hanjani M, et al. Clonal neoantigens elicit T cell immunoreactivity and sensitivity to immune checkpoint blockade. Science 2016;351:1463–9.

160. Turajlic S, Litchfield K, Xu H, Rosenthal R, McGranahan N, Reading JL, Wong YNS, et al. Insertion-and-deletion-derived tumour-specific neoantigens and the immunogenic phenotype: a pan-cancer analysis. Lancet Oncology 2017;18:1009–21.

161. Rosenthal R, Cadieux EL, Salgado R, Bakir M al, Moore DA, Hiley CT, Lund T, et al. Neoantigen-directed immune escape in lung cancer evolution. Nature 2019;567:479–85.

162. Jamal-Hanjani M, Wilson GA, McGranahan N, Birkbak NJ, Watkins TBK, Veeriah S, Shafi S, et al. Tracking the evolution of non-small-cell lung cancer. New England Journal of Medicine 2017;376:2109–21.

163. Meylan M, Petitprez F, Lacroix L, Tommaso L di, Roncalli M, Bougouin A, Laurent A, et al. Early hepatic lesions display immature tertiary lymphoid structures and show elevated expression of immune inhibitory and immunosuppressive molecules. Clinical Cancer Research 2020;26:4381–9.

164. Ben-David U, Ha G, Khadka P, Jin X, Wong B, Franke L, & Golub TR. The landscape of chromosomal aberrations in breast cancer mouse models reveals driver-specific routes to tumorigenesis. Nature Communications 2016;7:12160.

165. Song EK, Tai WM, Messersmith WA, Bagby S, Purkey A, Quackenbush KS, Pitts TM, et al. Potent antitumor activity of cabozantinib, a c-MET and VEGFR2 inhibitor, in a colorectal cancer patient-derived tumor explant model. International Journal of Cancer 2015;136:1967–75.

166. Matlung HL, Babes L, Zhao XW, van Houdt M, Treffers LW, van Rees DJ, Franke K, et al. Neutrophils kill antibody-opsonized cancer cells by trogoptosis. Cell Reports 2018;23:3946-3959.e6.

167. Xiao WK, Chen D, Li SQ, Fu SJ, Peng BG, & Liang LJ. Prognostic significance of neutrophil-lymphocyte ratio in hepatocellular carcinoma: A meta-analysis. BMC Cancer 2014;14.

168. Becht E, Giraldo NA, Lacroix L, Buttard B, Elarouci N, Petitprez F, Selves J, et al. Estimating the population abundance of tissue-infiltrating immune and stromal cell populations using gene expression. Genome Biology 2016;17:218.

169. Kelley RK, Rimassa L, Cheng AL, Kaseb A, Qin S, Zhu AX, Chan SL, et al. Cabozantinib plus atezolizumab versus sorafenib for advanced hepatocellular carcinoma (COSMIC-312): a multicentre, open-label, randomised, phase 3 trial. Lancet Oncology 2022;23:995–1008.

170. Anstee QM, Reeves HL, Kotsiliti E, Govaere O, & Heikenwalder M. From NASH to HCC: current concepts and future challenges. Nature Reviews Gastroenterology Hepatology 2019;16:411–28.

171. Dudek M, Pfister D, Donakonda S, Filpe P, Schneider A, Laschinger M, Hartmann D, et al. Auto-aggressive CXCR6+ CD8 T cells cause liver immune pathology in NASH. Nature 2021;592:444–9.

172. Dudek M, & Tacke F. Immature neutrophils bring anti-PD-1 therapy in NASH-HCC to maturity. Gut 2022;71:1937–8.

173. Pan X, Chiwanda Kaminga A, Liu A, Wen SW, Chen J, & Luo J. Chemokines in non-alcoholic fatty liver disease: A Systematic Review and Network Meta-Analysis. Frontiers in Immunology 2020;11:1802.

174. Ye D, Yang K, Zang S, Lin Z, Chau HT, Wang Y, Zhang J, et al. Lipocalin-2 mediates non-alcoholic steatohepatitis by promoting neutrophil-macrophage crosstalk via the induction of CXCR2. Journal of Hepatology 2016;65:988–97.

175. Sun L, Clavijo PE, Robbins Y, Patel P, Friedman J, Greene S, Das R, et al. Inhibiting myeloid-derived suppressor cell trafficking enhances T cell immunotherapy. JCI Insight 2019;4.

176. Moses K, Klein JC, Männ L, Klingberg A, Gunzer M, & Brandau S. Survival of residual neutrophils and accelerated myelopoiesis limit the efficacy of antibody-mediated depletion of Ly-6G+ cells in tumor-bearing mice. Journal of Leukocyte Biology 2016;99:811–23.

177. Bajaj JS, Kamath PS, & Reddy KR. The evolving challenge of infections in cirrhosis. New England Journal of Medicine 2021;384:2317–30.